TABLE II
Bulk Copolymerization of CF_3NO/C_2F_4 in Presence of Anionic Inhibitors

Inhibitor	Temp., °C.	Conversion to polymer, %	$\langle\eta\rangle$
—	−16	65	0.58
BF_3 etherate (5 wt.-%)	−16	60	0.56
$TiCl_4$ (20 wt.-%)	−16	55	0.44
CO_2 (5 wt.-%)	−16	65	0.55

water generally increases the molecular weight of the product formed, presumably by acting as a good heat transfer agent.

(*2*) Compounds such as BF_3, $TiCl_4$, and CO_2, which would be expected to inhibit an anionic polymerization such as that proposed by Barr and Haszeldine[2,3] have little or no effect on the polymerization (Table II). Any cationic mechanism proposed for the reaction would necessarily involve electrophilic attack on tetrafluoroethylene and an intermediate fluorocarbon carbonium ion, $\sim\sim CF_2CF_2^{\oplus}$. This would be contrary to all known experimental evidence concerning cationic polymerization and stability of carbonium ions.

(*3*) The reaction of CF_3NO and C_2F_4 takes place at low temperatures, which might seem at first to be evidence in favor of an ionic mechanism. However, the reaction rate shows a large direct temperature dependence, which is normal for a free-radical polymerization and in contrast to ionic polymerization rates which usually show little temperature dependence or increase with decreasing temperature. While a bulk polymerization of CF_3NO/C_2F_4 reaches a conversion of 70–80% in a few hours at −30°C., approximately 2 weeks are required to achieve 50% conversion at −65°C. The effect of temperature on molecular weight is shown in Table III.

(*4*) The molecular weight of the polymer is markedly decreased by the presence of small amounts of radical chain transfer agents. Trifluoromethyl iodide and trifluoromethyl bromide, starting materials for CF_3NO, are particularly effective in this respect, making monomer free from such agents essential to obtaining high molecular weight polymer.

Chain transfer reactions are also important in solution polymerization of CF_3NO/C_2F_4, as shown in Table IV. Solvents containing chlorine or hydrogen, which would be expected to act as chain transfer agents, result in polymer of lower molecular weight than that obtained in perfluorinated solvents.

TABLE III
Effect of Temperature on Molecular Weight for CF_3NO/C_2F_4 Copolymer

Expt.	Temp., °C.	$\langle\eta\rangle$
1	−65	0.86
2	−20	0.70
3	−10	0.61
4	25	0.15

TABLE IV
Effect of Solvent Type on Molecular Weight of CF_3NO/C_2F_4 Copolymer Polymerized at −20°C. at Monomer Concentrations of 30 wt.-%

Solvent	$\langle\eta\rangle$
CCl_3F	0.21
Cl_2FCCF_2Cl	0.24
C_3F_7H	0.20
n-C_7H_{16}	0.10
$C_8F_{16}O$	0.46
$(C_4F_9)_3N$	0.78

(5) The addition of DPPH to a solution polymerization of CF_3NO/C_2F_4 results in a color change of the DPPH (from violet to red-brown) and incorporation of the material into the polymer, indicating the presence of radicals during the polymerization.

With this evidence that the polymerization takes place by a radical mechanism, attention was focused on determination of the initiating species. The first possibility investigated was that initiation is due to undetectable amounts of impurities in the monomers. This theory was rejected on the basis of the following evidence. (1) The polymerization is quite reproducible among different batches of monomers (i.e., monomers prepared by different synthetic routes, stored for varying lengths of time, etc.). The reproducibility of initial polymerization rates is shown in Figure 1. (2) No change in the reaction was noted when polymerizations were carried out with monomers which had been removed from partially polymerized mixtures. If initiation were due to impurities, one would expect such a polymerization to show a difference in rate, molecular weight of final product, etc.

Another possibility for initiation involves homolytic cleavage of CF_3NO, a reaction which is known to occur readily under the influence of ultra-

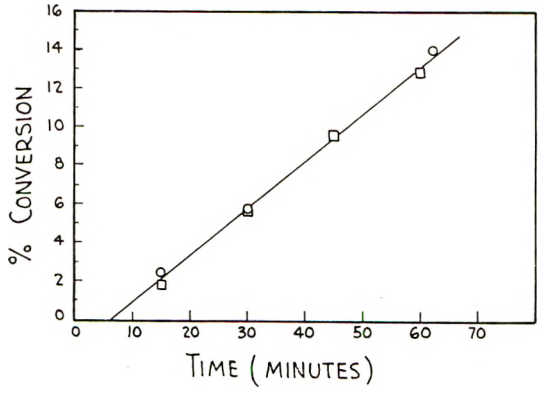

Fig. 1. Effect of monomer source on initial polymerization rate for CF_3NO/C_2F_4: (○) source A; (□) source B. Polymerization at −30°C., 35 wt.-% monomer in $(C_4F_9)_3N$, 1:1 molar ratio $CF_3NO:C_2F_4$.

violet irradiation. This is the basis of the mechanism proposed by Banks and co-workers,[5] i.e.,

$$CF_3NO \rightleftharpoons CF_3\cdot + NO$$

$$CF_3\cdot + CF_3NO \rightarrow (CF_3)_2NO\cdot$$

$$(CF_3)_2N{-}O\cdot + CF_2{=}CF_2 \rightarrow (CF_3)_2NO{-}CF_2CF_2\cdot \xrightarrow[C_2F_4]{CF_3NO} \text{etc.}$$

Several experiments were carried out to test the feasibility of this mechanism. First, the stability of CF_3NO was checked. Samples of pure CF_3NO were kept at room temperature in the dark for as long as three months without showing any change as determined by infrared or VPC (vapor phase chromatographic) analysis. If CF_3NO undergoes self-decomposition, formation of some NO would be expected. This would then react with CF_3NO. The reaction of CF_3NO with NO at room temperature was found to take place rapidly, probably by the following route:

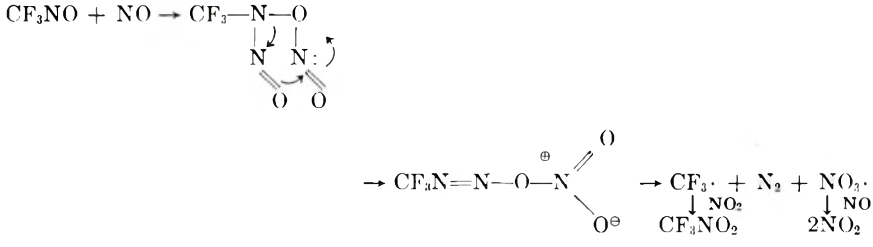

Trifluoronitromethane is the main product noticed in the reaction, along with carbonyl fluoride and silicon tetrafluoride, which could arise from the following reactions.

$$CF_3\cdot + NO_2 \rightarrow CF_3ONO \rightarrow CF_3O\cdot \xrightarrow{SiO_2} COF_2 + SiF_4$$

An attempt to detect $CF_3\cdot$ radicals in the monomer by use of DPPH was also made. A solution of CF_3NO and DPPH (10:1 mole ratio) in benzene was kept at room temperature in the dark for 2 months. At the end of this time, the CF_3NO was recovered quantitatively and spectral analysis showed no change. The DPPH showed no change in appearance or melting point. A qualitative test for fluorine was negative.

In addition to the above evidence against initiation by homolytic cleavage of CF_3NO is the fact that such a mechanism offers no explanation for the formation of oxazetidine along with polymer. Thus, one would have to postulate two distinct reactions occurring concurrently by different mechanisms.

The most plausible mechanism, based on existing data, is that the initiating species arises from the reaction of tetrafluoroethylene with CF_3NO, which is in the triplet or diradical state. Lewis and Kasha[6] have shown the existence of the triplet state in nitroso compounds and thioketones and have used this fact as an explanation for the abnormal colors of these compounds and for their tendency to dimerize and polymerize.

With initiation occurring in this way and assuming that one site of the initiating species, $CF_3\dot{N}$–$OCF_2CF_2\cdot$, is much less reactive than the other and does not take part in chain growth, the polymerization mechanism may be formulated as follows:

Initiation:

$$CF_3N{=}O \underset{k_{-1}}{\overset{k_1}{\rightleftharpoons}} CF_3\dot{N}{-}\dot{O} \tag{1}$$

$$CF_3\dot{N}{-}\dot{O} + C_2F_4 \xrightarrow{k_2} \cdot N(CF_3){-}O{-}CF_2CF_2\cdot \tag{2}$$

Propagation:

$$\cdot N(CF_3){-}O{-}CF_2CF_2\cdot + CF_3NO \xrightarrow{k_3} \dot{N}(CF_3){-}O{-}CF_2{-}CF_2{-}N(CF_3){-}O\cdot \tag{3}$$

$$\dot{N}(CF_3){-}O{-}CF_2CF_2{-}N(CF_3){-}O\cdot + C_2F_4 \xrightarrow{k_4} \dot{N}(CF_3){-}O{-}CF_2CF_2{-}N(CF_3){-}O{-}CF_2CF_2\cdot \tag{4}$$

Termination:

$$\sim\!\sim CF_2CF_2\cdot + \sim\!\sim CF_2CF_2\cdot \xrightarrow{k_5} \text{Polymer} \tag{5}$$

$$\sim\!\sim CF_2CF_2\cdot + \sim\!\sim N(CF_3){-}O\cdot \xrightarrow{k_6} \text{Polymer} \tag{6}$$

Rate expressions, based on the above scheme, may be derived as follows where M_1 denotes CF_3NO, M_2 denotes C_2F_4, DR denotes $CF_3\dot{N}{-}\dot{O}$, P_1 denotes $\sim\!\sim N(CF_3){-}O\cdot$, and P_2 denotes $\sim\!\sim CF_2CF_2\cdot$.

Under steady-state conditions,

$$d[DR]/dt = 0 \tag{7}$$

so that

$$k_1[M_1] = k_{-1}[DR] + k_2[DR][M_2] \tag{8}$$

or

$$[DR] = k_1[M_1]/(k_{-1} + k_2[M_2]) \tag{9}$$

Since the polymerization treated here is alternating

$$k_3[P_2][M_1] = k_4[P_1][M_2] \tag{10}$$

Assuming termination by eq. (5), we have

$$k_2[M_2][DR] = k_5[P_2]^2 \tag{11}$$

and

$$[P_2] = (k_2/k_5)^{1/2}[DR]^{1/2}[M_2]^{1/2} \tag{12}$$

Substituting the value of [DR] from eq. (9) yields

$$[P_2] = (k_1k_2/k_5)^{1/2}[M_1]^{1/2}[M_2]^{1/2}/(k_{-1} + k_2[M_2])^{1/2} \quad (13)$$

The polymerization rate R is given by

$$R = k_3\,[P_2][M_1] \quad (14)$$

Combining eqs. (13) and (14) yields

$$R = k_3\,(k_1k_2/k_5)^{1/2}[M_1]^{3/2}[M_2]^{1/2}/(k_{-1} + k_2[M_2])^{1/2} \quad (15)$$

Thus, the rate will be proportional to $[CF_3NO]^{3/2}$ and to a power of $[C_2F_4]$ between 0 and 0.5, depending upon the value of k_{-1} relative to $k_2[M_2]$. For termination by reaction (6), the rate depression becomes:

$$R = (k_3k_1k_2k_4/k_6)^{1/2}\,[M_1][M_2]/(k_{-1} + k_2[M_2])^{1/2} \quad (16)$$

and the rate will be proportional to the first power of $[CF_3NO]$ and to a power of $[C_2F_4]$ between 0.5 and 1. Since a combination of the two termination mechanisms would be expected, the rate of polymerization should show a dependence on $[CF_3NO]$ somewhat greater than 1 and on $[C_2F_4]$ less than 1.

Initial rates of polymerization in $(C_4F_9)_3N$ solution at $-30°C.$ were determined by polymer isolation techniques. It was necessary to use rather concentrated solutions in order to obtain a very high ratio of polymer to oxazetidine, so that solvent effects may be significant. Experiments conducted at the minimum concentrations which would yield polymer in essentially quantitative yield and limiting conversions to a maximum of 10% gave the results summarized in Table V.

TABLE V

Expt.	$[CF_3NO]$, moles/l.	$[C_2F_4]$, moles/l.	Rate of polymer formation, g./min.
1	2.81	2.81	0.0100
2	1.40	2.81	0.0041
3	2.81	1.40	0.0052

This gives the following reaction orders: $[CF_3NO]^{1.3}$, $[C_2F_4]^{0.9}$.

Similar experiments at lower concentrations lead to apparent lower orders of reaction due to a decrease in the ratio of polymer to oxazetidine. However, at all concentrations, there is a greater dependency on $[CF_3NO]$ than on $[C_2F_4]$ (Fig. 2) which is in agreement with the proposed mechanism. The same type of rate dependency was found when Freon 113 was used as a solvent, although rates are somewhat lower in this case (Fig. 3).

The effect of small amounts of chain transfer agents on initial polymerization rate is shown in Table VI. CF_3I, CF_3Br, and $CF_2ClCFCl_2$ show essentially no change in rate, indicating the radicals produced by transfer are capable of initiating new chains, presumably by attack on a

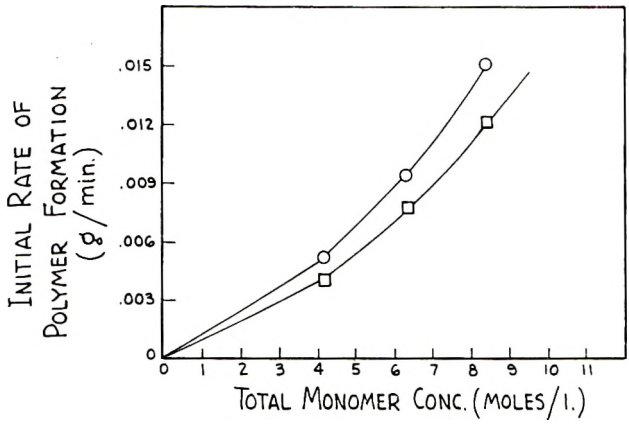

Fig. 2. Initial polymerization rate vs. total monomer concentration: (○) 2:1 molar ratio $CF_3NO:C_2F_4$; (□) 1:2 molar ratio $CF_3NO:C_2F_4$. Polymerization at −30°C. in $(C_4F_9)_3N$.

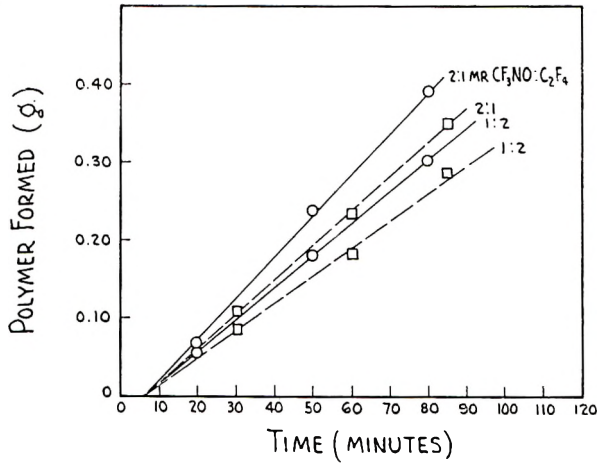

Fig. 3. Initial polymerization rates (○) in $(C_4F_9)_3N$ and (□) in $CF_2ClCFCl_2$. Total monomer concentration, 4.2 moles/l. at −30°C.

CF_3NO molecule. Small amounts of NO and NO_2 show a significant increase in rate as well as a decrease in molecular weight of the polymer. It is known that NO_2 reacts rapidly with C_2F_4 to give a mixture of products,[7,8] all arising from the intermediate, $O_2N–CF_2CF_2\cdot$. Since this species is comparable to the growing chain in CF_3NO/C_2F_4 copolymerization, the increase in rate is readily explained. As discussed previously, NO reacts with CF_3NO to produce NO_2 and $CF_3\cdot$, each of which could initiate new chains, thus increasing the polymerization rate.

In any diradical mechanism, of course, the possibility of self-termination of chains by intramolecular coupling must be considered. This readily accounts for the concurrent formation of perfluoro-2-methyl-1,2-oxazeti-

TABLE VI
Effect of Chain Transfer Agents on Initial Polymerization Rates. Polymerization in $(C_4F_9)_3N$ Solution at −30°C., Total Monomer Concentration 5.6 moles/l.

Chain transfer agent	Concn. chain transfer agent, moles/l.	Rate of polymer formation, g./min.
None	(control)	0.0114
CF_3I	7.4×10^{-3}	0.0116
CF_3Br	8.3×10^{-2}	0.0111
$CF_2ClCFCl_2$	8.3×10^{-2}	0.0110
NO	7.4×10^{-3}	0.0149
NO_2	7.4×10^{-3}	0.0149

dine in the copolymerization of CF_3NO/C_2F_4, but higher membered rings would also be expected. (These rings would contain 8, 12, 16, etc. atoms in the ring, maintaining the 1:1 stoichiometry of the reaction.) Barr and Haszeldine[3] dismissed the possibility of any cyclic structures of less than twenty atoms (other than the four-membered one) being present, on the basis of their inability to notice any distillable products below 400°C., at which temperature the polymer decomposed. Thermal stability studies carried out at Quartermaster Research and Engineering Center have shown that the raw polymer contains a considerable amount of volatile material. Samples heated at 100°C. at 20 mm. Hg pressure underwent a fairly rapid weight loss of 15–20%, after which further heating produced no additional weight loss. Samples of high molecular weight polymer, obtained by fractionation techniques, did not show any significant change in weight under these conditions, indicating the weight loss is volatilization rather than degradation. When a sample of CF_3NO/C_2F_4 copolymer was subjected to molecular distillation at room temperature, a low molecular weight fraction was obtained. Infrared and NMR spectra of this material were significantly different from those of the original sample, indicating that a structure rather different from that of the copolymer is involved. In particular, the NMR spectrum showed two types of $—CF_3$ and several types of $—CF_2$ (possibly as many as six, but all adjacent to N or O), compared to one type of $—CF_3$ and two types of $—CF_2$ in the crude copolymer. The relative amounts of $—CF_3$ and $—CF_2$ in agreement for a 1:1 ratio of CF_3NO to C_2F_4. While the material was probably a mixture, the spectra are not inconsistent with those expected from medium-sized cyclic structures. Work is currently underway to separate the volatile material into pure components and identify them.

Further evidence that polymerization initiation is due to the diradical character of the nitroso compound is afforded by the relative reactivities of different nitroso compounds. According to the theory of Lewis and Kasha, the reactivity of the nitroso group in R—NO is independent of the nature of R. Polymerization rates of CF_3NO, C_2F_5NO, C_3F_7NO, $C_8F_{17}NO$, $ClCF_2CF_2NO$, $CF_2ClCFClNO$, and $O_2NCF_2CF_2NO$ with C_2F_4 are all approxi-

mately the same, and terpolymers involving two nitroso compounds with C_2F_4 are readily prepared. On the other hand, the nature of the olefin has a very large effect on polymerization rate, and terpolymers involving two olefins and one nitroso compound are very difficult to prepare. The reactivity of olefins decreases with decreasing halogen substitution, e.g., $CF_2{=}CF_2 > CF_2{=}CFH > CF_2{=}CH_2 \gg CFH{=}CH_2$ and $CH_2{=}CH_2$.

Another phenomenon which may be explained by a diradical mechanism is that reaction of CF_3NO with an unsymmetrical olefin, $CF_2{=}CXY$, leads to an oxazetidine having predominantly the structure,

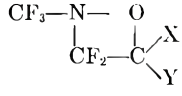

and a polymer having predominantly the structure,[5]

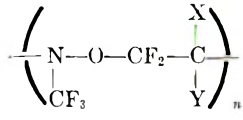

Free radical attack on $CF_2{=}CXY$ is known to occur at the CF_2 group. Thus, two possibilities exist for the initiating species:

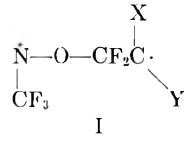

I

and

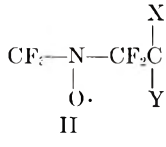

II

It can be postulated that both species are formed, with structure I predominating at temperatures of 0°C. or lower and the relative amount of structure II increasing with temperature. Through the use of molecular models it can be seen that the carbon atom, bearing the X and Y groups, is much less hindered in structure I than in structure II. Thus, structure I favors chain growth and polymer formation, while structure II favors self-termination or oxazetidine formation.

The foregoing has been an endeavor to clarify the mechanism of a reaction which is a useful method for the introduction of the heteroatoms nitrogen and oxygen into a carbon-carbon polymer chain, particularly one which is perhalogenated.

Note added in proof: Since this paper was submitted, electron paramagnetic resonance studies of the reactions of nitrosohaloalkanes have been carried out. These studies, reported elsewhere,[9,10] confirm the free radical nature of the process and identify the propagating radical species.

The writers wish to acknowledge the contributions and assistance of W. J. Fraser, J. J. McBrady, G. A. Morneau, P. I. Roth, and A. R. Shultz of the Central Research Department, 3M Company, J. C. Montermoso and C. B. Griffis of the Quartermaster Research and Engineering Center, and M. Szwarc, Syracuse University.

References

1. Crawford, G. H., D. E. Rice, and J. C. Montermoso, paper presented to Ind. Eng. Chem. Div., 137th Meeting, American Chemical Society, Cleveland, April 5–14, 1960.

2. Barr, D. A., and R. N. Haszeldine, *J. Chem. Soc.*, **1956**, 3424.

3. Barr, D. A., and R. N. Haszeldine, *J. Chem. Soc.*, **1955**, p. 1881.

4. Crawford, G. H., D. E. Rice, and J. C. Montermoso, Paper No. 45, presented at 6th Joint Army, Navy, and Air Force Conference on Elastomers, Boston, Mass., October 18–20, 1960.

5. Banks, R. E., J. M. Birchall, and R. N. Haszeldine, paper presented at Symposium on High Temperature Resistance and Thermal Degradation of Polymers, Society of the Chemical Industry, London, England, September 21–23, 1960.

6. Lewis, G. N., and M. Kasha, *J. Am. Chem. Soc.*, **67**, 994 (1945).

7. Knunyants, I. L., and A. V. Fokin, *Bull. Acad. Sci. USSR*, **1957**, 1463.

8. Crawford, G. H., *J. Polymer Sci.*, **45**, 259 (1960).

9. Crawford, G. H., D. E. Rice, and L. H. Piette, paper presented at the Second International Symposium on Fluorine Chemistry, Estes Park, Colorado, July 17–20, 1962.

10. Piette, L. H., and G. H. Crawford, paper No. 24 presented in the Division of Inorganic Chemistry, 142nd meeting, Am. Chem. Soc., Atlantic City, N. J., September 9–14, 1962.

Synopsis

The mechanism of copolymerization of fluoronitrosoalkanes with fluoroolefins was investigated. The reaction was not inhibited by water or other common ionic polymerization inhibitors but was greatly affected by free radicals or radical chain transfer agents, indicating a free radical polymerization mechanism. Evidence against initiation by impurities or by homolytic cleavage of the nitroso monomer was obtained. Initial rates of polymerization in solution were determined. The data obtained is consistent with a polymerization mechanism involving initiation by a radical formed through the interaction of the fluoroolefin with the fluoronitrosoalkane which has a significant diradical or triplet state population at the polymerization temperature. The reactivities of various monomers, the formation of low molecular weight product and the structures of the oxazetidine by-products are discussed in terms of this mechanism.

Résumé

On étudie le mécanisme de copolymérisation des fluoronitrosoalcanes et des fluorooléfines. La réaction n'est pas inhibée par l'eau ou par d'autres inhibiteurs habituels de la polymérisation ionique, mais elle est fortement influencée par les radicaux libres et les agents de transfert de chaîne radicalaires indiquant un mécanisme de polymérisation radicalaire. On constate une initiation par les impuretés ou par rupture homolytique du monomère nitrosé. On détermine les vitesses initiales de polymérisation en solution. Les résultats obtenus sont en accord avec un mécanisme de polymérisation comprenant l'initiation par un radical formé par interaction de la fluorooléfine avec le fluoronitrosoalcane qui possède à température de polymérisation, une population d'états diradicalaires ou triplets. On discute, sur la base de ce mécanisme, les réactivités de divers monomères, la formation de produit, de faible poids moléculaire et les structures des produits secondaires oxazétidiniques.

Zusammenfassung

Der Mechanismus der Copolymerisation von Fluornitrosoalkanen mit Fluorolefinen wurde untersucht. Die Reaktion wurde durch Wasser oder andere bekannte Inhibitoren für ionische Polymerisation nicht inhibiert, wohl aber durch freie Radikale oder Überträgerstoffe für Radikalketten stark beeinflusst, was für einen radikalischen Polymerisationsmechanismus spricht. Der Reaktionsstart erfolgt nicht durch Verunreinigungen oder homolytische Spaltung des Nitrosomonomeren. Die Anfangspolymerisationsgeschwindigkeit in Lösung wurde bestimmt. Die erhaltenen Ergebnisse stehen in Übereinstimmung mit einem Polymerisationsmechanismus mit Radikalbildung durch Reaktion des Fluorolefins mit dem Fluornitrosoalkan, das bei der Polymerisationstemperatur einen charakteristischen Anteil an Diradikal- oder Tripletform besitzt. Die Reaktivität verschiedener Monomerer, die Bildung niedrigmolekularer Produkte und die Struktur der Oxazetidin-Nebenprodukte werden anhand dieses Mechanismus diskutiert.

Received January 2, 1962

JOURNAL OF POLYMER SCIENCE: PART A VOL. 1, PP. 577–590 (1963)

Particle Size Distribution in Polymer Solutions

JOHN J. MAURER, *Chemicals Research Division, Esso Research and Engineering Company, Linden, New Jersey*

INTRODUCTION

Numerous investigators[1–3] have considered the problem of aggregate formation in polymer solutions and the effect of this process upon the properties of such solutions. However, convenient methods for measuring the size and the distribution of these aggregates have been lacking. This study was undertaken to determine whether the Coulter counter, which previously has been used to determine particle size distributions in various suspensions,[4,5] could be used to measure these particles and to study the properties of polymer solutions by this method. No previous work of this type has come to the author's attention, although Parks and Jurbergs[6] have used this instrument to measure the relative efficiency of filters in removing insoluble material from viscose solutions. It is shown in the present investigation that particle size distributions in certain polymer solutions can be measured by this technique. The method should be generally applicable to polymer solutions, provided that a suitable solvent is available and that the particles in solution are large enough to permit detection of a significant part of the distribution.

EXPERIMENTAL

Coulter Counter Principle

This counter is used to determine the number and size of particles present in a solution of electrolyte by forcing a sample of the solution through a calibrated orifice having an electrode on each side. Each particle, as it passes through the orifice, displaces its own volume of electrolyte and momentarily changes the resistance between the electrodes. This produces a voltage pulse of short duration, having a magnitude proportional to the volume of the particle. The voltage pulses, after amplification, are fed to a threshold circuit which has an adjustable screen-out level. If this level is equaled, or exceeded, a pulse will be counted. A series of counts is taken at varying threshold levels, and cumulative frequency plots of particle size are directly obtained from these counts.

Systems Studied

The polystyrene and the polyvinyltoluene used in this study were prepared by emulsion polymerization by standard techniques. Styrene-

maleic anhydride was prepared in methyl ethyl ketone with azobisisobutyronitrile as catalyst. Intrinsic viscosities of these polymers are shown in Table I. The former polymers were sulfonated by the method of Turbak[7] and then converted to the sodium salt. Styrenemaleic anhydride was converted to the sodium salt by treatment with aqueous sodium hydroxide.

TABLE I
Identification of Polymers

Polymer type	Code	Intrinsic viscosity (25°C.)
Polyvinyltoluene	PVT	6.5 (benzene)
Polyvinyltoluene sulfonate (Na^+)	$PVTSO_3Na$	
Polystyrene	PS	9.2 (benzene)
Polystyrenesulfonate (Na^+)	$PSSO_3Na$	
Styrenemaleic anhydride	SMA	1.8 (acetone)
Styrenemaleic anhydride (Na^+)	SMANa	

Particle size distributions were measured in aqueous sodium chloride solutions or in dimethylformamide–NH_4CNS solutions.

Measurement of Polymer Concentration

Two of the polymers (PS, SMA) were made by polymerizing C^{14}-labeled monomer. The concentration of polymer in solutions of these materials or of their derivatives was determined by drying a portion of the solution on glass beads, breaking up the dried mass, adding phosphor solution, and measuring the activity with a Packard liquid scintillation spectrometer. In a typical analysis, 4 ml. of polymer solution were pipetted into a liquid scintillation spectrometer vial (Wheaton Glass Company) containing 16.00 g. of glass beads (470 microns). The sample was dried for 24 hr. at 60°C., agglomerates were broken up, and 4 ml. of phosphor solution (4 g. diphenyloxazole and 0.05 g. 1,4-bis-2-(5-phenyloxazolyl)benzene per liter of toluene) were pipetted into the vial. The vial was then shaken thoroughly, tapped to settle the beads, and placed in the spectrometer for measurement of the C^{14} content. In this manner, it was shown that no change in polymer concentration took place during the measurement of the particle size distributions in solutions of these polymers.

Preparation of Solutions

The particle size distribution in a polymer solution is influenced by the thermal history of the solution and by the shearing forces to which it has been subjected. Therefore, care was taken to prepare and to measure all solutions under as nearly identical conditions as possible. Polymer was added to solvent in a glass flask, and was slowly stirred for 2 hr. at room temperature. The solution was then filtered through a coarse sintered-glass funnel, and the concentration was determined by measuring the C^{14} content by the procedure detailed above.

The concentration of polymer and of electrolyte in a solution was varied in such a way as to permit the detection of a maximum portion of the particle size distribution. This variation was necessary because the upper limit of polymer concentration is determined by the particular orifice being used and also by the counter. Deviations from true response occur when the total count (which is proportional to concentration) is too high. Also, viscosity considerations became important when measurements are to be made with polyelectrolytes in dilute salt solutions. The polymer concentrations used in this study are indicated in the appropriate figures.

All particle size measurements were made at room temperature, which was found to be 25 ± 1°C. This temperature variation had no significant effect on the particle size distributions in these systems.

Diffusion Measurements

The diffusion of polymer through a membrane (obtained from Millipore Filter Corporation, Bedford, Massachusetts) and into the appropriate solvent was studied at room temperature. The membrane, after having been conditioned by soaking for 18 hr. in the solvent to be used, was clamped between the halves of a polystyrene cell. Samples were periodically removed from each side of the cell, and the polymer concentration was determined by measuring the C^{14} activity as previously described.

Fractionation of Polystyrene

Polystyrene was fractionated by precipitation from methyl ethyl ketone solution with methanol at room temperature. Only a few fractions were collected, since it was felt that these would suffice to indicate the effect of high molecular weight species on particle distribution in $PSSO_3Na$ solutions. The fractionation data are indicated in Table II.

TABLE II
Fractionation of Polystyrene

Fraction	Weight fraction	Intrinsic viscosity (benzene, 25°C.)
I	0.504	11.5
II	0.269	7.4
III	0.227	4.2

These fractions were sulfonated by the method previously described, and particle size measurements were performed on solutions of fraction I and of fraction II.

Statistical Analysis of the Data

Kottler[8] has pointed out that particle size distributions should be log-normal, and Irani[9] has described the treatment of abnormalities in such systems. Both authors have described the presentation of data on prob-

ability paper (Codex Book Company No. 3127, 3128). This method of data analysis was used in this investigation because log-normal distributions give linear plots which are easily examined by regression techniques and because bimodal systems were easier to identify with these plots than was the case with differential plots. This latter was due to the fact that, in the systems studied, the distributions were very narrow. Thus, slight variations in particle counts caused appreciable scatter in a differential plot of the size distribution. In bimodal systems where the distributions are wider (i.e., in which σ is larger), differential plots can be used to detect bimodal systems.

The data are presented as cumulative per cent based on the number of particles counted. However, representative systems were examined to determine whether number-average or weight-average plots were more informative.[10] They did not differ significantly from the plots presented in this paper.

Although detection of the complete distribution was possible in most of the systems reported in this paper, there were cases in which truncated distributions were observed. This resulted from the fact that some of the particles were either too large or too small to be detected by the particular orifice used. It should be possible to calculate the complete distribution even for these systems because the point of truncation (i.e., the particle size at which the orifice becomes insensitive) is known with a fair degree of accuracy, and a statistical method is available[11] for calculating the complete distribution from a truncated distribution which has a known point of truncation.

RESULTS AND DISCUSSION

It was anticipated that the plots of particle size distribution obtained from these systems would be truncated at the low end because (*a*) the lowest molecular weight polymer, because of its solubility, may not be isolated with the bulk of the polymer after a polymerization, and (*b*) the orifice used in the determination has a lower size limit below which it is insensitive. However, as shown in Figure 1, the data indicated that complete distributions were being measured. In addition, the particle sizes were indicated to be in the micron range. These factors suggested that aggregates were the species being counted.

Membrane diffusion studies were performed to obtain an independent estimate of the particle sizes in several of these solutions. In one system (0.025% $PSSO_3Na$ in 0.15% NaCl solution), for example, only a trace of the polymer passed through a 5-micron membrane during one week at room temperature. Coulter counter evaluation of this same polymer solution indicated that most of the particles were above 4.5 microns. Thus the two measurements are in qualitative agreement. In contrast with the diffusion behavior of the above system, dilute salt solutions of low molecular weight $PSSO_3Na$ or more concentrated salt solutions of high molecular weight $PSSO_3Na$ were observed to pass readily through such a membrane.

Ultrafiltration experiments also indicated that solutions of the low molecular weight polymer passed readily through the membrane whereas those of the high molecular weight polymer did not. These results are interpreted as supporting evidence for the existence of aggregates in these polymer solutions.

There are several polymeric species which could account for the presence of aggregates in polymer solutions. These include (*a*) microgel due to

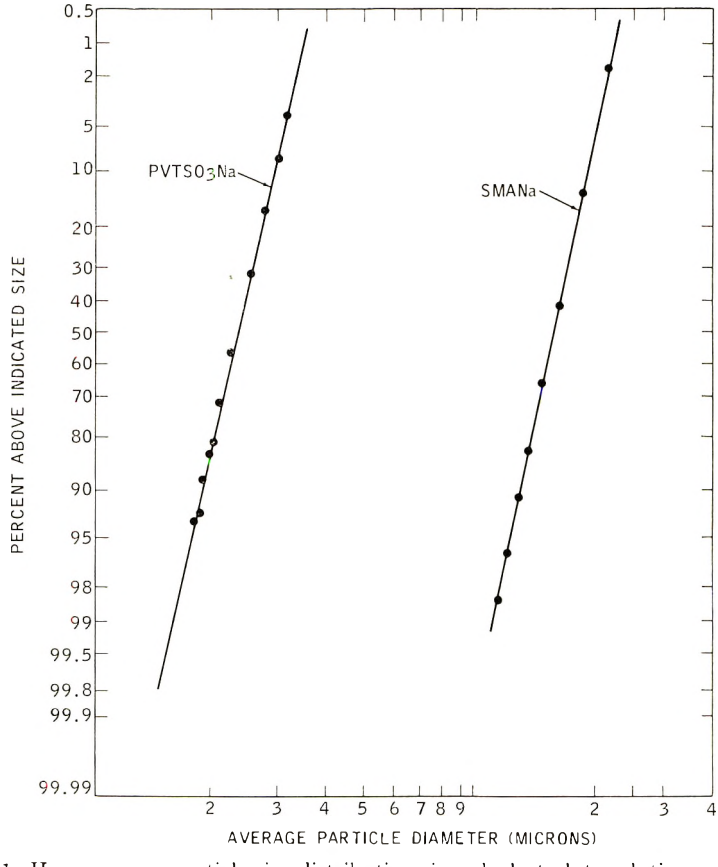

Fig. 1. Homogeneous particle size distributions in polyelectrolyte solutions; 0.025% polymer in 0.3% NaCl solution, 50 micron orifice for $PVTSO_3Na$, 30 micron orifice for SMANa.

very high molecular weight polymer or to crosslinked polymer, (*b*) incompletely-dissolved aggregates which originated in the polymerizations due to the high conversions attained,[1] or (*c*) aggregate formation in solution due to an equilibrium process. The first possibility is considered unlikely for reasons which become evident from the data throughout this paper. The remaining possibilities are discussed in the following experiments.

If an equilibrium process is involved in aggregate formation, it should be

possible to detect some dependence of the process on polymer concentration. Therefore, the effect of dilution upon the particle sizes present in a solution was studied. As shown in Figure 2, the particle sizes decrease with dilution. Curve *C*, which is typical of a system in which the low end of a distribution has been removed,[9] indicates that the average particle size was reduced to the extent that a portion of the distribution was too small to be detected by the orifice. The observed reduction in particle size may not be entirely due to decreasing polymer concentration because the dilution was not carried out at constant ionic strength. Katchalsky[12] has pointed out that solutions of constant ionic strength keep the shape of the poly-

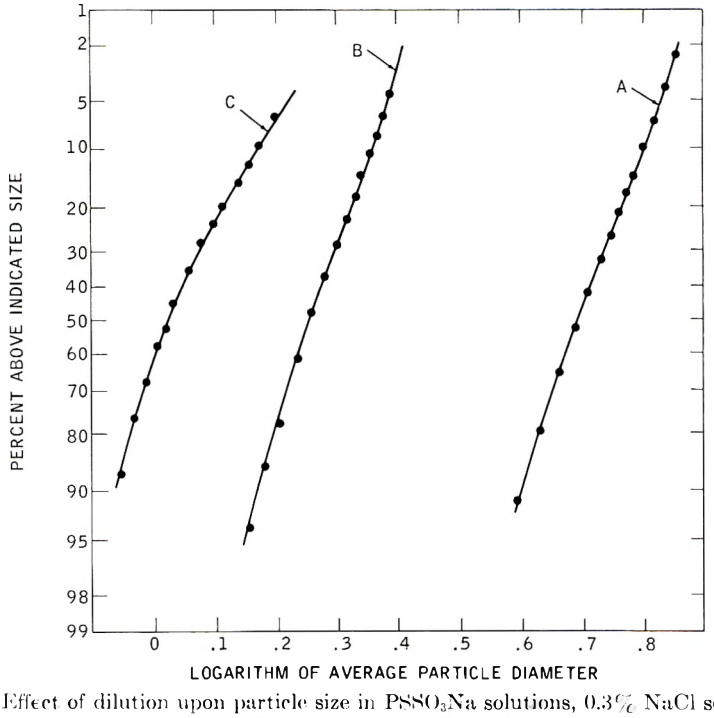

Fig. 2. Effect of dilution upon particle size in $PSSO_3Na$ solutions, 0.3% NaCl solution; 50 micron orifice: (*A*) 0.025% $PSSO_3Na$; (*B*) 0.013% $PSSO_3Na$; (*C*) 0.006% $PSSO_3Na$.

electrolyte molecule constant during dilution. Similar effects might be anticipated in the present systems.

A consequence of an equilibrium process, or of case (*c*), is that the particle size distribution should shift with temperature. Further, prolonged aging of a solution at high temperature, followed by cooling, might yield a system in which reaggregation would occur slowly. It is also possible that the solution would not return to its original state, and that this latter is one of the mechanisms by which polymer solutions degrade (i.e., lose viscosity) when they are aged at high temperatures.

To examine this point, the stability of a solution of SMANa (0.25% in 0.3% NaCl) was studied at 80°C. During four days' aging at this tem-

perature, the viscosity of the solution (measured at 25°C.) decreased from 6.1 to 3.1 cstokes. Particle size distributions (Fig. 3) were measured both before and after aging of the solution. They showed that an appreciable particle size decrease took place. Since the intrinsic viscosity of the system also decreased, as shown in the Fuoss plot[13] in Figure 4, molecular breakdown as well as aggregate breakdown has occurred. Thus, although disaggregation may facilitate polymer degradation by disentangling polymer molecules and thereby making weak links in these molecules more

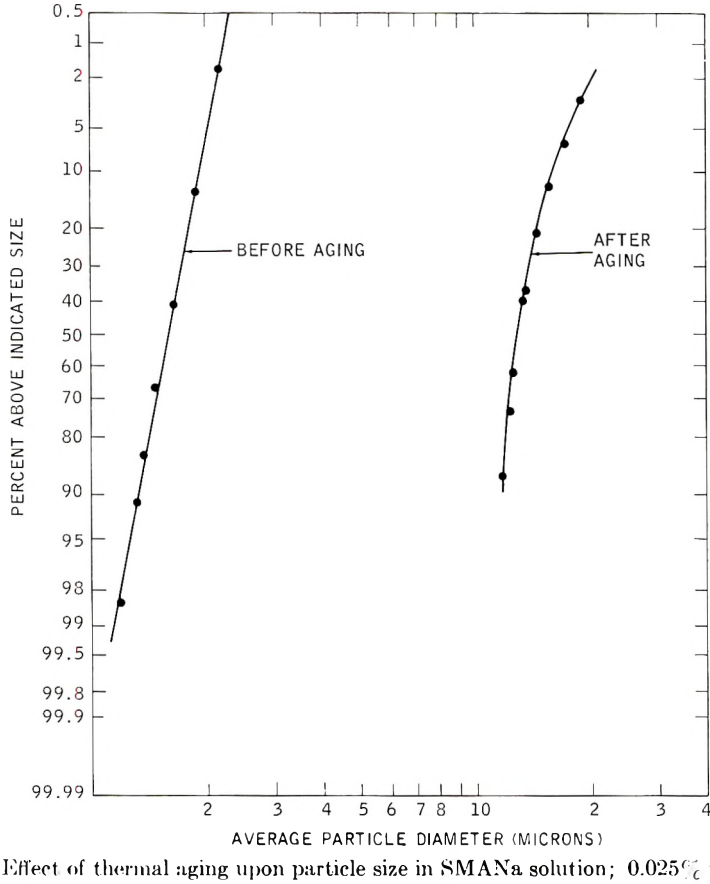

Fig. 3. Effect of thermal aging upon particle size in SMANa solution; 0.025% polymer in 0.3% NaCl solution, 30 micron orifice.

accessible, it is not the single mechanism by which degradation proceeds in this case. The above argument presupposes that intrinsic viscosity is not influenced by the presence of aggregates in the initial polymer solution. Frisch[2] presents evidence that this assumption is valid. On the basis of the foregoing evidence, mechanisms (*b*) and (*c*) could be sources of the aggregates in these systems. However, since no dependence of particle size upon time was found, mechanism (*b*) is favored.

Having evaluated some of the properties of the polymer species being

counted, attention was next directed to a study of the distribution curves thus obtained. There is a marked difference in the log-probability plot of a $PSSO_3Na$ solution (Fig. 5) as compared with those of solutions of SMANa or of $PVTSO_3Na$ (Fig. 1). Whereas the latter systems are represented by homogeneous, log-normal distributions, the former appear to be bimodal, log-normal. If this apparent bimodality is real and is not an artifact of this technique for measuring particle size, it has considerable physical significance. The following discussion is intended to resolve this question.

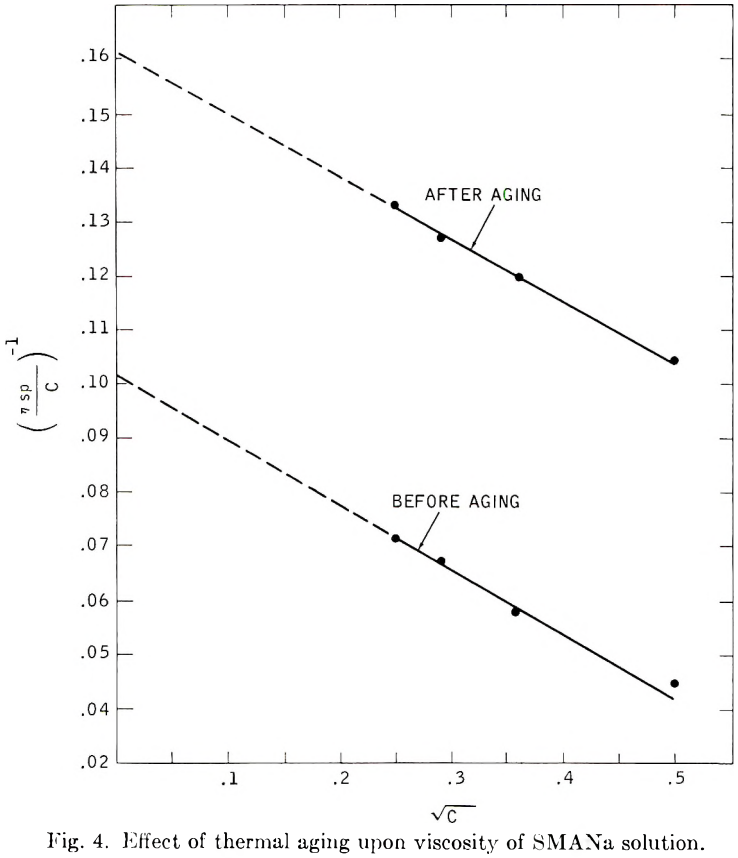

Fig. 4. Effect of thermal aging upon viscosity of SMANa solution.

Several methods which could give rise to "false" bimodal systems were considered. These were (*a*) that some peculiarity of polysulfonates, as opposed to the other types of polymers studied, led to erroneous results, (*b*) that improper sampling of the system had produced the equivalent of a kurtosis system, and (*c*) that some treatment of the polymer and/or the polymer solution had censored the distribution at both ends.[9] The first of these possibilities is not likely since a polyvinyltoluene sulfonate solution gave a homogeneous, log-normal plot (Fig. 1). The second possibility does not apply to measurements made with the Coulter counter because

the method of sampling the solution is random. The third possibility is also considered unlikely in these systems because (*a*) no significant change in the log-probability plots for $PSSO_3Na$ solutions was observed when the filtration step was omitted during solution preparation, (*b*) $PVTSO_3Na$, which was prepared by the same general method as was $PSSO_3Na$ exhibited homogeneous log-normal distributions, and (*c*) solutions of a sulfonate prepared from the highest molecular weight fraction of a polystyrene were bimodal (Fig. 6). One would expect that fractionation, by censoring the

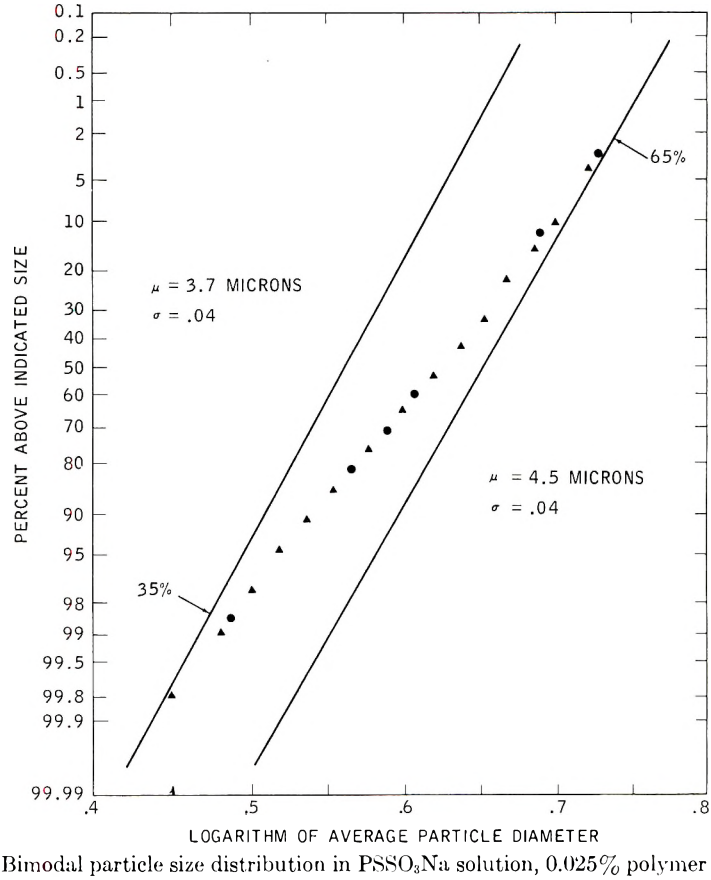

Fig. 5. Bimodal particle size distribution in $PSSO_3Na$ solution, 0.025% polymer in 0.3% NaCl solution, 50 micron orifice: (●) calculated; (▲) observed.

distribution, would have altered the shape of the log-probability plots. Since it did not, it is apparent that the shape of these plots is not very sensitive to removal of the "ends" of the polymer distribution.

Aitchison and Brown[14] describe a method for determining the parent distributions which make up a particular bimodal system. This technique was applied to a $PSSO_3Na$ system for the above purpose and also as a test of the bimodality of the distribution. As seen in Figure 5, a good fit was obtained by assuming that one of the parent distributions comprised 65%

of the mixture, and the other 35%. It is apparent from the geometric mean particle sizes μ and the dispersions σ that this system is composed of two distributions which are very similar. This is the reason that the log probability plot has such slight curvature. As a further test of the bimodality of this system, a chi-square test was performed. It indicated that there is good agreement between the calculated and the observed probability plots. On the basis of these results, it appears that the $PSSO_3Na$ systems are truly bimodal.

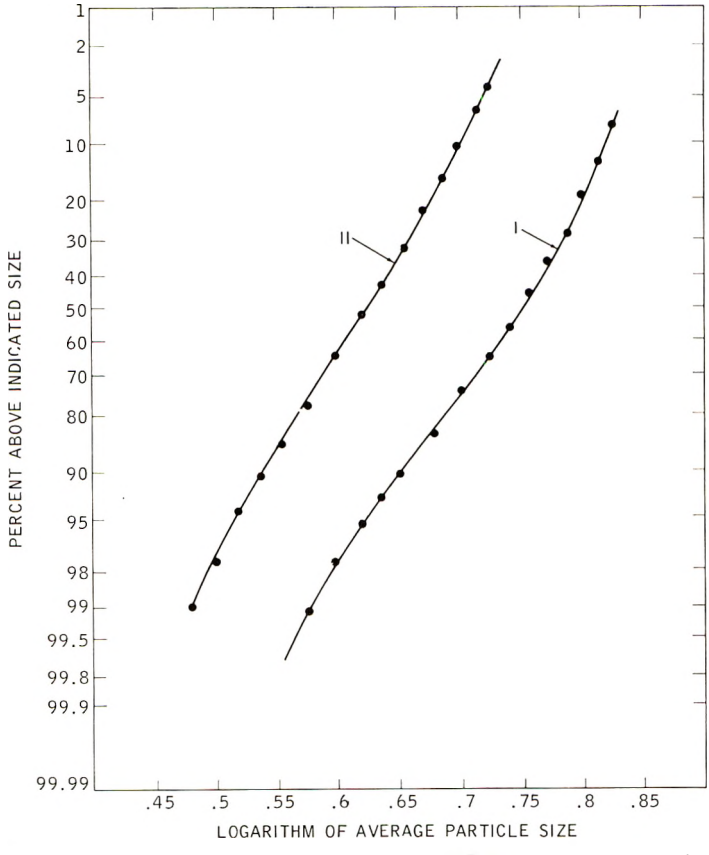

Fig. 6. Effect of fractionation upon particle size in $PSSO_3Na$ solutions; 0.025% polymer in 0.3% NaCl solution, 50 micron orifice.

The bimodal systems could have originated (*a*) during the polymerization of the styrene, (*b*) during the sulfonation of the polystyrene, or (*c*) in the aqueous solutions of the polystyrene sulfonate. Aqueous solutions of $PSSO_3Na$ were examined first. It was found that the appearance of bimodal behavior was not time-dependent within the limits studied (between one hour and two weeks from the start of sample preparation). Also, although particle size decreased with dilution in these systems (Fig. 2), the bimodal properties were retained until portions of the distribution became

too small to be detected (curve *C*, Fig. 2). Thus, there is little or no dependence of this property upon concentration in these solutions.

The effect of salt concentration upon particle size was also studied. As anticipitated from the polyelectrolyte character of $PSSO_3Na$, a decrease in particle size was observed when the salt concentration was increased from 0.3% to 0.9%. The data (Fig. 7) appear to represent a bimodal distribution for the former case and a homogeneous distribution for the latter. However, it is not certain whether the latter case is merely a result of a decrease in particle size to the extent that a bimodal distribution, even though present, cannot be detected. Although not shown in Figure 6, the

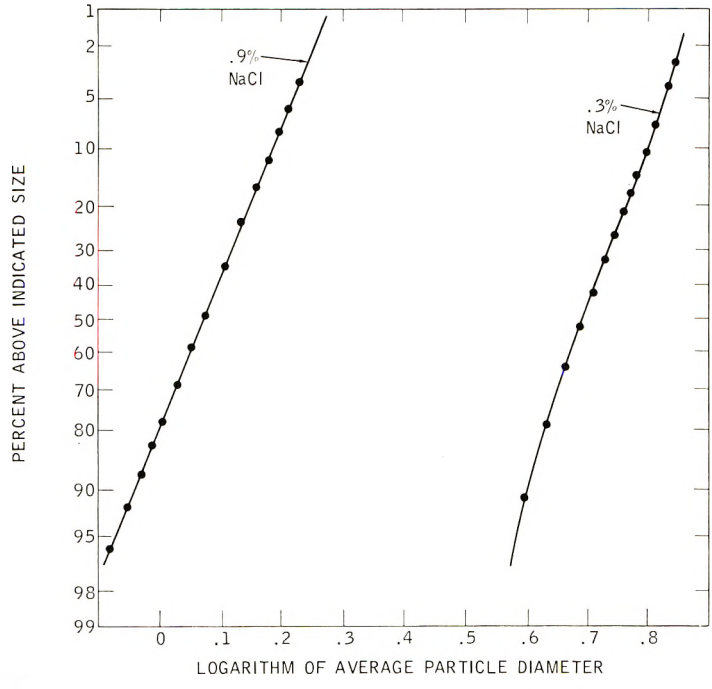

Fig. 7. Effect of salt concentration upon particle size in $PSSO_3Na$ solutions, 0.025% polymer in NaCl solution, 50 micron orifice.

particle size distribution in a 2% NaCl solution was measured. In that case, the system resembled curve *C* of Figure 2, an indication that a portion of the distribution was too small to be detected by the orifice. Further study will obviously be required before the dependence of particle size upon salt concentration can be firmly established.

To determine whether the bimodal properties of $PSSO_3Na$ are inherent in the parent polystyrene, dimethylformamide–NH_4CNS solutions of the latter were examined with the Coulter counter. It was found (Fig. 8) that such systems had bimodal particle size distributions. For comparison, a similar solution of SMA was examined and was found to exhibit a homogeneous log-normal distribution of particle sizes (Fig. 8). These experi-

ments and those shown in Figure 1 demonstrate that not all polymer solutions will appear to contain bimodal distributions when measured with this instrument. Thus, there is some support for the validity of this appearance in solutions of PS and of $PSSO_3Na$. Further, the evidence suggests that the bimodal properties of these polymers are inherent in the parent polystyrene.

There are several possibilities which could account for the presence of the

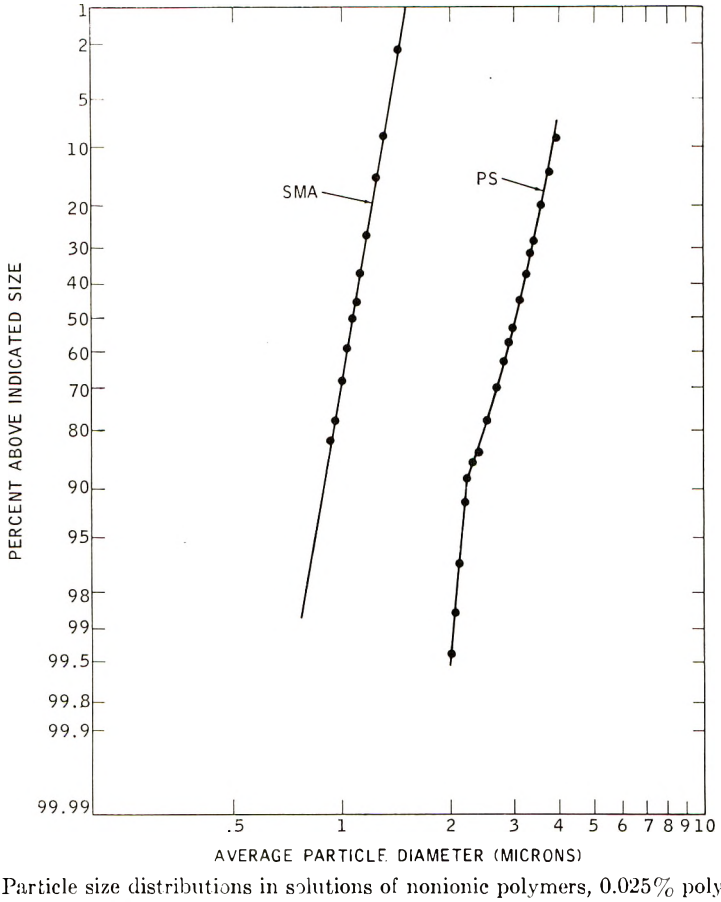

Fig. 8. Particle size distributions in solutions of nonionic polymers, 0.025% polymer in NH_4SCN (15%)–dimethyl-formamide solution, 50 micron orifice.

bimodal distributions in the above solutions. These are (*a*) two distributions of molecular weights or of particle size, due to different growth or termination mechanisms in the polymerization process, (*b*) different steric configurations (e.g., linear versus branched) present in the polymer, or (*c*) different states of aggregation in solutions of the polymers.

In a paper on the mechanism of emulsion polymerization of styrene, van der Hoff[15] presents data which indicate that bimodal distributions of particle size were formed when the soap concentration was near the critical micelle concentration. He considers that this arises from the consecutive formation of particles in two phases, micellar and aqueous. This mechanism is an example of the first possibility mentioned above. Thus,

study of particle size distributions as a guide to elucidating polymerization mechanisms may be another area where the Coulter counter can be employed. A 10-micron orifice has recently become commercially available and should permit the detection of particles in the size range encountered by van der Hoff.

Some support for the third possibility can also be found in the literature. Hastings et al.[16] describes experiments in which the electron microscope was used to detect the presence of two distributions in polystyrene. Light-scattering measurements, made on solutions of fractions of the same polymer, indicated the probable existence of two types of particles in solution; one was spherical and the other was rodlike. Such a differentiation according to shape is not possible with the Coulter counter technique, since the treatment assumes sphericity of the particles.

No example of the second possibility has come to the author's attention. However, starch solutions may be ideal for such a test, since they contain two components, amylose and amylopectin, which differ in branching. Since methods of separating the components are known, one could determine whether the whole-starch systems give bimodal particle size distributions, and whether the separate components give homogeneous distributions. It is possible that the Coulter counter will also provide a measure of the efficiency of the separation process.

The author is indebted to Mr. G. T. Davis, who developed the method used in analyzing the labeled polymers; to Dr. A. Noshay, who prepared the polymers used in this study; to Mr. Robert Phillips, for skillful assistance in particle size measurements; and to numerous co-workers, for many stimulating discussions.

References

1. Boyer, R. F., and D. J. Streeter, *J. Polymer Sci.*, **14**, 5 (1954).
2. Frisch, H. L., *J. Polymer Sci.*, **18**, 299 (1955).
3. Francis, P. S., *J. Appl. Polymer Sci.*, **5**, 261 (1961).
4. Berg, R. H., *ASTM Special Technical Publication*, No. 234, 245 (1958).
5. Petro, A. J., *J. Phys. Chem.*, **64**, 1508 (1960).
6. Parks, L. R., and K. A. Jurbergs, *J. Appl. Polymer Sci.*, **4**, 193 (1960).
7. Turbak, A. F., paper presented at 139th National Meeting of the American Chemical Society, St. Louis, Missouri, April 1961.
8. Kottler, F., *J. Franklin Inst.*, **250**, 339 (1950).
9. Irani, R. R., *J. Phys. Chem.*, **63**, 1603 (1960).
10. Maron, S. H., *J. Appl. Phys.*, **23**, 900 (1952).
11. Hald, A., *Statistical Theory with Engineering Applications*, Wiley, New York, 1952.
12. Katchalsky, A., *J. Polymer Sci.*, **12**, 159 (1954).
13. Fuoss, R. M., *Discussions Faraday Soc.*, **11**, 125 (1957).
14. Aitchison, J., and J. A. C. Brown, *The Lognormal Distribution*, Cambridge University Press, 1957.
15. van der Hoff, B. M. E., *J. Polymer Sci.*, **44**, 241 (1960).
16. Hastings, G. W., D. W. Ovenall, and F. W. Peaker, *Nature*, **177**, 1091 (1956).

Synopsis

Log-normal particle size distributions in polymer solutions have been measured with the Coulter counter. Qualitative membrane diffusion measurements were performed to

substantiate the presence in these solutions of particles in the micron size range. Particle size was found to be dependent upon the thermal history of a polymer solution and upon the shearing forces to which it had been subjected. Further, particle size decreased upon dilution of a polyelectrolyte solution or upon an increase in the salt content. It is concluded that polymeric aggregates are the species being counted. These aggregates apparently originated during the polymerization of the polystyrene or of the styrene maleic anhydride studied. Bimodal distributions were observed in polystyrene solutions and in polystyrene sulfonate (Na+) solutions. The latter bimodal systems were resolved by graphical means, and it was found that the two populations are present in the ratio 65:35. The two distributions have the same dispersions (0.04) and only slightly different means (3.7 versus 4.5 microns). The mechanism of formation of this bimodal system may be that proposed by van der Hoff; namely, that particles are formed consecutively in the micellar and in the aqueous phase of an emulsion polymerization system when the soap concentration is near the critical micelle concentration.

Résumé

On a mesuré au moyen d'un compteur Coulter les distributions logarithmiques normales de la dimension des particules dans des solutions polymériques. On a effectué des mesures qualitatives de diffusion de membrane pour établir la présence dans ces solutions de particules de la dimension du micron. On a trouvé que la taille des particules dépendait du traitement thermique de la solution polymérique et des forces de scission auxquelles elle eavait été soumise. De plus la taille de particules diminue par dilution de la solution de polyélectrolyte ou par augmentation de la quantité de sel. On en conclut que les aggrégats polymériques sont bien d'une espèce qui peut être comptée. On a étudié ces aggrégats apparemment produits pendant la polymérisation du polystyrène ou pendant la polymérisation du styrène et de l'anhydride maléique. On a observé des distributions bimodales dans les solutions de polystyrène et de sulfonate (Na^+) de polystyrène. Ce dernier système bimodal a été résolu graphiquement et on trouve que les deux espèces sont présentes dans le rapport 65/35. Les deux distributions ont les mêmes dispersions (0.04) et semblent seulement légèrement différentes (3.7 contre 4.5 microns). Le mécanisme de formation de ce système bimodal peut être celui proposé par van der Hoff; c'est à dire que les particules sont formées consécitivement dans la "micelle" et dans la phase aqueuse d'un système de polymérisation en émulsion lorsque la concentration en savon est proche de la concentration critique en micelles.

Zusammenfassung

Log-normale Teilchengrösseverteilungen wurden in Polymerlösungen mit dem Coulter-Zähler gemessen. Qualitative Membrandiffusionsmessungen wurden zum Nachweis des Vorhandenseins von Teilchen im Mikron-Grössenbereich in diesen Lösungen durchgeführt. Die Teilchengrösse war von der thermischen Vorgeschichte der Polymerlösung und von den Scherkräften, welchen sie unterworfen worden war, abhängig. Weiters nahm die Teilchengrösse bei Verdünnung einer Polyelektrolytlösung oder bei Ansteigen des Salzgehalts ab. Man kam zu dem Schluss, dass die Polymeraggregate die gezählten Teilchen sind. Diese Aggregate entstanden offenbar während der Polymerisation des untersuchten Polystyrols oder Styrolmaleinsäureanhydridcopolymeren. Bimodale Verteilungen wurden in Polystyrol- und Polystyrolnatriumsulfonat($Na+$) lösungen beobachtet. Das letztgenannte bimodale System wurde graphisch aufgelöst und es wurde gefunden, dass die beiden Verteilungen im Verhältnis von 65:35 vorliegen. Die beiden Verteilungen besitzen die gleiche Dispersion (0,04) und nur wenig verschiedene Mittelwerte (3,7 gegenüber 4,5 Mikron). Der Bildungsmechanismus diese bimodalen Systems entspricht möglicherweise dem von van der Hoff vorgeschlagenen: nämlich dass Teilchen fortlaufend in der micellaren und in der wässrigen Phase eines Emulsionspolymerisationssystems gebildet werden, wenn die Seifenkonzentration nahe der kritischen Micellkonzentration liegt.

Received December 7, 1961

JOURNAL OF POLYMER SCIENCE: PART A VOL. 1, PP. 591–597 (1963)

Some Aspects of the Production and Study of Semiconducting Polymeric Materials

A. V. TOPCHIEV, *Academy of Sciences of the U.S.S.R., Moscow, U.S.S.R.*

The present paper gives a brief survey of the work on the conductivity of organic materials and the synthesis of polymeric semiconducting materials carried out by the author and his co-workers in the laboratories of the Institute of Petrochemical Synthesis of the Academy of Sciences of the U.S.S.R. during 1958–60.

At the beginning of this century the photoconductivity of certain organic materials, especially of anthracene and its analogs, was noticed. The proper significance was not attached to this phenomenon at that time. Only in the last ten years has systematic research on the conductivity of organic compounds been developed in the U.S.S.R. and in other countries. Up to the present time many organic substances have been synthesized in which there is the temperature dependence of conductivity which is characteristic of semiconductors.

An analysis of the published data on conductivity of low molecular weight organic substances shows that the semiconducting properties are associated with the presence of conjugated bonds in aliphatic chains and rings. An investigation of the electronic absorption spectra of systems with conjugated bonds shows that some of the electrons in such bonds are delocalized. The interaction of π-electrons in such systems creates a single collective system of electrons. In such molecules the π-electrons may be considered quasi-free, and the system behaves like a metal from the point of view of conductivity.

In the investigation of polymers one is interested first in the polymer molecules themselves and secondly in the collection of macromolecular chains which constitutes the polymer in its entirety. Correspondingly, the study of electroconductivity in organic polymers may be divided into studies of (*1*) the movement of the current carriers in individual macromolecules and (*2*) of the movement of electrons (or holes) from molecule to molecule.

Let us examine the state of the electron in the isolated macromolecule. Three cases are possible: (*1*) the electron is in approximately the same state as in the isolated atom (free electron); (*2*) A pair of electrons is delocalized at a specific bond (σ-electrons); (*3*) The distribution of electrons is generalized for the molecule as a whole. Theory and experiment show that this is the case for π-electrons in the case of polyconjugation. Such a distribu-

tion of electrons appears to be most promising for the production of highly conducting materials, and thus our first attempts were the creation of polyconjugated polymers.

These may be obtained in two ways: (*1*) Modification of macromolecule chains; (*2*) Specific synthesis of the corresponding polymers.

Both methods have been used and produced polymers with specific electrical properties. The method of modifying the polymer to produce polyconjugation in the backbone chain has many advantages, in as much as it is hard to get a polymer of high molecular weight by direct synthesis and it is hard to regulate the molecular weight this way. In the polymerization of acetylene, which has been attempted by us and others, molecular weights rarely exceed 1000–2000. Furthermore these polymers have undesirable physical properties, i.e. do not melt, dissolve, extrude, etc.

Thus the method of modification of the chains of previously prepared polymers is more promising if the orientation of the initial material may be preserved.

However, the metallike character of the molecule itself is not sufficient to ensure that conductivity exists, e.g., while the single benzene molecule is a good conductor of electricity, this molecule in the condense state, liquid benzene, is an insulator. Polyconjugation is the optimum condition for the carrying of current down the molecule, but it does not decide the ease with which the current traverses the intermolecular potential barrier.

The potential barrier between molecules will depend on the following factors: (*1*) the character of the movement of electrons within the molecule; (*2*) the intermolecular distance; (*3*) the character of the intermolecular bonds.

These three factors must be studied in relation to each other, and may not be considered separately. The effect of heteroatoms on the electrical properties of the polymer are of especial interest, as they affect both the intramolecular movement of electrons and the intermolecular bonds.

The above considerations directed our experimental investigations. The investigations were directed at (*1*) the creation of systems with polyconjugated and heteroatoms in the main chain, and (*2*) the measurement of the effect of structure on the electrophysical properties of polymers.

Our investigations justified the above hypotheses. As an example I present the results of the study of polyconjugated systems obtained based on polyacrylonitrile.

We are of the view that thermal treatment produces a series of changes in polyacrylonitrile:

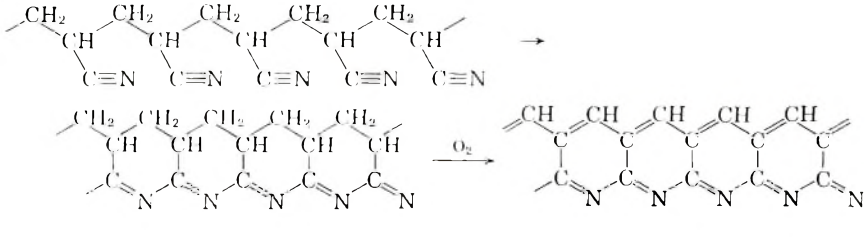

This process was believed until recently, to be a variation of the raising of the thermal stability of fibers of polyacrylonitrile. But, as seen in the scheme above, the change in this polymer leads us to a system of conjugated double bonds both along the —C=C— chain and the —C=N— chain. The thermal conversion of polyacrylonitrile led to a series of semiconducting materials differing in both conductivity and the temperature dependence of thermal conductivity over a wide range of values, depending on the conditions of thermal treatment, the structure of the initial material, and the introduction of various additives.

The investigations were directed at elucidating the effect of the duration and conditions of the thermal conversion, orientation, additives, and γ-radiation on the paramagnetic and semiconducting properties of the materials obtained and also at elucidating the mechanism of semiconductivity in these substances. The initial samples of acrylonitrile differed as to molecular weight, method of synthesis, amount of branching. Table 1 presents data on the paramagnetic properties of these products.

TABLE I
EPR Data

Method of preparation	Concentration of electrons with unpaired spins
Redox initiator system	4.0×10^{18}
Radiation polymerization	5.1×10^{18}
Ionic polymerization with LiC_4H_9	1.7×10^{18}
Ionic polymerization and exposure to light	1.5×10^{19}

Figure 1 presents data characterizing the electrophysical properties of a series of samples. An analysis of the data presented leads to the conclusion that during the thermal treatment of the samples two processes occur: (*a*) successive conversion within the molecule and (*b*) changes in the number and type of intermolecular bonds. The first is shown by the change in the

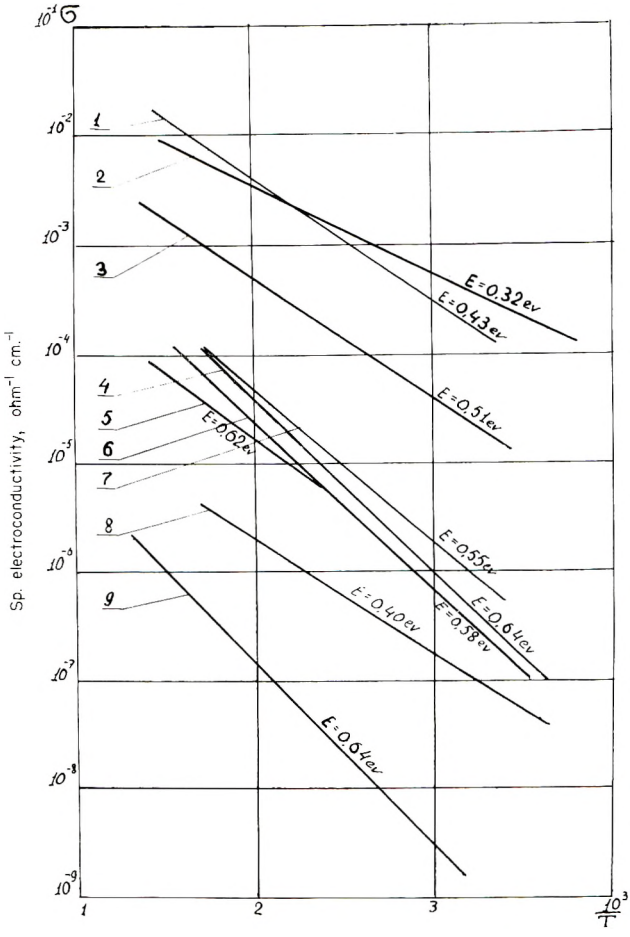

Fig. 1. Dependence of specific electroconductivity on temperature: (*1*) polyacrylonitrile (PAN) film 1; (*2*) PAN film 2; (*3*) PAN treated with saturated $CuCl_2$ and then heated at 400°C.; (*4*) PAN treated at 500°C. under NH_3; (*5*) PAN treated at 400°C. under NH_3; (*6*) polycondensation product of phthalic anhydride with hydroquinone and glycerol; (*7*) polycondensation product of phthalic anhydride and hydroquinone; (*8*) polyvinyl chloride heat-treated at 260°C.; (*9*) PAN heat-treated at 400°C.

energy of activation as compared to a sample heated for the same length of time in a vacuum. In as much as the former samples contain 2–3% more nitrogen than samples heated in a vacuum, this is indicative of the effect in the chain of the heteroatoms.

Similar patterns were observed for other polyconjugated systems studied. The products of intramolecular condensation of polyacryloamide and polymethacrylamide, of the dehydrochlorination of polyvinyl chloride, and modified polyconjugated copolymers of acrylonitrile with several monomers, etc. were investigated.

A series of compounds was synthesized in which there were systems of conjugated bonds and of aromatic rings in the chain.

Semiconducting polymeric materials were obtained by the polycondensation of phthalic anhydride with *p*-phenylenediamine and hydroquinone. The latter products are characterized by a specific electric conductivity at room temperature of 7×10^{-7}–9×10^{-7} ohm^{-1}cm.$^{-1}$, an energy of activation of 0.6–0.4 e.v. and a positive value of the thermal emf. The electrophysical properties of the polycondensates of α-diketones with diamines and hydrazine are being studied. Interesting results have been obtained with *para*-cyanogens and a series of other polymers.

We present some results of the study of the mechanism of conductivity in semiconducting polymeric materials. If we assume as is customary, that the electroconductivity σ is given by

$$\sigma = enu$$

where e is the electronic charge, n is the concentration of the carrier of current, and u is the mobility of the carrier, then the exponential dependence of the electric conductivity on temperature which, as indicated above, is characteristic for all our polymeric semiconductors may be explained either by an exponential growth in the number of carriers of current (n) or by the exponential growth of the mobility (u).

The answer to the above question may be given by studying the temperature dependence of the differential thermalelectromotive force.

If the increase in electroconductivity is due to an increase in current carrier concentration, then it follows that it must be accompanied by a sharp drop in differential thermal–emf. If the current carrier concentration is independent of temperature, then the thermal emf is only weakly dependent on temperature.

Figure 2 shows that there is practically no change in the thermal emf with temperature. We therefore conclude that the change of electroconductivity with temperature is due to the increase in current carrier mobility in the substances investigated.

The exponential dependence of electric conductivity on temperature is evidently due to the barrier between the geometric expanses of structural elements. Thermal activation is necessary to surmount the barrier between these elements. From this point of view it is interesting to observe the effect of addition of various elements on the conductivity of polymers.

Experiments have shown that addition of several metals significantly changes the thermal emf of semiconducting polymers and affect the electric conductivity comparatively weakly. Evidently, the number of carriers within the molecule changes in this case (and therefore the thermal emf changes), but the conditions of intramolecular transfer are not changed. On the other hand, thermal treatment under definite conditions, strongly changes the electric conductivity, and affects the thermal emf weakly.

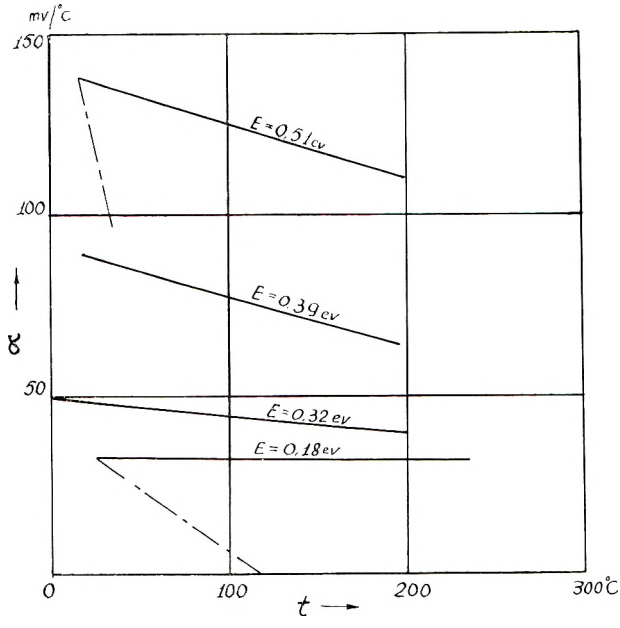

Fig. 2. Dependence of differential thermalelectromotive force on temperature for the samples PAN, treated at varial temperatures.

This is the case also in the addition of certain other elements. We are dealing here with the reverse phenomenon.

Orientation of the molecules (by fiber stretching) also increases the electric conductivity, but does not change the thermal emf or the energy of activation. In this case, the number of intermolecular transfers along the boundary corresponding to the length evidently increases.

In conclusion, I treat the catalytic properties of organic semiconductors. In the last few years many experimental data have been compiled that indicate that the electronic processes taking place in semiconductors and causing the electrical, magnetic, and optical properties also cause their catalytic activity. The basic position of semiconductor theory of catalysis led to a new approach to many questions of catalyst selection for a variety of chemical reactions, including polymerization.

The catalytic properties of the polymeric semiconductors are of interest. Experiments show that aside from their catalytic effect on decomposition of hydrazine hydrate to ammonia and nitrogen and on the decomposition of hydrogen peroxide they possess a catalytic activity in the decomposition of formic acid comparable in order of magnitude to the catalytic activity of a series of metallic catalysts and inorganic catalysts of the semiconductor type.

This deserves special attention, in as much as polymeric semiconductors are inactive in the decomposition of alcohols, differing in this respect from the usual inorganic semiconductors and metallic catalysts. The selectivity of polymeric semiconductors opens up new possibilities in heterogeneous

catalysis. It is possible that this will lead to the establishing of new rules in the relation of bonds between purely chemical and selective fermentation processes in biologically active substances.

Synopsis

The paper deals with theoretical and experimental data on polymeric products with semiconducting properties. The data show the possibility of producing, on the basis of polymers, particularly polyacrylonitrile, substances characterized by high electroconductivity and exponential dependence of the latter on temperature. Possible changes in electrophysical properties of the materials are discussed. A quasimetallic model of a polymeric semiconductor is described.

Résumé

Cet article traite des résultats théoriques et expérimentaux obtenus avec despolymères à propriétés semiconductrices obtenus par un groupe de chercheurs sous la direction de l'auteur. Les résultats obtenus montrent qu'il est possible de produire, à partir de polymères, en particulier du polyacrylonitrile, des substances caractérisées par une électro-conductivité élevée et une dépendance exponentielle vis-à-vis de la température. On discute des changements possibles dans des propriétés électrophysiques des matériaux obtenus. On décrit un modèle presque métallique d'un semiconducteur polymérique.

Zusammenfassung

Die Arbeit behandelt theoretische und experimentelle Ergebnisse an Polymeren mit Halbleitereigenschaften, die von einem Wissenschaftlerteam unter Leitung des Autors erhalten wurden. Die Ergebnisse zeigen die Möglichkeit, Substanzen auf Polymer-, besonders Polyacrylnitril-basis, herzustellen, die durch hohe elektrische Leitfähigkeit und eine exponentielle Temperaturabhängigkeit der Leitfähigkeit charakterisiert sind. Mögliche Veränderungen der elektrophysikalischen Eigenschaften der erhaltenen Stoffe werden diskutiert. Es wird ein quasi-metallisches Modell eines polymeren Halbleiters beschrieben.

Received May 1, 1961

JOURNAL OF POLYMER SCIENCE: PART A VOL. 1, PP. 599–604 (1963)

Synthesis of Nitroolefins and an Investigation of Their Ability to Polymerize

A. V. TOPCHIEV and V. P. ALANIYA, *Academy of Sciences of the U.S.S.R., Moscow, U.S.S.R.*

Little work has been done on nitroolefins since the turn of the century.

Recently, in connection with the interest in compounds with unsaturated bonds and in particular those in which multiple bonds are bonded with electrophilic groups (nitro, nitrile, etc.) much work has been devoted to nitroolefins.

Two types of nitroolefins exist: α-nitroolefins containing a nitro group bonded to an unsaturated carbon atom, and nitroolefins with the nitro group in the allyl position.

Results of the synthesis and study of nitroolefins of the first type are presented here.

Nitroolefins are either yellow liquids (aliphatic) or crystalline substances (aromatic and heterocyclic) and are lachrymators.

The presence of an active double bond and easily reduced nitro group promise a wide applicability of nitroolefins in organic synthesis (Fig. 1).

There are two basic paths of synthesis of nitroolefins: (*1*) nitration of olefins with nitric acid or nitrogen dioxide and (*2*) condensation of nitroparaffins with aldehydes and ketones. Also, many nitroolefins are synthesized by the condensation of diketones with nitroparaffins.

During the condensation of aliphatic aldehydes with nitroparaffins, the alcohol is formed first which on removal of water yields the nitroolefin. Condensation of nitoparaffins with aliphatic aromatic and heterocyclic compounds usually yields the nitroolefin directly.

The most promising method for industrial production of nitroolefins is direct nitration of olefins. The condensation reaction is more convenient for laboratory synthesis.

This latter method was used to prepare 1-nitropropylene, ω-nitrostyrene, and α-furyl nitroethylene. (Table I.)[1–3] The condensations were carried out in the presence of base. The synthesis of α-furyl nitroethylene was carried out in the presence of the anion-exchange resin AN-2F. The use of this resin for the reaction of furfural with nitromethane allows one to carry out the reaction at ordinary temperatures without cooling, and obtain the nitroolefins in good yield. The constants differ little from those in the literature (Table I).

These nitroolefins were then polymerized. Aliphatic nitroolefins poly-

TABLE I
Synthesis of Nitroolefins

Nitroolefin	Starting materials	Reaction conditions	Yield, % Nitroalcohol	Yield, % Nitroolefin	Observed constants M.W.	d_4^{20}	n_D^{20}	B.P., °C.	M.P., °C.	Literature constants M.W.	d_4^{20}	n_D^{20}	B.P., °C.	M.P., °C.
1-Nitropropylene	Acetaldehyde (2 moles) + nitromethane (2 moles)	0.5% base, 30–35°C.	80	89[a]	89	1.0654	1.4526	54–56	—	87	1.0661	1.4527	55–56	—
ω-Nitrostyrene	Benzaldehyde (0.5 mole) + nitromethane (0.5 mole)	0.5% base, 0°C.	—	85	150	—	—	—	58.5	149	—	—	—	58
α-Furylnitroethylene	Furfural (0.4 mole) + nitromethane (0.4 mole)	0.5% base, −50°C.	48	—	137	—	—	—	75	139	—	—	—	74–75
		15% AN-2F 200°C.	46	—										

[a] Dehydration of nitropropanol.

TABLE II
Results of Polymerization of Nitroolefins

Starting material	Catalysts studied	Optimum conditions for polymerization in presence of Na methylate: Temp., °C.	Catalyst, %	Time, hr.	Polymer yield, %	Polymer
1-Nitropropylene	BF_3, sat'd. soln. of $NaHCO_3$, Na methylate	−18	5	3	86	Light yellow powder (m.p. 115°C.)
ω-Nitrostyrene	BF_3, pyridine, benzoyl peroxide, Na methylate	−10	4	8	68	High polymer
α-Furylnitroethylene	BF_3, $(NH_4)_2S_2O_8$, Na methylate	−10	5	6	79	High polymer

TABLE III
Some Properties of Polymers Prepared

Monomer	Repeating unit of polymer	Polymer yield, %	Softening point, °C.	Character of polymer
1-Nitropropylene $CH_3CH{=}CHNO_2$	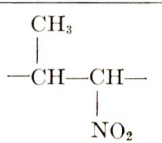	86	80	Amorphous, light yellow powder, partially soluble in dimethylformamide, easily ignitable
ω-Nitrostyrene $C_6H_5CH{=}CHNO_2$	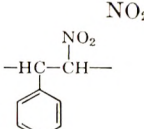	96	170	Amorphous, white powder, insoluble
α-Funylnitroethylene 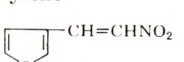	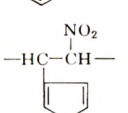	79	400	Amorphous, brown powder, insoluble, thermally stable

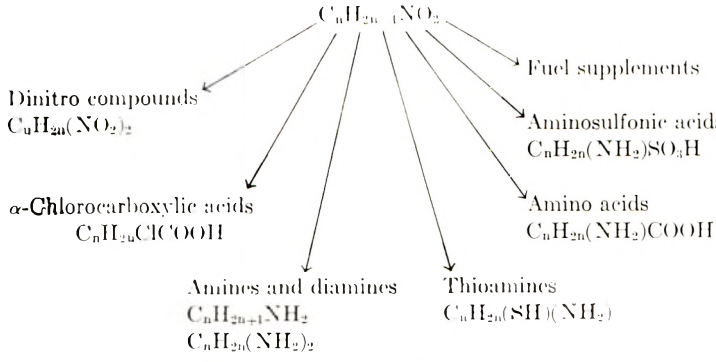

Fig. 1. Possible fields of application of nitroolefins.

merize easily in the presence of moisture and basic substances. Nitroethylene and nitropropylene are described in the literature,[4,5] as are dark, resinous substances easily soluble in acetone and benzene.

Very little appears in the literature concerning the polymerization of aliphatic nitroolefins.

No data appear in the literature concerning the polymerization of aliphatic aromatic nitroolefins and heterocyclic nitroolefins, but polymers of this type may be applicable in special uses (gunpowder, rockets, etc.).

In Table II we show the catalysts used to polymerize 1-nitropropylene, ω-nitrostyrene, and α-furyl nitroethylene.

For 1-nitropropylene: boron trifluoride, a saturated solution of sodium bicarbonate, and sodium methylate were used as catalysts; for ω-nitrostyrene BF_3, ammonium persulfate, and sodium methylate were used. No polymerization was observed in the presence of BF_3. The product of the polymerization of 1-nitropropylene in the presence of a solution of sodium bicarbonate was an amorphous powder melting at 115°C. Polymerization of ω-nitrostyrene is practically absent in the presence of benzoyl peroxide and pyridine.

The use of ammonium persulfate for the polymerization of α-furylnitroethylene leads to the production of an insoluble, amorphous, powdery polymer in 6–8% yield.

Polymerization of the nitroolefins in the presence of sodium methylate was investigated in more detail. High yields of the polymer of ω-nitrostyrene were obtained with this catalyst.[6] This monomer is of the type that polymerizes with difficulty, giving only dimers.

The following conditions were studied in the presence of the methylate: effect of temperature from −20 to +80°, amount of catalyst from 0.5 to 7%, reaction time from 30 min. to 12 hr. The optimum conditions for polymerization were found (see Table II).

The studies showed that the most important factor in the polymerization of nitroolefins is temperature; lowering the temperature increases yield and degree of polymerization. Dimers and trimers are produced along with high molecular weight products.

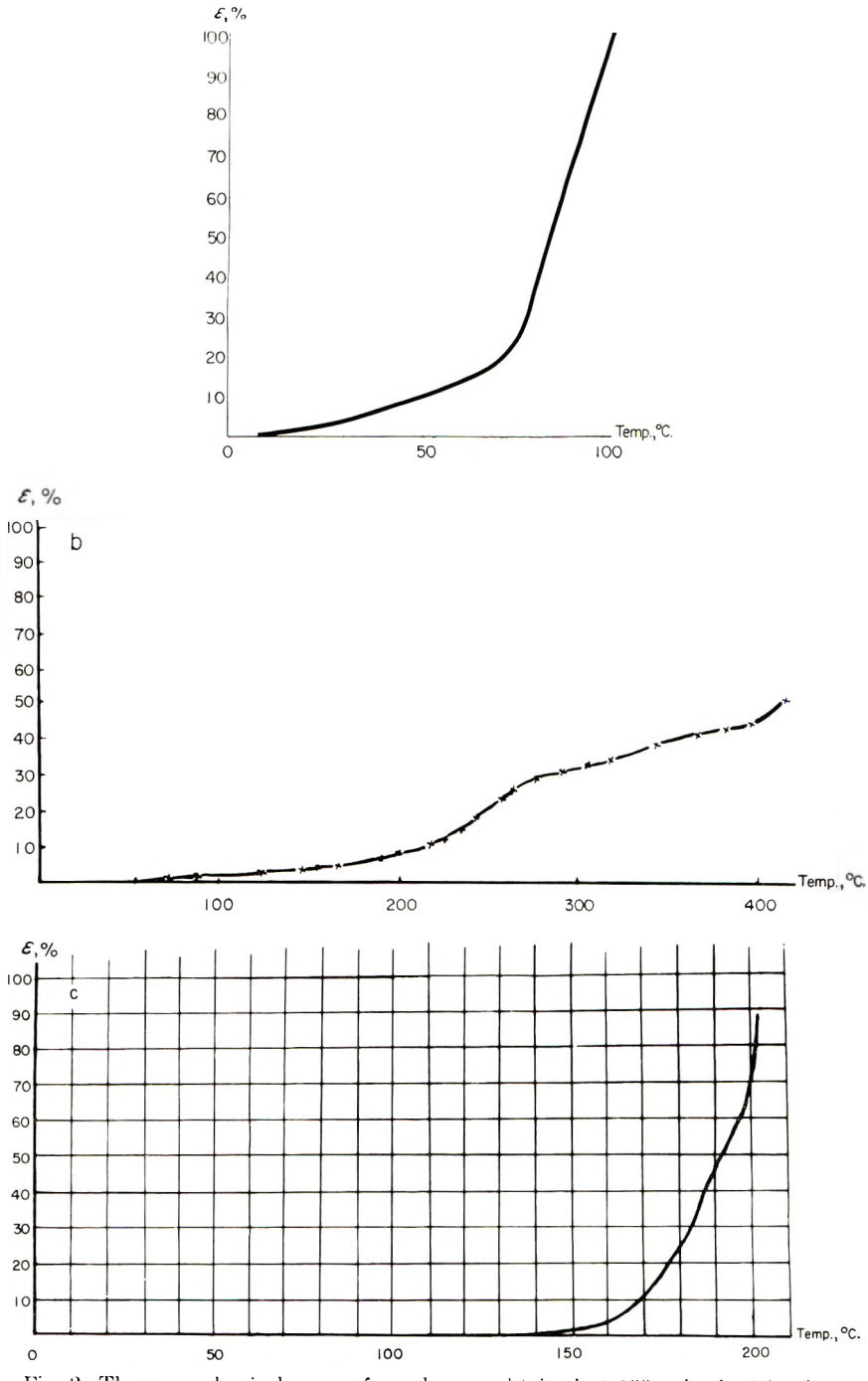

Fig. 2. Thermomechanical curves for polymers obtained at 100 g. load: (*a*) polymer of 1-nitropropylene; (*b*) polymer of ω-nitrostyrene; (*c*) polymer of α-furylnitroethylene.

High molecular weight, insoluble polymers were produced in good yield in the presence of sodium methylate. (Table II.) Thermomechanical curves were taken for the polymers with a force of 109 g. (Fig. 2). The softening points of the polymers are presented in Table III.

References

1. Buckley, G. D., and C. W. Scaife, *J. Am. Chem. Soc.*, **69,** 1471 (1947).
2. *Sintez organicheskikh.*
3. Chukervanik, I. P., and G. F. Iozeinia, *Doklady Akad. Nauk Uzbek. S.S.R.*, **8,** 26 (1951).
4. Noma, K., *Kobunshi Kagaku*, **5,** 29, 103 (1948).
5. Blomquist, Topp, and Johnson, *J. Am. Chem. Soc.*, **67,** 1879 (1948).
6. *Doklady Akad. Nauk S.S.S.R.*, **125** (1959).

Received May 1, 1961

JOURNAL OF POLYMER SCIENCE: PART A VOL. 1, PP. 605–623 (1963)

Electron Spin Resonance Study of Radiation Oxidation of Polymers. IIIA. Results for Polyethylene and Some General Remarks*

SHUN-ICHI OHNISHI, SHUN-ICHI SUGIMOTO, and ISAMU NITTA, *Osaka Laboratories, Japanese Association for Radiation Research on Polymers, Neyagawa City, Osaka, Japan*

In our previous papers,[3,4] Parts I and II of the present series dealing with electron spin resonance studies of irradiated polymers, we have reported ESR spectra of many polymers irradiated *in vacuo*. Free radicals produced by irradiation were identified for several polymers and some factors affecting ESR spectra were discussed in Part I.[3] In Part II,[4] the concentration of free radicals as well as free-radical formation curves were determined for some polymers, estimated G_R values also being tabulated. In the present investigations the effect of oxygen on the ESR spectra of various polymers has been examined. This may be of some significance to the study of radiation oxidation of high polymers. As for the effect of oxygen, several works have already been published which revealed formation of oxygenated radicals.[2,5–14] The ESR spectrum of the oxygenated radicals is known to be an asymmetric singlet in most cases.

On the other hand, the oxidation of high polymers induced by radiation (either ionizing radiation or ultraviolet radiation) or by heating has been investigated by several authors[15–21] by means of infrared spectroscopy, etc. more extensively than by the ESR study hitherto reported. Experimental results on model compounds have provided some generally accepted mechanisms for radiation-induced[22] or heat-induced[15] oxidation. We have studied the radiation oxidation of polymers by means of ESR spectroscopy mainly and also by infrared spectroscopy. The present paper contains the results for polyethylene with some general remarks as introduction. The following paper[1] will be concerned with similar studies for polypropylene and poly(vinyl chloride).

EXPERIMENTAL

Irradiations were carried out in vacuo with γ-rays from a Co^{60} source of 1,000 curies or with electrons accelerated by a 2 M.e.v. Van de Graaff

* This and the following work[1] make Part III of our series of papers on electron spin resonance studies of irradiated polymers. These works were presented in part at Conference on the Application of Large Radiation Sources in Industry, Warsaw, September 1959.[2]

accelerator. Irradiation doses were measured with Fricke dosimeter for γ-rays and by use of a calorimeter especially constructed for electron beams. After irradiation, air was introduced into the glass ampule containing the sample and subsequent oxidation was investigated by measuring changes in ESR and infrared spectra. In some experiments irradiation was carried out in the presence of air.

Marlex-50 inflation film having a thickness $\sim$30 μ was used. In some cases, thicker films, prepared by a piled-up sheet of thin films at some high temperatures, were used to observe the infrared carbonyl or unsaturation band more clearly.

ESR spectra were recorded at a room temperature or at low temperatures on a Varian V-4500 spectrometer with liquid-nitrogen and variable-temperature accessories. The operating frequency was about 9500 Mcycles/sec. The spectrometer can feed microwave power up to about 100 milliwatts to samples in the cavity. Hyperfine separations were determined by referring to the splitting value of the six lines of manganous chloride diluted in solid solution with cadmium chloride. The g factor was determined by measuring the operation frequency and by referring to the DPPH signal as a standard.

The Saturation Technique

Most free radicals trapped in polymers have relatively longer spin-lattice relaxation times (T_1), while the oxygenated radicals which are formed on introducing air to the radicals have smaller T_1's than the parent radicals.[23] Thus, ESR spectra of such free radicals can be recorded without saturation broadening at about 1–3 mw., while those of the oxygenated radicals can be represented without saturation even at maximum microwave power available ($\sim$100 mw.). Figure 1 shows a plot of the detected signal voltage V against the square root of the microwave power P for the oxygenated radical and for the parent radical trapped in irradiated polymer (polypropylene as a typical example), and it demonstrates clearly the differences in saturation behavior. Such differences in behavior can be made use of in differentiating the spectrum of the oxygenated radical from that of the parent one. If we run the spectrometer at a microwave power of, say 100 mw., V for oxygenated radicals is observed as magnified three times that of the parent one.

Figure 2 shows, for the case of irradiated polyethylene after introduction of air, changes with time of the ESR spectrum, recorded at a variety of power levels, illustrating usefulness of the discrimination technique by the saturation behavior. Series A, B, and C were recorded at power levels of $\sim$1, $\sim$50, and $\sim$80 mw., respectively. In series C at 80 mw. operation, we can clearly see the formation, at 3 min. after breaking of the vacuum, of a singlet peak of the oxygenated radical, having a higher g factor (2.014) than that of the parent one (2.0025). On the other hand, if we trace the change at 20 db. operation ($\sim$1 mw.), the formation of the singlet peak can only be recognized as a slight increase of the third peak of the spectrum

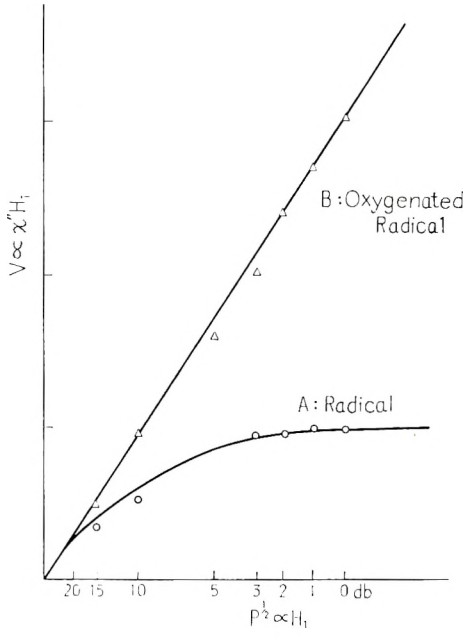

Fig. 1. Saturation effect of free radicals trapped in irradiated polypropylene for: (*A*) $-CH_2-\dot{C}(CH_3)-CH_2-$ (FR_{VIII}) and $-CH_2-\dot{C}(CH_3)_2$ (FR_{IX}); (*B*) for the oxygenated radicals produced on introduction of air to those radicals. Here V denotes the detected signal voltage; P is the microwave power to the cavity, 0 db. corresponding to approximately 100 mw; H_1 is the rotating magnetic field; χ'' is the magnetic susceptibility. The Sample was electron-irradiated with 1 Mrad.

of the parent radical (see the arrowed peak in Fig. 2, series A, curve 2). In short, to follow the behavior of the oxygenated radical, operation of the spectrometer at higher power levels will be more favorable.

RESULTS AND DISCUSSION

1. Change of ESR Spectrum of Irradiated Polymers after Introduction of Air

Before going into the study of polyethylene, some general aspects of behavior toward oxygen of the free radicals in various polymers will be discussed. The effect of air on ESR spectra has been examined for irradiated polyethylene (PE), polypropylene (PP), polytetrafluoroethylene (PTFE), poly(vinyl alcohol) (PVA), poly(ethylene glycol) (PEG), poly(vinyl chloride) (PVC), poly(methyl methacrylate) (PMMA), poly(ethylene terephthalate) (PET), nylon, and cellulose. Changes in the ESR spectra of these polymers irradiated *in vacuo* at a variety of doses produced by introducing air are shown in Figures 2, 4, and 7 for PE. From the observed differences in behavior toward oxygen of radicals trapped in polymers, the ESR study divides the polymers examined roughly into two groups: polymers which show the asymmetric singlet in the typical ESR

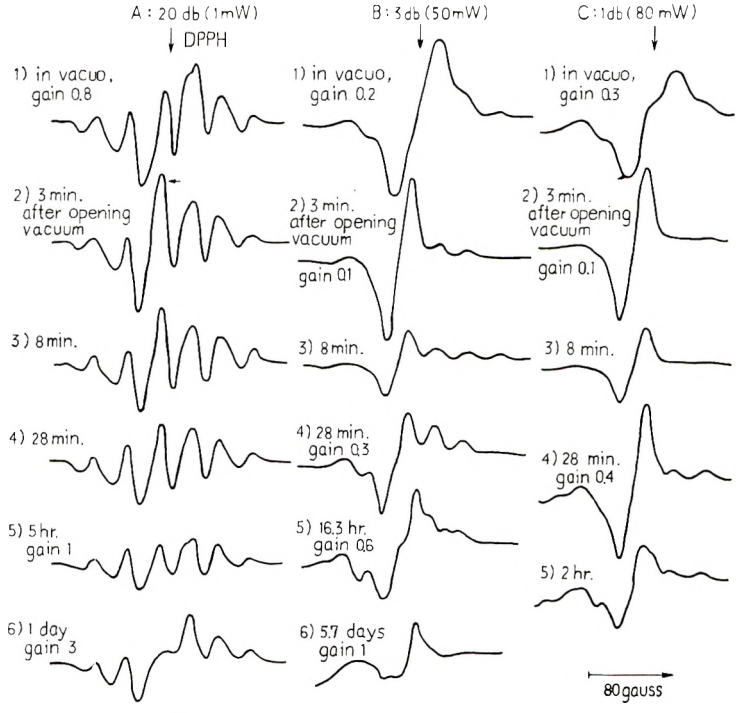

Fig. 2. Change of ESR spectrum after breaking of the vacuum to irradiated polyethylene. Series A was measured at a microwave power of ~1 mw, series B at ~50 mw., and series C at ~80 mw. The sample was electron-irradiated at —78°C., with 1 Mrad and then stored at room temperature for 2 hr.

spectrum of the oxygenated radical and those others which do not show such a singlet spectrum after introduction of air. To the first group belong PE,[2,6,13] PP,[7] PTFE,[5,7,8,10,12] PVC,[2,11,14] PMMA,[9] PET, and nylon; the second group includes the rest of the polymers mentioned above.

2. Identification of the Asymmetric Singlet Spectrum

The asymmetric singlet spectrum has been assigned to radicals of the type RO· or RO_2· because of the fact that g factor has a higher value than that of the parent radical.[2,5,6] The following experimental facts of the present investigations might be some additional support for the above assignment. (*1*) The spin-lattice relaxation time of the asymmetric singlet spectrum was found to be smaller than that of the parent radical. This is because of increased spin-orbit coupling in the RO· or RO_2· radical. (*2*) The asymmetric spectrum showed anisotropy, as shown in Figure 3. The sample used in the experiment was PE stretched yarn (cold-drawn to 20 times), irradiated *in vacuo* at —78°C. to a dose of 40 Mrad, and then exposed to air after one month storage at room temperatures. The spectrum was recorded at 50 min. after introduction of air as a function of the angle between the external field and the direction of stretching. The characteristic peak of the oxygenated radical varied as the angle changed.

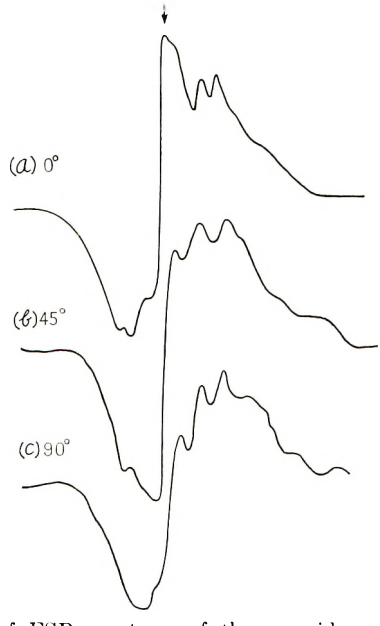

Fig. 3.—Anisotropy of ESR spectrum of the peroxide radical ($FR_{VII}O_2$) in polyethylene at various angles between the external field and the direction of stretching: (*a*) 0°; (*b*) 45°; (c) 90°.

This effect might be interpreted as arising from the spin density in the *p*-orbital of the oxygen atom of the RO· or RO_2· radical, the spin in the *p*-orbital possibly causing the *g* factor anisotropy.

According to the experimental results obtained on alkoxy radicals by Piette et al.,[24] the RO · radical would show hyperfine splitting of the order of 3 gauss. Although the splitting value may not be large enough for ESR spectra of solid polymer to be observed as resolved peaks, we would prefer RO_2 · of the two radical species.

PVA, cellulose, and PEG did not show the asymmetric spectrum. Kuri et al.[25] have attributed the reason for this to the presence of hydrogen bonds in the first two polymers. Although this could be a reason, of course, it may be suggested that as discussed later for the case of PE, the alkyl-type radical may not necessarily show the asymmetric spectrum.

3. Free Radicals Produced in Irradiated Polyethylene

Several kinds of radicals are generally produced in a polymer by irradiation *in vacuo*. It was shown in Part I,[3] however, that by irradiating under some suitable conditions one can obtain a sample in which a certain kind of radical is predominant. Short-living components predominate when polymers are lightly irradiated or irradiated at higher dose rates or at lower temperatures. For example, it is known that in the irradiated polyethylene there are produced at least three kinds of radicals of different lifetimes. The fast-decaying component (lifetime 1 day) gives the sextet

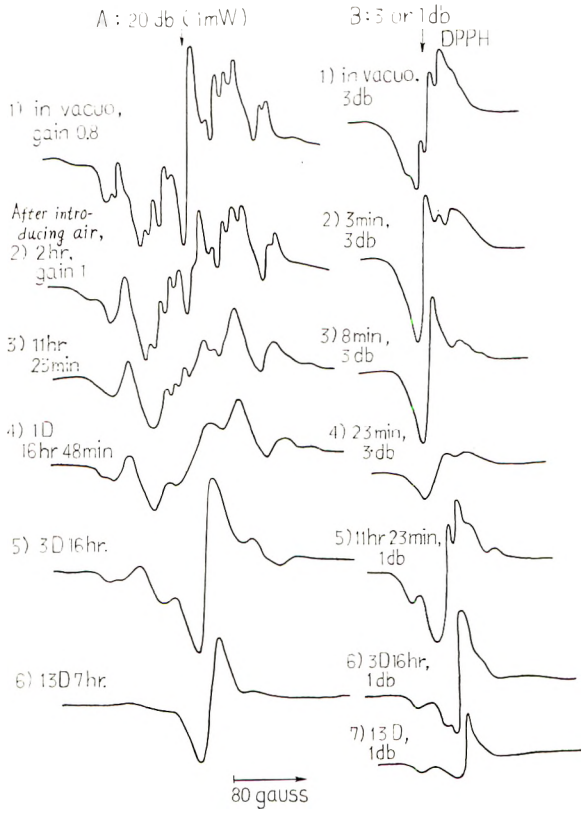

Fig. 4. Change of ESR spectrum after breaking of the vacuum of polyethylene electron irradiated at −196°C. with 60 Mrad and then stored at a room temperature for 2 days, showing reaction with oxygen of FR_{VII}(—$\dot{C}$H—CH=CH—). Series A was measured at 1 mw. and series B at 50 mw. or at 80 mw.

spectrum of the hyperfine splitting value 30 gauss. We refer to this radical as FR_{VI}. The FR_{VI} was assigned to the alkyl —CH_2—$\dot{C}$H—CH_2— radical by several authors.[3,26–28] The second component (lifetime several months) gives a spectrum of complex hyperfine structure, probably a septet spectrum of hyperfine separation 18 gauss, each peak having a doublet structure of 7 gauss splitting. And the spectrum, due to the radical denoted as FR_{VII} is possibly assigned to —CH_2—$\dot{C}$H—CH=CH—.[3,27,29] The last one, very stable at room temperature, gives singlet spectrum having ΔH_{msl} (line width at maximum slope) of about 25 gauss and was assigned to radicals of polyenyl type —CH_2—$\dot{C}$H—(—CH=CH—)$_n$—CH_2—.[30,31] We refer to this radical as FR_I. Thus when PE was irradiated lightly (dose $< \sim$1 Mrad) the main component of the radicals produced was FR_{VI} (—CH_2—$\dot{C}$H—CH_2—). In PE irradiated with intermediate doses (10–100 Mrad), FR_{VII} (—CH_2—$\dot{C}$H—CH=CH—CH_2—) was overwhelmingly predominant, while, with irradiation doses of up to 3000 Mrad, the spectrum was only the singlet which may be considered as due

to radicals of the type $-CH_2-\dot{C}H-(-CH=CH-)_n-CH_2-$ with varying n.

Since radicals of different kinds formed in the same polymer may behave differently on introduction of air we have examined the change in the spectra for the polymers which involved almost exclusively a specified radical as main component. Of the results obtained for PE, Figure 4 shows reaction of FR_{VII} with oxygen and Figure 7 shows reaction of the $-CH_2-\dot{C}H-(-CH=CH-)_n-CH_2-$ radicals, giving the singlet spectrum (ΔH_{msl} = 25.5 gauss). Figure 2 almost corresponds to the reaction with oxygen of FR_{VI}.

It should be added that it is sometimes difficult to identify the free radicals unequivocally from spectral shape, since there are some complicating factors. We have discussed the factors in Part I[3] to some extent and tried to identify the radicals. As for the above-mentioned identification of the radicals in PE, the interpretations of the sextet and the singlet spectra seem to be well established by several authors, while the identification of the second radical FR_{VII} seems to leave some questions. Voevodskiĭ et al.[27] first suggested that the spectrum should correspond to the $-CH_2-\dot{C}H-CH=CH-CH_2-$ radical, to judge from the smaller value of the hyperfine separation. We[3] have analyzed the spectrum based on the data of the spin densities on each carbon atom and showed the reasonableness of Voevodskiĭ's view. Recently, Lazurkin et al.[29] have published an interesting work on anisotropy of ESR spectrum of irradiated oriented polymers and confirmed the assignment. On the other hand, Lawton et al.[28] suggested a different view: that the spectrum mainly consisted of a five-line one, and it should correspond to a chain scission-type radical. However, their view does not seem to explain the smaller hyperfine splitting value (18 gauss, c.f. their value 20 gauss). It leaves some doubt in addition why the chain scission-type radical could survive until a temperature as high as its melting point (130°C.). Smaller and Matheson[26] irradiated many organic compounds at low temperatures and recorded ESR spectra. They could not detect the chain scission-type radical, and suggested, as one of the possible reasons, that such radicals could recombine instantaneously by the "cage" effect. Hence, and as we actually found septet spectra, we prefer the identification of the second radical (FR_{VII}) as $-CH_2-\dot{C}H-CH=CH-CH_2-$ at the present stage.

4. Reaction with Oxygen of FR_{VII}

The septet spectrum changes on introduction of air to the sample, as shown in Figure 4. The sample was irradiated *in vacuo* at −196°C. with a dose of 60 Mrad and then stored at a room temperature for 2 days. By this treatment the $-CH_2-\dot{C}H-CH_2-$ radical (FR_{VI}) coexisting at the irradiation almost decayed out and only the long-living FR_{VII} remained. Immediately after introduction of air, the peroxide singlet appeared in the region of high g factor (see Fig. 4, curve B2), but the concentration of the peroxide radical was small as observed in the spectrum (Fig. 4, curve A2)

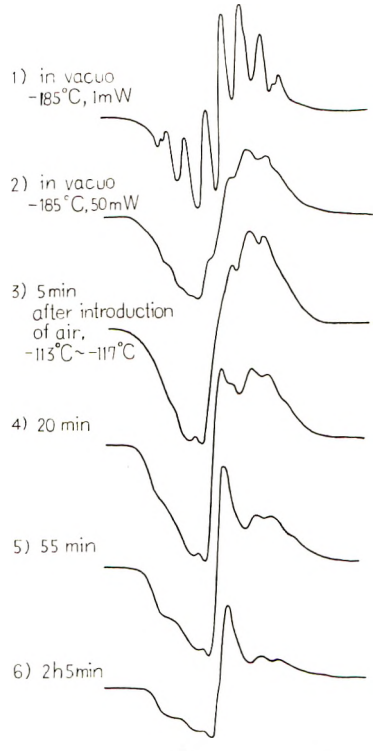

Fig. 5. Reaction with oxygen of FR_{VII} (—$\dot{C}$H—CH=CH—) in polyethylene at −113-−117°C. Spectra were recorded at 50 mw.

at the 20-db. operation. It is known from the decay curve at 3 db. operation that the peroxide radical, probably $FR_{VII}O_2$, decayed rather quickly (halflife about 20 min.). The decay curve at 20 db. operation shows that the total concentration of the free radicals, mainly FR_{VII}, decays faster after breaking vacuum than before (halflife 30 min.). After 11 hr. the ESR spectrum bore some different features (Figs. 4, curves A3 or A4). It might be interpreted as a superposition of the spectrum of FR_{VII} and that of some oxygenated radical other than the $FR_{VII}O_2$ mentioned above, its presence probably being shown at 1 db. operation (Fig. 4, curve B5). As time elapses, the septet spectrum decays, and after 13 days only a singlet spectrum remained (Fig. 4, curve A6). This might correspond to polyenyl radicals, since the singlet spectrum (ΔH_{msl} = 12 gauss) had a g factor very close to that for FR_{VII}.

Thus the ESR results might suggest that oxidation of FR_{VII} takes place in stages. Immediately after introduction of air, part of the FR_{VII} reacted to form the peroxide radical ($FR_{VII}O_2$), which decayed quickly to one half in 20 min. In the second stage (about 3–130 hr.), some oxygenated radicals of other type appeared. In the third stage (>130 hr.) FR_{VII} decayed almost entirely to form oxidation products, and polyenyl radicals of longer conjugations remained.

5. Oxygenation Temperature of FR_{VII}

In order to determine the oxygenation temperature air was introduced at −196°C. to a glass ampule containing sample in which only FR_{VII} was involved and then temperature of the sample in the cavity was gradually raised. When recorded at −185°C., the spectrum of the sample was as shown in Fig. 5, curve 1; it looked somewhat different from that recorded at a room temperature (cf. Fig. 4, curve A1). However, it is a well-known fact[28,32] that the same FR_{VII} gives the spectrum shown in Figure 5, curve 1, when recorded below about −30°C. and the spectrum of Figure 4, curve A1; above that temperature. When the temperature reaches about −113°C. the peroxide singlet begins to appear, as shown in Figure 5, curve 3, at 3 db. operation. After 2.1 hr. the oxidation proceeded so far as to give the ESR spectrum of Figure 5, curve 6. The sample was then evacuated again at −196°C. for 30 min., and evacuation was continued at a room temperature for 30 min. The ESR spectrum after evacuation was quite the same as that before introducing air (Fig. 5, curve 1), showing the reversible nature of such oxidation of FR_{VII}.

It might be somewhat remarkable that the oxidation began even as low as −113°C. The factor determining this temperature might be primarily mobility of the polymer chain in a certain mode, by which oxygen molecule can diffuse through polymer to the radical site, rather than the reactivity of each radicals, in view of the fact that radicals in different polymers had different reaction temperatures (cf. the following paper[1]). In this connection it should also be noted that the γ peak in the mechanical relaxation spectrum of PE lies near the above-mentioned temperature where, it is supposed, twisting of the main chain would begin to occur. Loy[13] has observed the build-up of the peroxide spectrum of PE at −80°C.

6. Reaction with Oxygen of FR_{VI}

It is difficult to prepare a sample in which only FR_{VI} is present. Irradiations with lower doses or at lower temperatures are more favorable.[3] Figure 2 shows result of an experiment in which the sample dipped in a Dry Ice–methanol mixture was irradiated *in vacuo* with electrons at a dose of 1 Mrad and then kept at a room temperature for 2 hr. before breaking of the vacuum. Another experiment (control), in which PE was irradiated under the same condition, evacuated again, and then kept for a long time without breaking of the vacuum, confirmed that before breaking the trapped radicals consisted of about 80% of FR_{VI} and about 20% of FR_{VII}.

On introduction of air to the sample the singlet spectrum of the peroxide radical appeared immediately (Fig. 2), and it decayed quickly (halflife about 10 min.). This is quite similar to the case of FR_{VII}. However, the behavior was remarkably different from that of the FR_{VII} case, in that the spectrum tended to pure sextet after introduction of air (see Fig. 2, curve A4 observed after 28 min.), while in this period the spectrum of the sample

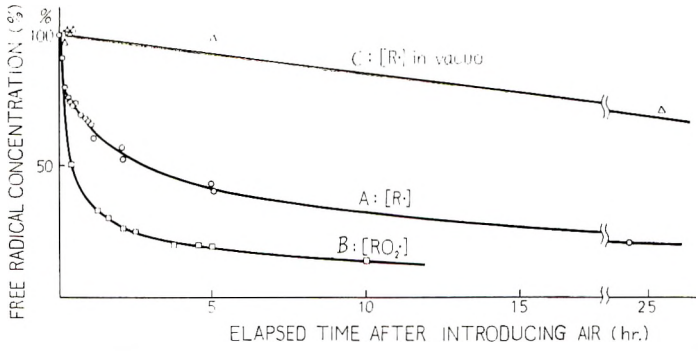

Fig. 6. Decay after breaking vacuum of the free radical in polyethylene electron-irradiated at —78°C. with 1 Mrad and then stored at a room temperature for 2 hr.; (*A*) measured at 1 mw., corresponds to decay of the free radical; (*B*) measured at 1 mw., corresponds to decay of the peroxide radical; (*C*) measured at 1 mw., shows decay of the free radical *in vacuo*.

kept in vacuum remained unchanged (sextet plus septet). Except for the remaining sextet, the change in the ESR spectrum can be interpreted as essentially the same as that due to FR_{VII}. Radical decay curves are shown in Figure 6, in which curve *A* almost corresponds to decay of the radicals, since the curve was plotted based on the data at 20 db. operation (Fig. 2, series A), while curve *B* almost corresponds to decay of the peroxide radical, since it was based on the data at 3 db. operation (Fig. 2, series B). Curve *C* is plotted according to the control experiment and shows free radical decay *in vacuo*. After breaking of the vacuum, the free radicals initially decayed quickly to a level of about 80% and thereafter decayed rather slowly (curve *A*), the decay being only slightly accelerated compared with that of the free radicals *in vacuo* (curve *C*). The peroxide radical decayed to one half in about 10 min. (curve *B*). Considering the decay data and also the behavior of free radicals after breaking of the vacuum, one might come to a conclusion that the oxidation process is due to FR_{VII} coexisting in the sample to an amount of about 20%. FR_{VII} decayed to a half in about 10 min. via $FR_{VII}O_2$, and as a result the spectrum observed at 28 min. after breaking of the vacuum tended to a pure sextet (FR_{VI}).

became negligibly small. The decay data for FR_I of PE are given in Figure 9 of the following paper,[1] together with data for PP and PVC. The ΔH_{msl} value of the singlet spectrum is larger, the shorter the conjugation length of polyenyl radical.[31] As a model compound showing such singlet

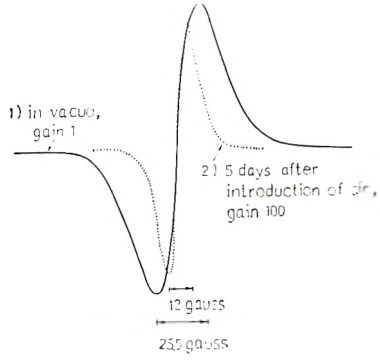

Fig. 7. Change of ESR spectrum after breaking of the vacuum for polyethylene irradiated with 4000 Mrad, showing reaction with oxygen of FR_I (polyenyl radicals). Power 1 mw.

spectrum we have chosen β-carotene, which has conjugated double bonds in the molecule. On irradiation *in vacuo*, β-carotene actually showed singlet spectrum of $\Delta H_{msl} = 17$ gauss, which might be attributable to a polyenyl radical of uniform length, probably an eleven-carbon conjugated system.[31] After introduction of air, the intensity of the singlet spectrum decayed quickly, while the peroxide singlet was not observed. This behavior is similar to that of the singlet of PE. However, unlike the case of PE, the ΔH_{msl} value remained unchanged. These results might be interpreted to show that polyenyl radicals react with oxygen, and the rate of reaction is larger, the shorter the conjugation. In irradiated PE, there are formed polyenyl radicals of various conjugation lengths, and after breaking of the vacuum oxygen attacks first the shorter polyenyl radicals, thus resulting in the decrease of ΔH_{msl} value due to quick decay of the radicals. After 40 hr. the radical concentration remained nearly constant with $\Delta H_{msl} = 12$ gauss. This result shows that polyenyl radicals of longer conjugations than that corresponding to $\Delta H_{msl} = 12$ gauss can react with oxygen only very slowly. It might be added in this connection that the singlet of $\Delta H_{msl} = 12$ gauss appeared in the course of oxidation of FR_{VII} (see Fig. 4, curve A6).

8. Oxidation Process Studied by Infrared Spectroscopy

In order to confirm the ESR results by other means, the same process of oxidation was followed by infrared spectra, i.e., the changes in the infrared spectra of polymers irradiated *in vacuo* were followed after introduction of air. Figure 8 shows the results for PE. In the experiment the sample, after having been irradiated at −196°C. *in vacuo* with a dose of 100 Mrad, was stored *in vacuo* at a room temperature for one week so that FR_{VI} produced at the irradiation decayed out and only the long-living FR_{VII} remained. The concentration of the remaining FR_{VII} was estimated to be 1.6×10^{-5} mole/g. This sample is referred to as sample I. The change of the infrared spectrum after introduction of air to sample I is given in

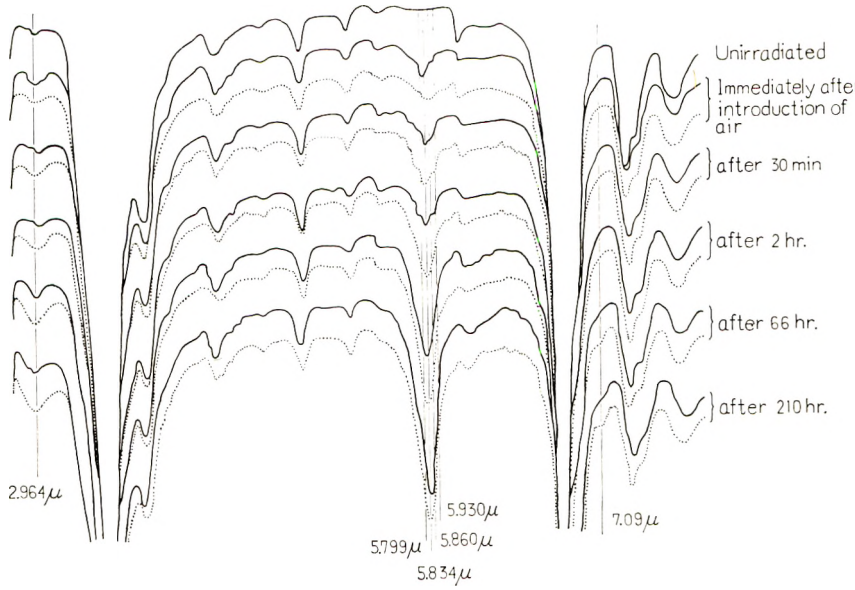

Fig. 8. Change of infrared spectrum after breaking of the vacuum for irradiated polyethylene: (··) sample II, electron-irradiated at −196°C. with 100 Mrad and then exposed to air immediately; (——) sample I, electron-irradiated under the same conditions as sample II and then stored at a room temperature for 1 week before breaking of the vacuum.

the solid curve of Figure 8. This will correspond to reaction of FR_{VII} with oxygen. In another experiment, to look for a reaction of the $-CH_2-\dot{C}H-CH_2-$ radical with oxygen, air was introduced to a PE sample at −196°C. immediately after irradiation under the same conditions as sample I. In fact, in this sample, referred to as sample II, the $-CH_2-\dot{C}H-CH_2-$ radical existed to an amount of 2.6×10^{-4} mole/g. before breaking of the vacuum, while FR_{VII} was involved to an amount nearly equal to or, exactly speaking, slightly more than that of sample I, 1.6×10^{-5} mole/g. The results for sample II are given in Figure 8 by the dotted curve.

On examining Figure 8 we found that subsequent oxidation produced carbonyl groups, mainly ketones (5.834 μ) and some aldehydes (5.799 μ), acids (5.860 μ), α,β-unsaturated ketones (5.961 μ), and a hydroxyl group, alcohols (2.964 μ). A slight increase in the 7.09 μ band, assigned to the methylenic rocking vibration of a ketone of the type $-(CH_2)_2C=O$ was also observed, showing that such ketone was actually involved. Another change was observed in 10.35 μ region (*trans*-vinylene band). A slight but definite decrease in intensity of the band was observed. Comparing the results for sample I with those for sample II we found that the infrared spectral changes in both samples are more or less similar to each other. The concentration of the carbonyl group of the ketones (5.834 μ) produced after breaking of the vacuum was calculated by taking the value of the

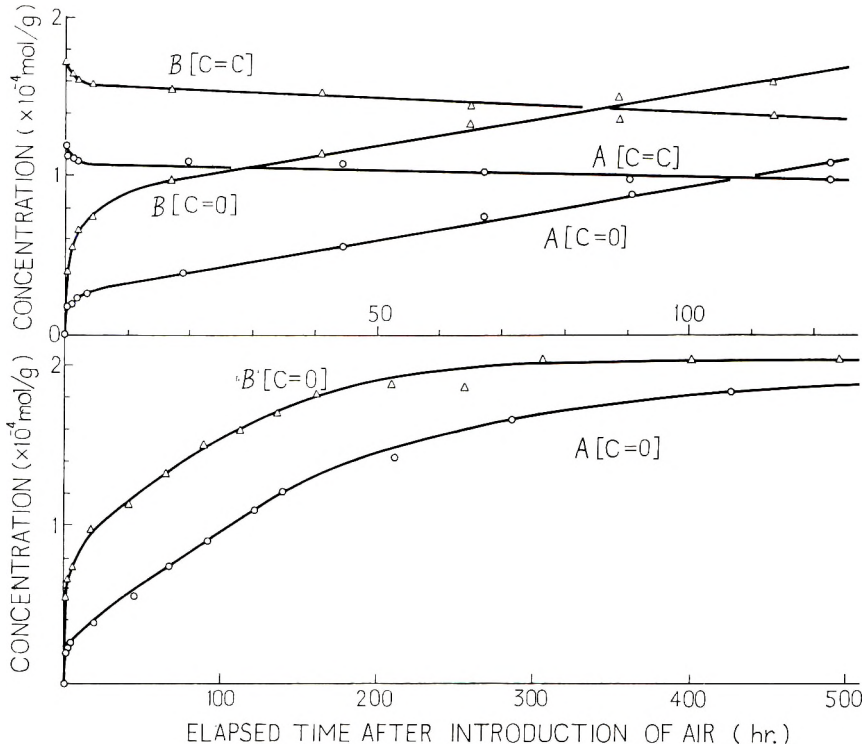

Fig. 9. Formation of the carbonyl group of the ketone (5.834 μ) and decay of the trans-vinylene group (10.35 μ) after introduction of air to irradiated polyethylene (cf. Fig. 8): (*A*) for sample I; (*B*) sample II.

molar extinction coefficient to be 188 mole/l. cm.[33] and was plotted in Figure 9 for both samples. On inspecting the figure it seems obvious that the carbonyl group is formed in nearly equal concentration in both samples (I and II). This might show a remarkable result that FR_{VI} involved in sample II in large concentration does not seem to contribute in a sensible manner to the carbonyl formation, while FR_{VII} does. This result is in accord with the ESR study (see Section 6).

The formation curve in Figure 9 seems to consist of three parts; the first rapidly increasing (<3 hr.), the next linearly increasing (3–130 hr.), and a gradually increasing section (>130 hr.) following the second. The curve finally reaches saturation. Comparing concentration of the ketonic group after 20 days (1.8×10^{-4} mole/g.) with the initial FR_{VII} concentration, we found about 12 carbonyl groups were eventually produced per FR_{VII}. The *trans*-vinylene group (10.35 μ) first decreased rapidly (<3 hr.), then in approximately a linear fashion with time (3–130 hr.), and in the final period more gradually (>130 hr.) (see Fig. 9). If we calculate the concentration by taking the molar extinction coefficient to be 139 mole/l. cm. as given by Hampton,[34] total decrease of the unsaturation group after 20 days was estimated as 2.2×10^{-5} mole/g. for sample I, a slightly

higher value than that of the initial FR_{VII} concentration (1.6×10^{-5} mole/g.). An equal concentration of the *trans*-vinylene group to that of the initial FR_{VII} decayed within 50 hr. It is interesting to note that the formation of the carbonyl group as a result of oxidation of FR_{VII}, the decrease of the *trans*-vinylene group, and also the ESR behavior of FR_{VII} after introduction of air (see Section 4), all proceed in three stages in the same manner. The fact might be additional evidence for the conclusion that the carbonyl group is produced mainly as a result of oxidation of FR_{VII}, FR_{VI} being almost inert.

The formation curves of the hydroxyl group were drawn for samples I and II. The relationship between samples I and II was quite similar to that in the case of carbonyl. The final concentration of the hydroxyl group was calculated as about $7\text{–}8 \times 10^{-5}$ mole/g. for sample I, and about 5 hydroxyl groups were produced per FR_{VII}.

On introduction of air to the PE sample showing singlet spectrum ($\Delta H_{msl} = 25.5$ gauss), the carbonyl and the hydroxyl groups were produced in nearly the same concentrations: 2.2×10^{-4} mole/g. and 3.5×10^{-4} mole/g. (after 40 days), respectively. Simultaneously the *trans*-vinylene band at 10.35 μ decreased. About 0.5 carbonyl groups were produced per polyenyl radical.

9. Comparison of the Carbonyl Formation by Post-Oxidation with in-Source Oxidation

When PE film (29 μ thick) was irradiated in the presence of air with a dose of 40 Mrad at a dose rate of 1.5×10^5 rad/hr., the produced carbonyl concentration was 5.5×10^{-4} mole/g., while post-oxidation of a PE film (29 μ thick) which was irradiated *in vacuo* with the same dose at dose rate of 1.7×10^5 rad/hr. and was exposed to air after irradiation produced eventually 9.5×10^{-5} mole/g. of the carbonyl group. Comparing the concentrations we found that the in-source oxidation produced more carbonyl groups (by a factor of about 6 times) than the post-oxidation. Similarly more hydroxyl groups were produced in the in-source oxidation. It was noted that the 7.09 μ band for $-(CH_2)_2C{=}O$ was observed clearly and intensely to an extent more than in the post-oxidation. The ESR spectrum observed in the sample irradiated in air to a dose of 40 Mrad looked like that observed at 13 hr. after introduction of air to another sample irradiated *in vacuo* with the same dose of 40 Mrad (cf. Fig. 4, curve A3).

10. Mechanism of Radiation Oxidation of Polyethylene

From experimental results of the present investigation a mechanism of radiation-oxidation of PE could be suggested as follows. Post-oxidation proceeds mainly via FR_{VII} ($-CH_2-\dot{C}H-CH{=}CH-CH_2-$), FR_{VI} ($-CH_2-\dot{C}H-CH_2-$) playing a minor role so that the decay was only somewhat accelerated in the presence of air. On introduction of air to FR_{VII} the first step is a diffusion-controlled process of oxygen to FR_{VII} trapped in the polymer [reaction scheme (1)]. Fr_{VII} is gradually con-

verted to $FR_{VII}O_2$, which reacts rather quickly to form hydroperoxide or peroxide [steps (2) or (2′)] ($FR_{VII}O_2$ decayed to a half in ~20 min.).

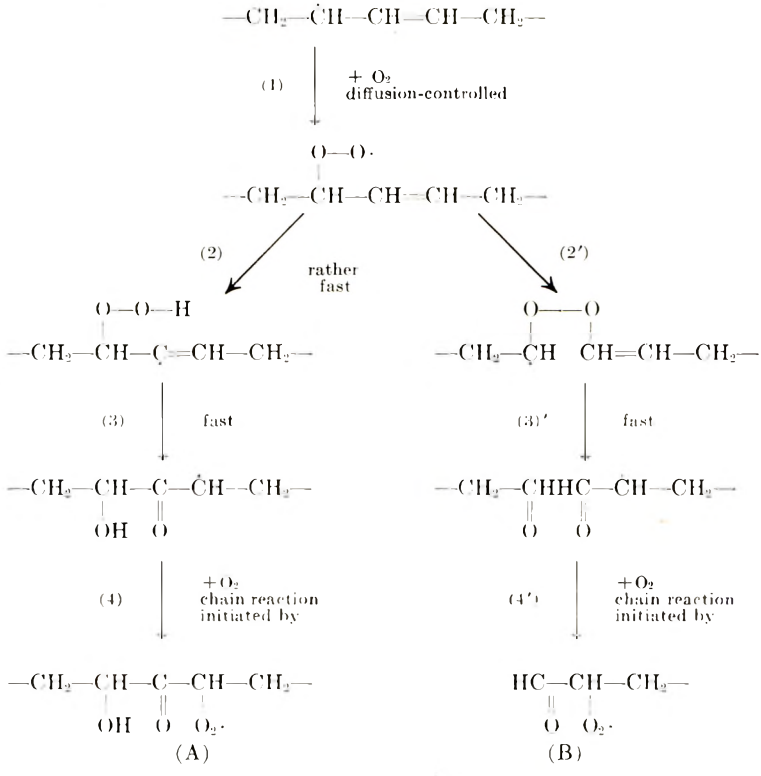

Fig. 10. The reaction scheme of —CH_2—$\dot{C}$H—CH=CH—CH_2— radical.

Of the possible reaction mechanisms to form hydroperoxide from $FR_{VII}O_2$ we would like to suggest, as shown in the reaction scheme (Fig. 10) that two mechanisms A and B, which assume an intramolecular feed-back mechanism of hydrogen to $FR_{VII}O_2$, are important. On the other hand, the currently prevailing reaction mechanism of peroxide radical $RO_2\cdot$[15,22] assumes implicitly an intermolecular reaction to form hydroperoxide from $RO_2\cdot$ and R′H; viz.

$$RO_2\cdot + R'H \rightarrow ROOH + R'\cdot$$

According to this intermolecular mechanism, hydroperoxide formation means a simultaneous formation of R′·, the —CH_2—$\dot{C}$H—CH_2— radical in our case. Our results suggested that the —CH_2—$\dot{C}$H—CH_2— radical plays only a minor role in the post-oxidation. Adopting the intermolecular mechanism, the chain reaction of oxidation should be interrupted and a —CH_2—CH—CH=CH—CH_2— radical would fail to produce overall 12 carbonyl groups. Also, the sextet spectrum should have been observed after introduction to air to FR_{VII}. These are the reasons why we do not prefer the intermolecular mechanism.

In our mechanism (Fig. 10), before the chain reaction starts, the scheme A produces a ketonic and a hydroxyl group in polymer chain, while the scheme B leads to oxidative chain scission accompanied by formation of aldehyde group. Both mechanisms result in disappearance of the double bond (*trans*-vinylene type) in FR_{VII}. These phenomena were in fact, observed experimentally. The concentration of the *trans*-vinylene group decreased by a factor equal to the concentration of FR_{VII} in the beginning stage of post-oxidation. The infrared hydroxyl band was observed at 2.96 μ, which might be attributable to an alcoholic hydroxyl group. The infrared aldehyde band (5.799 μ) is located so close to the ketonic band (5.834 μ) as to be resolved clearly by means of the NaCl prism. However, the oxidative chain scission seems to occur, in view of the well-known fact that the gelling dose is doubled and the formation of the *trans*-vinylene unsaturation is lowered to about one half if PE is irradiated in air.[20] The shape of the carbonyl band was quite similar to that of post-oxidized PE.

Of the two mechanisms suggested, we assume A is the major one. If only A occurs, the ketonic and the hydroxyl groups should be produced in the same way and in the same concentration. The formation curves of both groups were found to be quite similar in the beginning stage of post-oxidation, but the number of the carbonyl groups was found to be about 2.2 times that of the hydroxyl groups for both sample I (containing only FR_{VII}) and sample II (containing FR_{VI} and FR_{VII}). Since the concentration of the carbonyl group was estimated from the optical density at 5.834 μ (ketonic) by the base-line method, it would involve the concentration of aldehyde group to some extent. Therefore, the ratio of numbers of the ketonic to the hydroxyl groups could not be estimated exactly, although it must be smaller than 2.2. Step (3) in the scheme A might be imagined to proceed rather quickly, since the hydroperoxide band which should lie at 2.81 μ was not observed in the infrared spectrum.

Chain reactions of the oxidation [steps (4) and (4′)] initiated by the secondary radicals resulting from the beginning stage of oxidation might belong to the second stage of the post-oxidation, where peroxide radicals of other type than $FR_{VII}O_2$ appear (cf. three stages of post-oxidation as observed by ESR and infrared spectra). The chain length of the post oxidation (scheme A) might be about 5 as estimated from the hydroxyl concentration, a higher value compared with values of PP and PVC. In the third stage, ESR and infrared data might suggest that the oxidation of polyenyl radicals of longer conjugation proceeds at a very slow speed.

Lastly we mention the mechanism of in-source oxidation. ESR and infrared data seem to suggest that, as in post-oxidation, in-source oxidation proceeds mainly via the $-CH_2-\dot{C}H-CH=CH-CH_2-$ radical. Then the question arises why the in-source oxidation produced six times as many carbonyl groups as the number obtained in the post-oxidation. At the present stage we cannot tell the mechanism definitely, but some possibilities such as attack of O_2^- at the *trans*-vinylene group[35] might exist. In this connection we prefer Alexanders' conclusion[35] that irradiation in

the presence of air promotes the main-chain scission and thus the gelling dose doubles, to Charlesby's conclusion[20] that irradiation in air affects the crosslinking reaction itself. In fact, the ionizing radiation produces FR_{VI}'s located very closely to each other[28,36] and they may react with each other at a very fast rate without reacting with oxygen coming to the site at a diffusion-controlled rate. The formation of FR_{VI} clustering in spur might explain, in part, why most FR_{VI}'s failed to produce the carbonyl group in the course of oxidation (cf. section 8). The apparent inertness of most FR_{VI}'s in the radiation oxidation might be due, on the other hand, to the trapped site of the radicals where oxygen molecules cannot reach, owing to, for example, rigidness or perfectness of crystallites, in view of the fact that radicals produced in a single crystal of lower organic molecules were not affected in the presence of air.[37]

References

1. Ohnishi, S., S. Sugimoto, and I. Nitta, *J. Polymer Sci.*, **A2,** 625 (1963).
2. Ohnishi, S., M. Kashiwagi, Y. Ikeda, and I. Nitta, *Large Radiation Sources in Industry, Conference Proceedings, Warsaw, September 8–12,* **1959,** Vol. 1, International Atomic Energy Agency, Austria, 1960, p. 291.
3. Ohnishi, S., Y. Ikeda, M. Kashiwagi, and I. Nitta, *Polymer*, **2,** 119 (1961).
4. Ohnishi, S., Y. Ikeda, S. Sugimoto, and I. Nitta, to be published.
5. Ard, W. B., H. Shields, and W. Gordy, *J. Chem. Phys.*, **23,** 1727 (1955).
6. Abraham, R. J., and D. H. Whiffen, *Trans. Faraday Soc.*, **54,** 1291 (1958).
7. Ohnishi, S., M. Kashiwagi, Y. Ikeda, and I. Nitta, *Isotopes and Radiation*, **1,** 210 (1958).
8. Tsvetkov, Yu. D., N. N. Boubnov, M. A. Makoulskiĭ, Yu. S. Lazurskiĭ, and V. V. Volvodskiĭ, *Doklady Akad. Nauk. S.S.S.R.*, **122,** 1053 (1958).
9. Ohnishi, S., and I. Nitta, *J. Polymer Sci.*, **38,** 451 (1959).
10. Rexroad, H. N., and W. Gordy, *J. Chem. Phys.*, **20,** 399 (1959).
11. Kuri, Z., H. Ueda, and S. Shida, *J. Chem. Phys.*, **32,** 371 (1960).
12. Matsugashita, T., and K. Shinohara, *J. Chem. Phys.*, **32,** 954 (1960).
13. Loy, B. R., *J. Polymer Sci.*, **44,** 341 (1960).
14. Loy, B. R., *J. Phys. Chem.*, **65,** 58 (1961).
15. For the heat-induced and ultraviolet-induced oxidation, see, for example, N. Grassie, *Chemistry of High Polymer Degradation Processes*, Butterworths, London, 1956; also, J. P. Luongo, *J. Polymer Sci.*, **42,** 139 (1960).
16. Matsuo, H., and M. Dole, *J. Am. Chem. Soc.*, **63,** 837 (1959).
17. Schumacher, K., *Kolloid-Z.*, **157,** 16 (1958).
18. Lawton, E. J., J. S. Balwit, and R. S. Powell, *J. Polymer Sci.*, **32,** 257 (1958).
19. Lawton, E. J., R. S. Powell, and J. S. Balwit, *J. Polymer Sci.*, **32,** 277 (1958).
20. Black, R. M., and A. Charlesby, *Intern. J. Appl. Radiation and Isotopes*, **7,** 126 (1959).
21. Black, R. M., and A. Charlesby, *Intern. J. Appl. Radiation and Isotopes*, **7,** 134 (1959).
22. Bach, N. A., and V. V. Saraeva, *Zhur. Fiz. Khim.*, **32,** 209 (1958).
23. Nitta, I., S. Ohnishi, Y. Ikeda, and S. Sugimoto, *Ann. Repts. Japanese Assocn. Rad. Res. Polymers*, **2,** 215 (1960).
24. Piette, J. H., and W. C. Landgraf, *J. Chem. Phys.*, **32,** 1107 (1960).
25. Kuri, Z., Y. Fujiwara, H. Ueda, and S. Shida, *J. Chem. Phys.*, **33,** 1884 (1960).
26. Smaller, B., and M. S. Matheson, *J. Chem. Phys.*, **28,** 1169 (1958).
27. Koritskiĭ, A. T., Yu. N. Molin, V. N. Shamshev, N. Ya. Bouben, and V. V Voevodskiĭ, *Vysokomolekulyarnye Soedineniya*, **1, 1182** (1959).

28. Lawton, E. J., J. S. Balwit, and R. S. Powell, *J. Chem. Phys.*, **33**, 395 (1960).
29. Kiselev, A. G., M. A. Mokul'skiĭ, and Yu. S. Lazurkin, *Vysokomolekulyarnye Soedineniya*, **2**, 1678 (1960).
30. Lawton, E. J., J. S. Balwit, and R. S. Powell, *J. Chem. Phys.*, **33**, 405 (1960).
31. Ohnishi, S., Y. Ikeda, S. Sugimoto, and I. Nitta, *J. Polymer Sci.*, **47**, 503 (1960).
32. Nitta, I., Y. Ikeda, and S. Ohnishi, *Ann. Repts. Japanese Assocn. Rad. Res. Polymers*, **2**, 203 (1960).
33. Cross, L. H., R. B. Richards, and H. A. Willis, *Discussions Faraday Soc.*, **9**, 235 (1950).
34. Hampton, R. R., *Anal. Chem.*, **21**, 923 (1949).
35. Alexander, P., and D. Toms, *J. Polymer Sci.*, **22**, 343 (1956).
36. Ohnishi, S., *Bull. Chem. Soc. Japan*, **35**, 254 (1962).
37. For example, see the paper on irradiated glycine by D. K. Ghosh and D. H. Whiffen, *Molecular Physics*, **2**, 285 (1959).

Synopsis

The effect of oxygen on ESR spectra of various kinds of irradiated polymers has been examined by using a saturation technique developed in the present investigation. The radiation oxidation of some polymers has been studied by means of ESR as well as infrared spectroscopy. Results for polyethylene (PE) are given in this paper, with some general remarks as introduction. In PE three kinds of radicals are produced on irradiation: $-CH_2-\dot{C}H-CH_2-$ (FR_{VI}), $-\dot{C}H-CH=CH-$ (FR_{VII}), and $-\dot{C}H-(-CH=CH-)_n-CH_2-$ (FR_I). On introduction of air, FR_{VII} gave the asymmetric singlet of the peroxide radical which showed anisotropy. Reversible oxygenation of FR_{VII} took place even as low as $-113°C$. Radiation oxidation of PE proceeds mainly via FR_{VII}, which produced eventually about 12 carbonyl groups and about 5 hydroxyl groups in the course of post-oxidation, the *trans*-vinylene group decreasing by an amount nearly equal to the amount of initial FR_{VII}. FR_{VI} played only a minor role in the oxidation. An oxidation mechanism involving chain reaction has been proposed. It suggests an intramolecular free-back reaction of hydrogen to the peroxide radical of FR_{VII}. FR_I (polyenyl radicals of longer conjugations) is oxidized to form carbonyl and hydroxyl groups, although it does not give the spectrum of the peroxide radical. Polyenyl radicals of shorter conjugations reacted faster.

Résumé

On a étudié l'effet de l'oxygène sur les spectres ESR de diverses sortes de polymères irradiés à l'aide de la technique dite de saturation, développée dans le présent travail. On a étudié le processus d'oxydation par irradiation de certains polymères par spectroscopie ESR et IR. On donne, dans cette communication, les résultats relatifs au polyéthylène (PE), outre certaines remarques générales en introduction. Dans le PE, on produit trois sortes de radicaux par irradiation; $-CH_2-\dot{C}H-CH_2$ (FR_{VI}), $-\dot{C}H-$ $-CH=CH-$ (FR_{VII}), et $\dot{C}H-(-CH=CH-)_n-CH_2$ (FR_I). Par introduction d'air, FR_{VII} produit le singulet asymètrique du radical peroxyde, montrant de l'anisotropie. L'oxydation de FR_{VII} a lieu même à $-133°C$ de façon réversible. L'oxydation par irradiation du PE se produit principalement par l'intermédiaire de FR_{VII}, qui peut produire environ 12 groupes carbonyles, et environ 5 groupes hydroxyles durant la "post" oxydation, tandis que la teneur en groupe transvinylique décroît d'une quantité égale à la teneur initiale FR_{VII}. FR_{VI} joue uniquement un rôle secondaire dans l'oxydation. On propose un mécanisme d'oxydation suivant une réaction en chaîne. Ceci suppose une réaction intramoléculaire d'échange d'hydrogène sur le radical peroxydé de FR_{VII}. FR_I (radicaux polyényles de grandes conjugaisons) est oxydé en formant des groupes carboxyles et hydroxyles, bien qu'il ne donne pas le spectre du radical peroxydé. Les radicaux polyényles de faibles conjugaisons réagissent plus rapidement.

Zusammenfassung

Unter Benützung der in der vorliegenden Arbeit entwickelten "Sättigungs"-verfahren wurde der Einfluss von Sauerstoff auf die ESR-Spektren verschiedener Arten von bestrahlten Polymeren untersucht. Die strahlungsinduzierte Oxydation einiger Polymerer wurde mit ESR-und IR-Spektroskope untersucht. In der vorliegenden Mitteilung werden Ergebnisse an Polyäthylen (PE), nebst einigen allgemeinen Bemerkungen als Einleitung, angeführt. In Polyäthylen entstehen bei Bestrahlung drei Arten von Radikalen: $—CH_2—\dot{C}H—CH_2—$ (FR_{VI}), $—\dot{C}H—CH=CH—$ (FR_{VII}) und $—\dot{C}H—(—CH=CH—)_n—CH_2—$ (FR_I). Bei Luftzutritt lieferte FR_{VII} das asymmetrische Singlet des Peroxydradikals, welches Anisotropie zeigte. Reversible Oxydation von FR_{VII} fand sogar noch bei $-113°C$ statt. Die Strahlungsoxydation von PE verläuft hauptsächlich über FR_{VII}, das tatsächlich etwa 12 Carbonylgruppen und etwa 5 Hydroxylgruppen im Verlauf der "Nach"-oxydation erzeugt, wodurch die Anzahl der Transvinylengruppen um einen dem anfänglichen FR_{VII}-Gehalt fast gleichen Betrag abnahm. FR_{VI} spielte bei der Oxydation nur eine unbedeutende Rolle. Ein Oxydationsmechanismus unter Beteiligung von Kettenreaktionen wurde vorgeschlagen. Er nimmt eine intramolekulare Rückübertragung von Wasserstoff an das Peroxydradikal von FR_{VII} an. FR_I (Polyenylradikale mit längerer Konjugation) wird unter Bildung von Carbonyl- und Hydroxylgruppen oxydiert, obgleich es nicht das Spektrum des Peroxydradikals liefert. Polyenylradikale mit kürzerer Konjugation reagierten rascher.

Received June 14, 1961
Revised November 1, 1961

JOURNAL OF POLYMER SCIENCE: PART A VOL. 1, PP. 625–637 (1963)

Electron Spin Resonance Study of Radiation Oxidation of Polymers. IIIB. Polypropylene and Poly(Vinyl Chloride)*

SHUN-ICHI OHNISHI, SHUN-ICHI SUGIMOTO, and ISAMU NITTA, *Osaka Laboratories, Japanese Association for Radiation Research on Polymers, Neyagawa City, Osaka, Japan*

INTRODUCTION

As reported in the preceding paper,[1] ESR behavior toward oxygen of free radicals trapped in various polymers divides the polymers roughly into two groups, one showing an asymmetric singlet spectrum of peroxide radical on introduction of air and the other which does not. Radiation oxidation process of some polymers, i.e., polyethylene (PE), polypropylene (PP), and poly(vinyl chloride) (PVC), which belong to the first group has been studied in the present series of our investigations by means of ESR as well as infrared spectroscopy. Results for PE have been already given in the preceding paper with some general remarks and with discussion of the reaction mechanism. The present paper concerns with the results for PP and PVC.

Several works have already been published as for the effect of oxygen on ESR spectra of irradiated PP[3] and PVC.[4,5] Among them, Loy[5] has observed the rate of formation and decay of the peroxy radical in irradiated PVC and stated that the formation reaction was diffusion controlled. In the present investigations, the oxidation process has been studied for samples which involved a *specified radical* as the main component among the other various radicals produced on irradiation.

EXPERIMENTAL

Methods of irradiations and investigations are the same as described in the preceding paper.[1] Samples were irradiated *in vacuo* with γ-rays or with electron beams and air was introduced after irradiation. The subsequent oxidation process was investigated by measuring changes in ESR and infrared spectra. In some cases irradiation was carried out in presence of air. Materials used were Moplen A2 for PP, and a commercially available powder (Shin-etsu Chemicals, $DP = 1100$) for PVC. They were

* This and the preceding paper[1] make Part III of our series of papers on electron spin resonance studies of irradiated polymers. Part I has already been published[2] and Part II will be published soon.

prepared in thin films having a thickness of 20–35 μ, thicker films being used in some cases to observe infrared carbonyl or unsaturation bands more clearly. ESR spectra were recorded at a room temperature or at low temperatures on a Varian V-4,500 Spectrometer. The difference in saturation behavior of the peroxide radicals from their parent radicals was used to distinguish them on ESR observation.

RESULTS AND DISCUSSION

1. Free Radicals Produced in Irradiated PP and PVC

On irradiation of these polymers there are produced several kinds of radicals. Since radicals of different kinds may behave differently on introduction of air, we have examined changes of ESR and infrared spectra for the polymers which involved almost exclusively a specified radical as the main component. A method of obtaining such samples has been discussed in one[2] of our papers; it is based on the principle that irradiations with lower doses, or at lower temperatures, or at higher dose rates, are more favorable for observing the short-lived radicals. Although the assignment of the free radicals produced in PP and PVC is not yet well established, the following is our view[2] at the present stage.

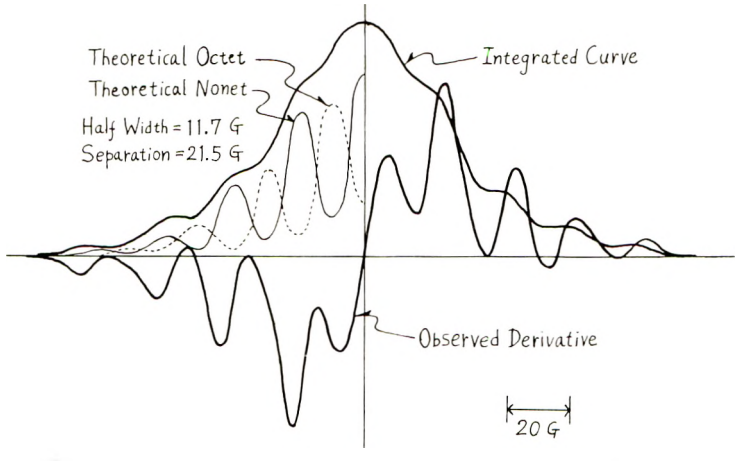

Fig. 1. ESR spectrum of the fast-decaying radicals in polypropylene and a tentative analysis of the spectrum. Irradiation at −196°C. with 3.4 Mrad with electron beam from a 2 M.e.v. Van de Graaff accelerator.

In irradiated PP are observed at least three different ESR spectra of different lifetimes.[2,6] The fast-decaying component could be interpreted as consisting of an octet and a nonet (see Fig. 1).[6] They are always observed as a pair on irradiation with low doses (<5 Mrad) or at low temperatures and have the same splitting value of 22 gauss. We refer to the radicals giving the octet and the nonet spectra as FR_{VIII} and FR_{IX}, respectively. The octet spectrum was assigned to the $-CH_2-\dot{C}(CH_3)-$

CH_2— radical[2] and the nonet tentatively to the —CH_2—$\dot{C}(CH_3)_2$ radical,[6] which might be imagined to appear as a result of the following secondary reaction of the primary —CH_2—$CH(CH_3)$—CH_2· radical:

$$—CH_2—CH(CH_3)—CH_2· \rightarrow —CH_2—\dot{C}(CH_3)_2$$

The second spectrum in irradiated PP, having relatively long lifetime at a room temperature, is a broad singlet having a line width at maximum slopes ΔH_{msl} = ~39 gauss (see Fig. 4, curve 1). An experiment on a stretched specimen showed that a certain hyperfine structure of smaller splitting was observed when the angle between the stretching direction and the applied field was 0°. The free radical giving the singlet spectrum, which is denoted as $FR_{I'}$ (the prime indicates the spectrum is apparently a broad singlet), consists of polyenyl radicals of shorter conjugations, i.e., —$\dot{C}(CH_3)$—(—CH=CH—)$_n$—CH_2—, where n is probably 1 or 2. The spectrum can be observed at irradiations with doses of 100 Mrad. The third one is also a singlet but has a narrower width, ΔH_{msl} = ~26 gauss. This is very stable and observable only on irradiation with high doses (~2000 Mrad). This component, denoted as FR_I, may be attributable to polyenyl radicals of longer conjugations as observed in irradiated PE.[2,10]

In irradiated PVC three spectra have been reported.[2,7,8] One of them is a sextet spectrum having a splitting value of 22 gauss which might be assigned to —CH_2—$\dot{C}H$—CH_2—.[7,8] This decays rather quickly, even at −78°C., so that it is difficult to keep the radical alive at room temperatures.[8] The second component, having a relatively long lifetime, is a singlet spectrum with a slight sign of hyperfine structure of smaller splitting value (see Fig. 7, curve 1). This radical (denoted as $FR_{I'}$) might be imagined to be polyenyl radicals with shorter conjugation lengths. A singlet spectrum of narrower width (ΔH_{msl} = 18 gauss) was observed in highly irradiated PVC. This shows that polyenyl radicals of longer conjugations, —CHCl—$\dot{C}$H—(—CH=CH—)$_n$—CHCl—, where n = ca. 11, are produced in PVC as in the cases of PE and PP.

2. Reaction with Oxygen of FR_{VIII} and FR_{IX} in PP

On introduction of air to the sample, the spectrum changed immediately to the typical asymmetric singlet of the peroxide radical (see Fig. 2). ESR measurements were made at a microwave power feeding to the cavity of 1 mw., so that the spectra in Figure 2 were recorded without a power. saturation effect for the parent radicals as well as for the peroxide onese Therefore, the result suggests that almost all FR_{VIII} and FR_{IX} were oxidized to form peroxide radicals immediately after introduction of air.

The free radical decay curve in Figure 3, which almost corresponds to that for the peroxide radical, shows that the halflife is nearly 2.5 hr.

On comparing the behavior toward oxygen of FR_{VIII} and FR_{IX} with that of the trapped radicals in PE,[1] some remarkable difference will be obvious. In PE, the alkyl-type radical FR_{VI} did not give such a peroxide spectrum,

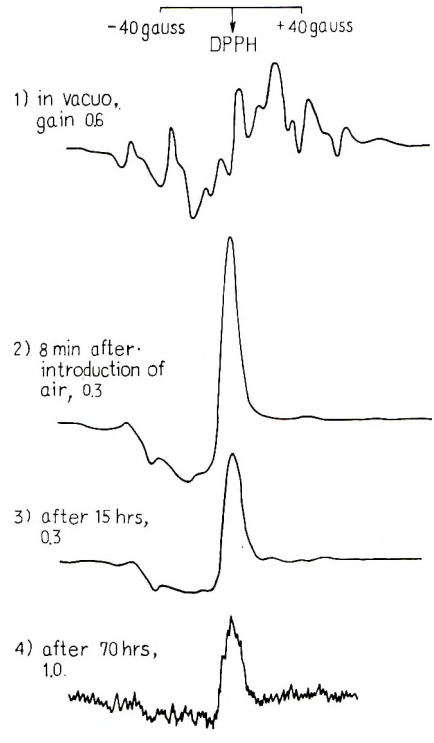

Fig. 2. Change in the ESR spectrum after breaking of the vacuum for polypropylene electron-irradiated at −78°C. with 1 Mrad, showing reaction with oxygen of $-CH_2-\dot{C}(CH_3)-CH_2-$ (FR_{VIII}) and $-CH_2-\dot{C}(CH_3)_2$ (FR_{IX}).

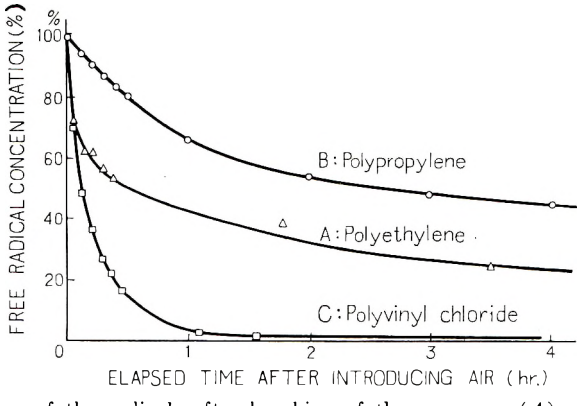

Fig. 3. Decay of the radicals after breaking of the vacuum: (*A*) polyethylene irradiated with 50 Mrad and stored at a room temperature for 3 days; (*B*) for polypropylene irradiated with 1 Mrad; (*C*) poly(vinyl chloride) irradiated with 2.9 Mrad. Power 1 mw.

which is almost inert to oxygen, while in PP the alkyl radicals did. In PE, the allyl-type radical FR_{VII} showed such a peroxide spectrum, but the peroxidation proceeded slowly. Immediately after introduction of air only a part of FR_{VII} was oxidized to form the peroxide radical (cf. Fig. 4,

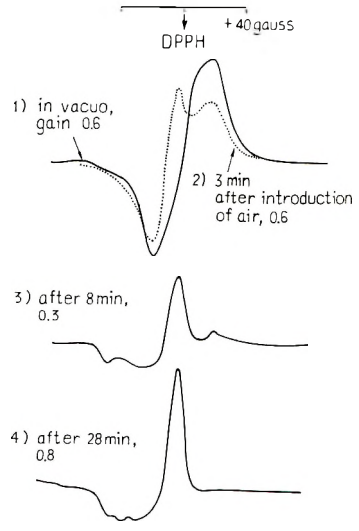

Fig. 4. Change in the ESR spectrum after breaking of the vacuum for polypropylene irradiated at −78°C. with 100 Mrad and then stored at a room temperature for 50 hr., showing reaction with oxygen of $FR_{I'}$ (polyenyl radicals with shorter conjugation lengths).

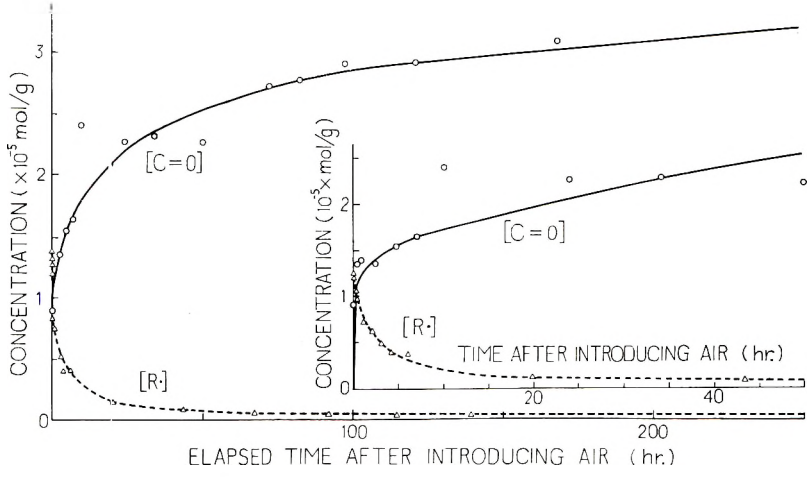

Fig. 5. Formation of the carbonyl group of the ketone (5.83 μ) and decay of the free radical ($FR_{I'}$) after introduction of air to polypropylene irradiated at −78°C. with 100 Mrad and then stored at a room temperature for 4 days (cf. Fig. 4).

curve A2 in the preceding paper[1]); on the other hand, in PP the alkyl radicals were oxidized immediately.

3. Reaction with Oxygen of $FR_{I'}$ in PP

In this case, the PP sample was electron-irradiated *in vacuo* at −78°C. with a dose of 100 Mrad and then stored at a room temperature for about 2 days. The sample gave only broad singlet spectrum (ΔH_{msl} = 39

gauss) as shown in Fig. 4, curve 1, FR_{VIII} and FR_{IX} produced at the irradiation having decayed out on storage at room temperatures. After introduction of air, $FR_{I'}$ gradually changed to the peroxide radical, the peroxidation being slower than the above case of FR_{VIII} and FR_{IX}. The spectrum of the parent radical, however, was not recognizable after 28 min. The decay curve, almost corresponding to that for the peroxide radical, is given in Figure 5.

The same process was followed by infrared spectroscopy with the use of a thicker film (about 61 μ). After introduction of air, some infrared bands, such as carbonyl (5.83 μ) and hydroxyl (2.96 μ) appeared (see Fig. 6A). Concentration of the carbonyl group of the ketone (5.83 μ) was calculated by taking the value[9] of the molar extinction coefficient to be 188 mole/l. cm. and was plotted in Figure 5 as a function of elapsed time after introduction of air. Most free radicals were oxidized rather quickly (within 10 hr. more or less) to form the carbonyl group via the peroxide radical. The formation curve of the carbonyl group gradually reaches saturation. Comparing the carbonyl concentration with the initial $FR_{I'}$ concentration, we can estimate that about 3.4 ketonic groups were eventually produced.

4. In-Source Oxidation of PP

The radiation oxidation of PP mentioned above was post-oxidation. In the in-source oxidation, irradiation was carried out in presence of air. Change with increasing dose in the infrared spectrum of a PP film (thickness 30 μ) is shown in Figure 6B for irradiation carried out in presence of air with γ-rays at a dose rate of 1.5×10^5 rad/hr. It is similar to the case of post-oxidation in that infrared bands of the carbonyl and the hydroxyl groups appeared. The ESR spectrum observed in the course of in-source oxidation was the asymmetric singlet. A comparison was made between the number of the ketonic groups produced by the in-source and post-oxidation processes on a specimen γ-irradiated with 54 Mrad at a dose rate of 1.5×10^5 rad/hr. It was found that the carbonyl groups produced by the in-source oxidation was about 9 times as large. The smaller number of carbonyl groups might be due to the situation that in the post-oxidation FR_{VIII} and FR_{IX} produced at the irradiation almost decayed out before introduction of air. It should be added that the shape of the infrared carbonyl band of PP had somewhat different features from that of PE or PVC; the absorption intensities of the bands at shorter wavelengths, e.g., at 5.660 μ (probably peresters[11]) being larger in the case of PP (cf. Fig. 6 and Fig. 8 in the preceding paper[1]).

5. Reaction with Oxygen of $FR_{I'}$ in PVC

The results of ESR and infrared studies on the post-oxidation of $FR_{I'}$ are shown in Figures 7 and 8. It can be seen from Figure 7 that the trapped radicals ($FR_{I'}$) reacted with oxygen immediately after introduction of air to form the peroxide radical. The oxidation products were the carbonyl group (5.78 μ) and the hydroxyl group (2.96 μ). Comparison of

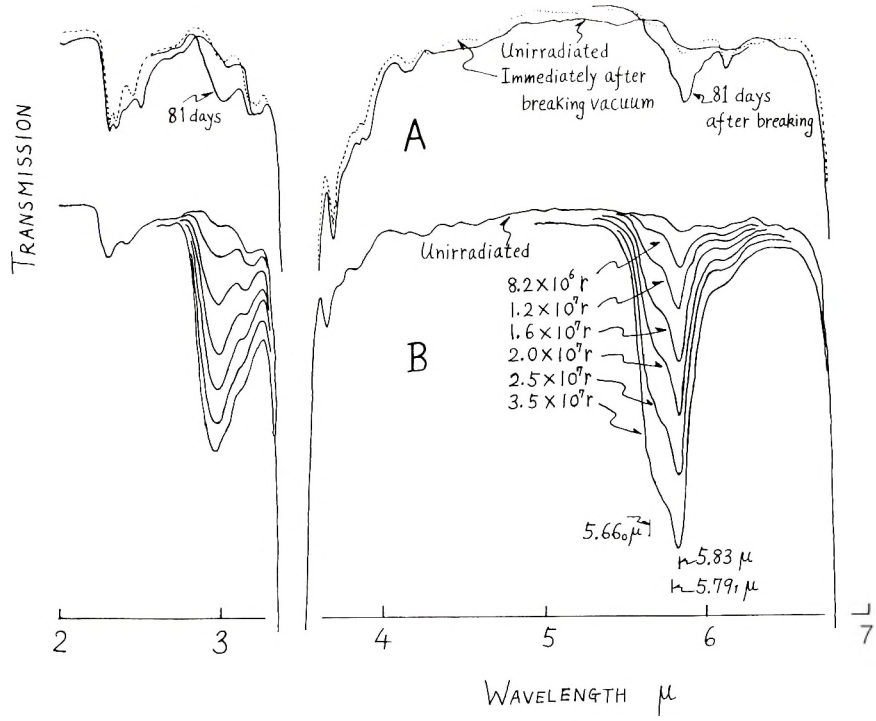

Fig. 6. Change in the infrared spectrum of irradiated polypropylene: (*A*) after breaking of the vacuum for a sample electron-irradiated at −78°C. with 100 Mrad and then stored at a room temperature for 2 days; (*B*) on irradiation in presence of air with γ-rays at a dose rate of 1.5×10^5 rad/hr.

the carbonyl concentration (see Fig. 8) with that of $FR_{I'}$ suggested that about 1.6 ketonic groups were eventually produced per $FR_{I'}$. In-source oxidation of PVC γ-irradiated with 30 Mrad at a dose rate of 4.8×10^4 rad/hr. produced about 10 times as many ketonic groups as the post-oxidation.

6. Oxygenation Temperature of the Free Radicals

Oxygenation temperatures of the radicals in PP and PVC were determined by the same technique as in the case of PE.[1] FR_{VIII} and FR_{IX} in PP began to react with oxygen to form the peroxide radicals at about −135°C. The oxygen molecule could no longer be removed from the peroxide radical by reevacuation. The temperature was −144°C. in the case of $FR_{I'}$ in PP. In this case, the oxygen molecule in the peroxide radical could be removed, so that ESR spectrum of the parent radical was restored after reevacuation. This is a similar reversible behavior to that seen in the case of PE. $FR_{I'}$ in PVC could start reacting with oxygen at the even lower temperature of −170°C. The oxygen molecule could be

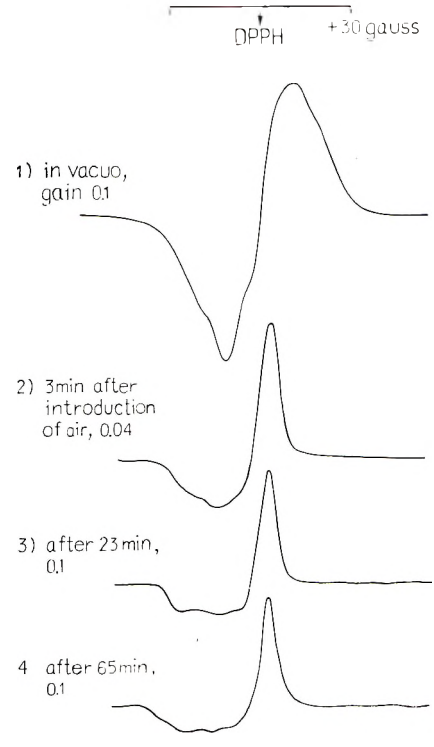

Fig. 7. Change in the ESR spectrum after breaking of the vacuum for poly(vinyl chloride) γ-irradiated with 2.9 Mrad, showing reaction with oxygen of $FR_{I'}$ (polyenyl radicals with shorter conjugation lengths). Power 1 mw.

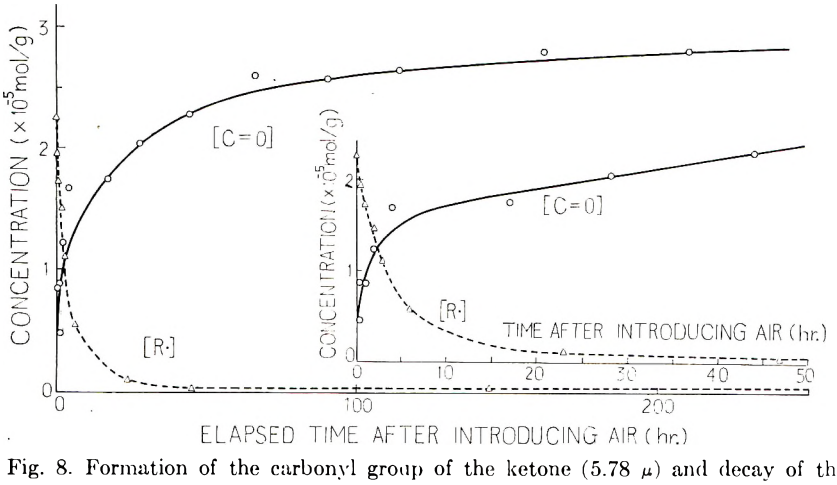

Fig. 8. Formation of the carbonyl group of the ketone (5.78 μ) and decay of the radicals ($FR_{I'}$) after introduction of air to poly(vinyl chloride) γ-irradiated with 45 Mrad.

Some features will be noted in the oxygenation and deoxygenation phenomena observed in PE, PP, and PVC. Oxygenation took place at low temperatures, and the oxygenation temperature was different among polymers. This fact might suggest that the primary factor determining such

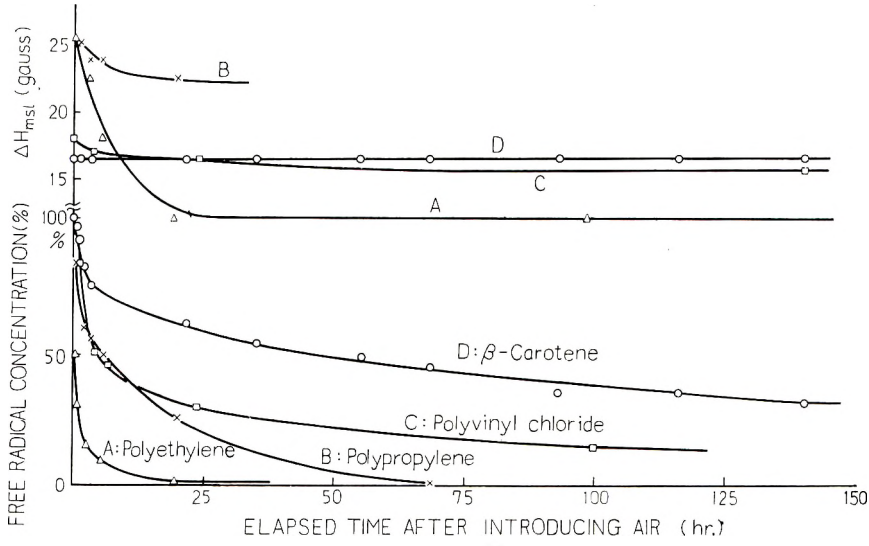

Fig. 9. Decay of the polyenyl radicals showing ESR singlet spectra and change of their ΔH_{msl} values after breaking of the vacuum: (*A*) polyethylene irradiated with 4000 Mrad; (*B*) polypropylene irradiated with 2300 Mrad; (*C*) for poly(vinyl chloride) irradiated with 500 Mrad; (*D*) for β-carotene irradiated with 50 Mrad.

temperature is mobility of polymer chain in a certain mode of vibration, by which oxygen molecule can diffuse to a radical site, rather than the reactivity of each radicals. Deoxygenation was possible for FR_{VII} in PE and $FR_{I'}$ in PP and PVC. These are the radicals in which unsaturation was involved, while, in the case of alkyl-type FR_{VIII} and FR_{IX} in PP, deoxygenation by recvacuation was impossible.

7. Reaction with Oxygen of Polyenyl Radicals

Highly irradiated PP (dose 2300 Mrad) and PVC (dose 500 Mrad) gave the singlet spectra of narrow widths, ΔH_{msl} was 25.5 gauss for PP and 18 gauss for PVC. As mentioned in the preceding paper,[1] PE irradiated with large doses (~4000 Mrad) gave the singlet spectrum of ΔH_{msl} = 25.5 gauss. Irradiated β-carotene also showed a similar singlet spectrum with ΔH_{msl} = 17 gauss. Probably these singlet spectra come from the same center,[10] i.e., polyenyl radicals of longer conjugations, —CH_2—$\dot{C}H$—(—CH=CH—)$_n$—CH_2—, although the number n and the distribution of n's may differ among polymers. On introduction of air the singlet spectra decayed rather quickly, although they are very stable *in vacuo*. Thereby the ΔH_{msl} values decreased, except for the case of β-carotene. Asymmetric singlet spectra of the peroxide radicals were not observed. These changes are shown in Figure 9, together with the results for PE and β-carotene which have already been discussed in the preceding paper.[1] As concluded there, these changes should be interpreted as showing that polyenyl radicals are oxidized rather quickly to form the carbonyl and the hydroxyl groups at the expense of the *trans*-vinylene group. The faster the oxidation proceeds, the shorter the conjugation, and, as a result, the ΔH_{msl} values

TABLE I
Reaction with Oxygen of Free Radicals as Studied by ESR

Polymer	Free radical[a]	Treatment of sample	Reaction with oxygen	Halflife[b]	Oxygenation temperature, °C.[c]	Number of carbonyl groups produced per radical
PE	FR_{VI} $[-CH_2-\dot{C}H-CH_2-]$	1 Mrad at −78°C.	Plays a minor role. The rate of decay becomes larger to some extent.			
	FR_{VII} $[-\dot{C}H-CH=CH-CH_2-]$	Irradiated at −196°C. with 30–60 Mrad, then stored at room temp. for 20 days	Formation of peroxide radical $FR_{VII}O_2$	30 min. (20 min.)	−113 (○)	12
	FR_I $[-\dot{C}H-(-CH=CH-)_n-CH_2-]$	4000 Mrad, ΔH_{msl} = 25.5 gauss	Reacts but does not show the asymmetric spectrum of peroxide radical, ΔH_{msl} decreasing.	21 min.		>0.5

PP	FR_{VIII}[—$\dot{C}(CH_3)$—CH_2—] FR_{IX}[—CH_2—$\dot{C}(CH_3)_2$]	1 Mrad	Rapid formation of peroxide radical	2.5 hr. (2.5 hr.)	−135 (×)	
	FR_I [Polyenyl radicals with shorter conjugation lengths]	100 Mrad at −78°C. and stored at room temp., for 2 days, ΔH_{msl} = 39.5 gauss	Rapid formation of peroxide radical	30 min. (2 hr.)	−144 (○)	3.4
	FR_I' [Polyenyl radicals with longer conjugation lengths]	2300 Mrad, ΔH_{msl} = 25.5 gauss	Same as FR_I of PE	5 hr.		
PVC	FR_I' [Polyenyl radicals with shorter conjugation lengths]	2.9 Mrad	Rapid formation of peroxide radical	8 min. (8 min.)	−170 (○)	1.6
	FR_I [—CHCl—$\dot{C}$H—(—CH=CH—)$_n$—CHCl—]	500 Mrad, ΔH_{msl} = 18 gauss	Same as FR_I of PE	5 hr.		
β-Carotene	$FR_{\bar{I}}$ [—$\dot{C}$H—(CH=CH—)$_{11}$—]	50 Mrad, ΔH_{msl} = 17 gauss	Reacts but does not show the asymmetric spectrum, ΔH_{msl} remaining constant.	45 hr.		

[a] Considering some uncertainties in assignment of free radicals, these are represented with an abbreviation such as FR_{VI} which indicates a free radical showing a sextet spectrum. Their possible identifications are shown in the bracket.

[b] Halflife of total concentration. Figures in parentheses are for the peroxide radicals.

[c] Where the asymmetric singlet of the peroxide radicals begins to appear; (○) denotes that oxygen molecule can be removed by evacuation from the peroxide radicals; (×) denotes that it cannot.

decrease. Polyenyl radicals of longer conjugations ($\Delta H_{msl} < 12$ gauss) can react with oxygen only very slowly. In the case of β-carotene, in which a polyenyl radical of uniform length[11] is supposed to be produced, the value remains constant. A comparison of ΔH_{msl} versus time curves in Figure 9 among polymers, suggests that the distribution of n in the polyenyl radicals $-CH_2-\dot{C}H-(-CH=CH)_n-CH_2-$ differs among them. Two extreme cases are PE and PVC. In PE, n seems to be distributed over wider range, while in PVC relatively over narrower range near 11. PP does not seem to have polyenyl radicals of longer conjugations ($\Delta H_{msl} <$ 22 gauss).

8. Summary

At the present stage we have only a few experimental results not sufficient to discuss further the mechanism of radiation oxidation of PP and PVC. The rate-determining step of the oxidation seems to be in the formation of hydroperoxide from peroxide radical, since, as shown in Figures 2 and 4 for PP and in Figure 7 for PVC, the ESR spectrum after introduction of air remained the asymmetric singlet of the peroxide radical. The chain reaction of the post-oxidation proceeded at a slow speed after about 20 hr. for $FR_{I'}$ in PP and PVC (see Figs. 5 and 8), and the chain length was found to be 3.4 for PP and 1.6 for PVC. Loy[5] has reported the chain length of PVC to be 1.5. In many respects the oxidation differs from that of FR_{VII} in PE.

The reactions with oxygen of various free radicals in PP and PVC are summarized in Table I together with the results for PE[1] for comparison.

References

1. Ohnishi, S., S. Sugimoto, and I. Nitta, *J. Polymer Sci.*, **A2**, 605 (1963).
2. Ohnishi, S., Y. Ikeda, M. Kashiwagi, and I. Nitta, *Polymer*, **2**, 119 (1961).
3. Ohnishi, S., M. Kashiwagi, Y. Ikeda, and I. Nitta, *Isotopes and Radiation*, **1**, 210 (1958).
4. Kuri, Z., H. Ueda, and S. Shida, *J. Chem. Phys.*, **32**, 371 (1960).
5. Loy, B. R., *J. Phys. Chem.*, **65**, 58 (1961).
6. Shioji, Y., S. Ohnishi, and I. Nitta, *Ann. Repts. Japanese Assocn. Rad. Res. Polymers*, **2**, 253 (1960).
7. Lawton, E. J., and J. S. Balwit, *J. Phys. Chem.*, **65**, 815 (1961).
8. Ohnishi, S., Y. Nakajima, and I. Nitta, *J. Appl. Polymer Sci.*, in press.
9. Cross, L. H., R. B. Richards, and H. A. Willis, *Discussions Faraday Soc.*, **9**, 235 (1950).
10. Ohnishi, S., Y. Ikeda, S. Sugimoto, and I. Nitta, *J. Polymer Sci.*, **47**, 503 (1960).
11. Luongo, J. P., *J. Polymer Sci.*, **42**, 139 (1960).

Synopsis

Results of ESR and infrared studies of radiation oxidation of polypropylene (PP) and poly(vinyl chloride) (PVC) are reported. The effect of oxygen on the free radicals, FR_{VIII} ($-CH_2-\dot{C}(CH_3)-CH_2-$) and FR_{IX} ($-CH_2-\dot{C}(CH_3)_2$), $FR_{I'}$ (polyenyl radicals with shorter conjugations), FR_I (polyenyl radicals with longer conjugations) in PP and $FR_{I'}$, FR_I in PVC was studied. On introduction of air, FR_{VIII} and FR_{IX} in PP and $FR_{I'}$ in PP and PVC showed the asymmetric singlet spectrum of the peroxide radical.

Oxygenation of the radicals began at low temperatures: −135°C. for FR_{VIII} and FR_{IX}, −144°C. for $FR_{I'}$ in PP, and −170°C. for $FR_{I'}$ in PVC. By reevacuation, the oxygen molecule could be removed from the peroxide radical of $FR_{I'}$ in PP and PVC, while deoxygenation was impossible from FR_{VIII} and FR_{IX}. Oxidation of the radicals in PP and PVC gave carbonyl and hydroxyl groups. The number of carbonyl groups produced per radical was estimated as 3.4 and 1.6 for $FR_{I'}$ in PP and PVC, respectively.

Résumé

On donne les résultats de l'étude par ESR et IR de la réaction d'oxydation sous irradiation du polypropylène (PP) et du chlorure de polyvinylle (PVC). On étudie l'effet de l'oxygène sur les radicaux libres FR_{VIII} (—CH_2—$\dot{C}$—(CH_3)—CH_2—) et FR_{IX} —(—CH_2—$\dot{C}$—(CH_3)$_2$), $FR_{I'}$ (radicaux polyényles avec faibles conjugaisons), FR_I (radicaux polyényles avec plus fortes conjugaisons) du PP et de radicaux FR_{I3} du PVC. Par introduction d'air, FR_{VIII} et FR_{IX} du PP, et $FR_{I'}$ du PP et du PVC montre le spectre du singulet asymétrique du radical peroxydique. L'oxydation des radicaux débute à faibles températures; −135°C pour FR_{VIII} et FR_{IX}, −144°C pour $FR_{I'}$ dans PP, et −170°C pour $FR_{I'}$ dans le PVC. En refaisant le vide on peut enlever une molécule d'oxygène du radical peroxydé de $FR_{I'}$ dans PP et PVC; cependant cette désoxygénation est impossible pour le radical peroxydé provenant de FR_{VIII} et de FR_{IX}. L'oxydation des radicaux du PP et du PVC produit des groupes carbonyles et hydroxyles. On estime le nombre de groupes carbonyles produit par le radical: 3.4 et 1.6 pour $FR_{I'}$ du PP et du PVC respectivement.

Zusammenfassung

Ergebnisse der ESR- und IR-Untersuchung der Strahlungsoxydation von Polypropylen (PP) und Poly(vinylchlorid) (PVC) werden mitgeteilt. Die Einwirkung von Sauerstoff auf die freien Radikale, FR_{VIII} (—CH_2—$\dot{C}$(CH_3)—CH_2—) und FR_{IX} (—CH_2—$\dot{C}$(CH_3)$_2$), $FR_{I'}$ (Polyenylradikale mit kürzerer Konjugation), FR_I (Polyenylradikale mit längerer Konjugation) in PP und $FR_{I'}$, FR_I in PVC wird untersucht. Bei Luftzutritt zeigt FR_{VIII} und FR_{IX} in PP, $FR_{I'}$ in PP und PVC das asymmetrische Singletspektrum des Peroxydradikals. Die Oxydation der Radikale setzte bei niedriger Temperatur ein; bei −135°C für FR_{VIII} und FR_{IX}, −144°C für $FR_{I'}$ in PP und bei −170°C für $FR_{I'}$ in PVC. Durch neuerliche Evakuierung konnte das Sauerstoffmolekül aus dem Peroxydradikal von $FR_{I'}$ in PP und PVC entfernt werden, während eine Sauerstoffabspaltung aus dem Peroxydradikal von FR_{VIII} und FR_{IX} unmöglich war. Oxydation der Radikale in PP und PVC lieferte Carbonyl- und Hydroxylgruppen. Die Anzahl der pro Radikal erzeugten Carbonylgruppen wurde für $FR_{I'}$ in PP zu 3,4 und in PVC zu 1,6 bestimmt.

Received June 14, 1961
Revised November 1, 1961

JOURNAL OF POLYMER SCIENCE: PART A VOL. 1, PP. 639–654 (1963)

Radiation-Induced Graft Polymerization of Styrene to Nylon

GEORGE ODIAN, MARJORIE SOBEL, ALBERT ROSSI, ROBERT KLEIN, and TERESE ACKER, *Radiation Applications Inc., Long Island City, New York*

It has previously been noted that the radiation-induced graft polymerization of styrene to nylon is a very inefficient reaction. Ballantine and co-workers[1] obtained a 10.5% graft of styrene to nylon with a gamma radiation dose of 31.1 Mrad. This paper deals with the enhancement of the yield of this particular graft polymerization reaction by the use of styrene-methanol solutions.

RESULTS AND DISCUSSION

Accelerative Effect of Methanol

It was observed in this laboratory that dilution of the styrene with methanol greatly accelerates the rate of graft polymerization of styrene to nylon. The results of the present investigation are shown in the rate curves in Figures 1–6. The initial grafting rates are shown in Table I and are plotted against the concentration of the methanol–styrene solution in Figure 7.

TABLE I
Effect of Methanol on the Graft Polymerization of Styrene to Nylon at 25°C. at a Dose Rate of 0.071 Mrad/hr.

Methanol in outside solution, vol.-%	Grafting rate, % graft/hr.
0	0.0
10	17.8
30	16.6
50	14.2
70	11.8
90	4.9

This large accelerative effect of methanol may be explained in terms of the extent of swelling of nylon by styrene–methanol as compared to that by undiluted styrene. The extent of swelling of nylon by the various monomer solutions as well as the concentrations of the solutions absorbed by the nylon were determined and are shown in Table II. These data indicate

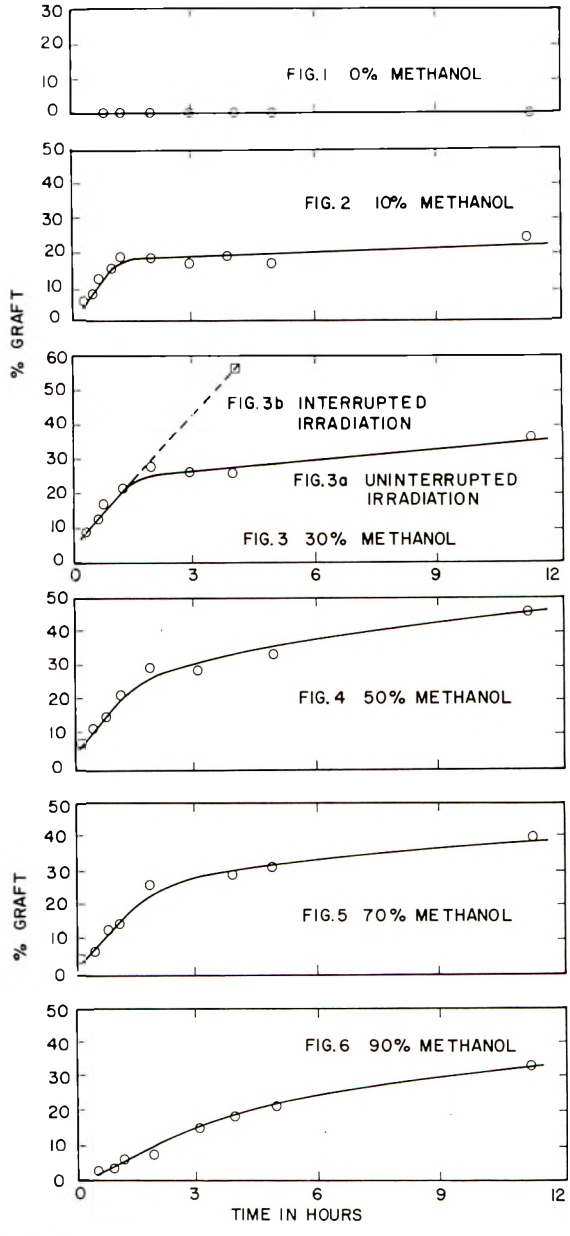

Figs. 1–6. Effect of methanol on the grafting of styrene to nylon. Dose rate = 0.071 Mrad/hr.

quite clearly that the concentration of styrene available for the grafting reaction is much greater when the styrene-methanol solutions are employed than when undiluted styrene is employed. This leads to an enhancement of the grafting rate since the latter is directly proportional to the monomer concentration.

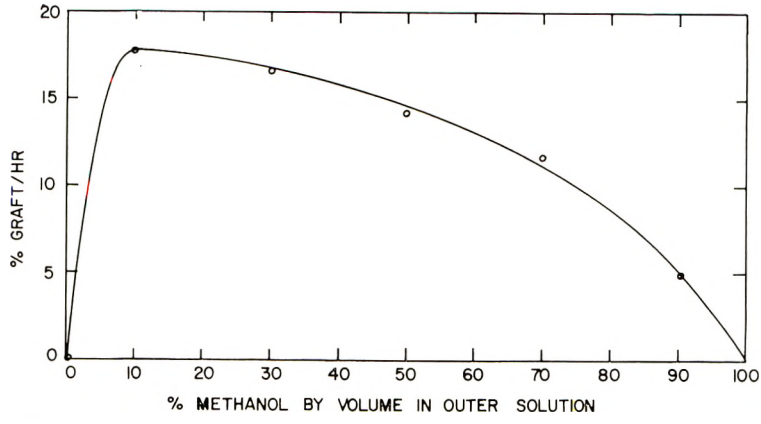

Fig. 7. Effect of methanol on the grafting of styrene to nylon. Dose rate = 0.071 Mrad/hr.

TABLE II
Swelling of Nylon by Styrene–Methanol

Methanol in outside solution, vol.-%	Swelling, %	Methanol in absorbed solution, vol.-%	[M]	$\rho_p \times 10^{-2}$, g./l.[a]	$\rho_s \times 10^{-2}$, g./l.[b]
0	0.2	0.0	0.05	10.6	
10	13.4	68.0	0.69	8.08	1.33
30	15.2	70.6	0.67	7.86	1.52
50	15.8	73.5	0.65	7.72	1.63
70	15.6	79.6	0.49	7.72	1.76
90	14.7	91.5	0.20	7.85	1.94

[a] Concentration of amorphous nylon in (amorphous nylon–methanol–styrene).
[b] Concentration of methanol in (amorphous nylon–methanol–styrene).

Effect of Diffusion

In considering Figures 2–6, one observes that the grafting rate decreases quite rapidly as the reaction proceeds. These results are not overly surprising and can be accounted for by a fast grafting rate coupled with a slow rate of diffusion of monomer into the nylon. That this is, indeed, the case was shown by taking grafted films (26.2% and 25.0% grafts, respectively) obtained via the use of the 30% methanol–70% styrene solution and 2 hr. of irradiation, re-equilibrating them with monomer solution and

TABLE III
Interrupted and Uninterrupted Irradiation in the Graft Polymerization of Styrene to Nylon

Irradiation	Grafting after 4 hr. of irradiation, %
Uninterrupted	26.2, 25.0
Interrupted	56.7, 52.4

then irradiating them for an additional 2 hr. These results are shown in Table III and Figure 3*b*. It is observed that with the same irradiation interval (4 hr.) the amount of graft polymer formed is approximately doubled when the grafting reaction is interrupted and the nylon re-equilibrated with the monomer solution.

Kinetics of Graft Polymerization

Let us consider the mechanism of this grafting process. Using a treatment similar to that in homogeneous homopolymerization[2] one may write, from a simplified kinetic scheme, the following series of equations for the various steps in the graft polymerization reaction

Initiation:

$$P \xrightarrow{r} P\cdot \tag{1}$$

$$P\cdot + M \xrightarrow{k_i} PM\cdot \tag{1a}$$

$$R_i = k_i[P\cdot][M] \tag{1b}$$

Propagation:

$$PM_n\cdot + M \xrightarrow{k_p} PM_{n+1}\cdot \tag{2}$$

$$R_p = k_p[PM_n\cdot][M] \tag{2a}$$

Termination:

$$PM_m\cdot + PM_n\cdot \xrightarrow{k_t} PM_{m+n} \text{ or } PM_m + PM_n \tag{3}$$

$$R_t = 2k_t[PM_n\cdot]^2 \tag{3a}$$

where P represents the nylon polymer chains, P· the nylon radicals, M the styrene monomer, $PM_n\cdot$, $PM_{n+1}\cdot$, $PM_m\cdot$ the graft copolymer radicals, k_p and k_t the rate constants for propagation and bimolecular termination, respectively.

For a long-chain process yielding high polymer, the rate of graft polymerization is given by eq. (2a). For the rate of change of concentration of graft copolymer radicals, one may write

$$d[\mathrm{PM}_n\cdot]/dt = k_i[\mathrm{P}\cdot][\mathrm{M}] - 2k_t[\mathrm{PM}_n\cdot]^2 \tag{4}$$

Introducing the conventional steady-state assumption that the rate of change of the concentration of $PM_n\cdot$ is small compared to its rates of formation and disappearance one obtains

$$[\mathrm{PM}_n\cdot] = (R_i/2k_t)^{1/2} \tag{5}$$

Combining eqs. (2a) and (5) one obtains for the rate of graft polymerization

$$R_p = k_p[\mathrm{M}]\,(R_i/2k_t)^{1/2} \tag{6}$$

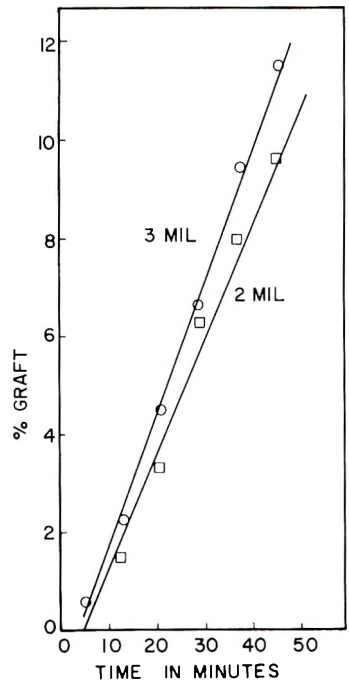

Fig. 8. Effect of film thickness on grafting rate with 50% styrene–50% methanol. Dose rate = 0.055 Mrad/hr.

It was experimentally found, for the 50% styrene–50% methanol solution, that the initial grafting rates were essentially the same for 2 and 3 mil nylon films when per cent graft was calculated as the grams of styrene grafted per gram of starting nylon × 100. These results are shown in Figure 8 and indicate that this grafting reaction is not diffusion-controlled in the initial stages of reaction, although, as was noted above, it is diffusion-controlled in the later stages. The results also indicate that the graft polymerization of styrene to nylon, employing styrene–methanol, is a volumetric reaction, i.e., it occurs homogeneously throughout the volume of the nylon. The various terms in eq. (6) are, therefore, defined in the following manner: R_p = moles of styrene graft polymerized per liter of (styrene–methanol–amorphous nylon) per second; [M] = moles of styrene monomer absorbed per liter of (styrene–methanol–amorphous nylon); R_i = moles of free radicals produced on amorphous nylon chains per liter of (styrene–methanol–amorphous nylon) per second. These definitions and the calculations of R_p, [M], and R_i (see Table IV) are based on the assumptions that (*1*) the swelling of nylon by the monomer solution, and consequently the grafting reaction, takes place only in the amorphous regions, and (*2*) the sum of the individual volumes of styrene, methanol, and amorphous nylon are additive without contraction or expansion of volume. The fact that the last is not a valid assumption in view of the positive interaction between nylon and methanol (see Table II) probably does not appreciably affect the relative validity of the various calculated terms.

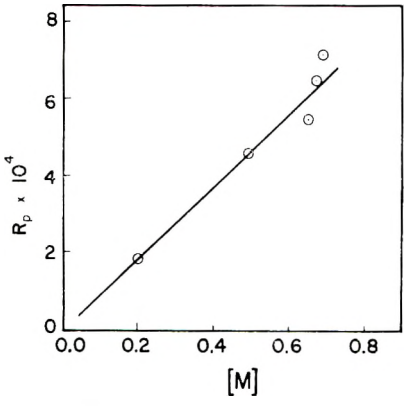

Fig. 9. Dependence of the grafting rate on the monomer concentration. Dose rate = 0.071 Mrad/hr.

Equation (6) is consistent with the results of the present investigation. Figure 9 shows the plot of the rate of graft polymerization, R_p, versus the monomer concentration. This verifies the dependence of R_p on the first power of the monomer concentration as required by eq. (6). Our data, however, covered only a $3^1/_2$-fold variation in styrene concentration. It was not possible to employ a wider range of styrene concentrations because of the positive interaction between nylon and methanol. Although the outside solutions were varied from 0 to 100% by volume of styrene, the concentration of the monomer solutions absorbed by the nylon varied only from 9 to 35% styrene.

The derivation of eq. (6) assumed that termination of the grafting reaction was bimolecular. Although this is the usual situation in homopolymerization, one might speculate that the mode of termination in the grafting reaction is monomolecular due to radical burial. These two modes of termination may easily be differentiated by a determination of the order of dependence of the graft polymerization rate on radiation intensity. Bimolecular termination results in a 0.5-order dependence of R_p on intensity as indicated in eq. (6), while monomolecular termination results in a first-power dependence. The results of a dose rate study of the 50% styrene–50% methanol–nylon grafting system are shown in Figures 10 and 11. As can be seen, a 0.5-order dependence by R_p on radiation intensity was found. This verifies the earlier assumption regarding bimolecular termination in the graft polymerization of styrene to nylon and the validity of eq. (6).

Determination of k_p^2/k_t

In order to further elucidate the mechanism of this grafting reaction, it was desirable to determine the k_p^2/k_t values for the various styrene–methanol–amorphous nylon systems. Rearranging and squaring eq. (6), one obtains

$$k_p^2/k_t = 2R_p^2/[\mathrm{M}]^2R_i \qquad (7)$$

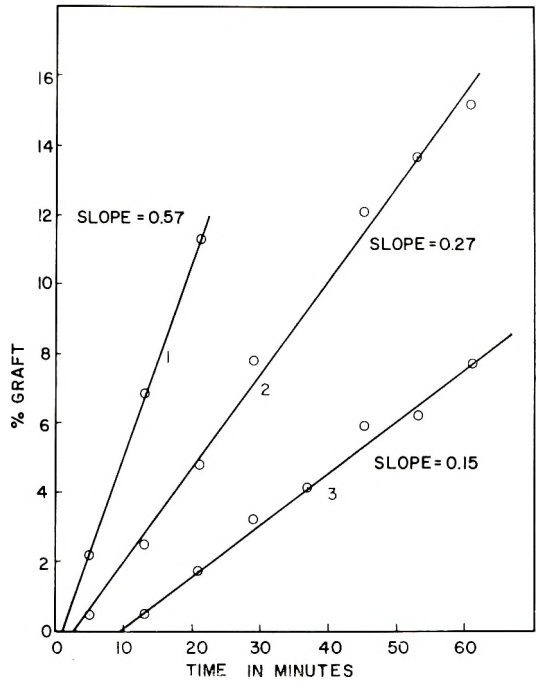

Fig. 10. Effect of radiation intensity on the rate of graft polymerization of styrene to nylon with 50% styrene–50% methanol at various dose rates: (*1*) 0.23 Mrad/hr.; (*2*) 0.054 Mrad/hr.; (*3*) 0.014 Mrad/hr.

The rate of initiation of the graft polymerization reaction, R_i, is given by the equation

$$R_i = G\phi\rho_p/(6.023 \times 10^{25}) \tag{8}$$

where G is the number of free radicals produced on amorphous nylon chains per 100 e.v. of radiation energy absorbed, ϕ is the radiation intensity in e.v. absorbed per gram of amorphous nylon per second, and ρ_p is the concentration of amorphous nylon in grams per liter of (styrene–methanol–amorphous nylon).

The rates of initiation for the various styrene–methanol–amorphous nylon systems were calculated from eq. (8) for a G value of 5.8 for amorphous nylon radical production.[3] These values were employed to determine the

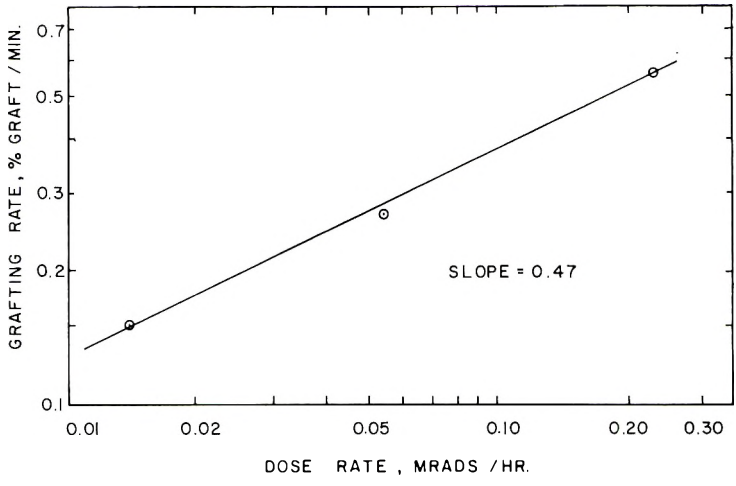

Fig. 11. Effect of radiation intensity on the rate of graft polymerization.

TABLE IV
Determination of Various Kinetic Terms in the Graft Polymerization of Styrene to Nylon

Methanol in outside solution, vol.-%	Methanol in absorbed solution, vol.-%	$R_p \times 10^4$	$R_i \times 10^8$	k_p^2/k_t
0	0	0.0	12.6	
10	68.0	7.2	9.6	22
30	70.6	6.5	9.3	19
50	73.5	5.5	9.2	16
70	79.6	4.6	9.2	19
90	91.5	1.9	9.3	20

Applicability of Steady-State Kinetics

The derivation above of eqs. (6) and (7) assumed steady-state conditions with regard to polymer radicals. This may not be a valid assumption in view of the greatly increased values of k_p^2/k_t. A cursory examination of the situation might lead one to postulate that the findings of various workers of the existence of long-lived radicals[7] produced via the irradiation of polyethylene and other polymers preclude any semblance of a steady-state situation in the grafting reaction. Under the experimental conditions employed in this investigation of mutual irradiation of polymer and monomer, one is concerned only with the lifetime of radicals formed in the amorphous regions of the nylon in the presence of monomer. The existing data on the life-time of radicals in irradiated polymers in the absence of monomers is not directly applicable to this situation.

Let us consider the kinetic equations which are applicable for the extreme case of nonsteady-state graft polymerization.

Integration of eq. (4) yields

$$\int_0^{[\mathrm{PM}_n\cdot]} d[\mathrm{PM}_n\cdot]/(R_i - 2k_t[\mathrm{PM}_n\cdot]^2) = \int_0^t dt \tag{9}$$

$$[\mathrm{PM}_n\cdot] = (R_i/2k_t)^{1/2}A \tag{10}$$

where

$$A = (e^{bt} - 1)/(e^{bt} + 1) \tag{11}$$

and

$$b = 2(2k_tR_i)^{1/2} \tag{12}$$

Combining eqs. (2a) and (10) one may obtain

$$R_p = k_p[\mathrm{M}](R_i/2k_t)^{1/2}A \tag{13}$$

and

$$k_p^2/k_t = 2R_p^2/[\mathrm{M}]^2R_iA^2 \tag{14}$$

It is apparent that eqs. (13) and (14) become essentially equivalent to eqs. (6) and (7), respectively, when A has a value close to unity. One may determine the error, if any, involved in the assumption of steady-state conditions and the use of eqs. (6) and (7) by determining the value of A under our experimental conditions. The proper evaluation of A is not possible, since the value of k_p in this graft polymerization reaction is not known. It is possible, however, to make various calculations based on certain assumed values of k_p.

If one assumes that the k_p value for the graft polymerization of styrene is the same as that for its homopolymerization[8] (k_p = 55 l./mole/sec.), A may be calculated to have a value of approximately 0.95 at t = 300 sec. and of 1.00 at t = 600 sec. Under these conditions one may employ eqs. (6) and (7) with negligible error for calculating values of k_p^2/k_t if one employed only data after t = 300 sec.

However, it would seem unlikely that k_p remains unchanged in view of the very large change in k_p^2/k_t. If k_p in the grafting reaction has decreased to one-tenth of its value in homopolymerization, then A will have a value of 0.32 at t = 600 sec., while if k_p has decreased to one-hundredth of its value, A will have a value of only 0.035 at t = 600 sec. Under these conditions, especially the latter, appreciable errors would ensue in the use of eqs. (6) and (7) due to inapplicability of the steady-state assumption.

In summary, one may state quite conclusively that the k_p^2/k_t values in the various grafting systems studied are increased by orders of magnitude relative to the value in homopolymerization. Only qualitative significance should be ascribed to these values. Their validation as quantitative values awaits an actual determination of k_p for these grafting systems. One last point that is apparent is that even if k_p = 55 (i.e., k_p is unchanged in grafting compared to homopolymerization), the time after the start of irradiation needed to attain or approach to within 95% of the steady-state situation is much longer than is required in the corresponding homopolymerization of styrene.

Competing Reactions

The kinetic scheme employed to derive eq. (6) and also eq. (13) is a simple one, as mentioned earlier, and does not take onto account any of the following possible reactions:

$$S \xrightarrow{\gamma} S\cdot \tag{14}$$

$$S\cdot + P \rightarrow P\cdot + S \tag{15}$$

$$S\cdot + M \rightarrow \text{Homopolymerization} \tag{16}$$

$$P\cdot + S \rightarrow S\cdot + P \tag{17}$$

$$P\cdot + M \rightarrow M\cdot + P \tag{18}$$

$$PM_n\cdot + S \rightarrow S\cdot + PM_n \tag{19}$$

$$PM_n\cdot + M \rightarrow M\cdot + PM_n \tag{20}$$

$$M_m\cdot + P \rightarrow P\cdot + M_m \tag{21}$$

$$PM_n\cdot + S\cdot \rightarrow \text{Termination} \tag{22}$$

$$PM_n\cdot + M_m\cdot \rightarrow \text{Termination} \tag{23}$$

where S represents the solvent (methanol), M the monomer (styrene), S· the solvent radicals, M· the monomer radicals, and M_m· the styrene homopolymer radicals.

The extent to which chain transfer reactions (17)–(21) occur may be ascertained by a consideration of the pertinent chain transfer constants. Primary alcohols are poor chain transfer agents. The transfer constant of *n*-butanol, for example, at 60°C., is 6×10^{-6} toward styryl radicals[9] and 2.5×10^{-5} toward methyl methacrylate radicals.[10] Thus, chain transfer from polyamide and graft copolymer radicals to methanol, reactions (17) and (19), would not be expected to be important. Chain transfer from polyamide and graft copolymer radicals to styrene monomer, reactions (18) and (20), would also be expected to be nil based on the reported value[11] of 6×10^{-5} for the self-transfer constant of styrene at 60°C. Chain transfer constants for amides are not available. However, those for comparable compounds,[9] such as propionic acid ($C = 5 \times 10^{-6}$) and diethyl malonate ($C = 4.7 \times 10^{-5}$) indicate that chain transfer from styrene homopolymer radicals to polyamide chains, reaction (21), is probably not occurring to any appreciable extent.

At first glance it might appear that the contribution of reaction (15), the formation of polyamide radicals by attack of solvent radicals on the nylon chains, would be quite high, since the G value for methanol[12] is 14.9 while that for nylon is 5.8. However, the concentration of amorphous nylon, ρ_p, in grams per liter of (amorphous nylon–methanol–styrene) is 4.2- to 6.2-fold greater than the concentration of methanol, ρ_s, in grams per liter of (amorphous nylon–methanol–styrene) (see Table II). Using

eq. (8), one calculates that the rate of initiation of graft polymerization, R_i, is 1.7- to 2.4-fold greater than the rate of initiation of homopolymerization, $R_{i,h}$. This difference in the rates of radical formation in combination with the competition of styrene monomer for the solvent radicals, reaction (16), should make the overall contribution of reaction (15) to the grafting process relatively small.

In our simplified kinetic scheme, bimolecular termination was assumed to be exclusively between graft polymer radicals, i.e., reaction (3). Other possible modes of bimolecular termination are those of graft polymer radicals with solvent radicals, reaction (22), or with homopolymer radicals, reaction (23). Termination via reaction (22) was deemed relatively unimportant due to the same reasons advanced for the unimportance of reaction (15).

Although termination via reaction (23) is probably quite important, it was ignored in our calculations because it would not alter qualitatively the values of the various calculated terms. That this is the case may be seen by deriving the kinetic equations for bimolecular termination via reaction (23). Assuming steady-state conditions one may obtain eq. (24) in a manner analogous to that employed to obtain eq. (5):

$$R_i = 2k_t[\mathrm{PM}_n\cdot]^2 + 2k_{t,c}[\mathrm{PM}_n\cdot][\mathrm{M}_m\cdot] \tag{24}$$

where $k_{t,c}$ is the rate constant for cross termination between "inside" homopolymer and graft polymer radicals via reaction (23).

Similarly, one may obtain the eq. (25) for the "inside" homopolymerization process (i.e., the homopolymerization which takes place inside the base polymer)

$$R_{i,h} = 2k_{t,h}[\mathrm{M}_m\cdot]^2 + 2k_{t,c}[\mathrm{PM}_n\cdot][\mathrm{M}_m\cdot] \tag{25}$$

where $R_{i,h}$ is the rate of initiation of homopolymerization and $k_{t,h}$ is the rate constant for the bimolecular termination of "inside" homopolymerization.

If one assumes that $k_t \cong k_{t,c} \cong k_{t,h}$, then eqs. (24) and (25) may be rewritten and rearranged to yield

$$R_i = 2k_t[\mathrm{PM}_n\cdot]([\mathrm{PM}_n\cdot] + [\mathrm{M}_m\cdot]) \tag{26}$$

and

$$R_{i,h} = 2k_t[\mathrm{M}_m\cdot]([\mathrm{PM}_n\cdot] + [\mathrm{M}_m\cdot]) \tag{27}$$

The available evidence indicates that this assumption is probably valid. It has been found in the grafting system styrene–cellulose acetate that the molecular weights of the styrene graft polymer and "inside" homopolymer are the same (and much higher than that of the homopolymer formed outside the cellulose).[13,14] Similar results have been observed in the graft polymerization of styrene to rubber.[15]

Equations (26) and (27) may be combined to yield

$$[M_m\cdot] = R_{i,h}[\mathrm{PM}_n\cdot]/R_i \tag{28}$$

Combining eqs. (26) and (28) yields

$$[\mathrm{PM}_m \cdot] = R_i^2/2k_t(R_i + R_{i,h})^{1/2} \tag{29}$$

Combining eqs. (2a and (29) yields

$$R_p = k_p[\mathrm{M}]\{R_i/[2k_t(R_i + R_{i,h})]^{1/2}\} \tag{30}$$

and

$$k_p^2/k_t = 2R_p^2/[\mathrm{M}]\{R_i^2/(R_i + R_{i,h})\} \tag{31}$$

On comparing eqs. (7) and (31) one notes that the latter differs from the former in that it contains an $R_i^2/(R_i + R_{i,h})$ term instead of an R_i term. Since $R_i \cong 2R_{i,h}$, $R_i^2/(R_i + R_{i,h})$ will be approximately 30% lower in value than R_i. This means that if one employs eq. (31) instead of eq. (7) to calculate the k_p^2/k_t values, the values so obtained will be approximately 30% higher than the k_p^2/k_t values calculated from eq. 7. Since we have ascribed only qualitative significance to the k_p^2/k_t values, it is apparent that the use of eq. (7) and the ignoring of termination via reaction (23) are justified.

EXPERIMENTAL

Materials

Methanol was dried over soda lime and then distilled. Styrene was washed with dilute sodium hydroxide solution, dried, and then vacuum distilled. Du Pont Zytel 101 nylon 66, as 2 and 3 mil film and 50 mil sheet, was employed. This particular nylon has a density of 1.140 g./ml. and contains 47% by weight of crystalline nylon.[16] The density of the amorphous regions is 1.069 g./ml., while that of the crystalline regions is 1.220 g./ml.

Procedure for Graft Polymerization

Strips of 2 and 3 mil nylon films measuring approximately 4 1/2 in. × 3/4 in., were washed with boiling benzene, vacuum-dried at 85°C. to constant weight, and then immersed in methanol–styrene solutions of known composition. The mixtures were purged with nitrogen for 15 min., equilibrated overnight at 25°C., and then irradiated at 25°C. in the RAI Co^{60} source at various constant dose rates for various time intervals. To avoid post-irradiation effects, samples were worked up immediately after completion of the irradiation. The film strips were freed of homopolymer and unreacted monomer by washing overnight with boiling benzene, and then vacuum-dried to constant weight by heating at 85°C. All experiments were performed in duplicate, and the per cent graft calculated from the equation

$$\% \text{ graft} = \frac{\text{final film weight} - \text{initial film weight}}{\text{initial film weight}} \times 100$$

The results of these experiments are shown in Tables V–VII.

TABLE V
Effect of Methanol on the Graft Polymerization of Styrene to Nylon[a]

Methanol in outside solution, vol.-%	Grafting, %, after irradiation at 0.071 Mrad/hr. for various times									
	0.33 hr.	0.58 hr.	0.75 hr.	0.92 hr.	1.25 hr.	2 hr.	3 hr.	4 hr.	5 hr.	11.25 hr.
0			0.6	0.0	0.0	0.0	0.3	0.0	0.0	0.0
			0.0	0.0	0.0	0.1	0.4	0.5	0.0	0.0
10	7.4	7.0	11.8	15.3	17.6	17.2	16.2	20.8	16.4	23.9
	3.9	9.1	12.6	15.6	17.1	19.3	16.1	15.5		25.4
										25.8
30	7.8	10.8	16.8	16.6	20.4	25.9	24.0	26.2	25.2	33.0
	7.5	10.6	16.0	19.2	20.1	27.8	24.4	25.0	27.4	38.0
						28.5	26.1			
						25.4	27.7			
50	7.7	11.9	14.9	14.9	21.1	29.3	28.5		32.8	43.2
	7.3	10.5	11.3	12.6	20.1	28.7	27.5		31.5	47.2
70	6.8	6.7	9.0	12.4	15.0	27.2		27.0	28.6	37.0
	5.2		12.2	11.9	14.1	24.9		30.0	31.8	39.6
					14.4					
90			2.7	4.4	4.5	7.0	14.1	18.3	22.3	34.6
			3.0	3.0	5.5	8.2	14.9	18.4	20.1	30.4

[a] 3-Mil film used.

TABLE VI
Effect of Dose Rate on the Graft Polymerization of Styrene to Nylon Using 50% Styrene–50% Methanol[a]

Dose rate, Mrad/hr.	Grafting, %, after irradiation for various times							
	5 min.	13 min.	21 min.	29 min.	37 min.	45 min.	53 min.	61 min.
0.23	2.2	6.9	11.2					
	2.2	6.7	11.5					
0.054	0.6	2.4	4.9	8.0		12.2	13.9	14.6
	0.4	2.5	4.8	7.5		12.0	13.5	15.6
0.014		0.6	1.8	3.1	4.2	6.1	6.2	7.8
		0.3	1.9	3.3	4.0	5.7	6.2	7.6

[a] 3-Mil film used.

TABLE VII
Effect of Film Thickness on the Graft Polymerization of Styrene to Nylon Using 50% Styrene–50% Methanol

Film thickness, mil	Grafting, %, after irradiation at 0.055 Mrad/hr. for various times					
	5 min.	13 min.	21 min.	29 min.	37 min.	45 min.
2		1.6	3.1	6.7	8.4	10.0
		1.5	3.6	5.8	7.6	9.2
3	0.6	2.2	4.6	6.5	9.8	12.1
	0.5	2.4	4.5	6.7	9.1	11.0

The interrupted experiments were performed in a similar manner with the exception that the irradiation was interrupted. Films were immersed in the 30% methanol–70% styrene solution and irradiated for 2 hr. to give 26.2% and 25.0% grafts. These grafts were then re-equilibrated with monomer solution and irradiated for an additional 2 hr. The total amount of graft for the duplicate samples after a total of 4 hr. of irradiation was 56.7% and 52.4%, respectively. These results are shown in Figure 3*b* and Table IV.

Procedure for Swelling Experiments

Strips of 50-mil nylon sheet, measuring approximately $1\frac{1}{2}$ in. $\times$ $\frac{1}{2}$ in., were washed in benzene, vacuum-dried at 85°C. for 3–4 days, and then immersed in the various styrene–methanol solutions and equilibrated at 25°C. for 28 days. This time interval was greater than that required to attain equilibrium swelling. The styrene was saturated at −20°C. with hydroquinone prior to the preparation of the solutions in order to prevent polymerization of the styrene during the course of the swelling experiments. The equilibrated samples were removed from the methanol–styrene solutions, their surfaces wiped dry with absorbent paper and weighed quickly. All experiments were performed in duplicate, and the per cent swelling of the nylon samples calculated from the equation;

$$\% \text{ swelling} = \frac{\text{wt. of equilibrated sample} - \text{initial wt.}}{\text{initial wt.}} \times 100$$

These results are shown in Table II.

In order to determine the composition of the liquid sorbed by the nylon, samples of nylon equilibrated in the various methanol–styrene solutions were placed in powdered Dry Ice and irradiated at 0.050 Mrad/hr. to a total dose of approximately 12.5 Mrad. The styrene in the sorbed solutions was "frozen in" (i.e., rendered nonvolatile) by this procedure due to homopolymerization and graft polymerization. The sorbed methanol, however, remained volatile. The samples were then vacuum-dried at 100°C. for 8–9 days to constant weight. The difference in weight between the equilibrated samples before and after irradiation is the amount of methanol which is sorbed by the nylon. From these data, the concentrations of monomer available for the grafting reaction in the various methanol–styrene–polyethylene system were calculated and are shown in Table II.

The authors are indebted to the Division of Isotopes Development of the United States Atomic Energy Commission for generous support of this work under Contract No. AT(30-1)-2318.

References

1. Ballantine, D. S., P. Colombo, A. Glines, B. Manowitz, and D. L. Metz., Brookhaven National Laboratory Report 414, T-81 (1956).
2. Walling, C., *Free Radicals in Solution*, Wiley, New York, 1957, Chap. 3.
3. Zimmerman, J., *J. Appl. Polymer Sci.*, **2**, 181 (1959).

4. Tobolsky, A. V., and R. B. Mesrobian, *Organic Peroxides*, Interscience, New York, 1954, p. 144.

5. Odian, G., A. Rossi, and E. N. Trachtenberg, *J. Polymer Sci.*, **42**, 575 (1960); G. Odian, M. Sobel, A. Rossi, and R. Klein, *J. Polymer Sci.*, **55**, 663 (1961).

6. Mock, R. A., and W. N. Vanderkooi, *J. Polymer Sci.*, **56**, 69 (1962).

7. Lawton, E. J., J. S. Balwit, and R. S. Powell, *J. Polymer Sci.*, **32**, 257 (1958); E. J. Lawton, R. S. Powell, and J. S. Balwit, *J. Polymer Sci.*, **32**, 277 (1958).

8. Matheson, M. S., E. E. Auer, E. B. Bevilacqua, and E. J. Hart, *J. Am. Chem. Soc.*, **73**, 1700, 5395 (1951).

9. Gregg, R. A., and F. R. Mayo, *J. Am. Chem. Soc.*, **75**, 3530 (1953).

10. Basu, S., J. N. Sen, and S. R. Rali, *Proc. Roy. Soc. (London)*, **A202**, 485 (1950).

11. Mayo, F. R., R. A. Gregg, and M. S. Matheson, *J. Am. Chem. Soc.*, **73**, 1691 (1951).

12. Charlesby, A., *Atomic Radiation and Polymers*, Pergamon Press, New York, 1960, p. 460.

13. Chaudhuri, D. K. R., and J. J. Hermans, *J. Polymer Sci.*, **51**, 381 (1961).

14. Kobayashi, Y., *J. Polymer Sci.*, **51**, 371 (1961).

15. Turner, D. T., *J. Polymer Sci.*, **35**, 17 (1959).

16. Crozier, V., E. I. du Pont de Nemours and Co., private communication.

Synopsis

It was observed in the gamma radiation-induced graft polymerization of styrene to nylon that dilution of the styrene with methanol greatly accelerates the rate of styrene grafting. The compositions of the solutions absorbed by the nylon on equilibration with the various methanol–styrene solutions were determined. These results showed that the concentration of styrene available for the grafting reaction is much greater when the styrene–methanol solutions are employed than when undiluted styrene is employed. It was found that the values of k_p^2/k_t for these graft polymerizations are increased by a factor of 10^5 compared to the corresponding value in homopolymerization. These increases in the k_p^2/k_t term are ascribed to the greater viscosity of the medium in which the grafting reaction takes place and to the immobilization of the graft polymer chains by the Trommsdorff-type effect of methanol. A discussion is presented of the applicability of steady-state kinetics, as well as of the various competing reactions, in the graft polymerization.

Résumé

On a observé que, dans la polymérisation greffée du styrène sur le nylon, induite par les rayons gamma, la dilution du styrène avec le méthanol augmente considérablement la vitesse de greffage du styrène. On a déterminé les compositions des solutions absorbées par le nylon, qui se trouve en équilibre avec les différentes solutions méthanol-styrène. Ces résultats ont montré que la concentration adéquate de styrène pour la réaction de greffage est plus grande lorsqu'on emploie des solutions styrène-méthanol que lors de l'emploi de styrène non dilué. On a trouvé que les valeurs k_p^2/k_t pour ces polymérisations greffées sont augmentées d'un facteur de 10^5 comparativement à la valeur correspondante pour l'homopolymérisation. Ces augmentations de la valeur du terme k_p^2/k_t ont été attribuées à la viscosité plus grande du milieu dans lequel se produit la réaction de greffage et à l'immobilisation des chaînes de polymère greffé par un effet du méthanol du type Trommsdorff. On présente une discussion au sujet de l'application de la cinétique de l'état stationnaire, ainsi que les différentes réactions compétitives dans la polymérisation greffée.

Zusammenfassung

Es wurde beobachtet, dass bei der durch γ-Bestrahlung induzierten Pfropfpolymerisation von Styrol auf Nylon eine Verdünnung des Styrols mit Methanol die Geschwindig-

keit der Styrolaufpfropfung stark beschleunigt. Die Zusammensetzungen der durch das Nylon im Gleichgewicht mit den verschiedenen Methanol-Styrol-Lösungen absorbierten Lösungen wurden bestimmt. Die Ergebnisse zeigten, dass die für die Pfropfreaktion verfügbare Styrolkonzentration bei Verwendung von Styrol-Methanol-Lösungen viel grösser ist als bei Verwendung von unverdünntem Styrol. Es wurde gefunden, dass die k_p^2/k_t-Werte für diese Pfropfpolymerisationen im Vergleich zu der entsprechenden Homopolymerisation um einen Faktor von 10^5 vergrössert werden. Das Ansteigen des k_p^2/k_t-Terms wird der grösseren Viskosität des Mediums, in dem die Pfropfreaktion stattfindet, und der Immobilisierung der Pfropfpolymerketten im Methanol durch einen Trommsdorffeffekt zugeschrieben. Eine Diskussion der Anwendbarkeit der Stationaritätsannahme in der kinetischen Behandlung wie auch der verschiedenen Konkurrenzreaktionen bei der Pfropfpolymerisation wird präsentiert.

Received April 4,1961
Revised September 11, 1961

JOURNAL OF POLYMER SCIENCE: PART A VOL. 1, PP. 655–670 (1963)

Polymerization of Allene by Organometallic Initiation*

WILLIAM P. BAKER, JR., *Film Department, Experimental Station, E. I. du Pont de Nemours and Company, Inc., Wilmington, Delaware*

Recently much information has been published concerning the polymerization of olefins and diolefins by organometallic initiators.[1] It is the purpose of this paper to present observations on the action of these initiators upon the cumulene, allene.

Prior to the advent of these initiators, no polymerization of allene to authentic high molecular weight polymer had been reported. Treatment of allene in the gas phase with α-rays had been reported to yield an off-white solid and brown viscous mass,[2] while gas phase photolysis had resulted in a small amount of uncharacterized, white, sublimable solid.[3] Literature had disclosed that allenes with allylic hydrogen react with dicobalt octacarbonyl to yield carbon monoxide and a product which polymerizes allene[4] and that various fluoroallenes are readily polymerizable, especially by radical means.[5,6]

The work contained herein reports the preparation of high molecular weight linear polyallene, the determination and kinetic control of the structural units of the polymer, a mechanistic interpretation of the results, and a few comments concerning the crystallinity of the polymer.

EXPERIMENTAL

The majority of infrared spectra was taken by a Perkin-Elmer Model 21 infrared spectrometer by both film and KBr pellet techniques. Some spectra were obtained on a Perkin-Elmer Model 13 infrared spectrometer for resolution purposes.

All polymerizations were performed by the batch process. Usually the stirred medium was first saturated with allene and the metallic salt to be reduced was added next, followed by addition of triisobutyl aluminum. Allene was bubbled through the stirred solution throughout the course of the polymerization. This procedure had the disadvantage that the latter part of the polymerization occurred in an environment of low allene concentration because of two factors: (*1*) the rapidity of the polymerization quickly increased the viscosity to such an extent that the allene monomer

* Presented in part before the Polymer Division at the 140th National Meeting of the American Chemical Society, Chicago, Ill., September 1961.

could not be uniformly distributed, and (*2*) under many conditions the polymer gelled from solution, which changed the environment. Nevertheless, the batch process was employed because it proved capable of meeting the objective of this program and because it was the simplest and most rapid method available.

All experiments were performed in glassware which was baked at least 24 hr. at 140°C. and cooled to room temperature under nitrogen containing less than 2.5 ppm water and less than 2.5 ppm oxygen. In a typical experimental procedure, 500 ml. of purified solvent was transferred into the flask under a nitrogen atmosphere, the flask being equipped with magnetic stirrer, thermometer, cooling bath, and an allene inlet and outlet. The medium was then saturated with allene (Caribou Chemical Company) which had been distilled at low temperature (by the Special Services Section) to yield a product having a minimum purity of 99.5% (principal impurity, dichloropropane) and which had been passed through a silica gel column. The allene was bubbled through the solution during the polymerization. After the solvent was saturated with allene, 0.05 ml. $VOCl_3$ was added, and the solution changed from colorless to dark red. ($VOCl_3$ alone did not cause polymerization.) Thereupon, 2.5 ml. of 2.2*M* triisobutyl aluminum in cyclohexane was added, and the color of the solution changed to a cherry red; this was followed shortly by the appearance of either very high viscosity or of gelled polymer, depending upon the conditions. After a suitable time interval, 50 ml. of ethanol was added, and shortly thereafter the polymer was collected by filtration. Evaporation of the filtrate left little or no residue. Then, the polymer was repeatedly washed in an Osterizer with 10% ethanolic HCl, ethanol, water, and acetone. The polymer was then dried. Control experiments demonstrated that the polymer did not pick up HCl and was not altered in other aspects by this work-up procedure.

A few experiments under a pressure of approximately 900 psi were run in a similar manner by conventional means in a 3-liter shaker tube.

The typical polymers produced by these experiments possessed an inherent viscosity of 1 to 5.5 (0.5%, bromobenzene, 110°C., antioxidant present). All polymers were film-forming and ranged from amorphous to highly crystalline. The polymers, although totally soluble, possessed low solubility, the crystalline samples being less soluble than the amorphous; the best solvents were halogenated hydrocarbons. The crystalline melting point was 122 ± 3°C. Most of the film-forming operations induced high crystallinity into the samples to yield brittle films; mechanical destruction of crystallinity yielded material having M/E/T values of the order of 115,000 psi/66%/5,000 psi.

INFRARED SPECTRA

It had been anticipated that the structure of the polymer would contain pendant methylene groups on alternate carbons of the polymer chain to

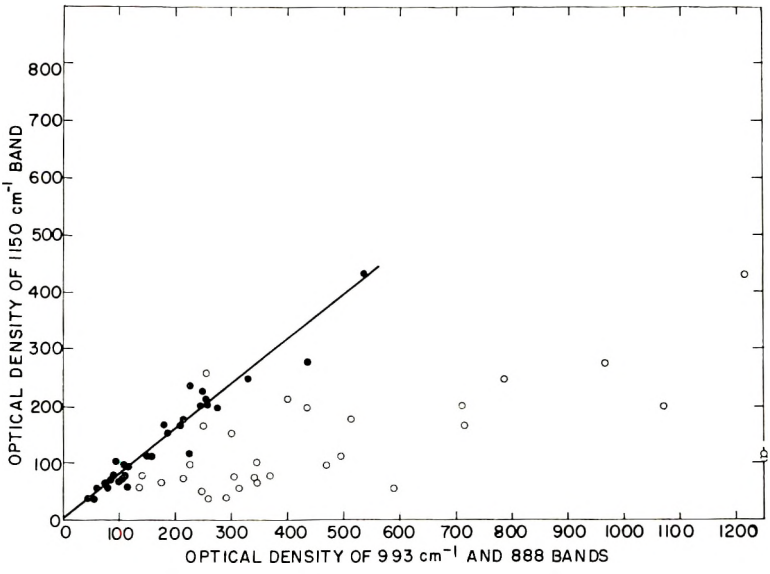

Fig. 1. Optical density of 1150 cm.$^{-1}$ band vs. (●) 993 cm.$^{-1}$ band and (○) 888 cm.$^{-1}$ band.

yield the following vinylidene structure (the α-disubstituted double bond being unreactive toward the type of catalyst employed):

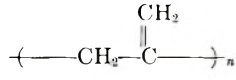

However, the presence of a strong absorption band at 993 cm.$^{-1}$ and a doublet at 696 and 708 cm.$^{-1}$ indicated that not only were vinyl and *cis* groups present in the polymer,[7] but that they were present as a large proportion of the total double bond content. Thus, the polymer samples possessed three unsaturated groupings and not just the anticipated vinylidene structure. A study of the infrared spectra was then undertaken to analyze the structural content of the various polymeric samples.

The Beer-Lambert law was found to be valid for the bands used in the analysis. The rather sharp symmetrical band at 993 cm.$^{-1}$ was employed as the criterion for vinyl absorption. The criterion for vinylidene absorption was not clear, because its main absorption band at 888 cm.$^{-1}$ had a shoulder at approximately 906 cm.$^{-1}$ due to vinyl absorption. However, it was found that the 888 cm.$^{-1}$ band could also be utilized if care was taken. Plots of the optical densities of the band in question were then made against both the 993 and the 888 cm.$^{-1}$ bands. These plots were made of 40 to 50 different polymeric samples. If one of the plots resulted in a straight line passing through the origin, the absorption of the band in question was considered totally due to the group that it was plotted against. If the line was reasonably straight but did not pass through the origin, a small contribution from another species was considered to be present. Typical results are shown in Figures 1 and 2.

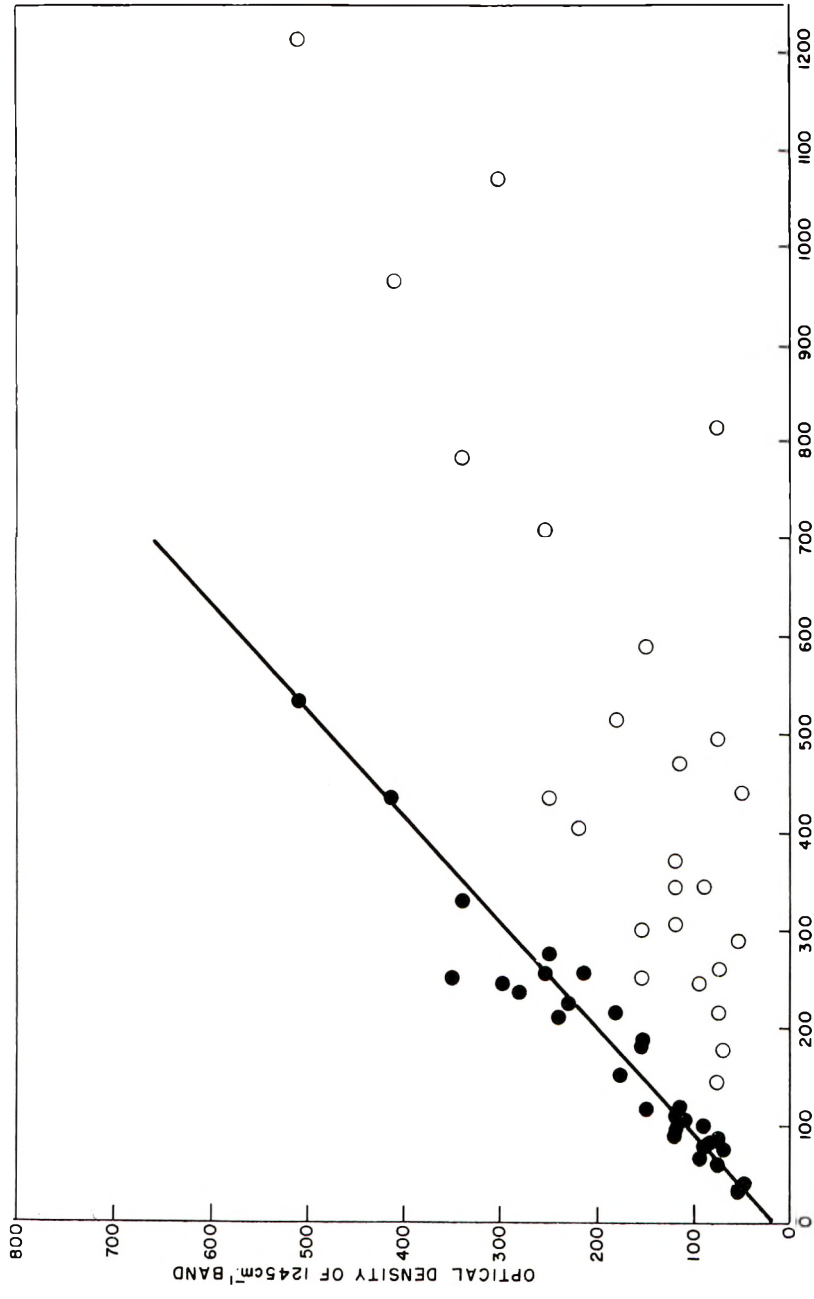

Fig. 2. Optical density of 1245 cm.$^{-1}$ band vs. (●) 993 cm.$^{-1}$ band and (○) 888 cm.$^{-1}$ band.

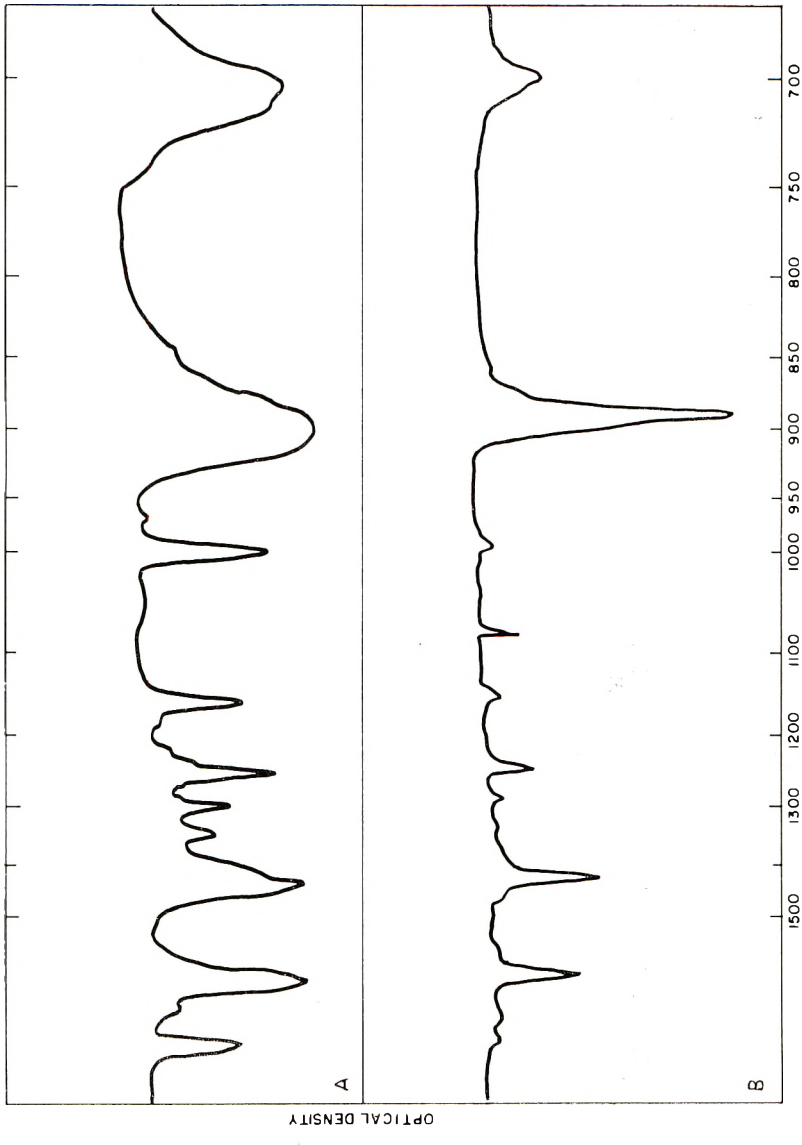

Fig. 3. Infrared spectra of polyallene of (*A*) high and (*B*) low vinyl content.

The spectra contained an absorption band at 696 cm.$^{-1}$; the band was a doublet, the main peak being at 696 cm.$^{-1}$ and a shoulder of moderate strength being present at 708 cm.$^{-1}$ This band was attributed to *cis* unsaturation. The ratio of the two bands of the doublet was 0.82; *cis* unsaturation has been reported to lead to an absorption doublet at 708 and 696 cm.$^{-1}$ with a ratio of 0.77.[8] Interestingly, a linear relationship for over a hundred different polymeric samples existed between the 696 and 993 cm.$^{-1}$ bands. This signified that the amounts of vinyl and *cis* groups were proportional to each other, even though the polymers had been synthesized over a wide range of temperature, solvent composition, and catalyst composition.

In no case was any indication of trisubstituted or *trans* unsaturation found in any of the spectra.

By the above method, the band assignments listed in Table I were made. These were later confirmed when it was possible to synthesize polyallene of pure vinylidene structure (for example, see Fig. 3).

TABLE I
Assignment of Infrared Bands

Frequency, cm.$^{-1}$	Primary species	Remarks
3050	Vinyl, vinylidene	C—H stretching of $=CH_2$
2971	Vinyl, *cis*	C—H stretching of =CH—
2916	Vinylidene, *cis*	C—H stretching of $—CH_2—$
2892, 2815 } 2853	Vinylidene, *cis*	$—CH_2—C=C$ 2853 cm.$^{-1}$ band split
1815	Vinyl	Overtone of 906 cm^{-1}
1634	Vinylidene	C=C stretching (as in isobutene) must also contain vinyl, *cis*
1425	Vinylidene	$—CH_2—$ bending deformation; shoulder must include vinyl and vinylidene $=CH_2$ in-plane deformation
1335	Vinyl, vinylidene	
1290	Vinyl	=CH in-plane deformation
1245	Vinyl and/or *cis*	
1150	Vinyl and/or *cis*	
993	Vinyl	=CH— out-of-plane deformation
906	Vinyl	$=CH_2$ out-of-plane deformation
888	Vinylidene	$=CH_2$ out-of-plane deformation
696	*cis*	

STRUCTURAL VARIATION OF POLYALLENE

The infrared study discussed above demonstrated that polyallene possessed vinylidene, vinyl, and *cis* unsaturation. Control of these groups was of importance both for contemplated end uses of the polymer requiring the unique methylene side chain unsaturation on alternate carbons and for

control of crystallinity and, hence, solubility. The mechanism detailed below was hypothesized and adopted in this work. It proved to predict accurately the effect of polymerization conditions upon the structure of the resulting polymers, and in no case did experimental evidence offer contradiction.

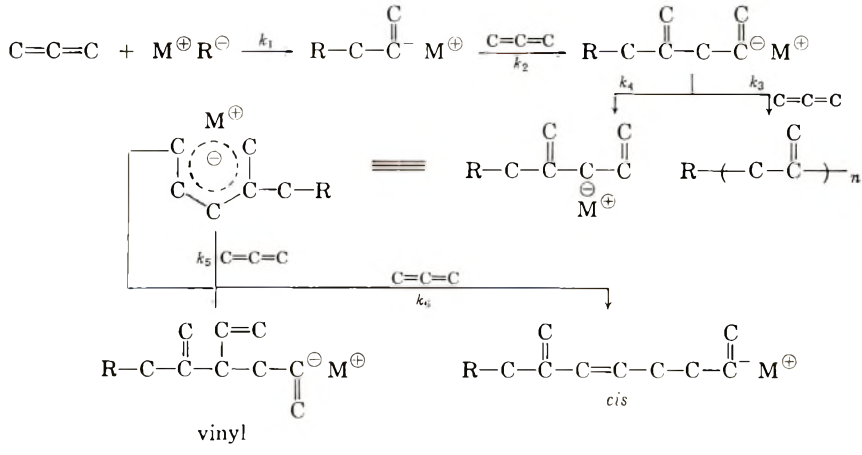

It was decided to consider the polymerization as a fundamentally anionic type. Since high molecular weight polyallene cannot be prepared by the usual methods of anionic polymerization, this representation of the polymeric growth as an ion pair species is oversimplified and the role of the transition metal minimized.

Several things should be noted concerning this mechanism. The proportion of vinyl groups occurring in the polymer will be determined by the r_4/r_3 ratio, i.e., the rate of monomer addition to the rate of a 1:2 proton transfer to yield a resonance stabilized six-membered ring. Thus, rate 4 would be emphasized by low monomer concentration, yielding polymer high in vinyl content. The mechanism accounts both for *cis* unsaturation and for a proportionality of *cis*-to-vinyl unsaturation. The *cis* content arises from attack of monomer upon the terminal carbon atom, the incipient double bond being forced to be *cis* by the ring configuration. The ratio of *cis*-to-vinyl unsaturation is the ratio of the corresponding rate constants, k_6/k_5, both rates being first order in monomer and first order in cyclized intermediate. The lack of trisubstituted unsaturation is thought to be due to steric hindrance by the growing chain and gegenion (with its environment).

One feature of the mechanism is of interest—the attack of anion on the terminal rather than the central carbon atom of allene:

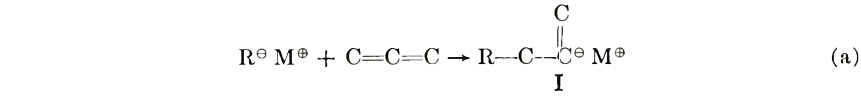

(a)

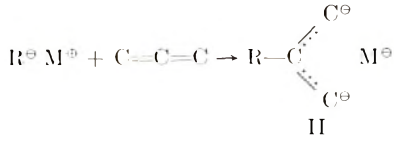

(b)

II

It can be hypothesized that (b) leads to a more thermodynamically stable intermediate and might be expected. However, since this reaction must be exothermic by about 20 kcal. (breaking of a C=C to form a C—C), application of the Hammond postulate[9] suggests that the transition state should resemble the reactants, i.e., the transition state should be loose, and hence, structure II would not be sufficiently formed to afford a significant contribution of its ultimate resonance energy. On the basis of the statistical factor and steric hindrance, it might be expected that terminal attack would be favored. (Recent evidence has shown that the Arrhenius frequency factor is about an order of magnitude lower for radical attack on the central carbon of allene than it is for attack on a conjugated diene carbon atom.)[11] On a polarity basis, terminal attack is favored since the central *sp* carbon atom of allene should be negative relative to the terminal sp^2 carbon atoms.

From this suggested reaction course, the conclusions listed below followed and were generally well substantiated by experimental results:

(*1*) The highest possible ratio of vinyl and *cis* to vinylidene unsaturation is 1:1. Regardless of the preparative conditions, it was found a maximum vinyl concentration would be reached but not surpassed. Use of literature extinction coefficients[8,10] indicated that this maximum concentration qualitatively corresponded to 2 *cis*:1 vinyl:3 vinylidene units. The correspondence was not exact but was felt to lie within the error inherent in use of literature values of infrared extinction coefficients of somewhat dissimilar compounds.

(*2*) The functionality of the solvent will play a large role in determining whether step 3 or 4 predominates due to specific interaction with the gegenion.

(*3*) Copolymerization should decrease the vinyl content because there is no chance of vinyl formation when the growing chain end contains the comonomer; for vinyl formation, an allene chain must attack an allene molecule, and the opportunity of such an occurrence during copolymerization is obviously less than in homopolymerization.

(*4*) Heterogeneous polymerization or low solubility and low swelling of polymer in the solvent will favor vinyl formation because of low monomer concentration at the growing site and because less coulombic and specific stabilization of the uncyclized gegenion is possible.

(*5*) The nature of the metallic gegenion will be of importance in the determination of the reaction path because of differences in cyclizing aptitudes.

(*6*) The dielectric constant of the medium may be expected to influence the reaction path taken, but its effect will be difficult to discern over other effects.

(7) If sufficient difference in enthalpy of activation exits between steps 3 and 4, then control of reaction path (structure) may be possible by temperature variation. However, thermally dependent factors such as polymer and monomer solubility may offset the effect of temperature.

(8) Control of the concentration of monomer will control the structure of the polymer, the greater the concentration, the more vinylidene units formed. Thus, in a batch process, the vinylidene content of the polymer will decrease with increasing conversion.

(9) The *cis*-to-vinyl ratio should be dependent upon the transition metal, but probably the enthalpies of activation will be too similar for the ratio to exhibit a temperature dependence.

RESULTS

In the following section the experimental results will be detailed and correlated with the suggested mechanism.

1. Effect of Solvent

It quickly became apparent that, although within a certain class of compounds there might be a change in structure with change in the dielectric constant of the solvent, the functionality of the solvent was the predominant factor. Some of these results are tabulated in Table II. The *cis*-to-vinyl ratio was not altered.

TABLE II
Effect of Solvent on Structure Obtained at 27 ± 2°C.

Expt. no.	Solvent[a]	ϵ	A_{888}/A_{993}[b]
FX-51-57	Tetrahydrofuran	7.39	6.60
FX-51-77	Dioxane	2.21	4.03
FX-51-100	Diphenyl ether		2.65
FX-51-72	Thiophene	2.76	8.10
FX-51-64	*o*-Dichlorobenzene	9.9	3.41
FX-51-96	Chlorobenzene	5.6	1.81
FX-51-26	Bromobenzene	5.4	2.27
FX-51-70	Toluene	2.38	2.42
FX-51-4	Benzene	2.28	3.31
FX-51-63	Dichloromethane	9.1	3.32
FX-51-65	1,1,2,2-Tetrachloroethane	8.2	6.20
FX-51-56	Tetrachloroethylene	2.3	1.70
FX-31-147	Cyclohexane	2.02	3.75
FX-51-62	Hexane	1.89	2.40
FX-51-102	Gas phase	—	5.1

[a] Most of solvents given special purification treatments.

[b] Optical density ratio of 888 cm.$^{-1}$ and 993 cm.$^{-1}$ bands; the higher the ratio, the less the vinyl content.

Superimposed on any interpretation of the results must be the question of the magnitude of differences of allene concentration among the solvents and differences in polymer solubility. Qualitatively, it appears that the

vinyl content may decrease with an increase of basicity of the solvent as displayed within the ether series. It is thought that solvation of the positive gegenion by the basic solvent competes with formation of the cyclized resonance stabilized carbanion and that solvation of the gegenion hinders incorporation of the ion into the cyclic structure.

2. Effect of Agitation

Polymerization under conditions of better agitation should decrease the vinyl content of the resulting polymer by maintaining the monomer concentration at the growing site of the chain. By the same reasoning, precipitated unswollen polymer should be high in vinyl content. A few such experiments are listed in Table III and demonstrate that this was indeed the case. The vinyl-to-*cis* ratio was not altered.

TABLE III
Effect of Agitation on Polymerization with $VOCl_3$ Catalyst

Expt. no.	A_{888}/A_{993}[a]	Conditions
FX-51-81	1.57	Hexane (500 ml.), 0°C. (polymer not appreciably swollen by solvent), magnetic stirring
FX-31-139	3.46	Benzene (500 ml.), magnetic stirring, 25°C.
FX-51-4	3.31	
FX-51-22	4.40	Benzene (500 ml.), polymerized in Osterizer, 27°C.
FX-51-28	5.70	Benzene (1000 ml.), mechanical stirring, 27°C.

[a] Ratio of optical densities of 888 cm.$^{-1}$ and 993 cm.$^{-1}$ bands; the higher the ratio, the less the vinyl content.

3. Effect of Metallic Catalyst

The effect of the transition metal contained in the gegenion should have a significant effect upon which reaction path will be followed. The results listed in Table IV show that such differences in cyclization tendencies do exist among the transition metals.

TABLE IV
Effect of Variation of Metallic Salt[a]

Expt. no.	Atomic no. of metal	Salt	Wt. salt, g.[b]	A_{888}/A_{993}[c]
FX-31-148[d]	22	$TiCl_4$	4.2	3.74
FX-31-139	23	$VOCl_3$	16.3	3.46
FX-51-106	26	$FeBr_3$	7.7	7.78
FX-51-107	27	$CoCl_2$	2.0	2.01
FX-51-111		$Co(NH_3)_6Cl_3$	14.4	4.60
FX-51-108	28	$NiCl_2$	0.4	3.08

[a] Polymerization conditions: 500 ml. benzene, triisobutylaluminum, 27 ± 2°C.

[b] 5×10^{-4} mole.

[c] Ratio of optical densities at 888 cm.$^{-1}$ and 993 cm.$^{-1}$; the higher the value, the less the vinyl content.

[d] In cyclohexane; $VOCl_3$ in cyclohexane yields A_{888}/A_{993} ratio of 3.75.

TABLE V

Effect of Temperature on Allene Polymerization by $VOCl_3$[a]

Solvent	ϵ	A_{888}/A_{993}[b]				Yield, g.			
		0°C.	30°C.	60°C.	>100°C.	0°C.	30°C.	60°C.	>100°C.
o-Dichlorobenzene	9.9	3.15	3.41	2.41	2.62[e]	6.5	4.9	7.7	3.0[e]
Chlorobenzene	5.6	2.21	1.81	2.04		11.4	13.0	11.1	
Bromobenzene	5.4	1.98	2.27	1.91	18[d]	4.4	14.4	8.0	2.6[d]
Benzene	2.3	2.41	3.46	2.71		5.8	16.3	4.5	
Cyclohexane	2.0	3.16	3.75	2.21		7.7	3.7	2.6	
Hexane	1.9	1.57	2.40	2.04		5.0	3.0	1.1	

[a] Polymerization conditions: 500 ml. solvent, 0.5 mmole $VOCl_3$, 4.4 mmole triisobutylaluminum.

[b] Ratio of optical densities of 888 cm.$^{-1}$ and 993 cm.$^{-1}$ bands; the higher the value, the less the vinyl content.

[c] Two experiments run at 140–145°C.; yields = 1.1, 4.9 g.; ratios = 2.60, 2.65.

[d] Three experiments run at 109–125°C.; yields = 2.5, 2.6, 3.0 g.; ratios = 7.7, 33, 14.

The diversity of the catalysts yielding positive results indicates that allene is polymerized by a rather large range of metallic salts coupled with a reducing compound. The transition metal involved might be expected to have some effect upon the ratio of *cis* to vinyl unsaturation. In the most thoroughly documented cases, mainly $TiCl_4$ and $VOCl_3$, there did seem to be a small but real difference in the ratio of *cis* to vinyl. The *cis* unsaturation was about 5% higher with $TiCl_4$. Insufficient work was done to compare relative cyclization tendencies of the other transition metals.

4. Effect of Temperature

The effects of temperature are listed in Tables V and VI. Unfortunately, polymer and monomer solubility are thermally dependent in opposite fashion, and no systematic trend of structure variation with temperature was found. It is, perhaps, worth noting that with the $VOCl_3$ catalyst an increase in vinyl content occurred in progressing from 30 to 60°C. in every case but one, in which the vinyl content remained about the same. Generally, the $TiCl_4$ catalyst showed a more marked thermal dependence than the $VOCl_3$ catalyst, but the small yields from the former prevent a more positive conclusion. No change in *cis*-to-vinyl ratio was caused by the temperature variations.

TABLE VI
Effect of Temperature on Allene Polymerization by $TiCl_4$[a]

Solvent	ϵ	A_{888}/A_{993}[b]			Yield, g.		
		0°C.	30°C.	60°C.	0°C.	30°C.	60°C.
o-Dichlorobenzene	9.9	4.65	3.85	2.18	0.5	0.7	0.6
Cyclohexane	2.0	4.94	3.74	7.28	0.8	4.2	0.5
Hexane	1.9	5.04	3.64	5.19	0.3	0.2	0.1

[a] Polymerization conditions: 500 ml. solvent, 0.5 mmole $TiCl_4$, 4.4 mmole triisobutylaluminum.

[b] Ratio of optical densities of 888 cm.$^{-1}$ and 993 cm.$^{-1}$ bands; the higher the value the less the vinyl content.

4. Effect of Catalyst Concentration

Catalyst concentrations were varied over very broad ranges without the appearance of a pronounced effect.

6. Effect of Copolymerization

The effect of copolymerization upon the structure of polyallene is detailed in Table VII. In each case in which the comonomer was incorporated into the resulting polymer, the vinyl content of the polymer was lower than in the control homopolymerization of allene. The *cis*-to-vinyl ratio was not altered.

TABLE VII
Effect of Comonomers[a]

M_1	M_2	Solvent	Polymer	A_{888}/A_{993}[b]
Allene	None	Benzene	Polyallene	3.31
Allene	Propylene	Benzene	$M_1 + M_2$	7.10
Allene	Ethylene	Benzene	$M_1 + M_2$	5.72
Allene	Styrene	Benzene	$M_1 + M_2$	5.82
Allene	Carbon monoxide	Benzene	Polyallene	1.37
Allene	Vinyl chloride	Benzene	Polyallene	1.60
Allene	none	Bromobenzene	Polyallene	2.27
Allene	Vinyl chloride	Bromobenzene	$M_1 > M_2$	3.37

[a] Polymerization conditions: $VOCl_3$–triisobutylaluminum catalyst, 500 ml. solvent, 27 ± 2°C.

[b] Ratio of optical densities of 888 cm.$^{-1}$ and 993 cm.$^{-1}$ bands; the higher the value, the lower the vinyl content.

TABLE VIII
Results of High Pressure Polymerizations[a]

Expt. no.	Temp., °C.	Yield, g.	A_{888}[a]/A_{993}[b]
FX-51-148	30–35	2.2	12.4
	Series A[c]		
	(30)[d]	(14.4)[d]	(2.3)[d]
FX-51-150	58–92	9.7	4.2
	(60)[d]	(8.0)[d]	(1.9)[d]
FX-68-1	109–146	25.6	4.2
FX-68-5	110–153	26.1	8.2
	(110)[d]	(2.6)[d]	(18)[d]
FX-68-3	151–156	2.7	11.8
FX-68-4	176–181	0.6	13.8
	Series B[e]		
FX-51-149	30–77	9.3	5.1
	(30)[d]	(14.4)[d]	(2.3)[d]
FX-51-151	61–64	1.7	6.6
FX-51-152	61–151	8.5	8.4
	(60)[d]	(8.0)[d]	(1.9)[d]
FX-68-6	91–115	8.3	4.5

[a] Average pressure approximately 900 psi.

[b] Ratio of optical densities of 888 cm.$^{-1}$ and 993 cm.$^{-1}$ bands; the higher the value, the less the vinyl content.

[c] Polymerization conditions for series A: 200 ml. Bromobenzene, 20 g. allene, 0.5×10^{-3} mole $VOCl_3$, 11×10^{-3} mole triisobutylaluminum.

[d] Values of experiments run in the laboratory at atmospheric pressure.

[e] Polymerization conditions for series B 100 ml. bromobenzene, 20 g. allene, 0.5×10^{-3} mole $VOCl_3$, 11×10^{-3} mole triisobutylaluminum.

7. Effect of Allene Concentration

To obtain a higher allene concentration than was possible in the laboratory experiments, a few polymerizations were performed under a pressure of about 900 psi of allene; these runs were accompanied by the usual

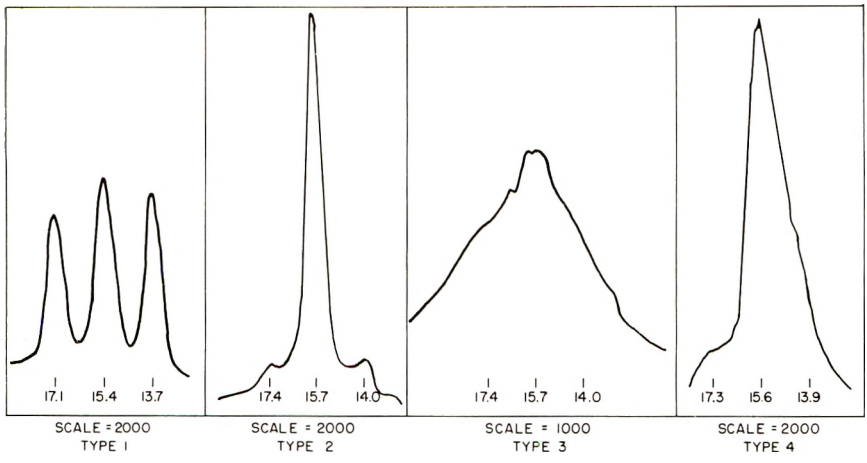

Fig. 4. X-ray goniometer traces of polyallene (numbers are 2θ angles).

difficulties inherent in work at high pressures. The results of such experiments are listed in Table VIII. As predicted from the mechanism, in all but the run at 110°C. vinyl content is less in the polyallene from the high pressure polymerization than in that produced from runs at atmospheric pressure. The relatively higher vinyl content of the polymer formed at 110°C. may be caused by the high conversion yielding a lowered allene concentration during the latter stages of the polymerization and by the increased polymer-to-solvent ratio which decreased the mobility of the system, resulting in decreased availability of monomer at the chain site. The increase of vinyl and *cis* content with extent of conversion was also quite noticeable in the runs at atmospheric pressure. The *cis*-to-vinyl ratio was not changed.

CRYSTALLINITY OF POLYALLENE

It was found that polyallene could be caused to exist in three distinct crystalline forms and an amorphous form. The corresponding x-ray goniometer scans are shown in Figure 4. All other types were metastable with respect to Type I. It was found possible to control the type of crystallinity by suitable choice of reaction conditions. Correlation between crystalline structure and polymeric structure is not available at this time. However, both x-ray and other experimental methods suggest that the polymers may be considered essentially as blocks of pure vinylidene structure and of blocks containing the mixed vinylidene–vinyl-*cis* structure.

POST-REACTIONS OF POLYALLENE

The unique structure of polyallene renders it susceptible to a great number of chemical reactions and modifications. It may be of interest to enumerate briefly a few such examples which have been performed.

Not only are internal double bonds thermodynamically more stable than terminal double bonds, but in the case of polyallene, conjugation would further increase the driving force for isomerization of the external double bonds into the chain. This isomerization to a polyene backbone was accomplished by treatment with several acids and was usually accompanied by some degradation. Polyallene could be oxidized to yield carbonyl groups by peracetic acid in acetic anhydride and with performic acid in formic acid. Attempts to add HCl across the double bonds of polyallene resulted in addition across the vinyl groups plus some isomerization of the pendant methylene double bonds to conjugated chain bonds and degradation of the polymer. Reactions of the Prins type were also found to be possible.

It is a pleasure to acknowledge the stimulating suggestions of Professor George S. Hammond of California Institute of Technology. The author is also indebted for valuable discussion to Drs. Frank P. Gay and William J. Pangonis of the Experiment Station Laboratory of the Film Department.

References

1. Gaylord, N. G., and H. F. Mark, *Polymer Reviews*, **2**, "Linear and Stereoregular Addition Polymers," Interscience, New York, 1959.
2. Heisig, G. B., *J. Am. Chem. Soc.*, **53**, 3245 (1931).
3. Lind, S. C., and R. Livingston, *J. Am. Chem. Soc.*, **55**, 1036 (1933).
4. Greenfield, H., I. Wender, and J. H. Wotiz, *J. Org. Chem.*, **21**, 875 (1956).
5. Jacobs, T. L., and R. S. Bauer, U.S. Application Serial No. 671,131.
6. Blomquist, A. T., and D. T. Longone, *J. Am. Chem. Soc.*, **79**, 4981 (1957).
7. Bellamy, L. J., *The Infrared Spectra of Complex Molecules*, Wiley, New York, 1954.
8. Anderson, J. A., and W. D. Seyfried, *Anal. Chem.*, **20**, 998 (1948).
9. Hammond, G. S., *J. Am. Chem. Soc.*, **77**, 334 (1955).
10. Bateman, L., J. I. Cunneen, J. M. Fabian, and H. P. Koch, *J. Chem. Soc.*, 936 (1950).
11. Rajbenbach, A., and M. Szwarc, *J. Am. Chem. Soc.*, **79**, 6343 (1957).

Synopsis

Allene has been polymerized to a high molecular weight by several transition metal salts reduced by aluminum triisobutyl. The polymer contained three types of unsaturation: vinylidene, vinyl, and *cis;* no *trans* unsaturation was found. A hypothesized mechanism accounted for these facts by two competitive rates: reaction of a linear intermediate with monomer to form again the linear intermediate plus one vinylidene unit, and isomerization of the linear intermediate to a cyclic intermediate which ultimately yielded one vinylidene and one vinyl or *cis* unit after reaction with monomer. Thus, the ratio of the two rates was controlled by the concentration of allene. The suggested mechanism proved to predict accurately the effect of the conditions of polymerization upon the structures of the resulting polymers. The nature of the transition metal also proved of importance in determining the path of polymerization as did temperature, solvent, degree of agitation, and copolymerization. Polyallene was found to exist in three crystalline forms as well as an amorphous form.

Résumé

On a polymérisé jusqu'à un poids moléculaire élevé de l'allène au moyen de plusieurs sels de métaux de transition réduits par du triisobutyl-aluminium. Le polymère

renferme trois types d'insaturation; les types vinylidénique, vinylique et cis; on n'a pas trouvé d'insaturation trans. On propose un mécanisme hypothétique qui rend compte de ces faits par deux vitesses compétitives: réaction d'un intermédiaire linéaire avec le monomère pour former à nouveau l'intermé diaire linéaire plus une unité vinylidénique, et isomérisation de l'intermédiaire linéaire en un intermédiaire cyclique qui fournit ultérieurement une unité vinylidénique et une unité vinylique ou cis après réaction avec le monomère. La rapport des deux vitesses a été contrôlé par la concentration en allène. Le mécanisme proposé tend à prouver qu'il est possible de prévoir exactement l'influence des conditions de polymérisation sur les structures des polymères qui en résultent. La nature du métal de transition est également importante pour déterminer l'évolution de la polymérisation au même titre que la température, le solvant, la vitesse d'agitation et la copolymérisation. On a trouvé que le polyallène existe sous trois formes cristallines ainsi que sous une forme amorphe.

Zusammenfassung

Allen wurde mit einigen durch Triisobutylaluminum reduzierten Übergangsmetallsalzen zu hochmolekularen Produkten polymerisiert. Die Polymeren enthielten drei Typen von Ungesättigtheit: Vinyliden, Vinyl und *cis;* es wurde keine *trans*-Ungesättigtheit gefunden. Ein Mechanismus mit zwei kompetitiven Reaktionen wurde zur Erklärung dieser Tatsachen als Arbeitshypothese aufgestellt: Reaktion eines linearen Zwischenstoffs mit Monomeren unter wiederholter Bildung des linearen Zwischenprodukts plus einer Vinylideneinheit und Isomerisierung des linearen Zwischenprodukts zu einem cyklischen Zwischenprodukt, das schliesslich nach Reaktion mit dem Monomeren eine Vinyliden- und eine Vinyl- oder *cis*-Einheit liefert. Das Geschwindigkeitsverhältnis wird durch die Allenkonzentration bestimmt. Der vorgeschlagene Mechanismus kann den Einfluss der Polymerisationsbedingungen auf das entstehende Polymere genau angeben. Die Natur des Übergangsmetalls hatte, ebenso wie Temperatur, Lösungsmittel, Rührung und Copolymerisation Einfluss auf den Reaktionsweg. Für Polyallen wurden drei kristalline und eine amorphe Form nachgewiesen.

Received November 17, 1961

JOURNAL OF POLYMER SCIENCE: PART A VOL. 1, PP. 671–685 (1963)

Crystallinity and the Structure of Celluloses

K. J. HERITAGE,* J. MANN,† and L. ROLDAN-GONZALEZ,‡ *British Rayon Research Association, Heald Green Laboratories, Wythenshawe, Manchester, England*

INTRODUCTION

Many methods of determining the crystallinity of celluloses have been proposed,[1] most of which suffer from the disadvantage that they are based on the study of extents or rates of chemical reactions and therefore the interpretation of the results which they yield in terms of structure necessarily involves assumptions. Of the physical techniques which study structure in a more direct way only the infrared-deuteration technique[2] seems to give a well defined crystallinity value. The density method suffers from the disadvantage that the density of amorphous cellulose is not known,[3] while a successful solution of the problem of determining crystallinities by x-ray diffraction has yet to be achieved.[4]

The fact that the different methods of determining crystallinity give different values has been cited as evidence that the simple crystalline-amorphous concept does not provide an adequate picture of cellulose structure.[5] However, although it has been suggested that it is necessary to take into account the existence of a continuous range of degrees of order to describe the structure of celluloses,[5] it is unfortunately true that no clear picture of structure has emerged from the experimental measurements which have been made. The main reason for this is probably that most measurements have been made by techniques which yield results of uncertain structural significance.

To provide a more definite and reliable picture of structure it seems desirable to use physical methods which study structure in a rather more direct way. In the present paper crystallinities of a regenerated cellulose determined by x-ray diffraction and by the infrared-deuteration technique are compared, and a study of hydrogen bonding in amorphous regions is reported.

* Present address: Plant Protection Ltd., Jealott's Hill Research Station, Bracknell, Berks, England.

† Present address: Shell Chemical Co. Ltd., Carrington Research Laboratory, Urmston, Manchester, England.

‡ Present address: Allied Chemical Corporation, Central Research Laboratory, Morristown, New Jersey.

EXPERIMENTAL

X-Ray Measurements

The x-ray diagrams were obtained with CuKα radiation monochromatized by reflection from a pentaerythritol crystal. A flat-plate vacuum camera was used to eliminate air scattering, the specimen–film distance being 10 cm.; the collimator was 0.8 mm. in diameter. The intensity of the x-ray beam was monitored by means of a Goppel-type camera in which reflections from a polyethylene sample were recorded near the center of the film.[6]

The samples were in the form of disks approximately 0.5 cm. in diameter and 1 mm. in thickness. In the case of powder samples these were prepared in a press by means of a circular die. Cellulose samples were prepared by cutting film with a special tool. The weights of the samples per unit area were measured on dry samples and were the same for different samples to within 5%; absorption of the x-ray beam was effectively constant therefore.

The x-ray diagrams were measured with a microdensitometer of a type previously described.[7]

Infrared Measurements

A Grubb-Parsons double-beam spectrometer equipped with a 60° lithium fluoride prism was used for measurements in the region 3600–2200 cm.$^{-1}$. A 60° rock salt prism was used for measurements at lower frequencies. For measurements of the shape of OD bands the strong absorption of atmospheric carbon dioxide near 4μ was reduced by placing trays of Carbosorb in the spectrometer casing and sweeping out with a stream of dry nitrogen.

The celluloses were examined as films approximately 3μ in thickness which were clamped between brass rings mounted in a brass cell fitted with calcium fluoride windows. Provision was made for passing a steady stream of D_2O vapor through the cell or alternatively for evacuating the cell through a liquid oxygen trap to dry the samples.

Titration of Cellulose

A film of viscose rayon weighing about 2 mg. was mounted in a brass cell fitted with calcium fluoride windows. The cell was connected to a vacuum line and source of T_2O by a standard cone and socket joint and a Pyrex glass tap lubricated with Apiezon N grease. The cell was evacuated, and T_2O vapor was then admitted (97 atom-% of tritium) at a pressure of 18 mm. and a temperature of 21°C. The total activity of tritium in the cell was about 0.5 curies. After 16 hr. the vapor was pumped out, the cell isolated and placed in a desiccated canister which was then sealed. It is estimated that the total energy absorbed by the cellulose was about 2×10^7 rad. The first spectrum was measured 9 hr. after the end of the tritiation experiment.

Samples

Viscose rayon films were prepared by spreading viscose solutions on glass plates followed by successive immersion in baths of 15% ammonium sulfate solution and 15% sulfuric acid solution. After washing the films in water, sulfur was removed by steeping the films in sodium sulfide solution, and the films were finally washed in distilled water.

Saponified secondary acetate films were regenerated from films of secondary cellulose acetate by a 2% solution of potassium hydroxide solution in a 50–50 mixture of water and methyl alcohol. They were washed in the same solvent and finally in water.

Viscose rayon film of increased crystallinity was obtained by steeping a viscose rayon film in 20% aqueous caustic soda solution and transferring it to boiling water.

Viscose rayon film was also modified by heating in water at 90°C. for one week.

Skin viscose rayon films were prepared from viscose solution containing a polyethylene oxide type modifier. The regeneration was carried out in a low acid, high zinc bath (6% acid, 8% zinc sulfate, and 12% sodium sulfate) at 50°C.

Bacterial cellulose was grown from *Acetobacter acetigenum*. It was purified by boiling in 1% caustic soda solution under oxygen-free nitrogen. The film was then washed successively in water, dilute hydrochloric acid, and finally water.

Ball-milled samples were prepared in a vibratory ball mill equipped with stainless steel balls and a stainless steel container. The samples did not discolor during this process.

The oligosaccharides were prepared by hydrolyzing Whatman's cellulose powder with fuming hydrochloric acid. The mixture of sugars was separated on an acid extracted charcoal–Celite column by Jermyn's method.[14] Crystalline oligosaccharides were recovered from solution by precipitation with acetone. The amorphous oligosaccharides were prepared by freeze-drying the solutions.

The oriented cellulose film was prepared by spontaneous extension of secondary cellulose acetate followed by regeneration in caustic soda solution.

RESULTS

X-Ray Diffraction

Scattering by Amorphous Cellulose. In order to determine the crystallinity of a polymer by x-ray diffraction it is necessary to be able to separate scattering by crystalline material from scattering by noncrystalline material. Since these two types of scattering overlap considerably in cellulose,[8] the first essential step is to establish a detailed shape for the scattering curve of amorphous cellulose. Ball-milled cellulose has been used by previous

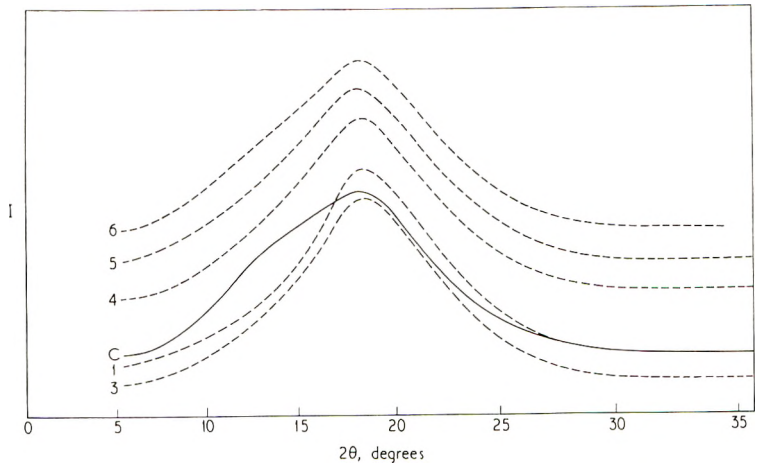

Fig. 1. Scattering curves of amorphous oligosaccharides and ball-milled cellulose (curves displaced along intensity axis): (*1*) glucose and cellobiose; (*3*) cellotriose; (*4*) cellotetraose; (*5*) cellopentaose; (*6*) cellohexaose; (*c*) ball-milled cellulose.

workers to provide this information. In the present work the products from ball-milling Fortisan and cotton fibers were found to show the same scattering curve within the experimental error; the mean curve is shown in Figure 1. It is evident therefore that ball-milled cellulose is a noncrystalline material, the scattering curve of which has the same shape, independent of the crystal lattice of the starting material. It is questionable however whether the scattering of ball-milled cellulose is typical of truly amorphous cellulose.

For this reason the scattering curves of amorphous oligosaccharides were compared with that of ball-milled cellulose with the results shown in Figure 1. It can be seen that the maxima of all the scattering curves are at the same angle and that their high-angle sides are very similar in shape. However there are differences in the shapes of the scattering curves on the low-angle sides of the maxima. The scattering curve of glucose is convex to the 2θ axis and there is a gradual transition in shape as the oligosaccharide series is ascended. The curve is almost a straight line with cellohexaose and becomes concave to the 2θ axis in cellulose. This gradual transition in the shape of the scattering curves suggests that the scattering curve of ball-milled cellulose is a close approximation to that from amorphous cellulose.

A similar trend in shape is found when cellulose is compared with its derivatives. This comparison is shown in Figure 2, where the scattering curves of ball-milled cellulose derivatives are reproduced. The curve for cellulose butyrate is reproduced from the work of Baker, Fuller, and Pape[9] and represents scattering by a quenched sample. All these curves represent scattering from the most highly disordered states of cellulose derivatives which it has been possible to obtain and they all show two peaks.

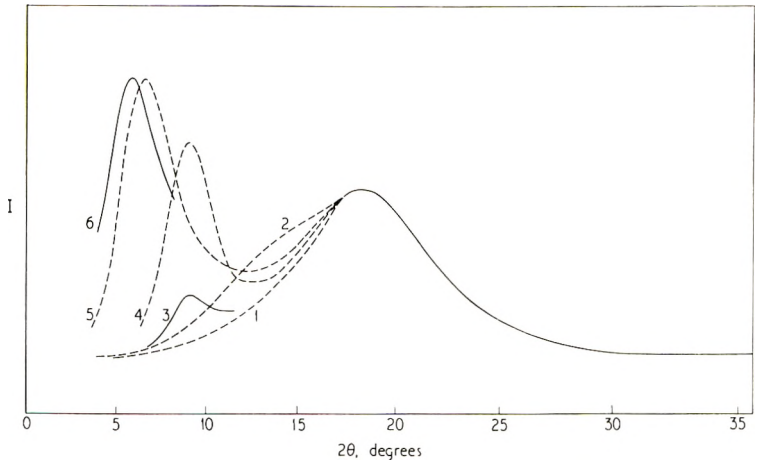

Fig. 2. Scattering curves of ball-milled cellulose and its derivatives: (*1*) Amorphous glucose; (*2*) cellulose; (*3*) sodium carboxymethyl cellulose; (*4*) methyl cellulose; (*5*) ethyl cellulose; (*6*) cellulose butyrate.

It can be seen that the peak at higher angles is at the same position and has the same shape in the different materials. The inner peak, however, is variable in position, and there is a gradual trend with the size of the substituent. As the substituent on the cellulose hydroxyl groups decreases in size, the peak moves to higher angles, corresponding to smaller spacings. It can be seen that the scattering curve of ball-milled cellulose represents a logical consequence of this trend, the shoulder on the low-angle side of the maximum being the analog of the resolved inner peak observed with the cellulose derivatives. In view of the relation between position of the inner peak and size of the substituent, it seems likely that this peak is connected with lateral spacings between long-chain molecules which are governed by the width of the molecules parallel to the "plane" of the glucose rings. The results again suggest that the scattering curve observed for ball-milled cellulose is a close approximation to that from amorphous cellulose.

These findings, however, do not show that the noncrystalline component of normal celluloses has an x-ray scattering curve which shows a similar shape. For this reason the diagram of a highly oriented cellulose, namely Fortisan H, was studied. On diagrams obtained from long exposure times a weak, diffuse halo is visible. This halo shows orientation and is strongest towards the equator, where it merges with the 002 and 101 crystalline reflections and extends out through the 021 reflections towards the meridian. By photometering the diagrams along directions at an angle to the equator it was possible to record the shape of this diffuse halo with little interference from crystalline reflections. The result of a photometric scan taken at 30° to the equator is shown in Figure 3, and it can be seen that the shape of the halo is very similar to the shape of the scattering curve for ball-milled cellulose. This finding confirms that there is a component of cellulose fibers

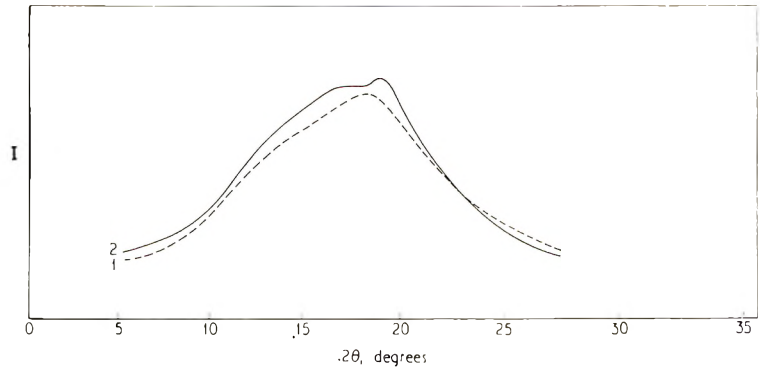

Fig. 3. Amorphous halo of Fortisan: (*1*) ball-milled cellulose; (*2*) Fortisan photometered at 30° to equator.

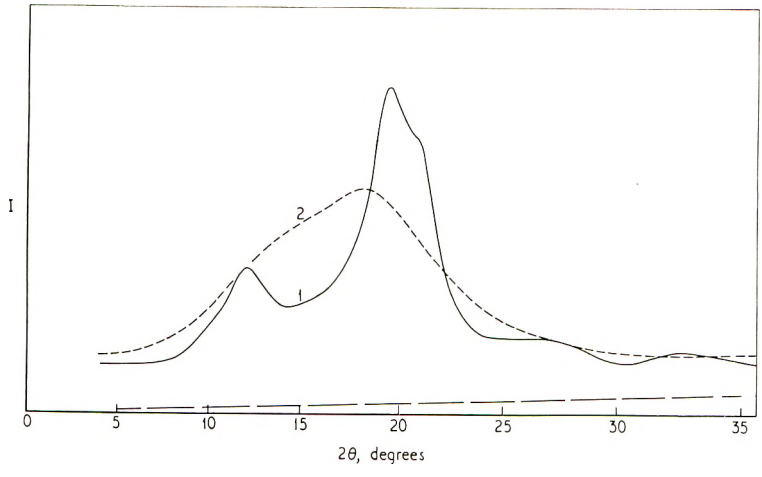

Fig. 4. Normalized scattering curves: (*1*) unoriented viscose rayon; (*2*) ball-milled cellulose.

which scatters x-rays in a way very similar to ball-milled cellulose and which may be termed amorphous cellulose.

Estimation of Crystallinity. The observations on band shapes of disordered materials suggest that a crystallinity can be determined for celluloses by use of ball-milled cellulose as a standard for 100% amorphous material. It must be admitted, however, that it has not been possible to show whether or not cellulose fibers show a component of scattering which has precisely the same shape as the scattering of ball-milled cellulose. For this reason, two standards for 100% amorphous cellulose have been used, amorphous cellotetraose and ball-milled cellulose.

The method used to determine crystallinity is similar to that used by Goppel and Arlman in their work on natural rubber.[6] The recorded scattering curves of cellulose film, ball-milled cellulose, and amorphous

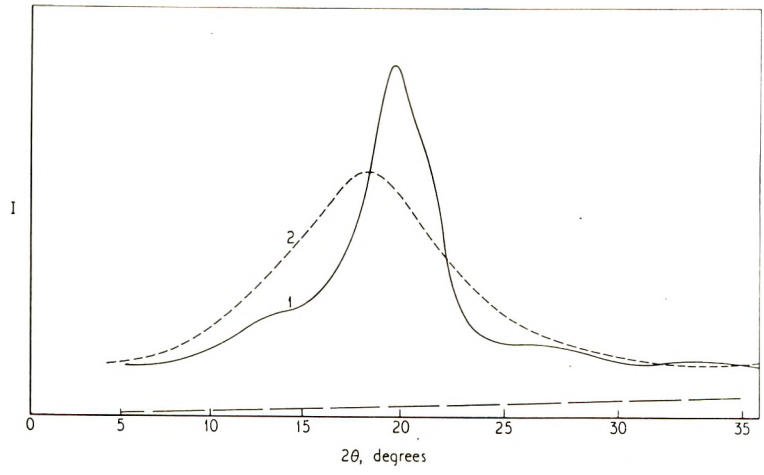

Fig. 5. Normalized scattering curves: (*1*) planar-oriented viscose rayon; (*2*) amorphous cellotetraose.

cellotetraose were converted to intensity of scattered radiation per unit weight of cellulose irradiated per unit amount of incident x-radiation. This was achieved by using the measured weights per unit area of the sample and the measure of incident x-ray intensity obtained from the polyethylene lines recorded near the center of the film in the small auxiliary camera. The curves shown in Figures 4 and 5 have been converted to this common basis. The level of incoherent radiation which is also shown was obtained by using the calculated data of Ellefsen et al.[8]

The amorphous content was determined by drawing in amorphous scattering curves under the total scattering curves of cellulose samples in such a way that the amorphous curves touched the total curve in the region between the 101 and $10\bar{1}$ reflections. The amorphous content was then taken to be equal to the ratio of the area under the drawn amorphous curve and the area under the corresponding normalized curve for 100% amorphous material. The results of determinations on unoriented and planar-oriented viscose rayon films are shown in Table I.

The planar-oriented cellulose was included in this work since the minimum crystallinity value is influenced by any overlap between the tail of the

TABLE I
Percentage Crystallinities of Viscose Rayon Films

	X-Ray crystallinity, %		
Amorphous standard	Unoriented films	Planar-oriented film	Infrared crystallinity, %
Ball-milled cellulose	43	43	26
Amorphous cellotetraose	40	42	26

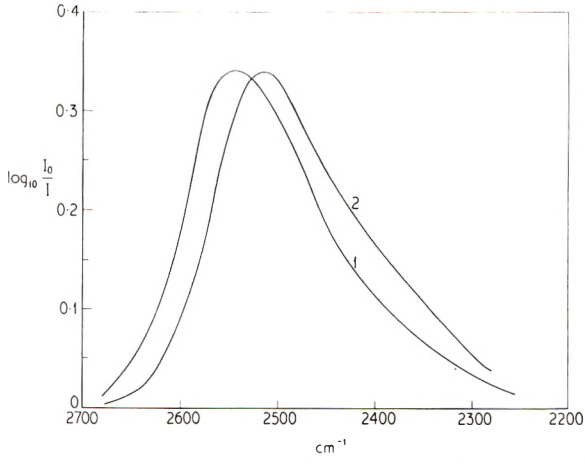

Fig. 6. OD bands of celluloses: (*1*) regenerated cellulose; (*2*) bacterial cellulose.

101 reflection and the tail of the $10\bar{1}$ reflection, and, since the planar-oriented film shows only a weak 101 reflection, it was thought possible that the minimum crystallinity figure might be higher with the oriented film than with the unoriented film. In fact the crystallinities are not very different. This implies either that there is little overlap between the 101 and $10\bar{1}$ reflections or that the reduction in intensity of the 101 reflection is offset by the increase in the intensity of the $10\bar{1}$ reflection.

Infrared Spectra

Measurement of the true shape of the OD bands of celluloses in which OH groups in amorphous regions have been deuterated is complicated by the fact that undeuterated celluloses show absorption in this region. The extent and nature of this absorption is shown in previously published spectra.[2] This absorption cannot be used as the background from which to measure the OD absorption because part of it is caused by OH groups in amorphous regions and is therefore removed on deuteration. To overcome this difficulty and to obtain a measure of the change in this absorption, an exchange reaction was carried out with the vapor of tritium oxide instead of deuterium oxide. By this procedure accessible OH groups were converted into OT groups which absorb near 2100 cm.$^{-1}$, so leaving the 2500 cm.$^{-1}$ region clear. The residual absorption in the 2500 cm.$^{-1}$ region measured in this way was taken into account in determining the OD band shapes of regenerated celluloses. No significant differences were found in the band shapes of the five regenerated celluloses studied, and the band shown in Figure 6 represents the mean of the measurements on all five celluloses. This band shape was also found to be independent of the extent of deuteration of OH groups in amorphous regions of the sample.

In the case of the bacterial cellulose band shown in Figure 6 the absorption of the undeuterated material was used as the background from which

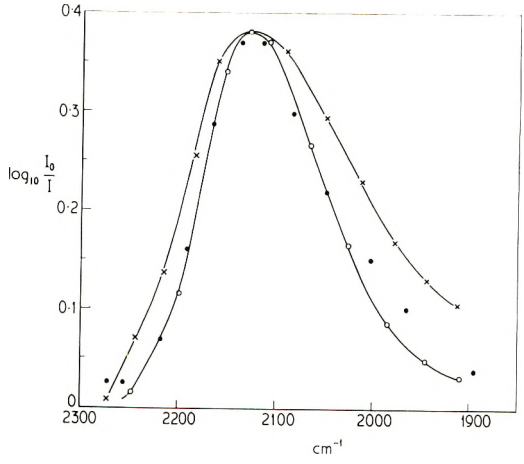

Fig. 7. Bands of tritiated cellulose: (○) OT band; (●) OD band (transposed); (×) OH band 30 days after tritiation (transposed).

to measure OD absorption. No allowance was made for the reduction in this background which must occur on deuteration since bacterial cellulose has a high crystallinity and the correction for this effect would be small. Neglect of this correction could not account for the differences between regenerated celluloses and bacterial cellulose which are discussed in the next section.

Figure 7 shows the band due to stretching of the OT groups introduced into cellulose by tritiation; the OH band was considerably reduced in intensity and showed the characteristic absorption pattern of crystalline material. The OT band is clearly due to OT groups in amorphous regions and is similar in shape to the corresponding band of OD groups in deuterated cellulose. The OD band is also shown in Figure 7 transposed by the appropriate frequency factor. The ratio of the peak frequency of the OT band (2126 cm.$^{-1}$) to that of the OD band (2527 cm.$^{-1}$) is 0.841, which is of the order expected from the mass ratio of deuterium to tritium. For harmonic oscillators the frequency ratio should be 0.816.

On storing the cellulose changes occurred in its spectrum. The OT band became weaker and a new band appeared at 1735 cm.$^{-1}$ with a shoulder at 1625 cm.$^{-1}$. The OH band at first increased in intensity but after about 10 days began to decrease in intensity. Over a period of 3 months there was little change in the optical density of the CH band, apart from the appearance of a shoulder at 2880 cm.$^{-1}$.

The rate of decrease of the OT band was far too high to be attributed to radioactive decay; thus the optical density was reduced by 50% in 10 days, whereas the halflife time of tritium is 12.5 yr. It seems certain, therefore, that the reduction in the OT band and the accompanying increase in the OH band were caused by a reversal of the exchange reaction. Changes also occurred in the crystallinity of the film, since the OH band showed no sign of its original crystalline component. This band is shown

in Figure 7 transposed by the appropriate frequency factor for comparison with the OT and OD bands. The film itself appeared to become brittle and cracked. There is little information available on the action of β-particles on cellulose, but it is known that large doses of γ-radiation produce a drop in the degree of polymerization.[10]

The band at 1735 cm.$^{-1}$ can be attributed to the introduction of carbonyl groups. Spedding[11] reports a strong band at 1734 cm.$^{-1}$ in cellulose which has been oxidized by periodate. Carbonyl groups formed at the expense of hydroxyl groups would explain why the optical density of the OH band falls after first increasing owing to rehydrogenation. The production of carbonyl groups is presumably initiated by β-particles expelled from decaying tritium atoms and it is clear that the quantum yield must be much larger than unity, since only a small fraction of the tritium can have decayed during the period of the experiment.

DISCUSSION

Previous work[2] has shown that the infrared-deuteration technique allows a well defined crystallinity determination to be made on cellulose. This crystallinity is defined as the fraction of OH groups which are hydrogen-bonded in the regular manner characteristic of crystalline material and which therefore give well defined infrared absorption bands. The amorphous portion is defined as the fraction of OH groups which are hydrogen-bonded in the irregular manner of disordered material and which therefore give a broad, diffuse, absorption band.

In the case of the x-ray diffraction technique, however, no such well defined crystallinity can be determined. The basic reason for this is that the scattering from crystalline and noncrystalline material overlap and it is doubtful whether there is any angle at which crystalline or noncrystalline scattering can be measured with no interference from the other. In these circumstances a unique separation of the total scattering into scattering from the two types of material can be made only if the detailed shapes of the two types of scattering are known.

The observations on ball-milled cellulose, amorphous oligosaccharides, and the diffuse halo of Fortisan II have led to a shape which can be used as a reliable approximation for the scattering by the noncrystalline component. However, lack of knowledge of the detailed shape of scattering by crystalline material allows a wide range of crystallinities to be determined according to the assumptions which are made about the form of this scattering.[4] Thus, at the present state of knowledge, the x-ray diagram of a cellulose is consistent with a range of contents of crystalline material.

A maximum can be fixed for the content of noncrystalline material, however, by making use of the fact that it is impossible for the noncrystalline component to scatter more radiation at any angle than the total radiation scattered by the sample. This maximum can be fixed by separating the total scattering curve into scattering by crystalline and non-

crystalline material in such a way that the scattering curve of noncrystalline material touches the total scattering curve at some point. This is the procedure used by Ellefsen et al.[8] in determining "amorphicities" of celluloses, and the crystallinities recorded in Table I were determined in this way.

The crystallinities in Table I represent, therefore, the minimum crystallinities consistent with the observed x-ray diagrams, and the true crystallinities cannot be smaller than those measured. It is evident on comparing x-ray crystallinities with the infrared-deuteration crystallinities also shown in Table I that there is a large discrepancy between them. Since the x-ray crystallinity is the larger of the two, this discrepancy must be significant.

When the definition of the infrared-deuteration crystallinities is remembered one reason for such a discrepancy becomes clear. Some of the OH groups of chains which lie in the surface of crystallites will be readily accessible to D_2O and will therefore deuterate rapidly. The OD band of deuterated celluloses shows no structure, and this implies that the vast majority of OH groups which lie in the surface of crystallites do not exhibit the sharp bands characteristic of OH groups in crystalline regions. Conversely, the fact that OH groups which show the characteristic absorption pattern of crystalline material deuterate slowly implies that they are protected from easy access by D_2O by being in the interior of the crystallites.

The difference between the infrared-deuteration crystallinity of 26% and the minimum x-ray crystallinity of 40% implies that 35% of the material which is measured as being crystalline by x-ray diffraction is hydrogen-bonded in an irregular manner and is counted as amorphous material by the infrared method. Now cellulose crystallites are agreed to be tabular in shape with the (101) plane forming the plate face.[12] From the known unit cell dimensions and inclinations of the glucose rings in the unit cell it can be calculated that crystallites 29 A. × 65 A. would have 35% of their OH groups in their surfaces. These figures are similar to those reported for cellulose crystallites from electron microscope observations,[12] and it follows therefore that on this basis the discrepancy between the infrared-deuteration and the x-ray crystallinities can be accounted for in terms of crystallite size. However, it must be remembered that although a crystallite thickness of 29 A. is consistent with electron microscope observations, it implies that crystallites are only 4 glucose units thick. It seems doubtful to the authors whether the broadening of the x-ray reflections is consistent with such a small thickness, i.e., only two unit cells.

The fact that 35% of the material registered as crystalline by x-ray diffraction does not show the sharp infrared absorption bands characteristic of crystalline material has an important bearing on the validity of the simple crystalline-amorphous concept of cellulose structure. The two sharp infrared bands of crystalline cellulose at 3484 and 3444 cm.$^{-1}$ are due to intramolecular hydrogen bands between the two glucose groups of the cellobiose repeating unit and hence characterize molecular form.[13]

It follows that a substantial fraction of the material registered as crystalline by x-ray diffraction does not have the precise molecular configuration typical of chains in crystalline regions. Thus the observations show that a substantial fraction of material in a regenerated cellulose cannot be characterized as being truly crystalline or truly amorphous and that the simple crystalline-amorphous concept does not provide an adequate explanation of cellulose structure. The extent to which the material of intermediate order departs from the precise molecular configuration characteristic of chains in crystalline regions is uncertain. The distortion may not be very large, however, in view of the sensitivity of the lengths of the intramolecular hydrogen bands ($O_3 \rightarrow O_5$[1]) to rotations of the glucose units around the C—O bands which join successive glucose units.

The fact that part of the material characterized as amorphous by infrared is not truly amorphous material suggests that the infrared amorphous portion may vary in structure from one cellulose to another. The shape of the amorphous OD band is closely connected with the distribution of strengths of hydrogen bands formed by these OD (or OH) groups and therefore provides a way in which the structure of the infrared amorphous material can be investigated. Differences in structure between different celluloses would be expected to be reflected in differences in the shapes of their amorphous OD bands.

The results of measurements of OD band shapes on regenerated celluloses show that no significant differences exist among the five materials examined. The OD band of bacterial cellulose is, however, significantly different from the bands of the regenerated celluloses. Although the shapes of the bands are similar, the band of bacterial cellulose is shifted by 25–30 wave numbers to lower frequencies. This suggests that the average hydrogen-bond strength of OH (OD) groups in bacterial cellulose is greater than the average strength in the regenerated celluloses. The fact that no differences could be found between the regenerated celluloses may be due to the fact that they did not differ greatly in crystallinity. The bacterial cellulose, on the other hand, represents not only a cellulose with a different crystal lattice but also a cellulose which has a crystallinity much higher than that of the regenerated celluloses.[2]

Since the material which is crystalline to x-ray diffraction but amorphous to infrared must be oriented in a cellulose which is highly oriented, its presence might also be revealed in infrared dichroism of the amorphous OD band. Preliminary measurements of infrared dichroism have shown that the amorphous OD band of a highly oriented regenerated cellulose is in fact dichroic. In the frequency range corresponding to the two sharp absorption bands of crystalline cellulose, the amorphous OD band showed parallel dichroism. Since the two sharp bands of crystalline cellulose also show parallel dichroism,[13] it seems possible that the absorption bands of the material of intermediate order in this frequency region are a blurred version of the bands of crystalline cellulose. This view is consistent with

the conclusion that the molecular chains in the material of intermediate order are distorted from the precise molecular configuration of perfectly crystalline material, since the two sharp bands characterize molecular form. It is also consistent with the difference found between regenerated and bacterial celluloses, since the strongest bands of crystalline material are at a lower frequency in bacterial cellulose than in regenerated cellulose.

The findings on material of intermediate order and on variations in the distribution of hydrogen-bond strengths in different celluloses seem at first sight to provide a striking confirmation of the theories of Howsman[5] regarding cellulose structure, since these two features are integral parts of his theory. However, in the theory of Howsman[5] the material of intermediate order lies not in the surfaces of crystallites but in the chains which join two adjacent crystallites. It has been shown above that the amount of material of intermediate order found in the present work can be attributed entirely to material in the surfaces of crystallites. In order to provide a more rigorous test of Howsman's theory by the methods outlined in the present paper it seems desirable to specify more accurately the size of crystallites, since the dimensions used in analyzing the results represent minimum dimensions. In addition, the x-ray crystallinities measured in the present work represent minimum values, and the development of an x-ray method which measures crystallinity more precisely seems desirable. The key to this problem lies in fixing the shape of the scattering from crystalline regions more accurately.

The authors wish to acknowledge the help of Dr. E. J. Wilson of the Radiochemical Centre, Amersham who carried out the tritiation, and Dr. K. Gray of Courtaulds Limited, who supplied the samples of skin viscose rayon.

References

1. Howsman, J. A., and W. A. Sisson, in *Cellulose and Cellulose Derivatives*, Part I, E. Ott, H. M. Spurlin, and M. W. Grafflin, Eds., Interscience, New York, 1954, p. 231.

2. Mann, J., and H. J. Marrinan, *Trans. Faraday Soc.*, **52,** 481 (1956).

3. Hermans, P. H., *Physics and Chemistry of Cellulose Fibres*, Elsevier, Amsterdam, 1949, p. 205.

4. Gjönnes J., N. Norman, and H. Viervol, *Acta Chem. Scand.*, **12,** 489 (1958).

5. Howsman, J. A., and W. A. Sisson, in *Cellulose and Cellulose Derivatives*, Part I, E. Ott, H. M. Spurlin, and M. W. Grafflin, Eds., Interscience, New York, 1954, pp. 251, 277; J. A. Howsman and R. H. Marchessault, *Textile Research J.*, **27,** 30 (1957).

6. Goppel, J. M., *Appl. Sci. Research*, **A1,** 3 (1949); J. M. Goppel and J. J. Arlman, *Appl. Sci. Research*, **A1,** 462 (1949).

7. Mann, J., L. Roldan-Gonzalez, and H. J. Wellard, *J. Polymer Sci.*, **62,** 165 (1960).

8. Ellefsen, O., E. W. Lund, B. A. Tonnesen, and K. Oien, *Norsk Skogind.*, **11,** 284, 349 (1957).

9. Baker, W. O., C. S. Fuller, and N. R. Pape, *J. Am. Chem. Soc.*, **64,** 776 (1942).

10. Clegg, R. E., and K. I. Kertesz, *J. Polymer Sci.*, **26,** 289 (1957).

11. Spedding, H., *J. Chem. Soc.*, **1960,** 3147.

12. Mukherjee, S. M., and H. J. Woods, *Biochim. Biophys. Acta*, **10,** 449 (1953).

13. Mann, J., and H. J. Marrinan, *J. Polymer Sci.*, **32,** 357 (1958).

14. Jermyn, M. A., *Australian J. Chem.*, **10,** 55 (1957).

Synopsis

Observations on the x-ray scattering by ball-milled cellulose and cellulose derivatives, amorphous oligosaccharides, and Fortisan H are reported and an approximate shape is established for the scattering curve of the noncrystalline component of celluloses. Using this shape measurements have been made of the minimum crystallinity which is consistent with the observed x-ray diagram of regenerated cellulose.

From a comparison of this minimum crystallinity with crystallinity determined by the infrared-deuteration method, it is concluded that at least 14% of the total material cannot be truly described as either perfectly crystalline or perfectly amorphous. This fraction of material of intermediate order is registered as crystalline by x-ray diffraction, but infrared spectroscopy suggests that it does not possess the precise molecular configuration characteristic of crystalline material. Support for this view of structure is reported from observations of differences in hydrogen-bonding in amorphous regions of regenerated and bacterial celluloses. Infrared results show that OH groups which lie in the surface of crystallites are hydrogen-bonded in a random amorphous manner and it is concluded that the material of intermediate order can be accounted for in terms of chains lying in the surface of crystallites of cross-section 29 A. × 65 A.

Résumé

Des observations sur la diffusion des rayons-X par la cellulose broyée, les dérivés de la cellulose, les oligosaccharides amorphes et la Fortisan H sont rapportées; on a établi la forme approximative de la courbe de diffusion du constituant non-cristallin des celluloses. En se servant de cette courbe, on a mesuré la cristallinité minimum qui est en accord avec le diagramme observé aux rayons-X dans le cas de la cellulose régénérée. En comparant cette cristallinité minimum avec la cristallinité déterminée par la méthode infrarouge se basant sur la réaction d'échange avec le deutérium, on peut conclure qu'il existe au moins 14% de l'ensemble de la substance qui ne peut être considéré avec exactitude ni comme parfaitement cristallin ni comme parfaitement amorphe. Cette fraction de la substance qui est d'ordre "intermédiaire" est enrégistrée comme cristalline par la diffraction des rayons-X, mais la spectroscopie infrarouge fait penser qu'elle ne possède pas la configuration moléculaire précise caractéristique d'une substance cristalline. Cette façon d'envisager la structure est confirmée par les différences observées pour les liens hydrogène des régions "amorphes" de la cellulose régénérée et de la cellulose bactérielle. Les résultats de l'infrarouge montrent que les groupes OH qui se trouvent à la surface des cristallites présentent des liens hydrogène statistiques et amorphes et on conclut que la substance d'ordre intermédiaire peut être expliquée en considérant qu'il y a des chaînes à la surface de cristallites ayant une section transversale de 29 A. × 65 A.

Zusammenfassung

In der Kugelmühle gemahlene Cellulose und Cellulosederivate, amorphe Oligosaccharide und Fortisan H werden in bezug auf ihre Röntgenstreuung untersucht und die ungefähre Gestalt der Streukurve der nichtkristallinen Komponente der Cellulose wird aufgestellt. Unter Verwendung dieser Kurve wurde eine Bestimmung der Mindestkristallinität durchgeführt, die mit dem beobachteten Röntgendiagramm von regenerierter Cellulose vereinbar ist. Durch einen Vergleich dieser Mindestkristallinität mit der mittels der Infrarot-Deuterierungsmethode ermittelten Kristallinität wurde festgestellt, dass mindestens 14% des Gesamtmaterials exakt weder als vollkommen kristallin noch als vollkommen amorph beschrieben werden können. Dieser Materialanteil mit "mittlerer" Ordnung wird durch Röntgenstreuung als kristallin erfasst, die Infrarotspektroskopie weist jedoch darauf hin, dass er nicht die exakte molekulare Konfigurationscharakteristik eines kristallinen Materials besitzt. Unterstützt wird diese Ansicht über die Struktur durch Beobachtung von Unterschieden in der Wasser-

stoffbindung in "amorphen" Bereichen von regenerierter und bakterieller Cellulose Infrarotdaten zeigen, dass an der Oberfläche der Kristallite liegende OH-Gruppen Wasserstoffbindungen von statistischem, amorphen Charakter bilden; es wird geschlossen, dass das Material mit mittlerer Ordnung durch die Annahme von Ketten in der Oberfläche der Kristallite mit einem Querschnitt von 29 A. × 65 A. beschrieben werden kann.

Received September 25, 1961

JOURNAL OF POLYMER SCIENCE: PART A VOL. 1, PP. 687–703 (1963)

Termination of the Anionic Polymerization of Acrylonitrile at Low Catalyst Concentrations*

ARIEL OTTOLENGHI and ALBERT ZILKHA, *Department of Organic Chemistry, The Hebrew University, Jerusalem, Israel*

INTRODUCTION

The anionic polymerization of acrylonitrile in different systems, such as, butyllithium in petroleum ether,[1] metal ketyls in tetrahydrofuran,[2] sodiomalonic ester in dimethylformamide,[3] and quaternary ammonium hydroxides in dimethylformamide,[4] has already been studied. In all these systems the termination step in the mechanism of the polymerization is believed to be by chain transfer to monomer, as proved by the independence of the molecular weights obtained of both catalyst and monomer concentrations.

In the course of studying the acrylonitrile polymerization by electron transfer catalysts, such as sodium naphthalene or anthracene, it was found[5] that at low catalyst concentrations, the molecular weights increased with increasing monomer concentration and decreased with increasing catalyst concentration, i.e., the principle of termination by chain transfer to monomer is not being followed. Since these catalysts are able to initiate polymerization either anionically or radically, the cause for the increase in molecular weight at low catalyst concentrations may be due either to the radical or to the anionic mechanism. To verify this point, we undertook the study of the homogeneous polymerization of acrylonitrile in dimethylformamide by the classical anionic catalyst butyllithium, especially at relatively very low catalyst concentrations, which had not been investigated before. Dimethylformamide was chosen as the solvent for this polymerization because, contrary to other solvents, it led to high conversions even with very small catalyst concentrations.

RESULTS

The effect of the *n*-butyllithium concentration on the acrylonitrile polymerization in dimethylformamide was studied at three different monomer concentrations (Table I): (A), 0.45 mole/l.; (B), 0.90 mole/l.; and (C), 1.80 mole/l., and at different temperatures (Table II).

* Part of a Ph.D. Thesis to be submitted by A. Ottolenghi to the Hebrew University, Jerusalem.

TABLE I Effect of Catalyst Concentration on the Polymerization of Acrylonitrile[a]

Run no.	Amt. catalyst, mmole	[Catalyst], mmole/l.	Yield, %	$[\eta]$, dl./g.	$\overline{M}_w$	[Monomer]/[Catalyst]
Series A[b]						
10	0.056	1.12	45	0.198	8,000	400
11	0.056	1.12	40	0.198	8,000	400
2	0.112	2.24	90	0.188	7,500	201
48	0.112	2.24	95	0.194	7,800	201
51	0.125	2.50	95	0.178	7,000	180
34	0.225	4.50	95	0.122	4,200	100
33	0.450	9.00	90	0.106	3,500	50
24	3.400	68.00	95	0.085	2,600	6.6
25	3.400	68.00	100	0.078	2,350	6.6
Series B[c]						
6	0.056	1.12	60	0.392	20,000	800
5	0.112	2.24	90	0.348	17,000	403
15	0.112	2.24	90	0.336	16,300	403
38	0.125	2.50	90	0.320	15,200	360
39	0.125	2.50	85	0.302	14,100	360
44	0.125	2.50	90	0.325	15,600	360
4	0.225	4.50	85	0.236	10,200	200
19	0.450	9.00	90	0.190	7,600	100
13	0.900	18.00	90	0.128	4,500	50
8	1.700	34.00	100	0.110	3,700	26.5
9	1.700	34.00	95	0.106	3,500	26.5
22	3.400	68.00	100	0.087	2,700	13.2
23	3.400	68.00	100	0.085	2,600	13.2
29[d]	3.400	68.00	100	0.075	2,200	13.2
28[e]	3.400	68.00	90	0.074	2,150	—
57[e]	3.400	68.00	85	0.085	2,600	—
Series C[f]						
7	0.056	1.12	40	0.642	38,600	1,614
3	0.112	2.24	90	0.592	34,700	807
16	0.125	2.50	85	0.552	31,600	723
17	0.125	2.50	90	0.578	33,600	723
18	0.125	2.50	95	0.580	33,800	723
36	0.225	4.50	95	0.366	18,250	401
35	0.450	9.00	100	0.338	16,400	200
37	0.450	9.00	100	0.300	14,000	200
14	0.900	18.00	95	0.204	8,400	100
30	1.700	34.00	100	0.152	5,650	53
26	3.400	68.00	100	0.106	3,500	26.5
27	3.400	68.00	100	0.099	3,200	26.5
53	6.500	130.00	95	0.078	2,350	13.8
54	6.500	130.00	90	0.074	2,150	13.8

[a] The polymerizations were carried out by adding catalyst in petroleum ether to the monomer dissolved in dimethylformamide. The total volume of monomer, petroleum ether (2 ml.), and dimethylformamide was kept constant (50 ml.). Polymerization temp. 0 ± 2°C.; time 15 min.

[b] Monomer used 1.5 ml.; 0.45 mole/l.

[c] Monomer used 3 ml.; 0.90 mole/l.

[d] After 15 min. another 3 ml. monomer were added; the polymerization was stopped 15 min. later; the yield was 100% based on the total amount of monomer (6 ml., 1.80 mole/l.).

[e] The monomer was added dropwise during 5 min.

[f] Monomer used 6 ml.; 1.80 mole/l.

TABLE II
Effect of Temperature on the Polymerization of Acrylonitrile[a]

Run no.	Temp.,	[Monomer], mole/l.	[Catalyst], mmole/l.	Yield, %	$[\eta]$, dl./g.	$\bar{M}_w$
8	0	0.90	34.00	100	0.110	3,700
9	0	0.90	34.00	95	0.106	3,500
59	−50	0.90	34.00	95	0.304	14,200
60	−50	0.90	34.00	100	0.310	14,600
28[b]	0	0.90	68.00	90	0.074	2,150
57[b]	0	0.90	68.00	85	0.085	2,600
55[b]	−50	0.90	68.00	95	0.204	8,400
56[b]	−50	0.90	68.00	100	0.208	8,600
39	0	0.90	2.50	85	0.302	14,100
44	0	0.90	2.50	90	0.325	15,600
20	−30	0.90	2.50	85	0.518	29,000
21	−30	0.90	2.50	90	0.528	29,700
40	−50	0.90	2.50	38	0.584	34,000
41[c]	−50	0.90	2.50	45	0.606	35,700
42[d]	−50	0.90	2.50	42	0.606	35,700
43	−50	0.90	2.50	35	0.552	31,600
16	0	1.80	2.50	85	0.552	31,600
17	0	1.80	2.50	90	0.578	33,600
18	0	1.80	2.50	95	0.580	33,800
45	−50	1.80	2.50	40	0.678	41,500
46	−50	1.80	2.50	45	0.730	45,800

[a] The experiments were carried out as described in Table I. Reaction time for experiments carried out at −30 or −50°C. was 30 min. and for those at 0°C., 15 min.

[b] The monomer was added dropwise during 5 min.

[c] After 30 min. another 3 ml. monomer was added; the polymerization was stopped 30 min. later; the yield was 45% based on the total amount of monomer (6 ml.) i.e., about 45% of the added monomer was polymerized.

[d] Polymerizations carried out for 60 min.

Effect of Catalyst

The effect of the catalyst on the molecular weight was studied on a wide range of concentrations, at each of the above monomer concentrations, under otherwsie constant conditions. At the low catalyst concentrations, increase of catalyst concentration was accompanied by a decrease in molecular weight. The molecular weight became constant at the high catalyst concentrations (Table I and Fig. 1).

Effect of Monomer

At relatively high catalyst concentrations of about 70 mmole/l. and above, the molecular weights obtained were the same for the three monomer concentrations investigated. The same molecular weight was obtained when monomer was slowly dropped on to the catalyst so that only a very low concentration of it was present. However, at relatively low catalyst concentrations of about 2.5 mmole/l. there was a sharp increase in molecular weight with increase in monomer concentration. This increase is linear

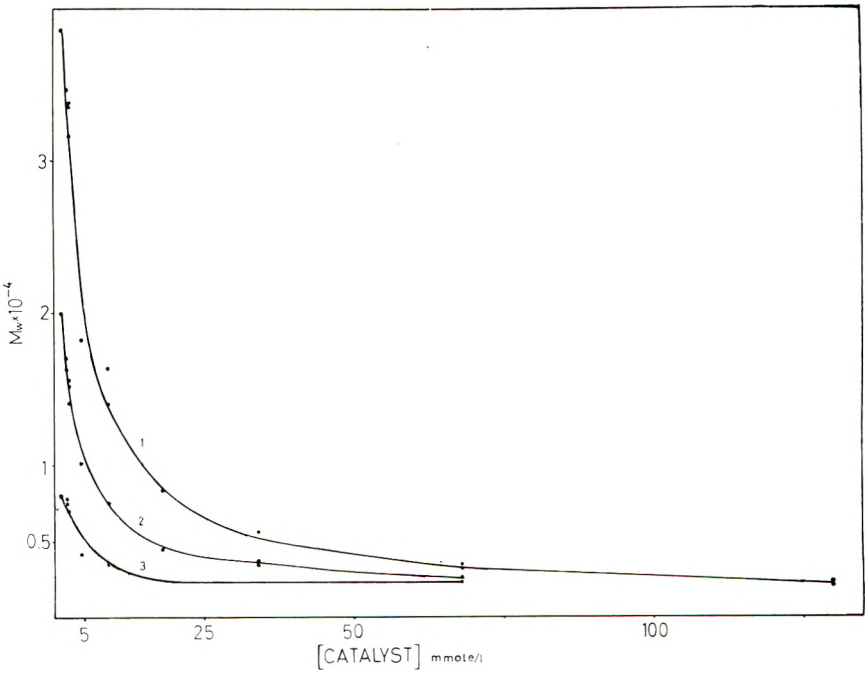

Fig. 1. Dependence of molecular weight on catalyst concentration at various initial monomer concentrations: (*1*) 1.80 mole/l.; (*2*) 0.90 mole/l.; (*3*) 0.45 mole/l.

(Fig. 2). Thus, a fourfold increase in monomer concentration gave approximately a fourfold increase in molecular weight. Between these two extreme concentrations there was a smaller increase in molecular weight with increase in monomer concentration.

Effect of Temperature

The effect of temperature on molecular weight was investigated at 0, −30, and −50°C. under otherwise constant conditions (Table II). It was found that the increase in molecular weight with the decrease in temperature was more pronounced in polymerizations at high catalyst concentrations than in those carried out at low catalyst concentrations. Thus, at monomer concentration of 0.90 mole/l. and 34 mmole/l. catalyst (runs 59 and 60 at −50°C.; runs 8 and 9 at 0°C.), the molecular weight obtained at −50°C. was higher by some 400% than that obtained at 0°C. A similar change of molecular weight with temperature was obtained when monomer (0.90 mole/l.) was slowly dropped on to 68 mmole/l. catalyst (runs 55 and 56 at −50°C.; runs 28 and 57 at 0°C.). A semilogarithmic plot of molecular weight against the reciprocal of the polymerization temperature gave a straight line whose slope corresponds to a difference in activation energy between propagation and termination of 4 kcal./mole.

At the same monomer concentration and with a decrease of catalyst concentration to 2.5 mmole/l. the increase in molecular weight between

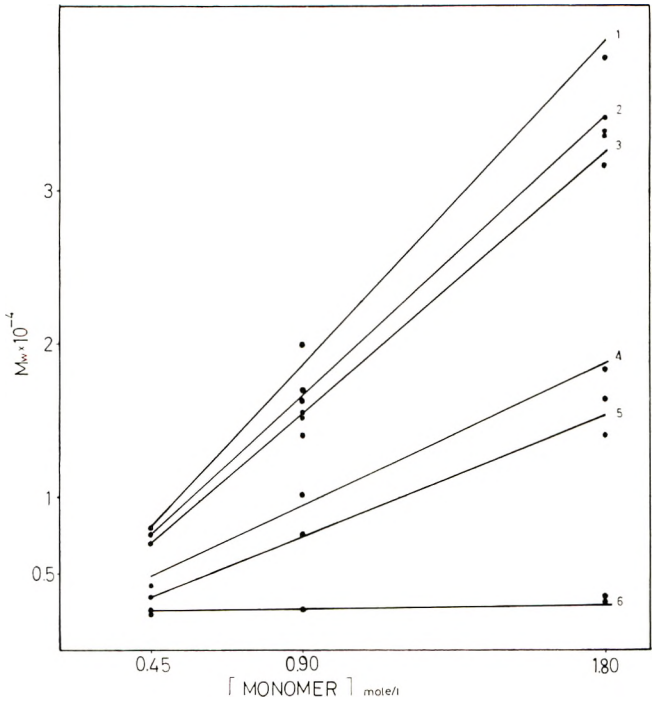

Fig. 2. Dependence of molecular weight on monomer concentration at various initial catalyst concentrations: (*1*) 1.12 mmole/l.; (*2*) 2.24 mmole/l.; (*3*) 2.50 mmole/l.; (*4*) 4.50 mmole/l.; (*5*) 9.00 mmole/l.; (*6*) 68.00 mmole/l.

the two temperatures was smaller: about 250% (runs 40 and 42 at −50°C.; runs 39 and 44 at 0°C.). However, when the last conditions were kept constant and only a greater monomer concentration 1.80 mole/l. was used, the change in the molecular weights was still smaller: about 25% (runs 45 and 46 at −50°C.; runs 16 and 17 at 0°C.). At −30°C. intermediate values were obtained.

Effect of the Degree of Conversion on Molecular Weight

At low catalyst concentrations, the molecular weight was found to increase linearly with the per cent conversion (or the concentration of monomer consumed) up to about 30–50% independently of polymerization temperature; then the molecular weight remains approximately constant with per cent conversion. The point of deviation from linearity depends upon the polymerization temperature and monomer concentration (Table III and Fig. 3).

The results also show (Fig. 3) that for polymerizations carried out at 0°C., all molecular weights obtained at 30% conversion and above can be safely compared between themselves, as conversion then has no effect on the molecular weight.

TABLE III
Dependence of Molecular Weight on Per Cent Conversion[a]

Run no.	[Monomer], mole/l.	Temp., °C.	Conversion, %	[η], dl./g.	$\bar{M}_w$
9k	1.80	−30	3[b]	0.248	10,900
7k	1.80	−30	5	0.258	11,500
8k	1.80	−30	15	0.415	21,600
3k	1.80	0	17[c]	0.436	23,100
6k	1.80	0	18	0.442	23,500
10k	1.80	−30	21	0.483	26,300
2k	1.80	0	25	0.496	27,400
1k	1.80	0	29	0.544	31,000
45	1.80	−50	40	0.678	41,500
46	1.80	−50	45	0.730	45,800
16	1.80	0	85	0.552	31,600
17	1.80	0	90	0.578	33,600
18	1.80	0	95	0.580	33,800
4k	0.90	−30	7.5	0.306	14,400
5k	0.90	−30	13	0.324	15,500
11k	0.90	−30	16	0.426	22,400
12k	0.90	−30	17.5	0.463	25,000
13k	0.90	−30	22	0.464	25,100
14k	0.90	−30	26	0.538	30,500
15k	0.90	−30	39	0.504	28,000
43	0.90	−50	35	0.552	31,600
40	0.90	−50	38	0.584	34,000
42	0.90	−50	42	0.606	35,700
38	0.90	0	90	0.320	15,200
39	0.90	0	85	0.302	14,100
44	0.90	0	90	0.325	15,600
20	0.90	−30	85	0.518	29,000
21	0.90	−30	90	0.528	29,700

[a] Catalyst concentration was held constant (0.125 mmole, 2.50 mmole/l.), other conditions as in Table I (except time of polymerization).

[b] Polymer obtained after 60 sec.

[c] Polymer obtained after 6 sec.

Catalyst Consumption

Had all the catalyst molecules started polymerization, the maximum molecular weight obtainable should have been determined by the monomer/catalyst ratio [M]/[C].

At the high catalyst concentrations, the molecular weights obtained can be seen to be much higher than those theoretically calculated according to [M]/[C]. This fact indicates clearly that not all the catalyst starts polymerization, i.e., free active carbanions, either as catalyst molecules or as active monomer anions, formed by chain transfer, are still present at the end of the polymerization. Evidences for this conclusion are supported either by the results of runs 28 and 57 (Table I-B) in which monomer was dropped on to the catalyst and the molecular weights obtained were nevertheless the same and by run 29 (Table I-B), where monomer

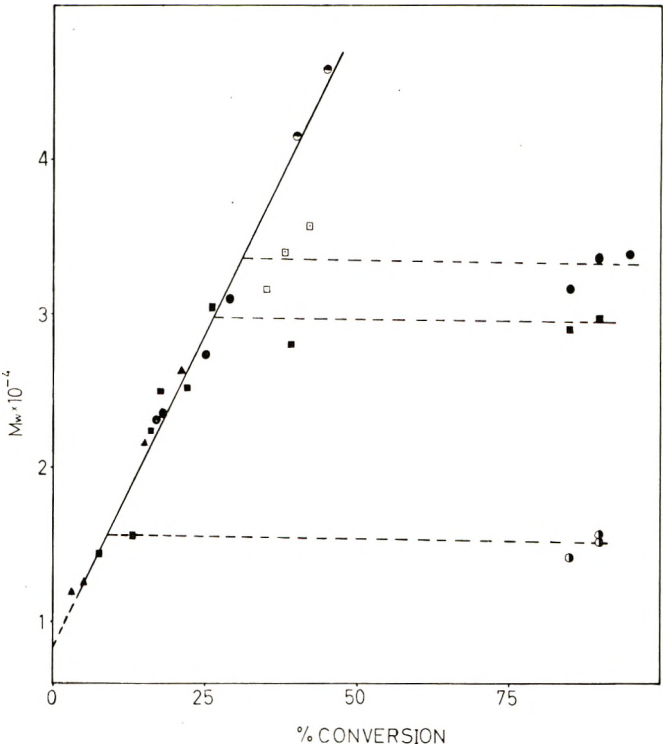

Fig. 3. Dependence of molecular weight on per cent conversion at various initial monomer concentrations: (●) 1.80 mole/l.,temp. of polymerization = 0°C.; (▲) 1.80 mole/l., temp. of polymerization = −30°C.; (◓) 1.80 mole/l., temp. of polymerization = −50°C.; (◑) 0.90 mole/l., temp. of polymerization = 0°C.; (■) 0.90 mole/l., temp. of polymerization = −30°C.; (⊡) 0.90 mole/l., temp. of polymerization = −50°C.

added at the end of the polymerization after all the initial monomer was consumed was also polymerized completely without any change in the resulting molecular weight. This catalyst low efficiency was similarly found in the polymerization of acrylonitrile by butyllithium in toluene at −78°C.[6]

Relative Effectiveness of Catalyst and Monomer

From Table I it is seen that for the same [M]/[C] values the molecular weights obtained were higher when greater concentrations of monomer and catalyst correspondingly were used. This shows that the monomer concentration is more effective than that of the catalyst in increasing the molecular weight. This greater influence of the monomer is reasonable taking into consideration the following evidence.

(*1*) While all the monomer enters polymerization as indicated from the quantitative yields of the obtained polymers, not all the catalyst is consumed, as shown above, for the higher catalyst concentrations.

(*2*) From Table I and Figure 1 it is clearly seen that the rate of increasing

the molecular weight on decreasing catalyst concentration, increases always more by passing from the lowest to the highest monomer concentrations.

(3) On doubling the monomer concentration at a constant catalyst concentration (out of the chain transfer region, see discussion) the molecular weights are also doubled, while on halving the catalyst concentrations at a constant monomer concentration, the molecular weights increased much less.

Infrared Spectra

The infrared spectra of the polymers obtained at high catalyst concentrations, showed relatively strong (CH_2=) double bond absorptions at 6.1–6.2 μ, as well as absorptions at 4.55 μ due to conjugation between the triple bond of the cyano groups and the terminal double bonds,[7] while the infrared spectra of the polymers obtained at low catalyst concentrations showed only very weak absorptions at 6.1–6.2 μ, no absorptions at 4.55 μ, but new absorptions at 5.8 μ which can be due to cyclic ketones β- to cyano groups.[8]

DISCUSSION

The present study of the homogeneous polymerization of acrylonitrile by butyllithium in dimethylformamide at a wide range of catalyst concentrations shows that at relatively high catalyst concentrations the molecular weights of the polymers are independent of both catalyst and monomer concentrations, while at low catalyst concentrations the molecular weight increases considerably with increase in monomer concentration and with decrease in catalyst concentration.

Obviously there should be different termination mechanisms that are responsible for these changes in molecular weight.

It may be noted that in previously studied anionic polymerizations of acrylonitrile the catalyst concentrations used were generally in the relatively high concentration region, and no dependence of molecular weight with changes in monomer and catalyst concentrations was observed.

Termination by Chain Transfer

From Table I and Figures 1 and 2 it is seen that at catalyst concentrations of about 70 mmole/l. or higher the molecular weights are constant and independent of both catalyst and monomer concentrations. This is consistent with the assumption that termination is by chain transfer to monomer.[9] The region where chain transfer termination occurs is found to be also connected with the ratio of monomer to catalyst concentration [M]/[C]. At values of [M]/[C] $\leq$ 15, there is a constancy in molecular weight. At higher values of [M]/[C] (to about 30), the molecular weights obtained are higher but still in the vicinity of the order of molecular weights obtained for pure chain transfer, showing that at these [M]/[C] values termination is also mostly dominated by chain transfer.

The existence of pure chain transfer termination is even evident at extremely low [M]/[C] values, as seen from the resulting molecular weights (runs 28 and 57, Table I-B) in which monomer was dropped on to the catalyst and thereby the initial concentration of monomer was very small.

Furthermore, as shown by the infrared absorption bands already described in the results, the polyacrylonitriles obtained at values of [M]/[C] $\leq$ 30 contain terminal $CH_2{=}C(CN){\sim\sim}P$ double bonds conjugated to the triple bonds of the cyano group as required by the chain transfer termination:

$$P{\sim\sim}CH_2C^-H(CN) + CH_2{=}CH(CN) \rightarrow P{\sim\sim}CH_2CH_2(CN) + CH_2{=}C^-(CN)$$

Monomolecular Termination

In the present polymerization two extreme cases are apparent. One is the independence of molecular weight on monomer concentration at high catalyst concentrations (chain transfer conditions); the second is the direct proportionality of molecular weight to monomer concentration at low catalyst concentrations.

Considering the following polymerization steps it is possible to arrive to the conclusion that a monomolecular termination may have occurred at low catalyst concentration.

Initiation:

$$C + M \xrightarrow{K_i} CM^-$$

Propagation:

$$CM_n^- + M \xrightarrow{K_p} CM^-_{n+1}$$

Termination, bimolecular (chain transfer):

$$CM^-_n + M \xrightarrow{K_{tr}} CM_nH + M^-$$

Termination, monomolecular:

$$CM_n^- \xrightarrow{K_t} CM_n$$

For bimolecular termination

$$\overline{DP} = (K_p/K_{tr})\ [M][CM_n^-]/[M][CM_n^-] = \text{Constant}$$

For monomolecular termination

$$\overline{DP} = (K_p/K_t)\ [M][CM_n^-]/[CM_n^-] = (K_p/K_t)\ [M]$$

The linear dependence of molecular weight to monomer concentration found is in accordance with this relationship for monomolecular termination.

This monomolecular termination can be an inner cyclization reaction which had been postulated for acrylonitrile[10] or for methyl methacrylate[8,11] polymerizations. The cyclization can occur as a result of the interaction

of the carbanion growing end with the positive carbon of a cyano group, the third in the chain, so that a stable, six-membered ring is obtained:

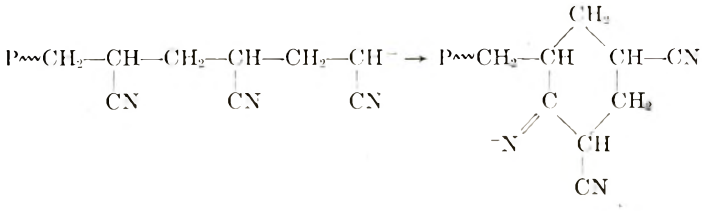

The imine anion is capable of undergoing further cycling reactions with the pendant nitrile groups, and thus subsequent hydrolysis would yield more than one carbonyl group per chain.[12] However, since the polymers obtained were perfectly white, such a further cycling reaction could have occurred only to a small extent. The imine ion is insufficiently basic (much less basic than a carbanion) to be able to initiate further polymerization. On termination of the polymerization with acid we get a C=NH group, which as known is easily hydrolyzed to a carbonyl group. Evidence for the presence of the cyclic carbonyl group is shown by the absorption band at 5.8 μ in the infrared, as was found in the case of the anionic polymerization of methyl methacrylate.[8,11]

It seems that the interaction of the carbanion chain end takes place exclusively with the γ-cyano group and not with any random cyano group of polymer, otherwise insoluble crosslinked polymers might have been formed. The driving force for such a reaction seems to be the formation of a stable, six-membered ring, otherwise such a reaction may not have taken place.

The fact that only soluble polymers were obtained also indicates that the possibility of chain transfer to polymer with the subsequent possibility of branching is not of importance.

The existence of monomolecular termination is clearly reflected in the results of the dependence of molecular weight on per cent conversion (Fig. 3). From these results it is seen that there is a linear relationship between molecular weight and monomer consumed up to about 30% conversion, after which the molecular weights stopped to increase and remained constant. In "living" polymerizations there is a linear increase of molecular weight with conversion. This was found, for example, in the anionic polymerization of nitroethylene.[13] In our polymerization, the linear initial dependence of molecular weight on consumed monomer may be due to such a behavior. In such a case, the molecular weights are proportional to [M]/[C], and therefore from the slope of the curve relating molecular weight with monomer consumed it is possible to calculate [C], the catalyst concentration which has initiated polymerization. This value of [C] is 1.2 mmole/l. as calculated from the reciprocal of the slope (Fig. 3) if the initial monomer concentration was 1.80 mole/l., or 0.6 mmole/l. if the initial monomer concentration is 0.90 mole/l.; i.e., it is about half the initial catalyst concentration (2.5 mmole/l.) has initiated polymerization at the

first high monomer concentration, and only about a quarter of the initial catalyst concentration started polymerization at the second lower monomer concentration. The abrupt stopping in the increase of the molecular weight with per cent conversion, is due to monomolecular termination in which $\overline{DP} = (K_p/K_t)$ [M₀], so that for any given initial monomer concentration only a certain determined value for the molecular weight is obtainable.

From the slope of the curve (Fig. 2) relating molecular weight to monomer concentration (for the catalyst concentration at which the conversion studies had been carried out, namely, 2.5 mmole/l.) calculation of the ratio of the rate constants K_p/K_t for the monomolecular termination gives the value of 350 ± 5%. From this value of K_p/K_t it is possible to see from the above relationship for $\overline{DP}$ that the maximum molecular weights that can be obtained for the monomer concentrations studied (Fig. 3) are 33,400 ± 5% for 1.80 mole/l. monomer and 16,700 ± 5% for 0.90 mole/l. monomer.

This is in complete agreement with the results found in Figure 3, where at about 30% conversion molecular weights of 33,000 and 15,600 were correspondingly obtained and did not increase further.

The molecular weights obtained at the low conversions where there is a linear dependence of molecular weight on monomer consumption are independent of polymerization temperature, as seen from Figure 3 where the values of the molecular weight at different temperatures (0, −30, and −50°C.) fall on the same curve. This independence of molecular weights on the polymerization temperature has been found in "living" polymer systems, where the molecular weights generally depend on the ratio of [M]/[C].

Furthermore, monomolecular termination requires a certain activation energy, and on lowering the temperature, it will occur less frequently leading to increase in molecular weight; thus, although there is an initial independence of molecular weight on temperature in the region where termination is not occurring, nevertheless termination will occur at the higher temperature before it does at the lower, and hence there is an increase in molecular weight with decrease in temperature (Fig. 3). In the absence of termination, the linear increase of molecular weight with the consumed monomer is continuous. Extrapolation of the linear curve (Fig. 3) shows that at zero conversion the molecular weight is not zero but about 8000; this may be due to unsteady-state conditions at the start of the polymerization.

Reason for the Presence of Chain Transfer at High Catalyst Concentrations and Its Absence at Low Catalyst Concentrations

It was shown that termination by chain transfer with monomer occurred only at high catalyst concentrations and was absent at low catalyst concentrations. This might suggest the possible participation of the catalyst in the chain transfer termination.

Chain transfer with monomer occurs by collision of a growing polymer end with a monomer molecule followed by abstraction of the acidic α-hydrogen atom of the monomer:*

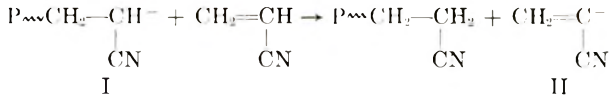

The energy differences between carbanions I and II may be deduced from a comparison of the acidities of γ-cyanobutyric acid and acrylic acid, respectively. These acids can be reasonably compared to the above carbanions regarding the inductive effects contributed by the same substituents. Carbanion I is stabilized by the $-I$ effect of the cyano groups at the α- and the γ-positions, while carbanion II is stabilized by the effect due to the α-cyano group and the vinyl double bond. The formation of carbanion II (or in other words the transfer reaction) is slightly favored on energy grounds. This can be seen from the small difference in the acidities of acrylic acid ($pK_a = 4.25$) and that of γ-cyanobutyric acid[14] ($pK_a = 4.4$), and from the resonance stabilization that is possible in II due to conjugation between the vinyl double bond and the triple bond of the cyano group. However, in the presence of excess butyllithium this reaction of chain transfer may be much more favored. Butyllithium, for example, in the vicinity of the collision of the growing chain with monomer (unreacted butyllithium solvates the growing end) can help in the transfer of the acidic hydrogen atom from the monomer to the growing end by a possible 1,4 mechanism:

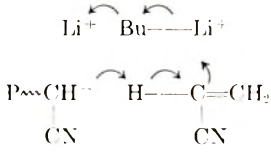

* The alternative possibility of chain transfer by hydride transfer to monomer is not favored on energy grounds. The energy differences

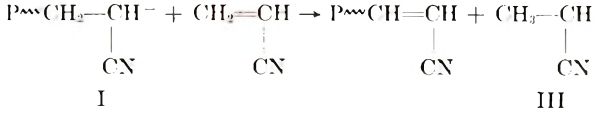

between carbanions I and III seems to be greater than that of I and II, and are in the opposite direction not favoring the transfer reaction, due to the +I effect of the methyl group. Furthermore, it is not so probable that a hydride transfer occurs from a position which is α to a very strong electron-withdrawing group such as the cyano group. Furthermore, in the anionic polymerization of styrene, living polymers were obtained whose molecular weight was given by $[M]/[C]$,[15] i.e., no termination by hydride transfer was energetically possible, even with a weak electronegative group. Also, in the anionic polymerization of methacrylonitrile (which has no acidic α H-atom) with lithium in liquid ammonia[12] and with quaternary ammonium hydroxides[4] no chain transfer to monomer occurred, showing that the possibility of hydride transfer is ruled out.

For such a mechanism it is plausible that a certain effective limiting concentration of free butyl lithium in solution is necessary, below which termination by chain transfer will become gradually smaller and unimportant; and above which, free catalyst may be in excess so that it will not influence the rate of termination to a greater extent.

It may be mentioned that the results obtained with the butyl lithium in dimethylformamide system show that for catalyst concentrations $\geq$ 70 mmole/l. and [M]/[C] values of $\leq$15–30, pure chain transfer occurs. For other systems this range of catalyst concentrations where chain transfer occurs may of course be different.

Dependence of Molecular Weight on Catalyst Concentration

As seen from Figure 1, the molecular weights depend on the catalyst concentration. At high catalyst concentrations (chain transfer region) the molecular weights are independent of catalyst concentration. At the low catalyst concentrations the molecular weights increase with decrease in catalyst concentration, but the increase is not linear. It was also shown that not all the catalyst added is consumed. In the chain transfer region, as seen from the use of very high catalyst concentrations only a small fraction of the catalyst initiated polymerization. On the other hand, as was found for the low catalyst concentration of 2.50 mmole/l. a significant part of the initial catalyst initiates polymerization depending on monomer concentration. It may be that at still lower catalyst concentrations, most or all of the catalyst initiates polymerization.

From the values of the molecular weights in the chain transfer region (2,150–2,700) the ratio of the rate constants K_p/K_{tr} is found to be equal to 45 $\pm$ 5. Assuming that the rate propagation constant K_p, is the same for both monomolecular and bimolecular termination it can be seen from the above calculated value of K_p/K_t for monomolecular termination that the rate constant for chain transfer termination is about eight times that for monomolecular termination ($K_{tr} \simeq 8K_t$).

Since the molecular weights were found to depend on catalyst concentration, this large change in the rate termination constants seems to be connected with the change in the catalyst concentration. It is plausible to assume that the large change of the termination rate constants is gradual, i.e., there cannot be an abrupt passage from one mode of termination to another with a continuous change of catalyst concentration. It is quite possible that at intermediate catalyst concentrations, both monomolecular and bimolecular termination (chain transfer) might be occurring side by side to different extents, and the results are reflected in the molecular weights. At catalyst concentrations which are near the chain transfer region, the chain transfer termination will be more dominant, while at low catalyst concentrations the monomolecular termination will be more dominant.

We have pointed out that free catalyst molecules can be probably taking part in the chain transfer termination and that a certain critical concentra-

tion of catalyst is probably needed to ensure complete chain transfer conditions. Below this critical concentration, termination by chain transfer will become smaller, while above it even free catalyst in excess will not influence the rate of termination to a greater extent.

These considerations require that the free catalyst concentration which did not initiate polymerization should be taken as a factor in the elementary steps of the polymerization.

Thus termination by chain transfer to monomer should be expressed by:

$$CM^- + M + C \xrightarrow{K_{tr}} CMH + M^- + C$$

Since two kinds of terminations can take place at the same time, namely, monomolecular and chain transfer, then $\overline{DP}$ should be given by:

$$\overline{DP} = R_p/(R_{tr} + R_t) = K_p[M][CM^-]/(K_{tr}[CM^-][M][C] + K_t[CM^-])$$

$$\overline{DP} = \frac{K_p\,[M]}{(K_{tr}\,[M][C] + K_t)}$$

and

$$1/\overline{DP} = (K_{tr}[C]/K_p) + (K_t/K_p\,[M])$$

Now, since the catalyst concentration was found not to change the molecular weight in the chain transfer region i.e., after a certain critical concentration $[C^+]$ there is no more change in the molecular weight with increase in the catalyst concentration, then [C] will become constant and will enter the rate constant for chain transfer termination to give a new constant K_{tr}^+ (given by $K_{tr}^+ = K_{tr}\,[C^+]$) i.e.,

$$\overline{DP} = K_p[M]/(K_{tr}^+\,[M] + K_t)$$

From the above general relationship for $\overline{DP}$, three cases may be considered.

(*1*) Case of $K_{tr}\,[C][M] \gg K_t$: This will occur when [C] is large (equal to $[C^+]$) so that K_{tr} has its maximum value (K_{tr}^+). Then $\overline{DP}$ would be equal to K_p/K_{tr}^+ equal constant, i.e., the chain transfer region. We have shown that for chain transfer $K_p/K_{tr}^+ = 45$ and $K_{tr}^+ = 8K_t$, so that K_t compared to $K_{tr}^+\,[M]$ can be neglected.

(*2*) Case of $K_t \gg K_{tr}\,[C][M]$: Here, $\overline{DP}$ should be equal to $K_p\,[M]/K_t$, i.e., we have monomolecular termination. This case will occur when [C] is very small.

(*3*) Case of $K_t \lesssim K_{tr}\,[C][M]$: This occurs at intermediate catalyst concentrations and both terminations are working. A plot of $1/\overline{DP}$ versus 1/[M] at various catalyst concentrations shows that at the catalyst concentration of about 2.5 mmole/l. a positive intercept is not obtained

on the $1/\overline{DP}$ axis. Since this intercept should give the value of K_{tr} [C]$/K_p$, then no chain transfer termination is occurring. On the other hand, a positive intercept is obtained at catalyst concentrations of 4.5 mmole/l. and higher, showing that chain transfer termination is also occurring.

EXPERIMENTAL

Materials

Nitrogen was freed from oxygen by passage through a quartz tube containing fresh copper turnings at 600°C., then through a 5% alkaline permanganate solution, a 10% solution of pyrogallol in 20% sodium hydroxide, concentrated sulfuric acid followed by a solution of sodium benzophenone in tetrahydrofuran, and was dried by concentrated sulfuric acid. Dimethylformamide (B.D.H.) was dried by azeotropic distillation with benzene and then was fractionally distilled under nitrogen. Acrylonitrile was purified according to Bamford and Jenkins.[16] *n*-Butyllithium prepared in petroleum ether as before[17] was kept in a refrigerator and its concentration in the solvent checked by titration before use. Only freshly prepared catalyst was used.

Polymerization of Acrylonitrile

All manipulations were carried out under nitrogen. The polymerizations were carried out in three-necked flasks fitted with a high speed stirrer, a gas adapter for introducing nitrogen, a thermometer, and an outlet fitted with a self-sealing rubber cap. The apparatus was flushed immediately before use with a stream of hot air, and then cooled under a stream of nitrogen. Freshly distilled monomer and solvent were transferred with syringes, the flask cooled to the required temperature of polymerization and kept thereat. The required amount of catalyst solution was then added from a syringe with fine graduations. The polymerization was stopped after the required time by adding 20% aqueous acetic acid (50 ml.). The polymer was filtered off, washed with water and methanol to remove monomer, and sucked dry on the water-pump. It was further purified by trituration with water and with methanol and then filtered, washed with methanol and ether, and dried to constant weight in an oven at 60°C.

Viscosities of polymer solutions were measured in dimethyl-formamide with the use of an Ostwald viscometer. The weight-average molecular weights were determined from intrinsic viscosities by use of the equation of Cleland and Stockmayer:[18]

$$[\eta] = 2.33 \times 10^{-4} \bar{M}_w^{0.75}$$

The authors are pleased to acknowledge partial support of this work by the Israeli National Council for Research and Development.

References

1. Frankel, M., A. Ottolenghi, M. Albeck, and A. Zilkha, *J. Chem. Soc.*, **1959**, 3858.

2. Zilkha, A., P. Neta, and M. Frankel, *J. Chem. Soc.*, **1960**, 3357; *Bull. Research Council Israel*, **9A**, 185 (1960).

3. Cundall, R. B., J. Driver, and D. D. Eley, *Proc. Chem. Soc.*, **1958**, 170

4. Zilkha, A., B. A. Feit, and M. Frankel, *J. Polymer Sci.*, **49**, 231 (1961).

5. Zilkha, A., and Y. Avny, *J. Polymer Sci.*, **A1**, 549 (1963).

6. Miller, M. L., paper presented at the 139th Meeting of the American Chemical Society, St. Louis, March 1961.

7. Bellamy, L. J., *The Infrared Spectra of Complex Molecules*, 2nd Ed., Methuen, London, 1958, p. 264.

8. Goode, W. E., F. H. Owens, and H. L. Myers, *J. Polymer Sci.*, **47**, 75 (1960).

9. Flory, P. J., *Principles of Polymer Chemistry*, Cornell Univ. Press, Ithaca, N. Y., 1953, p. 223.

10. Szwarc, M., *Fortschr. Hochpolymer Forsch.*, **2**, 281 (1960).

11. Glusker, D. L., I. Lystoff, and E. Stiles, *J. Polymer Sci.*, **49**, 315 (1961).

12. Overberger, C. G., E. M. Pearce, and N. Mayes, *J. Polymer Sci.*, **34**, 109 (1959).

13. Grodzinski, J., A. Katchalsky, and D. Vofsi, *Makromol. Chem.*, **44–46**, 591 (1961).

14. Braude, E. A., and F. C. Nachod, *Determination of Organic Structures by Physical Methods*, Academic Press, New York, 1955, p. 578.

15. Waack, R., A. Rembaum, J. D. Coombes, and M. Szwarc, *J. Am. Chem. Soc.*, **79**, 2026 (1957).

16. Bamford, C. H., and A. D. Jenkins, *Proc. Roy. Soc. (London)*, **A216**, 515 (1953).

17. Frankel, M., J. Rabani, and A. Zilkha, *J. Polymer Sci.*, **28**, 387 (1958).

18. Cleland, R. L., and W. H. Stockmayer, *J. Polymer Sci.*, **17**, 473 (1955).

Synopsis

The homogeneous anionic polymerization of acrylonitrile in dimethylformamide with *n*-butyllithium was studied. Two different termination reactions were found to exist depending on catalyst concentration. At high catalyst concentrations termination was bimolecular by chain transfer to monomer, while at relatively low catalyst concentrations termination was monomolecular, by an inner cyclization reaction of the growing chain end. The existence of chain transfer only at high catalyst concentrations suggests the possibility of free catalyst molecules participating in the transfer reaction. At intermediate catalyst concentrations, both monomolecular and bimolecular terminations were found to occur side by side, and $\overline{DP} = K_p[M]/(K_{tr}[C][M] + K_t)$. Study of the dependence of molecular weight on per cent conversion at low catalyst concentrations showed that, up to about 30% conversion, there is a linear relationship between molecular weight and concentration of monomer consumed which is independent of temperature and monomer. After this degree of conversion, molecular weight stopped to increase and remained constant due to monomolecular termination. All over the wide range of catalyst concentrations investigated, the catalyst efficiency in initiating polymerization was found to be low. In the lowest range where there is a linear dependence of molecular weight on per cent conversion it was also found that the molecular weights are proportional to [M]/[C], which is a property of "living" systems.

Résumé

On a étudié la Polymérisation anionique homogène de l'acrylonitrile dans le diméthylformamide catalysée par le *n*-butyllithium. On a trouve qu'il existait deux réactions de terminaison différentes suivant la concentration en catalyseur. A concentration élevée en catalyseur, la terminaison est bimoléculaire par transfert de chaîne sur monomère tandis qu'à concentration relativement basse en catalyseur, la terminaison est

monomoléculaire par une réaction de cyclisation interne de l'extrèmité de la chaîne en croissance. L'existence d'un transfert de chaîne seulement pour des concentrations élevées en catalyseur suggère la possibilité de molécules libres de catalyseur participant à la réaction de transfert. A des concentrations intermédiaires en catalyseur on a trouvé que les terminaisons bi- et monomoléculaires se produisaient côte à côte et que $\overline{DP} = K_p[M]/(K_{tr}[C][M] + K_t)$. L'étude de la relationent re le poids moléculaire et le pourcentage de conversion aux basses concentrations en catalyseur montre que jusqu'à environ 30% de conversion, il y a une relation linéaire entre le poids moléculaire et la concentration de monomère consummé qui est indépendante de la température et du monomère. Au dela de ce degré de conversion le poids moléculaire cesse de troître et demeure constant à cause de la terminaison monomoléculaire. Dans tout le large domaine des concentrations en catalyseur étudié, on a trouvé que l'efficacité du catalyseur à initier la polymérisation était faible. Dans le domaine inférieur de concentration, où il existe une relation linéaire entre le poids moléculaire et le pourcentage de conversion, on a également trouvé que les poids moléculaires sont proportionnels à [M]/[C], ce qui est une propriété des systémes "vivant."

Zusammenfassung

Die homogene anionische Polymerisation von Acrylnitril in Dimethylformamid mit *n*-Butyllithium wurde untersucht. Für die Beendigung des Wachstums einer Kette bestehen zwei verschiedene, von der Katalysatorkonzentration abhängige Reaktionen. Bei hohen Katalysatorkonzentrationen findet eine bimolekulare Kettenübertragung zum Monomeren statt, bei relativ geringen Katalysatorkonzentrationen verläuft der Abbruch monomolekular als innere Ringschlussreaktion des wachsenden Kettenendes. Die Beschränkung der Kettenübertragung auf hohe Katalysatorkonzentrationen weist auf die Möglichkeit hin, dass freie Katalysatormoleküle an der Übertragungsreaktion teilnehmen. Bei mittleren Katalysatorkonzentrationen wurde gefunden, dass mono- und bimolekularer Abbruch nebeneinander verlaufen und $\overline{DP} = K_p[M]/(K_{tr}[C][M] + K_t)$. Die Untersuchung der Abhängigkeit des Molekulargewichts vom Umsatz bei geringen Katalysatorkonzentrationen zeigte, dass bis zu 30% Umsatz zwischen Molekulargewicht und der Konzentration des verbrauchten Monomeren eine lineare Beziehung besteht, die von der Temperatur und vom Monomeren unabhängig ist. Nach Erreichung dieses Umsatzes steigt das Molekulargewicht nicht weiter an und bleibt wegen des monomolekularen Abbruchs konstant. Im gesamten untersuchten grossen Konzentrationsbereich an Katalysator wurde gefunden, dass die Katalysatorwirksamkeit beim Start der Polymerisation gering ist. Weiters wurde gefunden, dass im niedrigsten Bereich, wo eine lineare Abhängigkeit des Molekulargewichts vom Umsatz besteht, das Molekulargewicht proportional [M]/[C] ist, was eine Eigenschaft von "lebenden" Systemen darstellt.

Received September 11, 1961
Revised November 20, 1961

JOURNAL OF POLYMER SCIENCE: PART A VOL. 1, PP. 705–714 (1963)

Copolymerization of Acrylonitrile and *p*-Sodium Styrene Sulfanate

Z. IZUMI, H. KIUCHI, and M. WATANABE, *Central Research Laboratories, Toyo Rayon Company, Otsu, Japan*

INTRODUCTION

The reactivity ratios in the copolymerization of acrylonitrile (AN) and sodium-*p*-styrenesulfonate (SSS) were reported by Grabiel,[1] but no mention was made of the copolymerization rates of these two monomers. In this report the authors present the reactivity ratios and the rates of copolymerization of AN and SSS in aqueous solution at pH 3 and pH 7. Two aspects of the copolymerization of AN and SSS, which we have recently studied, drew our attention. Firstly, SSS is a strongly electrolytic vinyl monomer and the kinetic behavior of AN and SSS during copolymerization shows a considerable dependence on the pH of the reaction medium. Secondly, copolymers of low SSS content are insoluble in aqueous solution, whereas those of high SSS content are soluble. It is therefore possible merely by changing the molar ratio of the two monomers, to determine whether any change occurs in the copolymerization rate on passing from a heterogeneous to a homogeneous system. These two phenomena are dealt with in this report, and factors causing them are herein discussed.

EXPERIMENTAL

Materials

SSS was prepared from phenyl ethyl alcohol as a starting material by the method of Wiley[2] and purified by recrystallizing from 90% ethanol twice. The purity of this monomer was determined to be 98.5% by bromine addition method. Polymer grade AN (supplied by Nitto Chemical Co.) was dried with calcium chloride and then distilled under nitrogen twice. Ammonium persulfate (APS) (supplied by Wako Chemical Co.) was purified by recrystallization from water, and then the solution, of which the concentration was determined by the iodo method, was stored in a refrigerator to minimize thermal decomposition.

Other reagents were considered to be extremely pure and were used without further treatment.

Copolymerization Technique

Copolymers for the determination of the monomer reactivity ratios were prepared in a sealed tube *in vacuo*, the pH of the reaction mixtures being

adjusted to 3 or 7 by addition of hydrochloric acid or sodium hydroxide, respectively.

Rates of copolymerization were obtained from the observed rates of volume contraction in a dilatometer. By assuming that the change in specific volume in conversion from monomer to polymer of both AN and SSS is the same as in their homopolymerization and that these are additive in the copolymer, the total mole fraction α consumed in the reaction is readily obtained from eq. (1)

$$\alpha = (1000/V)(Ah/M_1 + M_2)\ [(R + 1)/(\Delta_1 R + \Delta_2)]$$

where h is the observed change in the height of the liquid in a dilatometer capillary at time t, A is the cross-sectional area of the capillary, V is the volume of the dilatometer bulb, $[M_1]$ and $[M_2]$ are the initial concentrations of AN and SSS monomer in the feed in moles/liter, respectively, Δ_1 and Δ_2 are the change in volume which is caused from complete polymerization of 1 mole of the monomer to the polymer, and R is the molar ratio of AN/SSS in the initial copolymer. Equation (1) was used in the copolymerization of styrene and α-vinylnaphthalene by Loshaek and Broderick.[3] The numerical values used here at 45°C. are $V = 11.25$ cm.^{3}, $[M_1] + [M_2] = 0.5$ mole/l., $\Delta_1 = 15.67$ cm.^{3}/mole, $\Delta_2 = 12.82$ cm.^{3}/mole and $A = 5.291 \times 10^{-3}$ cm.^{2}. The following eq. (2) is obtained by substituting the values described above.

$$\alpha = [0.941(R + 1)/(15.67R + 12.82)]h \qquad (2)$$

Initial rates of copolymerization were obtained from tangents to the curve of α against t at low conversion.

The copolymers were quantitatively precipitated with alkaline ethanol and washed with hot 90% ethanol using a centrifugal separator till no further chloride ion was detected. The copolymers were filtered in glass crucibles and dried to constant weight in a vacuum oven kept at 50°C. under 1 mm. for about 50 hr.

The compositions of the AN–SSS copolymers were determined from nitrogen contents obtained by the Dumas method. In order to confirm the validity of the method, the sulfur content was also determined for three samples, and consistent results were obtained within 1% analytical error.

RESULTS AND DISCUSSION

Monomer Reactivity Ratios

The data for calculating monomer reactivity ratios are listed in Table I. Monomer reactivity ratios were determined graphically by the method of Mayo and Lewis.[4] The intersections coincidate fairly well, and from these intercepts were obtained the values r_1 (AN) = 0.10 ± 0.02, r_2 (SSS) =

1.20 ± 0.10 at pH 3; r_1 (AN) = 0.05 ± 0.01, r_2 (SSS) = 1.40 ± 0.04 at pH 7. The solid lines in Figure 1 were calculated from these reactivity ratios and the differential copolymerization equation. From these reactivity ratios and the Q and e values for AN (Q_1 = 0.44, e_1 = 1.2), Price Q and e for SSS are calculated; Q_2 (SSS) = 0.76, e_2 (SSS) = −0.26 at pH 3; Q_2 (SSS) = 1.24, e_2 (SSS) = −0.43 at pH 7. The values which are shown above were obtained from the investigation both in the range of homogeneous system (above 5 mole-% SSS in the monomer feed) and in that of heterogeneous system where the polymer was precipitated but highly swollen (0.5 mole-% and 2 mole-% SSS in the monomer feed). We can not find any difference in the monomer reactivity ratios between these two regions, and the absence of a change in reactivity ratios in passing from a homogeneous system to one in which the polymer is precipitated but highly swollen is not surprising; such phenomena were discussed by Bamford et al.[5] A different value may be obtained in the range where the copolymer is precipitated and not swollen; these conditions are however, different from those of our study, and we did not study these conditions because of the experimental difficulties resulting from the higher reactivity of SSS and the great affinity of copolymer to water. It has been reported that when a substituent is introduced into benzene ring of styrene, the e value is markedly affected, whereas the influence on the Q value is not so large.[6] Electron-withdrawing substituents, such as —No_2 or —CN, behave—through the ring—to make the ethylenic double bond more "positive."

TABLE I
Copolymerization of AN and SSS[a]

pH	SSS in the monomer feed M_2, mole-%	Monomer reacted, wt.-%	SSS in the copolymer m_2, mole-%
3.0	2.0	16.8	10.5
	5.0	21.5	20.4
	10.0	5.44	39.0
	20.0	10.1	54.7
	30.0	10.1	57.5
	50.0	9.5	67.0
	70.0	16.6	77.4
	90.0	17.5	91.6
	95.0	15.6	96.1
7.0	0.5	5.46	7.90
	1.0	14.21	13.50
	5.0	4.30	34.5
	10.0	7.13	44.9
	30.0	6.11	59.6
	50.0	4.04	69.3
	90.0	1.59	92.1
	95.0	2.35	96.5

[a] Copolymerization conditions: 0.5 mole/l. monomer, 0.01 mole/l. APS as initiator at 45°C.

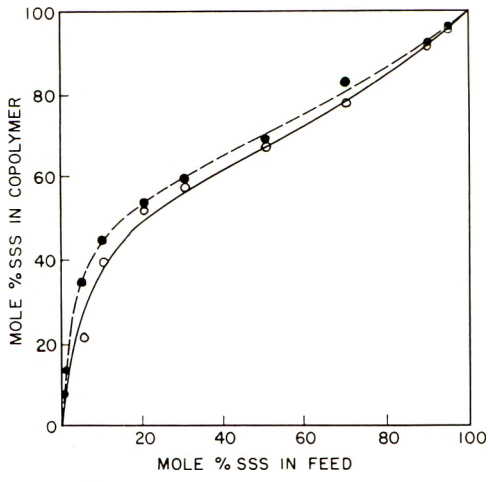

Fig. 1. Plot of mole-% SSS (m_2) in the copolymer against mole-% SSS (M_2) in the monomer feed: at pH 3 (○) experimental points; (—) calculated for $r_1 = 0.10$ and $r_2 = 1.20$; and at pH 7: (●) experimental points; (---) calculated for $r_1 = 0.05$ and $r_2 = 1.40$.

Electron-donating groups, such as $-OCH_3$ or $-N(CH_3)_2$ feed electrons into the double bond via benzene ring. In Table II substituent effects are tabulated on the basis of Hammett's σ value, the order of the *meta*-directing power in the benzene ring, and the polar value of the ring-substituted styrene. Table II shows that there is a close relation among the Hammett's σ value, *meta*-directing activity, and the polar factor e, which is in accord with the work of Price.[7] The σ value of SO_3H is not known, but the strength of the *meta*-directing power lies between —COOH and —CN; the e value of $-SO_3H$ therefore can be placed between 0.3 and −0.2. When the polar groups are dissociated into ions, the e values tend to be more negative, as mentioned later. Therefore, these obtained values, −0.27 at pH 3 and −0.43 at pH 7, could be reasonably understood.

TABLE II

The Effect of Ring Substituents on the Hammett σ Value, the *meta*-Directing Power, and the Polar Factor e

Ring substituents	Hammett σ value	Order of *meta*-directing power	Polar factor e
p-NO_2	1.27	1	0.4
p-CN	1.00	2	0.3
p-COOH	0.728	3	
p-Br	0.232	4[a]	−0.2
p-Cl	0.227		−0.3
	0.000	*ortho, para*-	−0.8
m-CH_3	−0.069	5 directing	−0.8
p-CH_3	−0.170		−0.9
p-CH_3O	−0.268	6	−1.0

[a] The *ortho, para*-directing influence of the halogen atom can be interpreted as a consequence of the resonance effect.

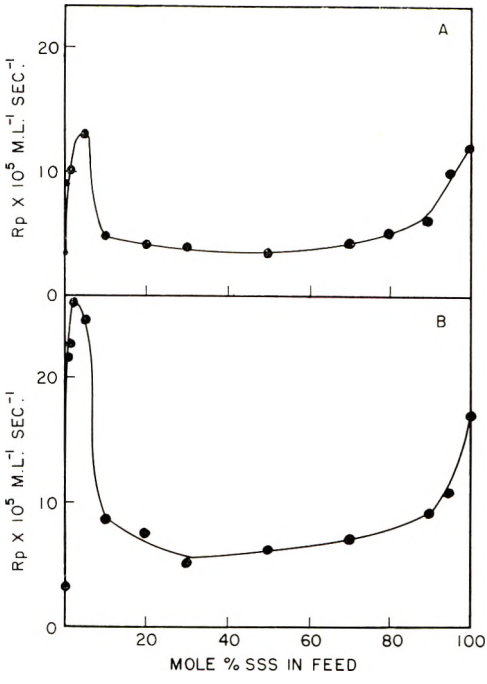

Fig. 2. Plot of initial rate of copolymerization R_p against mole-% SSS in the monomer feed at (*A*) pH = 3; (*B*) pH = 7.

On comparing the e values at pH 3 and pH 7, the polar values are found to decrease when SSS is dissociated into ions. This tendency is in accord with other electrolytic monomers.[8–10]

Thus, when the polar group is dissociated and the monomer becomes an anion, the electron-withdrawing power is diminished, giving the double bond a negative character. In the case of SSS, which is a strong electrolyte, this difference seems rather small, but this coincides with other electrolytic monomers clearly.

Copolymerization Rates

The initial rates of copolymerization R_p at 45°C. in the presence of 1×10^{-2} mole/l. of APS as the initiator are given in Table III and Figure 2. From Figure 2, a sharp rise in copolymerization rates in the range of 0.2–5 moles-% monomer feed is noticeable, sometimes being eight times larger than those in the neighboring range. There have been few examples which showed the existence of a maximum in the copolymerization rate in certain monomer feeds. Akazome[11] reported that there was a maximum in the rates of copolymerization of AN and dodecyl vinyl ether at about 1.5 mole-% of dodecyl vinyl ether in the monomer feed, the rates being three times larger than those at the neighboring monomer feed compositions. He explained this by stating that the occlusion of the radical would be disturbed by long-chain alkyl groups and the propagation constant might

be higher. In our experiments the polymerization was carried out in aqueous medium. Therefore the acrylonitrile homopolymer is separated as a solid polymer from aqueous phase, i.e., heterogeneous polymerization occurs, whereas *p*-sodium styrene sulfonate homopolymer is soluble in the medium, i.e., homogeneous polymerization occurs. The copolymerization in the SSS monomer feed at 0.2–5 mole-% occurs in the transition phase from homogeneous to heterogeneous, and the system becomes very viscous and slightly cloudy. It is well known that the rates of polymerization are greatly affected by the physical conditions of the polymerization system. Palit and Guha[12] studied the connection between polymerization rate and the colloidal nature of the precipitating polymer. They found by a careful visual examination that the faster polymerization is linked with the production of a stabler sol. Bamford[5] has shown that in the copolymerization of styrene and maleic anhydride, there is a sharp rise in the reaction rate when the polymer contains sufficient maleic anhydride to be insoluble in the reaction mixture.

TABLE III
Initial Rate of Copolymerization of AN and SSS[a]

SSS in monomer feed M_2, mole-%	Rate of copolymerization $R_p \times 10^5$, mole/l. sec.	
	At pH 3	At pH 7
0	3.12	3.33
0.5	8.78	21.9
1.0	—	22.8
2.0	10.0	26.1
5.0	13.0	24.6
10.0	4.58	8.44
20.0	3.89	7.50
30.0	3.59	5.01
50.0	3.11	6.90
70.0	4.04	6.90
80.0	4.96	—
90.0	5.79	9.15
95.0	9.92	10.0
100.0	12.2	17.0

[a] All experiments at 45°C., at 0.5 mole/l. monomer concentration and with 0.01 mole/l. APS as initiator.

For the further investigation of the transition state, where the reaction rate is surprisingly high, the effect of initiator concentration on the copolymerization rate in the monomer feed consisting of AN (98.0 mole-%)–SSS (2.0 mole-%) was studied. Table IV shows the results, and the rates are plotted against the initiator concentration in a logarithmic graph (Fig. 3). From these experiments it was observed that the copolymerization rate first increases with a change in the catalyst exponent from 1 to $^1/_2$, then reaches a constant value, and finally begins to decrease. These regions coincide with changes in appearance of the reaction mixture from a trans-

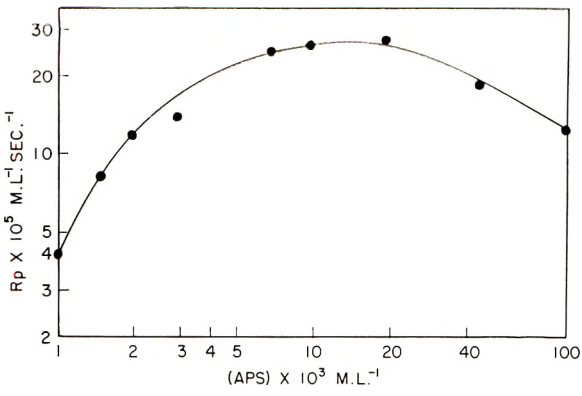

Fig. 3. Dependence of rate of copolymerization in the monomer feed of AN (98.0 mole-%)–SSS (2.0 mole-%) on catalyst concentration at 45°C.

TABLE IV
Dependence of Rate on Initiator Concentration[a]

Initiator concentration, mole-%	Reaction rate $R_p \times 10^5$, mole/l. sec.	Appearance of polymerization system (at about 45% conversion)
1	4.16	Transparent, low viscosity
1.5	8.34	"
2	11.90	Slightly cloudy
3	13.89	Cloudy
7	25.25	White cloudy, high viscosity
10	26.10	"
20	27.8	"
45	18.5	Milky dispersion
100	12.4	Coarse precipitate

[a] Polymerization conditions: AN, 0.490 mole/l. (98.0 mole-%); SSS, 0.010 mole/l. (2.0 mole-%); 45.00 ± 0.02°C.; pH 7; initiator APS.

parent solution to a slightly cloudy solution, then to a fine sol, a milky dispersion, and a coarse precipitate. For the direct observation of the copolymerization system of different monomer feed ratios, we examined them by an electron microscopy. Figure 4 shows the electron micrograph negative print of the conversion of 30% of (*a*) acrylonitrile homopolymer, (*b*) the copolymer obtained from a monomer feed of AN(99.75 mole-%)–SSS (0.25 mole-%) and (*c*) the copolymer obtained from a monomer feed of AN(97.3 mole-%)–SSS(2.7 mole-%). From Figure 4 it may be seen that the AN homopolymer coagulates markedly, whereas the AN–SSS copolymer disperses in fine particles, and that faster polymerization is linked with smaller size and larger numbers of particles. The rate of homopolymerization of AN in aqueous solution is greatly enhanced by the addition of AN–SSS copolymer, and polymerization seems to occur in many particles, as is seen in the presence of emulsifier such as sodium lauryl sulfate. (The details of this investigation will be published later.) There-

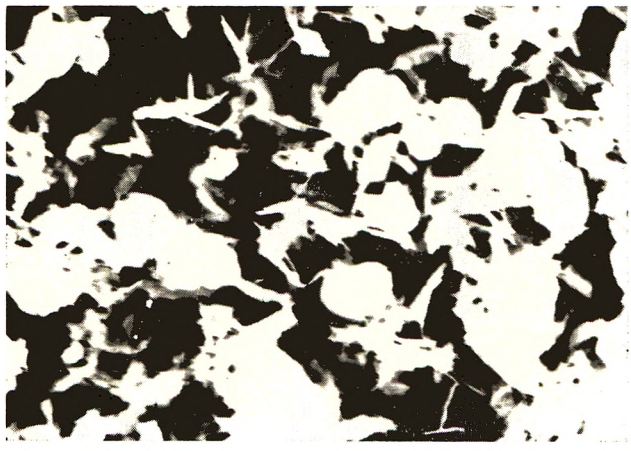

(*a*)

(*b*)

(*c*)

Fig. 4. Electron micrographs of (*a*) AN homopolymer; (*b*) the copolymer obtained from a monomer feed of AN (99.75 mole-%)–SSS (0.25 mole-%); and (*c*) the copolymer obtained from a monomer feed of AN (97.3 mole-%)–SSS (2.7 mole-%). Negative prints, 12.500×.

fore it is suggested that the AN–SSS copolymer produced under these conditions acts as an excellent emulsifier in the polymerization system, and that the fine sol of apparent slight cloudiness is indeed an aggregate of independent numerous particles, and that polymerization occurs mainly in each particle like emulsion polymerization. This might be the reason for the striking increase in the reaction rate, sometimes eight times as large as the value which would be expected from the usual polymerization mechanism. The dependence of the copolymerization rate on the initiator concentration may be interpreted from this point of view by considering the numbers and sizes of polymer particles produced in the earlier stages, and the coagulating effect of APS.

The authors wish to express their sincere gratitude to Dr. Kobayashi for his help and permission to publish the results.

References

1. Grabiel, C. E., and D. L. Decker, paper presented at the 138th Meeting of the American Chemical Society, New York, N. Y., September 11–16, 1960.
2. Wiley, R. H., N. R. Smith, and C. C. Kettner, *J. Am. Chem. Soc.*, **76**, 720 (1954).
3. Loshaek, S., and E. Broderick, *J. Polymer Sci.*, **39**, 241 (1959).
4. Mayo, F. R., and F. M. Lewis, *J. Am. Chem. Soc.*, **66**, 1594 (1944).
5. Bamford, C. H., and W. G. Barb, *Discussions Faraday Soc.*, **14**, 208 (1953).
6. Alfrey, T., Jr., J. J. Bohrer, and H. Mark, *Copolymerization*, Interscience, New York, 1952, p. 91.
7. Price, C. C., *Discussions Faraday Soc.*, **2**, 304 (1947).
8. Chapin, E. C., and G. E. Ham, *J. Polymer Sci.*, **4**, 597 (1949).
9. Suzuki, S., and H. Ito, *J. Chem. Soc. Japan, Ind. Chem. Sect.*, **58**, 627 (1955).
10. Alfrey, T., Jr., C. G. Overberger, and S. H. Pimer, *J. Am. Chem. Soc.*, **75**, 4221 (1953).
11. Akazome, G., and K. Murai, *J. Chem. Soc. Japan, Ind. Chem. Sect.*, **63**, 1446 (1960).
12. Palit, S. R., and T. Guha, *J. Polymer Sci.*, **36**, 243 (1959).

Synopsis

The copolymerization of acrylonitrile (AN) with sodium *p*-styrenesulfonate (SSS) in aqueous solutions (of pH 3 and pH 7) has been investigated. Monomer reactivity ratios at 45°C. for AN and SSS are found to be $r_1 = 0.10 \pm 0.02$, $r_2 = 1.20 \pm 0.10$ at pH 3 and $r_1 = 0.05 \pm 0.01$, $r_2 = 1.40 \pm 0.04$ at pH 7, from which Price Q and e values for SSS of 0.76 and -0.26 at pH 3 and of 1.25 and -0.43 at pH 7 are calculated. Initial rates of copolymerization at 45°C. with ammonium persulfate (APS) as initiators were determined over the entire range of composition from pure AN to pure SSS, and it has been found that there is a sharp rise in copolymerization rates within 0.2–5 mole-% monomer feed, sometimes being eight times larger than those in the neighboring range. The copolymerization in SSS monomer feed of 0.2–5 mole-% occurs in the transition phase from homogeneous to heterogeneous, and the system is very viscous and slightly cloudy. From the investigation of the effect of initiator concentration on the copolymerization rate and the direct observation by an electron microscope, the sharp rise in copolymerization rates may reasonably be interpreted in terms of the emulsion copolymerization mechanism.

Résumé

La copolymérisation de l'acrylonitrile (AN) avec le *p*-styrènesulfonate de sodium (SSS) fur effectuée en solution aqueuse (de pH 3 à 7). On trouve des rapports de réactivité du monomère à 45°C d'une valeur égale à $r_1 = 0.10 \pm 0.02$, $r_2 = 1.20 \pm 0.10$ à pH 3 et à pH 7, $r_1 = 0.05 \pm 0.01$, $r_2 = 1.40 \pm 0.04$ desquelles sont extraites par calcul, les valeurs Q et e pour SSS de 0.76 et -0.26 à pH 3 et 1.25, -0.43 à pH 7. Les vitesses nitiales de copolymérisation à 45°C, avec le persulfate d'ammonium comme initiateur, sont déterminées sur une échelle de composition allant de l'AN pur à l'SSS pur et il fut trouvé qu'il y avait augmentation aigue dans les vitesses de copolymérisation pour une solution de monomères de 0.2 à 5 moles-%; elle peut être dans certains as huit fois plus élevée que dans le domaine voisin. C'est lors de la phase de transition de l'homogène à l'hétérogène que la copolymérisation des monomères SSS en solution de 0.2 à 5 mole-% se produit; le système devient très visqueux et légèrement trouble. On peut interpréter la montée aigue dans les vitesses de copolymérisation comme un mécanisme de copolymèrisation en émulsion en s'aidant de l'étude de l'effet de la concentration en initiateur sur la vitesse de copolymérisation et de l'observation directe par un microscope électronique.

Zusammenfassung

Die Copolymerisation von Acrylnitril (AN) und *p*-Natriumstyrolsulfonat (SSS) in wässriger Lösung (p_H 3 und 7) wurde untersucht. Die Monomerreaktivitätsverhältnisse bei 45°C für AN und SSS betrugen $r_1 = 0{,}10 \pm 0{,}02$, $r_2 = 1{,}20 \pm 0{,}10$ bei p_H 3 und $r_1 = 0{,}05 \pm 0{,}01$, $r_2 = 1{,}40 \pm 0{,}04$ bei p_H 7; aus diesen Werten wurden Q- und e-Werte nach Price für SSS von 0,76 und $-0{,}26$ bei p_H 3 und 1,25 und $-0{,}43$ bei p_H 7 berechnet. Die Anfangsgeschwindigkeit der Copolymerisation bei 45°C mit Ammonpersulfat (APS) als Starter wurde über den gesamten Zusammensetzungbereich von reinem AN bis zu reinem SSS bestimmt, und es wurde bei Monomermischungen mit 0,2–5 Molprozent ein scharfer Anstieg der Copolymerisationsgeschwindigkeit gefunden, machmal achtmal grösser als im angrenzenden Bereich. Die Copolymerisation in einer SSS-Monomerischung mit 0,2–5 Molprozent verläult in der Übergangsphase vom homogenen zum heterogenen Bereich und das System erweist sich als sehr viskos und schwach trüb. Auf Grund der Untersuchung des Einflusses der Starterkonzentration auf die Copolymerisationsgeschwindigkeit und der direkten Beobachtung mit einem Elektronenmikroskop kann man den scharfen Anstieg der Copolymerisationsgeschwindigkeit in Analogie zum Mechanismus der Emulsionscopolymerisation verständlich machen.

Received September 27, 1961
Revised December 4, 1961

JOURNAL OF POLYMER SCIENCE: PART A VOL. 1, PP. 715–723 (1963)

Crystalline Order in Nylon 66

HOWARD W. STARKWEATHER, JR., JOHN F. WHITNEY, and DONALD R. JOHNSON, *E. I. du Pont de Nemours & Company, Inc., Plastics Department, Du Pont Experimental Station, Wilmington, Delaware*

I. Introduction

It has been reported by Geil[1] that polyamides, like polyethylene and polyoxymethylene, crystallize from solution to form lamellar structures in which the chains are normal to the plane of the platelets. The thickness of these lamellae (50–100 A.) is about the same as the long-period spacings which can be detected by small-angle x-ray diffraction in the same polymers when crystallized from the melt. Thus, it seems that lamellae, perhaps in a distorted form, may be basic structural units in all crystalline polymers, including polyamides. In view of this possibility it is important to reexamine the concept of per cent crystallinity, particularly for specimens which have densities and other properties indicating large amorphous fractions, to decide whether there are discrete crystalline and amorphous regions or merely varying degrees of disorder in the crystalline structure.

It is most convenient to calculate the per cent crystallinity of nylon 66 from the density by use of a linear interpolation on a specific volume scale between values for the amorphous and crystalline densities of 1.069 g./cc. and 1.220 g./cc. respectively.[2]

The effects of various thermal treatments on the per cent crystallinity of nylon 66 at room temperature are shown in Figure 1. In all cases, the films were molded between aluminum foils and were quenched rapidly to 0°C. or below following the thermal treatment. When samples are quenched from the melt to 0°C. and then annealed for 10 min., the crystallinity increases with increasing annealing temperatures to a maximum of 56% at 250°C. Annealing at 255–270°C. reduces the level of crystallinity to 22–24%. The last evidence of crystallinity in these samples disappears at 272°C.

The procedure of cooling abruptly from the melt to an elevated temperature, holding for 15 min., and then quenching at 0°C. has been called hot quenching.[3] A maximum of 52% crystallinity was obtained by hot quenching at 225°C. X-ray diffraction studies have shown that this lies in a narrow temperature range within which occurs the greatest development of the high temperature crystalline modification (discussed in the next section). However, this changes to the triclinic form on quenching to 0°C. The per

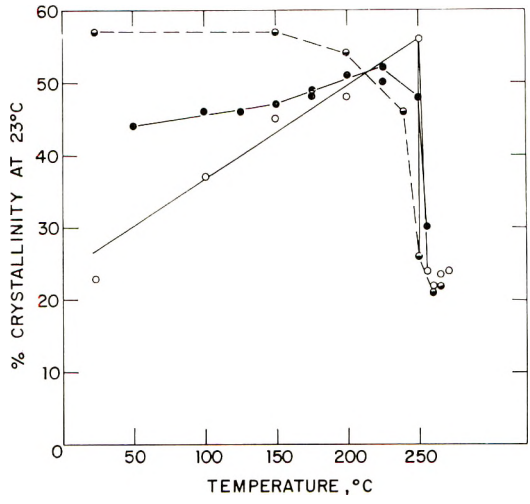

Fig. 1. Effect of thermal treatments on the crystallinity of nylon 66: (○) annealing temperature following quenching in ice water; (●) hot quench temperature; (◒) temperature at which slow cooling was interrupted.

cent crystallinity is less dependent on the temperature of crystallization for hot quenching than for cold quenching followed by annealing. When the polymer is cooled slowly from the melt, the greatest increase in crystallinity occurs between 250 and 240°C.

II. Types of Large-Angle Diffraction Patterns

The four basic types of x-ray diffractometer scans which are obtained for unoriented samples of nylon 66 are shown in Figure 2. At room temperature, samples which have been annealed at 175–250°C. display the triclinic crystal structure which has been described by Bunn and Garner.[4] The four peaks correspond to the (001), (002), and (100) spacings and the (110), (010) doublet. The first two peaks are due to order along the polymer chain, and their intensities are quite small. The two strong peaks are due to lateral order. In the range 200–272°C. a pseudohexagonal structure is observed.[5–8] The diffraction angle for the (002) reflection is about the same as in the triclinic state, but only one lateral spacing is observed, and this is close to the (100) spacing at room temperature. From this it is concluded that the polymer chains are still tilted with respect to the *ab* plane and that the separation between the sheets containing the amide–amide bonds has increased until the projection of the unit cell on the plane normal to the *c*-axis gives a two-dimensional hexagonal lattice.

When nylon 66 is quenched rapidly from the melt, a diffraction pattern is obtained at room temperature which has only one peak corresponding to the lateral packing of the chains.[6,8] Quenched specimens differ from the pseudohexagonal structure which is stable at elevated temperatures in the absence of the (002) reflection. They also differ from the melt in having a

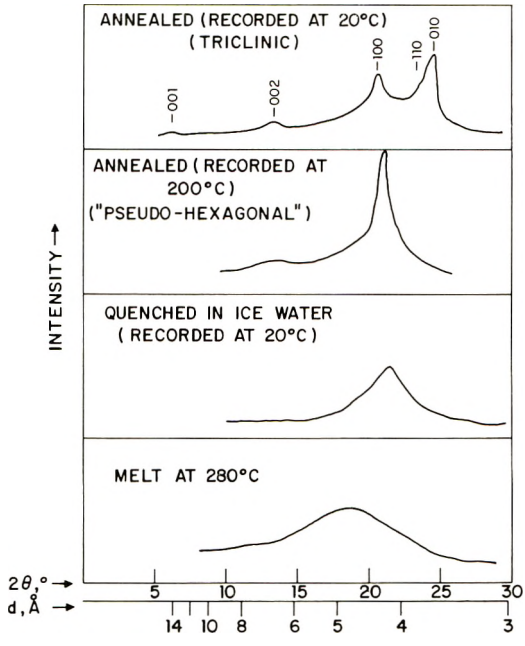

Fig. 2. X-ray diffractometer scans for nylon 66: intensity vs. scattering angle.

much sharper diffraction maximum. Specimens giving this type of diffraction pattern should not be considered amorphous, because they commonly have densities between 1.09 and 1.13 g./cc., while the amorphous density at room temperature is 1.069 g./cc. We believe that in the quenched specimens, the neighboring polymer chains have a greater tendency to be parallel to each other than in the melt, but that the sheets containing the amide–amide bonds are not well formed and are not in register with each other.

When nylon 66 is cooled slowly from the melt, it first crystallizes in the pseudohexagonal form. At about 175°C. the crystal structure begins to change into the triclinic form, but the change is a gradual shift in the lattice parameters rather than an abrupt change in the degree of order.[5,6,8]

When the triclinic form is heated to the melting point, the changes are essentially the reverse of those which occur during slow cooling. This is shown in Figure 3. In the pseudohexagonal form, the lateral diffraction peak becomes sharper and higher as the temperature is increased up to about 250°C. Above 255°C., this peak decreases in intensity but remains sharp as the melting point (272°C.) is approached.

When a quenched specimen is heated, the lateral spacing changes gradually all the way up to the melting point, but the height of the peak increases steadily from 100°C. to 250°C., indicating improved packing of the chains. There seems to be no tendency for the quenched state to change directly into the triclinic form without first going through the pseudohexagonal structure.

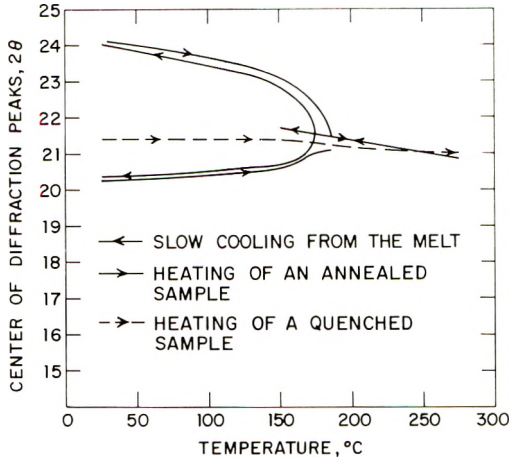

Fig. 3. Changes in the diffraction pattern of nylon 66 with temperature.

From the work of Trifan and Terenzi[9] and Cannon,[10] it appears that in polyamides the amide groups are always almost all bonded to each other, even in the disordered regions and in the melt. At temperatures where the pseudohexagonal structure is stable, it seems to be fairly easy for the amide groups to change their bonding partners. The fraction of amide groups making this change at any moment is probably very small. Below 175°C., where the triclinic form is stable, such shifts are much more difficult. This follows from the existence and relatively high stability of the quenched structures. The quenched structures may be compared with liquid crystals.[11] Since the only degree of order in which they differ from the melt is the greater tendency for neighboring chains to be parallel to each other, we prefer to describe them as a nematic rather than a smectic state, in contrast with the usage of Schmidt and Stuart.[8]

As applied to quenched structures, the term per cent crystallinity is construed to be an index of the overall quality of packing rather than the amount of a phase having true three-dimensional order.

III. Small-Angle Diffraction

In addition to the diffraction pattern at large angles, nylon 66 also exhibits characteristic x-ray diffraction patterns at small angles.[12,13] These small-angle patterns reflect organization on a scale larger than the unit cell. The angle for which the intensity of this diffraction is a maximum corresponds to a Bragg spacing which varies from 56 A. to 108 A., depending on the thermal history. This is shown in Figure 4. For a given crystallization temperature, hot quenching results in a larger long-range spacing than annealing after quenching to 0°C. or below. However, the dependence of the long-range spacing on per cent crystallinity is the same for all thermal treatments (Fig. 5).

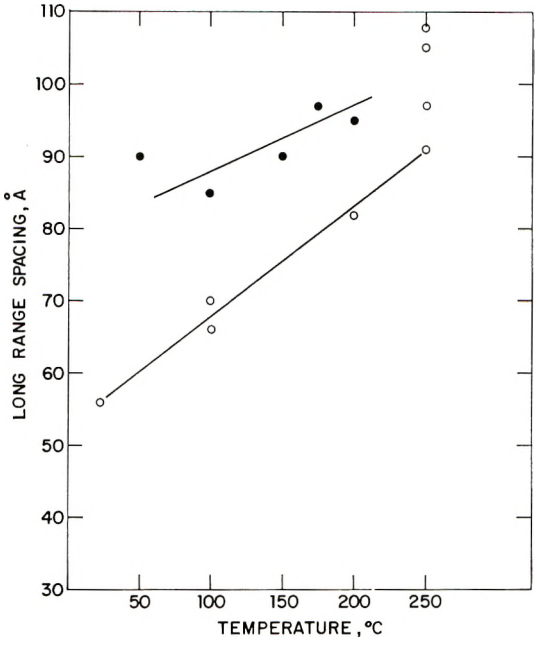

Fig. 4. Effect of thermal treatment on the long-range spacing in nylon 66: (○) annealing temperature after quenching in ice water; (●) hot quench temperature.

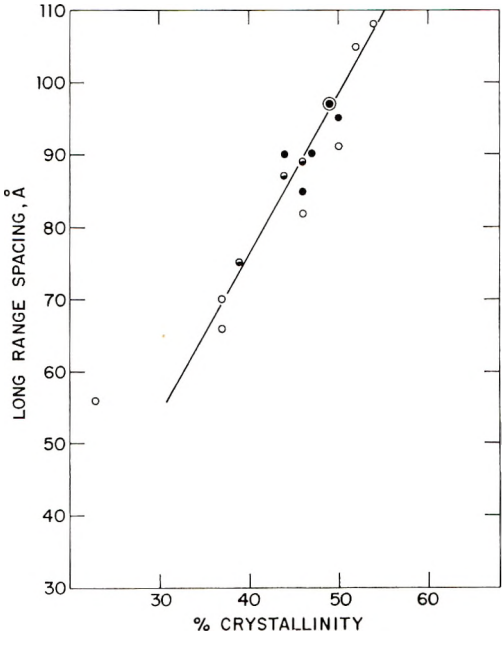

Fig. 5. Dependence of the long-range spacing in nylon 66 on per cent crystallinity: (○) annealed after quenching in ice water; (●) hot quenched; (◒) injection molded.

Annealing at 250°C. produces a long-range spacing which increases from 91 A. to 105 A. as the annealing period is increased from 5 sec. to 1 min. More prolonged annealing at 250°C. produces another type of small-angle scattering in which the intensity decreases continuously with increasing scattering angle. This type of diffraction is due to random variations in density from point to point and has been attributed[13] to voids which form in the highly annealed specimens. When it is sufficiently intense, void scattering can obscure the diffraction maximum due to the long-range spacing.

In nylon fibers, the long-range periodicity is in the direction of the polymer chains.[12,13] It is believed that this is also true in unoriented specimens. This is consistent with the lamellar structures which have been described by Geil.[1]

IV. Size and Perfection of Crystallites

The width of the diffraction peaks in most polymers suggests that the size of the crystallites is of the order of 50–200 A. However, part of the broadening may be due to imperfections in the crystallites. Thus, the crystallite sizes calculated in this way are minimum values. If thin lamellae in which the chains are normal to the principal surfaces are basic structural units in semicrystalline polymers, it seems probable that the width of the (001) and (002) peaks is primarily indicative of the thickness of the crystallites. Statton[13] has compared the long-range spacing for nylon fibers with the size of the crystallites calculated from the width of a meridional reflection in the wide-angle diffraction pattern. He considers the long period to be the sum of the lengths of crystalline and amorphous

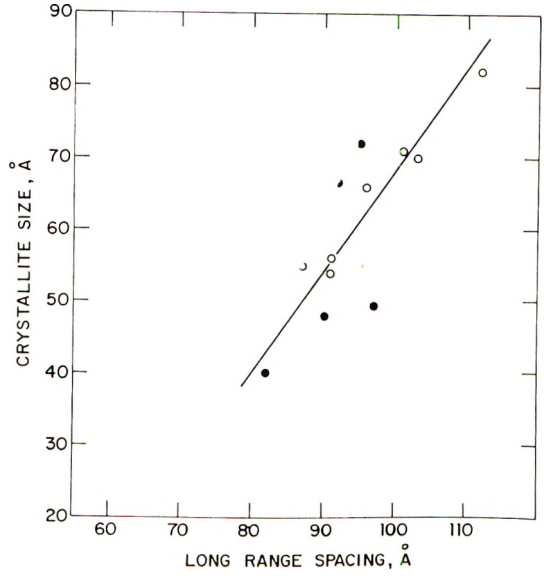

Fig. 6. Comparison of the crystallite size and long-period spacing in nylon 66: (○) oriented fibers (data of Statton[13]); (●) unoriented films.

segments. Within the limits of experimental uncertainty, the data shown in Figure 6 indicate that the relationship between the long-range spacing and the crystallite size is similar for drawn fibers and unoriented films. The difference between these quantities is about 30–40 A. This suggests that the lamellae consist of a central crystalline portion and outer amorphous portions, each of which is about as thick as the length of a repeat unit (17 A.).

V. The Meaning of Per Cent Crystallinity

The term per cent crystallinity, as applied to nylon 66, is based on a linear interpolation between the best estimates of the specific volumes of completely crystalline and amorphous phases.[2] This means that the amorphous fraction may include both completely disordered regions and any imperfections which reduce the density of the ordered or crystalline regions. One index of the degree of crystallinity is the ratio of the crystallite size in the chain direction to the long-period spacing. This ratio increases from 0.48 to 0.69 as the crystallinity varies from 40 to 55%. If the outer portions of the lamellae have the amorphous density, this would mean that the central, ordered portions are 80% crystalline.

Several other properties of nylon 66 correlate with the density or per cent crystallinity. At room temperature, the quenched structure occurs below 40–45% crystallinity, and the triclinic structure occurs above this level. The triclinic structure and the low-angle diffraction pattern are detected only when the size of the crystallites in the chain direction corresponds to at least 2–3 repeat units. As the per cent crystallinity is increased, the intensity of the small-angle diffraction increases, and eventually the void scattering appears. Thus, in nylon 66, the per cent crystallinity is a unifying concept expressing the overall degree of order, including mesomorphic structures, the relative amounts of ordered and disordered material, and the quality of the ordered regions.

VI. Melting

The melting points of polyamides are much higher than those of the corresponding polyesters. This is due not to a larger heat of melting but to a smaller entropy of melting. This, in turn, could mean either that the entropy of the solid just below the melting point is high because of partial disordering at lower temperatures[14] or that polyamides possess greater order above the melting point than other linear polymers. The latter view is supported by studies on the dependence of the entropy on temperature[15] and the changes in the infrared spectrum on melting.[9,10]

In order to interpret the entropy of melting, one should separate the portion due to expansion.[16] The entropy of melting corrected to constant volume, $(\Delta S_m)_v$, can be calculated from the total entropy of melting, ΔS_m, by (1), where T_m is the melting temperature:

$$(\Delta S_m)_v = \Delta S_m[1 - (\partial P/\partial T)_v(dT_m/dP)] \quad (1)$$

The results of this calculation for nylon 66 are given in Table I.

TABLE I
Entropy of Melting of Nylon 66

Heat of melting, cal./g.	45[a]
Melting point, °C.	272
ΔS_m, cal./°K. mole of repeat units	18.7
$(\partial P/\partial T)_v$, psi/°K.	134[b]
dT_m/dP, °K./psi	1.9×10^{-3} [b]
$(\Delta S_m)_v$, cal./°K. mole of repeat units	13.9

[a] Data of Dole and Wunderlich.[15]
[b] Data of Tordella.[17]

For polyethylene, $(\Delta S_m)_v$ is 1.77 cal./°K. per mole of CH_2 groups.[16] Thus, the entropy of melting of nylon 66 corrected to constant volume is equal to that of 7.8 CH_2 groups in polyethylene. In linear polymers, variations in $(\Delta S_m)_v$ are related to rotations about the primary bonds in the chain. Let us assume that in polyamides only rotation about bonds connecting two CH_2 groups contribute significantly. There are eight such bonds in a repeat unit of nylon 66.

The entropy of melting is consistent with Cannon's observation that only the infrared bonds associated with methylene groups changed on melting.[10] Undoubtedly, there are other effects making small contributions to the entropy of melting, but the factor outlined above seems to be the predominant one. The ability of polyamides to flow above their melting points proves that the bonded amides are not permanently associated, but the fraction which is unbonded at any moment is very small.

References

1. Geil, P. H., *J. Polymer Sci.*, **44**, 449 (1960).
2. Starkweather, H. W., Jr., and R. E. Moynihan, *J. Polymer Sci.*, **22**, 363 (1956).
3. Starkweather, H. W., Jr., and R. E. Brooks, *J. Appl. Polymer Sci.*, **1**, 236 (1959).
4. Bunn, C. W., and E. V. Garner, *Proc. Roy. Soc. (London)*, **A189**, 39 (1947).
5. Brill, R., *J. prakt. Chem.* [2], **161**, 49 (1942).
6. Sandeman, I., and A. Keller, *J. Polymer Sci.*, **19**, 401 (1956).
7. Slichter, W. P., *J. Polymer Sci.*, **35**, 77 (1958).
8. Schmidt, G. F., and H. A. Stuart, *Z. Naturforsch.*, **13a**, 222 (1958).
9. Trifan, D. S., and J. F. Terenzi, *J. Polymer Sci.*, **28**, 443 (1958).
10. Cannon, C. G., *Spectrochim. Acta*, **16**, 302 (1960).
11. Kast, W., in *Die Physik der Hochpolymeren*, Vol. 3, H. A. Stuart, Ed., Springer Verlag, Berlin, 1955, pp. 18–20.
12. Hess, K., and H. Kiessig, *Naturwissenschaften*, **31**, 17 (1943); *Z. physik. Chem.*, **A193**, 196 (1944); *Kolloid-Z.*, **130**, 10 (1953).
13. Statton, W. O., *J. Polymer Sci.*, **41**, 143 (1959).
14. Flory, P. J., H. D. Bedon, and E. H. Keefer, *J. Polymer Sci.*, **28**, 151 (1958).
15. Dole, M., and B. Wunderlich, *Makromol. Chem.*, **34**, 29 (1959).
16. Starkweather, H. W., Jr., and R. H. Boyd, *J. Phys. Chem.*, **64**, 410 (1960).

Synopsis

The x-ray diffraction patterns of nylon 66 at small and large angles have been correlated with the densities of samples prepared in various ways. Quenching from the melt to 0°C. produces structures which are less than 40% crystalline, as determined by density and have structures similar to nematic liquid crystals. More dense specimens have a triclinic structure and appear to contain lamellae 50–100 A. thick which consist of outer amorphous layers and a central portion which is about 80% crystalline. Thermodynamic and spectroscopic evidence indicates that the disorder on melting consists of rotations about the bonds connecting CH_2 groups.

Résumé

La diffraction aux rayons-X du nylon 66 aux petits et grands angles a été comparée aux densités d'échantillons préparés de différentes manières. Le refroidissement brutal au départ de l'état fondu à 0°C produit des structures qui sont cristallines à moins de 40%, ainsi qu'il résulte de la détermination par densité; ces structures sont similaires aux cristaux liquides nématiques. Des échantillons plus denses ont une structure triclinique et semblent contenir des lamelles ayant une épaisseur de 50–100 Å, constituées de couches amorphes àl 'extérieur et dont la région centrale est environ 80% cristalline. L'analyse thermodynamique et spectroscopique indique que le désordre à l'état fondu est dû aux rotations des liaisons liant les groupes CH_2.

Zusammenfassung

Eine Korrelation der Röntgenbeugungsdiagramme von Nylon 66 bei kleinen und grossen Winkeln mit den Dichten von verschieden hergestellten Proben wurde aufgestellt. Abschrecken aus der Schmelze auf 0°C erzeugt Strukturen mit einer aus der Dichte bestimmten Kristallinität von weniger als 40% und mit einem den mneatischen flüssigen Kristallen ähnlichen Aufbau. Dichtere Proben besitzen eine trikline Struktur und scheinen Lamellen mit 50–100 Å Dicke zu enthalten, die aus äusseren amorphen Schichten und einem inneren Anteil von ungefähr 80% iger Kristallinität bestehen. Thermodynamische und spektroskopische Befunde weisen darauf hin, dass die Unordnung beim Schmelzen in einer Rotation um die Bindungen zwischen den CH_2-Gruppen besteht.

Received December 22, 1961

JOURNAL OF POLYMER SCIENCE: PART A VOL. 1, PP. 725–732 (1963)

Strain Birefringence of Sodium Hyaluronate Films

VAHAK M. DERSARKISSIAN and FREDERICK A. BETTELHEIM,
Chemistry Department, Adelphi College, Garden City, New York

Introduction

Hyaluronic acid is one of the most widely distributed mucopolysaccharide components of the connective tissues.[1,2] Mechanical, elastic, and flow properties of such systems are influenced greatly by the contribution of hyaluronic acid.[3–8] Since most of these systems form loose gel structures[9,10] or very viscous liquids,[3,5] the molecular parameters obtained from measurements of infinitely dilute solutions do not fully explain the physical properties of the physiological states. The aim of our investigation was to provide information on the behavior of hyaluronic acid in the gel. Mechanical and elastic properties depend largely upon the degree of orientation of the molecules when they are subjected to stresses. The total strain birefringence of swollen polymeric films is the sum of two factors: (*a*) orientation birefringence and (*b*) form birefringence.[11] If one lets the films swell in liquids of different refractive indices, one obtains Wiener-type curves,[12] the minima or maxima of which give the orientation birefringence alone. Hence, strain birefringence measurements on swollen sodium hyaluronate films at different elongations can enlighten our knowledge on the ease and degree of orientation of hyaluronate in gel.

Material

Sodium hyaluronate was isolated from human umbilical cords which were stored in acetone for six weeks. The method used was a combination of those of Jeanloz and Forchielli[13] and Schiller et al.[14] The hyaluronate was purified from proteins by subsequent enzymic hydrolyses with pepsin and trypsin. The remaining polymeric material was precipitated from the solution with two volumes of ethanol after the pH was adjusted to 4.6 with acetate buffer. Further purification from proteins was achieved by repeated Sevag procedures also with the use of Lloyd's Reagent.[13] The separation of hyaluronate from admixed sulfated polysaccharides was accomplished by cetyl pyridinium chloride precipitation and subsequent solubilization with 0.4*M* NaCl solution.[14] The yield of hyaluronate was 1.2% on the basis of the dry weight of the umbilical cords.

The product from the above isolation procedure was analyzed, and the following results were obtained.

Acid hydrolysis with 4*N* HCl and subsequent paper chromatography showed only D-glucuronic acid and D-glucosamine spots. No amino acids were present in the hydrolyzate. Anderson's micro method for sulfur determination[15] gave negative results. Dische's method for the determination of uronic acid content[16] gave 53% uronic acid as anhydrosodium glucuronate. A modification of the Elson-Morgan method[17] gave 41% *N*-acetyl glucosamine. The preparation contained 3.2% nitrogen as determined by a micro-Kjeldahl method.

Methods

To prepare the films, purified sodium hyaluronate was dissolved in a small amount of water. This solution was poured onto a ferrotype plate and placed in a vacuum oven. The films, after drying for 24 hr. at a pressure of approximately 127 mm. Hg at room temperature, were easily removed from the plate.

Film strips, approximately $1\frac{1}{2} \times 5$ cm., were prepared. These strips were marked at $\frac{1}{2}$ cm. intervals with inked lines and were then placed in the jaws of a lathe-type stretching device. This device and the film were placed in a tray containing 82% ethanol, and the films were slowly elongated. The amount of elongation was determined by measuring with a caliper the average distance between the inked lines after stretching. After stretching, the films were clamped in a jig and kept under absolute alcohol prior to birefringence measurements. Films were stretched to 10, 20, 30, 40, and 50% elongation.

The clamped, elongated films were immersed in liquids of different refractive indices. In order to exchange the 82% ethanol solution for the solvent desired, eight to ten immersions, each for 12 hr., were needed. The criterion for equilibrium swelling was a constant thickness measurement of the swollen film at least throughout three subsequent immersions.

To obtain the thickness of the films, an American Optical Spencer Metalstar compound microscope with a tungsten light source and green filter was used. The vertical illumination was restricted to a small area in the total field by means of a hexagonally shaped iris.

By means of the calibrated fine adjustment the edges of the hexagon were first focused on the top and then the bottom of the film. The difference of readings gave the apparent thickness of the film in microns. The actual thickness was obtained from the following relationship:

$$\text{Actual thickness} = \text{Apparent thickness} \times \text{average refractive index of the film}$$

The average refractive index of the film was obtained by placing small pieces of film in various solvents. The refractive index of the solvent in which the film was no longer visible was taken to be the average refractive index of the film. This solvent was found to be benzene, the refractive index of which is 1.50.

Birefringence measurements were taken with the use of 5461 A. radiation of a mercury lamp. The sample cell and the quartz halfwave plate compensator were placed between a polarizer set at a 45° angle to the vertical and an analyzer set 90° to the axis of the polarizer. Blank measurements for the retardation of the solvent were taken with the sample cell filled with liquid but without the stretched and preswollen film.

The elongated sodium hyaluronate film in its special jig was then placed in the cell with the direction of stretched parallel to the orientation of the electric vector of the polarized radiation. The halfwave plate was rotated, and the point of total extinction was again determined. The reading in degrees of the halfwave plate with the film in the solvent minus the reading given by the solvent alone was a measure of the retardation caused by the film.

The film was then rotated, and similar readings were taken with the electric vector perpendicular to the direction of stretch. The average of the readings obtained with the film placed perpendicular and parallel provided a measure of the total amount of retardation caused by the film.

The method for calculating the birefringence is as follows:

$$N = (n_{\parallel} - n_{\perp})d/\lambda_0$$

where N is the retardation or number of waves of path difference, d is the thickness of the film, and λ_0 is the wavelength of monochromatic light. Here, $(n_{\parallel} - n_{\perp})$ is the difference in refractive indices with the polarized parallel and perpendicular to the direction of stretch, i.e., the birefringence.

Results and Discussion

The swelling ratios of sodium hyaluronate film in various liquids of different refractive indices are given in Table I.

TABLE I

Liquid	Refractive index	Swelling ratio, %
Ethyl alcohol	1.36	1
Triethylamine	1.40	49
Cyclohexene	1.44	21
Benzene	1.50	56
α-Chlorotoluene	1.54	50
Bromobenzene	1.56	21

These swelling ratios were determined in order to ascertain the degree to which solvent molecules had penetrated the films, giving rise to the form birefringence observed. Had the measurements been taken in air alone (refractive index = 1.00), the form birefringence would have been very high.

The results of the total birefringence readings are given in Figure 1.

The total birefringence as measured is the sum of orientation and form birefringence. Since the entanglement and interaction of hyaluronate

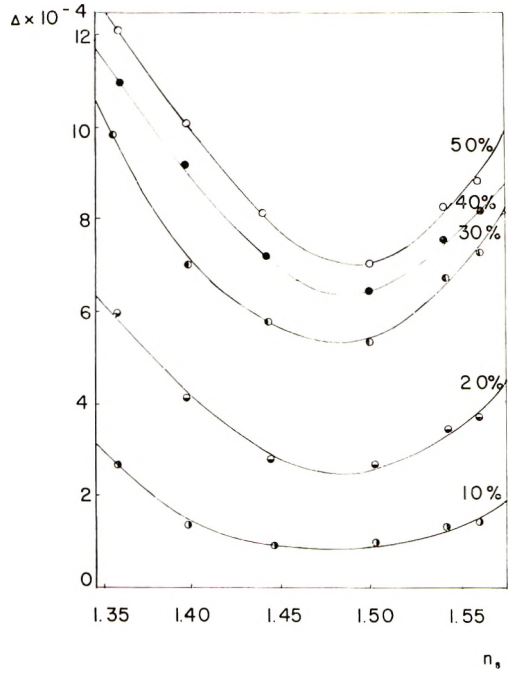

Fig. 1. The variation of the birefringence of stretched sodium hyaluronate films with refractive index of the swelling liquids for several elongations.

chains with each other is reflected in the degree of orientation, one wants to correlate the orientation birefringence with elongation. This is done by the separate evaluation of form birefringence in different swelling liquids.

In Figure 1, the birefringence measurements are plotted against the refractive index of different liquids. The birefringence plots indicated a minimum in the manner predicted by Wiener,[12] whose theory predicts such a minimum for the form birefringence of rodlets elongated in the direction of stretch. The curvature of the graph obtained increased with stretching, indicating that the orientation increased as the film was elongated.

Sterling[18] obtained similar curves in dried alginate samples. The form birefringence values of the dried alginate were found to be of the same magnitude as that of the sodium hyaluronate samples in this study. This value is approximately 2×10^{-4}. According to Wiener, at the minimum of the curves in Figure 1, there is no form birefringence and the only contributing factor to the birefringence values of the swollen films is the orientation birefringence.

In Figure 2, orientation birefringence is plotted against per cent elongation. The graph shows an increase in orientation birefringence with increasing elongation. This is interpreted as being due to the arrangement of the polymer chains in a parallel distribution. The curve appears to be reaching a maximum beyond which rupture of the film results.

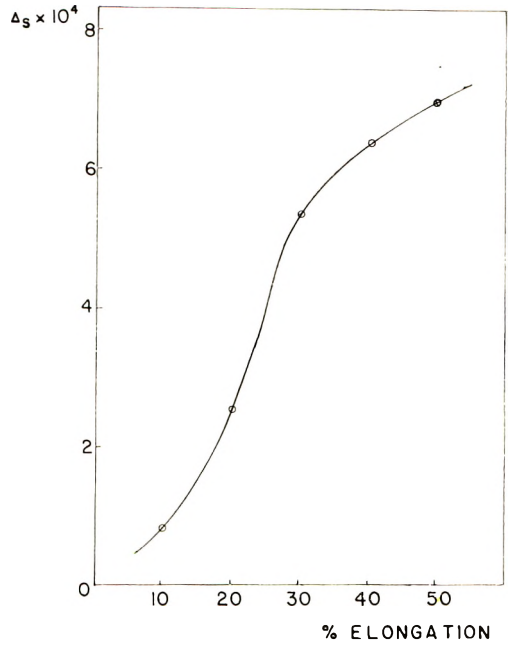

Fig. 2. The variation of strain or orientation birefringence (minimum of the curves from Fig. 1) of stretched swollen sodium hyaluronate films with elongation.

Initially, the sodium hyaluronate aggregates orient themselves in a manner resembling the arrangement in a rubberlike material. This arrangement persists up to approximately 25% elongation and gives curves corresponding to the Kuhn-Treloar theories.[19,20] The indication is, therefore, that at small elongations, first the free nonhydrogen-bonded parts of the amorphous chains will orient in the direction of stretch, as one expects from rubberlike behavior. Above 25% elongation, however, the orientation birefringence increases only slightly with elongation asymptotically approaching a maximum birefringence. The swollen films, however, break before this value can be reached. The molecular interpretation may be that once the free amorphous segments have oriented themselves, little further orientation can occur due to the strong intermolecular hydrogen bonding, and further stresses cause slippage of chains and breaking hydrogen bonds which will result in mechanical break.

The absolute values of orientation birefringence obtained are small compared to those reported in the literature. Sylven and Ambrose[21] prepared thin fibers of hyaluronic acid which showed a maximum value of 1.5×10^{-2}. This is a magnitude greater than our data. The disagreement can be explained on the basis of molecular weights on one hand and due to the difference between the measured quantities on the other. Bettelheim[22] has shown that if the hyaluronate chain is degraded to low molecular weight, a crystalline material can be obtained which possesses a great deal of chain stiffness. However, the sodium hyaluronate of the present

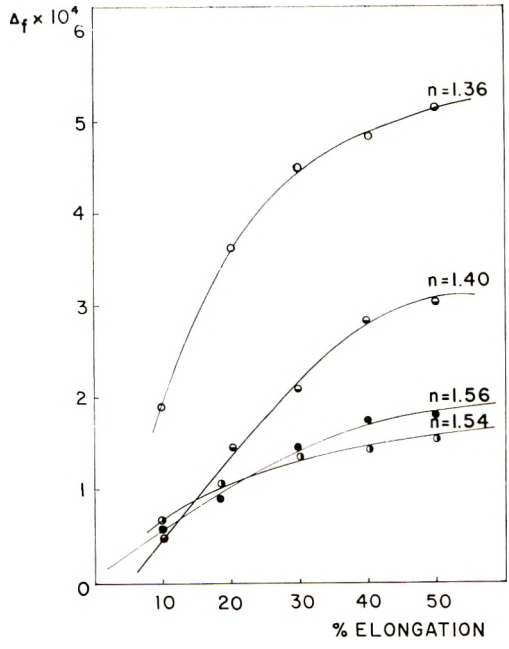

Fig. 3. The variation of form birefringence of stretched swollen sodium hyaluronate films in a medium of refractive index n at several elongations.

study had a molecular weight of 1.2×10^6, and it was amorphous. Care was taken to avoid excessive degradation for the reason that the total orientation birefringence should be interpreted unequivocally, that is, no need should arise to separate the crystalline and amorphous orientation birefringence. Since the molecular weights are high, one can expect greater random entanglement and hence a lower birefringence.

The main reason for the difference between values of Sylven and Ambrose and our own is that we measured a different quantity. At zero stress and zero elongation the films showed no birefringence, i.e., there was a random orientation of the chains in the film. The values thus obtained are solely due to the strain exerted on the swollen gel and not to surface orientation introduced in the liquid state and preserved in the dry fibers.[21] Therefore, our values correspond more to the action in a physiological gel under stress when the tendency for orientation is counterbalanced by the hydrogen bonds between neighboring chains.

Beside this, the value given by Sylven and Ambrose represents the total birefringence, in which case, the air being the embedding medium, the contribution of the form birefringence might be quite appreciable.

In Figure 3, form birefringence is plotted against elongation in liquids of different refractive indices. The graph indicates an increase in form birefringence with increasing elongations. The existence of the Wiener curves[12] indicates that the hyaluronate chains aggregate into a rodlet shape which cause form birefringence. As these rodlets orient with elon-

gation, the form birefringence increases. The minima of the Wiener curves lie at refractive indices where the solvent matches the refractive index of the imbedded particle perpendicular to the direction of stretch. One can see (Fig. 1) that these minima lie at lower refractive indices the higher the elongation, indicating slight orientation of the rodlets with their long axis toward the direction of stretch.

This investigation was supported in part by Grant C-3984 (BBC) of the National Cancer Institute, Public Health Service.

References

1. Meyer, K., *Physiol. Rev.*, **27**, 335 (1947).
2. Whistler, S., *Polysaccharide Chemistry*, Academic Press, New York, 1953, p. 417.
3. Ogston, A. G., and J. B. Stanier, *Biochem. J.*, **46**, 364 (1950).
4. Ogston, A. G., and J. B. Stanier, *Biochem. J.*, **49**, 585 (1951).
5. Ogston, A. G., and J. B. Stanier, *Biochem. J.*, **52**, 149 (1952).
6. Ogston, A. G., and J. B. Stanier, *Discussions Faraday Soc.*, **13**, 275 (1953).
7. Egelius, N., E. Jonsson, and L. Jundblad, *Ann. Rheumatic Diseases*, **15**, 357 (1956).
8. Balazs, E. A., and L. Sundblad, *Acta Soc. Med. Upsaliensis*, **64**, 137 (1959).
9. Pigman, W., B. Gramling, and H. L. Holley, *Biochim. et Biophys. Acta*, **46**, 100 (1961).
10. Whistler, S., *Polysaccharide Chemistry*, Academic Press, New York, 1953, Chapt. 5.
11. Bettelheim, F. A., and R. S. Stein, *J. Polymer Sci.*, **27**, 567 (1958).
12. Wiener, O., *Abhandl. kgl. Sachs. Ges. Wiss. Math.-Physik. Klasse*, **32**, 509 (1912).
13. Jeanloz, R. W., and E. Forchielli, *J. Biol. Chem.*, **186**, 495 (1950).
14. Schiller, S., G. A. Slover, and A. T. Dorfman, *J. Biol. Chem.*, **236**, 983 (1961).
15. Anderson, L., *Acta Chem. Scand.*, **7**, 689 (1953).
16. Dische, Z., *J. Biol. Chem.*, **167**, 189 (1947).
17. Johnston, J. P., A. G. Ogston, and J. B. Stanier, Analyst, **76**, 88 (1951).
18. Sterling, C., *Biochim. et Biophys. Acta*, **26**, 191 (1957).
19. Kuhn, W., and H. Grün, *Kolloid Z.*, **101**, 248 (1942).
20. Treloar, L. R. G., *Trans. Faraday Soc.*, **42**, 83 (1946).
21. Sylven, B., and E. J. Ambrose, *Biochim. et Biophys. Acta*, **18**, 587 (1955).
22. Bettelheim, F. A., *J. Phys. Chem.*, **63**, 2069 (1959).

Synopsis

Strain birefringence of swollen sodium hyaluronate films was measured. Typical Wiener curves were obtained in solvents with different refractive indices. The orientation birefringence of sodium hyaluronate was evaluated from the minima of the Wiener curves and was found to increase with increasing elongation. Up to 30% elongation, the swollen hyaluronate films show quasi-rubberlike behavior. Above this elongation, the interchain hydrogen bonding further hinders the chain mobility and the orientation increases only slightly.

Résumé

La biréfringence due à la tension a été mesurée sur des films fondus d hyaluronate de sodium. On a obtenu des courbes typiques de Wiener dans des solvants ayant différents indices de refraction. On a mesuré la biréfringence d'orientation de l'hyaluronate de sodium à partir des minima des courbes de Wiener et on a trouvé que ceux-ci augmentent avec une augmentation d'élongation. Jusqu'à 30% d'élongation le film fondu d'hyaluronate a un comportement quasi identique au caoutchouc. Au-dessus de 30% d'élongation la liaison hydrogène entre les chaînes inhibe la mobilité de la chaîne et l'orientation augmente seulement lentement.

Zusammenfassung

Die Spannungsdoppelbrechung von gequollenen Natriumhyaluronatfilmen wurde gemessen. In Lösungsmitteln mit verschiedenem Brechungsindex wurden typische Wiener-Kurven erhalten. Die Orientierungsdoppelbrechung von Natriumhyaluronat wurde aus den Minima der Wiener-Kurven berechnet und es wurde gefunden, dass sie mit zunehmender Dehnung ansteigt. Bis zu einer 30% igen Dehnung zeigen die gequollenen Hyaluronatfilme ein quasi-kautschukartiges Verhalten. Oberhalb dieser Dehnung behindern die Wasserstoffbrücken zwischen den Ketten eine weitere Kettenbeweglichkeit und die Orientierung nimmt nur mehr wenig zu.

Received December 4, 1961

JOURNAL OF POLYMER SCIENCE: PART A VOL. 1, PP. 733–749 (1963)

Thermodynamic Properties of Solutions of Cellulose Acetate and Cellulose Nitrate

W. R. MOORE and R. SHUTTLEWORTH, *Polymer Research Laboratories, Department of Chemical Technology, Bradford Institute of Technology, Bradford, Yorkshire, England*

INTRODUCTION

Thermodynamic properties of dilute solutions of cellulose derivatives have been fairly extensively studied.[1–7] Comparable studies of more concentrated solutions are less complete and mainly restricted to cellulose nitrates[1,8,9] and relatively high polymer concentrations. The high osmotic pressures and viscosities of such systems preclude the use of osmometry, and vapor pressure measurements have been used. Schulz[1] and Takenaka[8] used the lowering of vapor pressure in studies of cellulose nitrate–acetone systems, and Baughan, Jones, and Stewart[9] weighed films of cellulose nitrates at measured vapor pressures of different solvents. Both methods were used by Jeffries[4] in studies of solutions of secondary cellulose acetate in phenol and acetone. The vapor pressure lowering for solutions containing up to 30 wt.-% of moderately high molecular weight cellulose derivatives is small, and solutions covering this concentration range have received little study.

Previous studies on dilute solutions of cellulose derivatives[6,7] have shown that in certain cases heats of dilution are positive, and, if solvation is taken into account, results are capable of interpretation in terms of current polymer-solvent interaction theory. To what extent such interpretation is possible at higher concentrations is not clear. Solvation may lead to

TABLE I
Characteristics of Polymers

Polymer	$\bar{M}_n$	D.S.	d_4^{25}, g./cc.
Cellulose acetate	104,000	2.50	1.397
Cellulose nitrate	94,000	2.36	1.628

changes in the magnitude and sign of thermodynamic quantities and parameters at higher concentrations. The results of measurements of the vapor pressure lowering of moderately concentrated solutions (10–50 wt.-% of polymer) of secondary cellulose acetate in four representative solvents over a range of temperature are given in this paper. Comparable solutions of a cellulose nitrate of similar degree of substitution and molecular

weight in two solvents have also been studied for purposes of comparison with other results and those for the less polar acetate. Thermodynamic data are obtained and discussed.

EXPERIMENTAL

Materials

The cellulose acetate and nitrate were fractions obtained by methods previously described.[10,11] Their characteristics are given in Table I. Number-average molecular weights, $\bar{M}_n$, were obtained osmotically in acetone at 25°C. Degrees of substitution, D.S., were determined by standard methods and densities in aromatic-free hexane at 25°C.

Acetone, methyl acetate, pyridine, and dioxane were used as solvents for the cellulose acetate, and acetone and methyl acetate were used for the nitrate. Careful purification of solvents is an essential for measurements of vapor pressure. Acetone was refluxed with potassium permanganate and calcium oxide and then distilled, the distillate being further purified by the method of Felsing and Durban.[12] A middle fraction was converted to the crystalline addition compound $NaI \cdot (CH_3)_2CO$ by treatment with vacuum-dried sodium iodide. The crystals were heated and the acetone produced refractionated twice. About 100 ml. of the final middle fraction was collected in a tube containing anhydrous magnesium sulfate. The tube was connected to a vacuum system, cooled, and the contents degassed in high vacuum. The acetone was then fractionated in vacuum, about 10 ml. of the middle fraction being finally distilled into the apparatus for measuring vapor pressure. The vapor pressure was measured at temperatures of 15–40°C. Values agreed closely with those given in the literature,[9,12,13] and the density at 25°C. agreed with that given by Hughes and Dippy[14] for anhydrous acetone.

Methyl acetate was refluxed with acetic anhydride and then distilled. The distillate was shaken with anhydrous potassium carbonate, redistilled, and the distillate allowed to stand over anhydrous sodium sulfate. It was then thrice refractionated, and the final middle fraction was cooled and degassed in vacuum. It was finally refractionated in vacuum and a middle fraction collected in the apparatus for measuring vapor pressure. Vapor pressures in the range 15–40°C. and the density at 25°C. were in close agreement with values given by Timmermans.[13]

Pyridine was refluxed with solid caustic soda, thrice fractionally distilled, stored over solid caustic soda, and then refractionated, the final middle fraction being cooled and degassed in vacuum. It was then refractionated in vacuum and a middle fraction collected in the apparatus for vapor pressure measurement. Vapor pressures in the range 15–40°C. and the density at 25°C. agreed closely with values given by Timmermans.[13]

Dioxane was refluxed with 1*N* hydrochloric acid for several hours. Caustic potash was added to neutralize acid and the aqueous layer removed. After standing over caustic potash for 24 hr. the dioxane was refluxed with

sodium for 12 hr. and twice refractionated from sodium. The final middle fraction was cooled and degassed in vacuum and refractionated in vacuum, a middle fraction being collected in the apparatus for measuring vapor pressure. Vapor pressures in the range 15–40°C. agreed closely with values given in the literature.[9,15,16] The melting point and density at 25°C. were in good agreement with those given by Timmermans.[13]

All distillations other than those in vacuum were carried out with suitable precautions to exclude water vapor, and the final transfer to the apparatus for measurement of vapor pressure involved passage of the vapor over phosphorus pentoxide. Densities were determined by means of pyknometers.

Measurement of Vapor Pressure Lowering

The method of direct measurement of the difference in vapor pressure between solvent and solution was used and the apparatus was essentially that of Bawn, Freeman, and Kamillidin[17] as modified by Bawn and Wajid.[18] It consisted of a U-tube connected at the base of a mercury reservoir, one limb of the U-tube being connected to a small bulb which contained the solution. The other limb, leading initially to a vacuum line, was also sealed to a calibrated side tube containing the solvent. The U-tube manometer and mercury reservoir were immersed in a water bath which could be thermostatically controlled to ±0.01°C. at temperatures in the range 15–45°C.

Polymer was weighed into the small bulb which was then sealed on to the U-tube and the polymer degassed by evacuating the bulb which was heated by boiling water. Solvent was distilled in vacuum into the calibrated side tube which was then sealed off. Vapor pressures of the pure solvent were then measured at 25, 30, 35, and 40°C. Solutions of known concentration were obtained by distilling known amounts of solvent from the calibrated side tube into the bulb containing polymer and vice versa.

Differences between the vapor pressures of solvent and solution were determined at 25, 30, 35, and 40°C. by direct measurement of the mercury levels in the U-tube with a cathetometer. Measurements were first made at increasing concentrations of polymer and then at decreasing concentrations. About 3 hr. was required for equilibrium to be reached. At the end of a series of measurements all the solvent was distilled on to the polymer. The vapor pressure of the resulting dilute solution was the same as that of the pure solvent, so that no volatile substances were produced during measurements. Two separate series of measurements were made with each polymer–solvent combination, fresh polymer and solvent being used for each. The volume of the system was accurately calibrated and corrections made for the mass of solvent in the vapor phase. Thermometers were calibrated and could be read to better than 0.01°C.

Calculation of Activities

Since the solvent vapor is nonideal, corrections must be made for gas imperfection. The activity of the solvent, a_1, is given by:

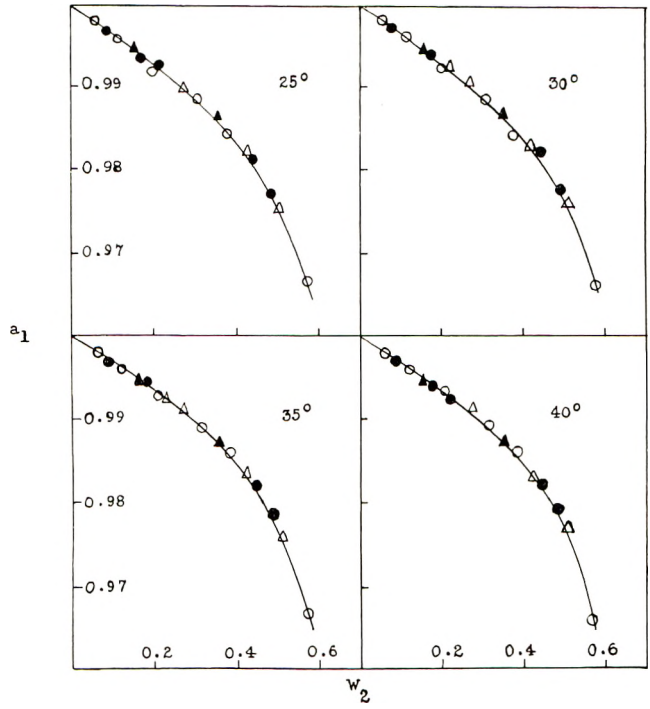

Fig. 1. a_1 as a function of polymer weight fraction for the cellulose acetate–acetone system: (○) first series of measurements at increasing concentration; (●) first series of measurements at decreasing concentration; (△) second series of measurements at increasing concentration; (▲) second series of measurements at decreasing concentration.

$$a_1 = f_1/f_{01} \tag{1}$$

where f_1 and f_{01} are the fugacities of the vapor above solution and solvent, respectively. The fugacity ratio may be related to the vapor pressure ratio p_1/p_{01} by:[9]

$$\log (f_1/f_{01}) = \log (p_1/p_{01}) + X(1 - p_1/p_{01}) \tag{2}$$

where

$$X = -[(B - V_1)p_{01}]/(2.303RT) \tag{3}$$

B is the second virial coefficient of the vapor, R is the gas constant, and V_1 is the molar volume of the liquid at the absolute temperature T. This method was used to correct pressure ratios to activities. Values of B for acetone, methyl acetate, and pyridine were obtained by the method of Lambert et al.[19] Values of B for dioxane were estimated from that given for 20°C. by Baughan, Jones, and Stewart.[9]

RESULTS

Figures 1–6 show a_1 as a function of polymer weight fraction w_2 at each temperature. Hysteresis effects are seen to be absent, and the results of the

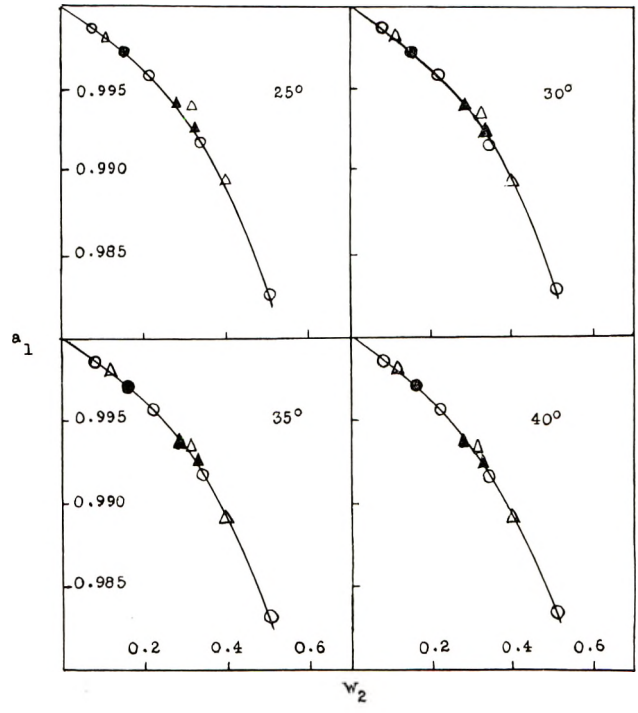

Fig. 2. a_1 as a function of polymer weight fraction for the cellulose acetate–methyl acetate system. Points indicated as in Fig. 1.

two separate series of measurements on each system are in good agreement. Where comparison is possible, results are in general agreement with those of other workers. Values of a_1 for the cellulose acetate–acetone system are similar to those of Jeffries.[4] Those for the cellulose nitrate–acetone system agree generally with those of Schulz[1] and with those of Baughan et al.[9] if the higher degree of substitution of the nitrates used by the latter workers is taken into account.

Free energies of dilution $\Delta\bar{F}_1$ at $w_2 = 0.1, 0.15, 0.2, 0.25, 0.3, 0.35, 0.4, 0.45$ and 0.5 were obtained from

$$\Delta\bar{F}_1 = RT \ln a_1 \tag{4}$$

values of a_1 being interpolated from the smooth curves in Figures 1–6. Heats $\Delta\bar{H}_1$ and entropies $\Delta\bar{S}_1$ of dilution were calculated by use of the relationships:

$$\Delta\bar{H}_1 = \delta(\Delta\bar{F}_1/T)/\delta(1/T) \tag{5}$$

and

$$-\Delta\bar{S}_1 = \delta\Delta\bar{F}_1/\delta T \tag{6}$$

Values of $\Delta\bar{F}_1$, $\Delta\bar{H}_1$, and $T\Delta\bar{S}_1$ at 30 and 35°C. are given in Tables II and III which also include "ideal" values of $T\Delta\bar{S}_1$ obtained from:

$$\Delta\bar{S}_1 \text{ (id)} = R x_2 \tag{7}$$

where x_2 is the mole fraction of polymer. Values of $\Delta\bar{H}_1$ and $T\Delta\bar{S}_1$ are estimated to be $\pm 10\%$ with perhaps somewhat larger errors at the lowest concentrations.

a_1 may be related to the composition of a polymer–liquid system by:

$$\ln a_1 = \ln (1 - \phi_2) + (1 - 1/x)\phi_2 + \chi_1\phi_2^2 \tag{8}$$

TABLE II
Cellulose Acetate–Solvent Systems

		30°C.			35°C.			
Solvent	w_2	$-\Delta\bar{F}_1$, cal./mole	$\Delta\bar{H}_1$, cal./mole	$T\Delta\bar{S}_1$, cal./mole	$-\Delta\bar{F}_1$, cal./mole	$\Delta\bar{H}_1$, cal./mole	$T\Delta\bar{S}_1$, cal./mole	$T\Delta\bar{S}_1$ (id)
Acetone	0.1	1.9	4.7	6.6	1.9	4.4	6.3	0.04
	0.15	3.0	4.6	7.6	3.0	4.4	7.4	0.06
	0.2	4.2	0.2	4.4	4.2	−0.1	4.1	0.08
	0.25	5.2	−4.2	1.0	5.2	−4.4	0.8	0.11
	0.3	6.6	−13.0	−6.4	6.4	−13.0	−6.6	0.14
	0.35	8.1	−17.3	−9.2	7.8	−17.4	−9.6	0.18
	0.4	9.3	−24.0	−14.7	9.1	−24.7	−15.6	0.22
	0.45	11.4	−27.4	−16.0	11.1	−26.7	−15.6	0.28
	0.5	14.0	−28.1	−14.1	13.7	−25.8	−12.1	0.34
Methyl acetate	0.1	1.0	2.4	3.4	1.1	1.5	2.6	0.05
	0.15	1.5	2.8	4.3	1.7	2.5	4.2	0.08
	0.2	2.2	3.1	5.3	2.3	3.2	5.5	0.11
	0.25	3.0	2.4	5.4	3.1	2.5	5.6	0.14
	0.3	4.0	1.8	5.8	4.1	1.5	5.6	0.18
	0.35	5.1	0.7	5.8	5.2	0.8	6.0	0.23
	0.4	6.3	0.1	6.4	6.4	−1.0	5.4	0.29
	0.45	7.8	−1.7	6.1	7.8	−2.5	5.4	0.35
	0.5	10.0	−7.6	2.4	10.1	−8.5	1.6	0.43
Pyridine	0.15	2.4	0.1	2.5	2.4	0.1	2.5	0.08
	0.2	6.0	−0.1	5.9	6.1	−0.2	5.9	0.11
	0.25	10.8	−0.6	10.2	11.0	−0.5	10.5	0.15
	0.3	16.9	−0.8	16.1	17.2	−0.9	16.3	0.20
	0.35	25.4	−1.3	24.1	25.8	−1.2	24.6	0.25
	0.4	35.4	−1.8	33.6	36.1	−1.7	34.4	0.31
	0.45	47.4	−2.2	45.2	48.2	−2.1	46.1	0.37
Dioxane	0.15	2.5	−0.1	2.4	2.5	−0.2	2.3	0.09
	0.2	4.3	−2.2	2.1	4.4	−2.2	2.2	0.13
	0.25	6.3	−4.9	1.4	6.4	−5.1	1.3	0.17
	0.3	8.4	−8.6	−0.2	8.4	−8.7	−0.3	0.22
	0.35	10.6	−11.7	−1.1	10.6	−11.8	−1.2	0.27
	0.4	13.0	−15.5	−2.5	12.9	−15.5	−2.6	0.34
	0.45	15.6	−20.0	−4.4	15.6	−19.9	−4.3	0.42
	0.5	19.4	−24.7	−5.3	19.5	−24.4	−4.9	0.51

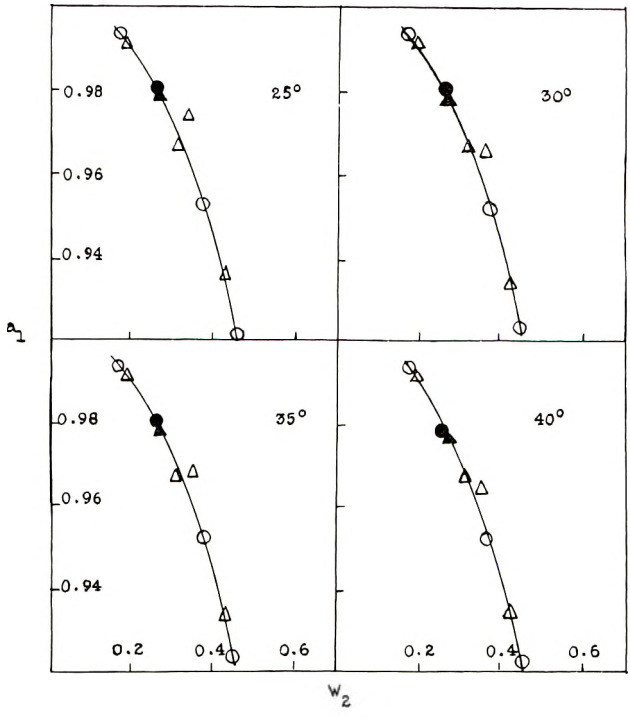

Fig. 3. a_1 as a function of polymer weight fraction for the cellulose acetate–dioxane system. Points indicated as in Fig. 1.

TABLE III
Cellulose Nitrate–Solvent Systems

		30°C.			35°C.			
Solvent	w_2	$-\Delta\bar{F}_1$, cal./mole	$\Delta\bar{H}_1$, cal./mole	$T\Delta\bar{S}_1$, cal./mole	$-\Delta\bar{F}_1$, cal./mole	$\Delta\bar{H}_1$, cal./mole	$T\Delta\bar{S}_1$, cal./mole	$T\Delta\bar{S}_1$ (id)
Acetone	0.1	0.5	−0.5	—	0.5	−0.5	—	0.04
	0.15	1.1	−1.1	—	1.1	−0.9	0.2	0.07
	0.2	2.2	−2.1	0.1	2.2	−2.1	0.1	0.09
	0.25	4.0	−3.9	0.1	4.0	−3.5	0.5	0.12
	0.3	7.3	−6.1	1.2	7.3	−5.8	1.5	0.16
	0.35	14.3	−11.2	3.1	14.4	−10.3	4.1	0.20
	0.4	33.8	−25.2	8.6	33.9	−22.9	11.0	0.25
	0.45	75.2	−42.5	32.7	75.7	−37.8	37.9	0.30
Methyl acetate	0.1	0.8	−0.7	0.1	0.8	−0.6	0.2	0.05
	0.15	1.9	−1.7	0.2	1.9	−1.6	0.3	0.08
	0.2	4.2	−3.2	1.0	4.2	−3.0	1.2	0.12
	0.25	7.6	−5.5	2.1	7.6	−4.8	2.8	0.16
	0.3	14.4	−8.4	6.0	14.5	−7.8	6.7	0.20
	0.35	27.9	−12.6	15.3	28.1	−11.7	16.4	0.26
	0.4	52.9	−18.1	34.8	53.5	−15.4	38.1	0.32
	0.45	104.3	−27.1	77.2	105.6	−21.1	84.5	0.39

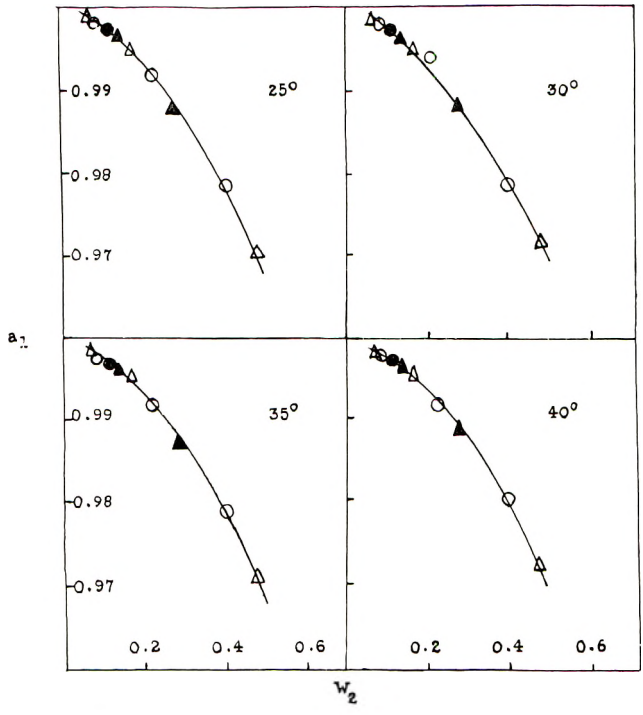

Fig. 4. a_1 as a function of polymer weight fraction for the cellulose acetate–pyridine system. Points indicated as in Fig. 1.

where ϕ_2 is the volume fraction of polymer, x the number of segments in the polymer chain, and χ_1 the polymer–solvent interaction parameter. Values of χ_1 are plotted against ϕ_2 in Figures 7 and 8. Additivity of volumes was assumed, and the density of the dry polymer was used in the calculation of ϕ_2. The validity of the assumption and the use of the density of the dry polymer will be considered later, as will the significance of the broken lines in Figure 7.

DISCUSSION

At each concentration in the cellulose acetate systems $-\Delta\bar{F}_1$ increases in the order methyl acetate < acetone < dioxane < pyridine, in agreement with results for dilute solutions.[6] The cellulose acetate systems involving acetone, methyl acetate, and pyridine are endothermal at lower concentrations, becoming exothermal at polymer weight fractions of about 0.2, 0.4, and 0.2 respectively. The dioxane system is exothermal at all concentrations studied, in agreement with the results of Kunze.[20] Values of $-\Delta\bar{F}_1$, $\Delta\bar{H}_1$, and $T\Delta\bar{S}_1$ for the cellulose acetate–acetone system differ somewhat from those of Jeffries.[4] The change from endothermal to exothermal character occurs at a lower value of w_2 in this work and at $w_2 = 0.4$, the lowest value at which comparison is possible, $-\Delta\bar{F}_1$ is larger and the signs of both $\Delta\bar{H}_1$ and $T\Delta\bar{S}_1$ differ from those given by Jeffries. Reasons for

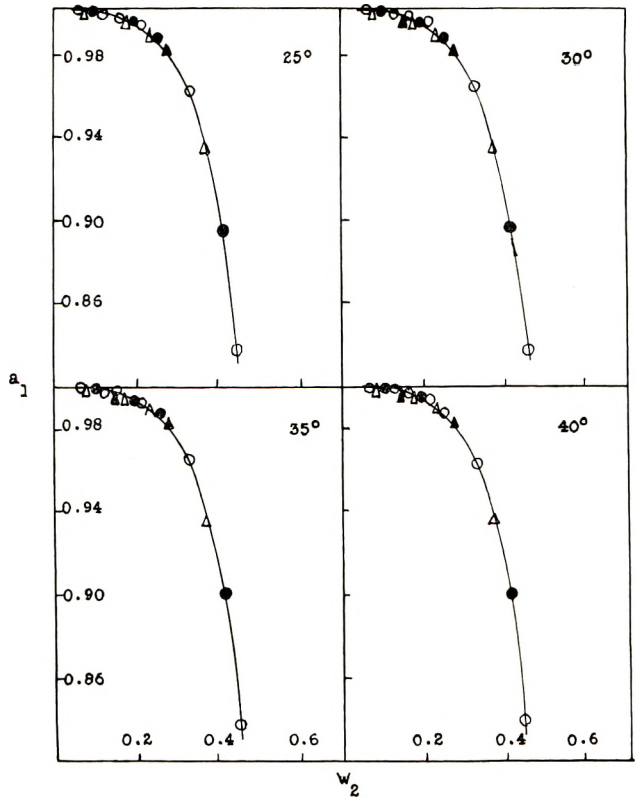

Fig. 5. a_1 as a function of polymer weight fraction for the cellulose nitrate–acetone system. Points indicated as in Fig. 1.

such differences are not clear, but they might be due to differences between the cellulose acetates used or to the presence of water in Jeffries' acetone.[4]

$\Delta\bar{S}_1$ also changes from positive to negative values at higher concentrations in the cellulose acetate–acetone and cellulose acetate–dioxane systems, and values for the cellulose acetate–methyl acetate system suggest the possibility of this at values of w_2 greater than 0.5. Positive values of $T\Delta\bar{S}_1$ for these systems are much larger than ideal values, and at the lowest concentrations, at which errors are likely to be greatest, seem to be similar to values predicted by lattice theories[21] for comparable systems involving flexible, less polar polymers. At higher concentrations, however, they become appreciably less than such predicted values. $T\Delta\bar{S}_1$ is positive at all concentrations studied in the cellulose acetate–pyridine system and increases with concentration of polymer. The values are not very different from those predicted by lattice theories for comparable systems involving flexible, less polar chains. Values of $-\Delta\bar{F}_1$, $\Delta\bar{H}_1$, and $T\Delta\bar{S}_1$ for the cellulose acetate systems seem to be little affected by small temperature changes.

The cellulose nitrate systems are exothermal at all concentrations, but values of $T\Delta\bar{S}_1$ are positive with values close to ideal ones at the lowest

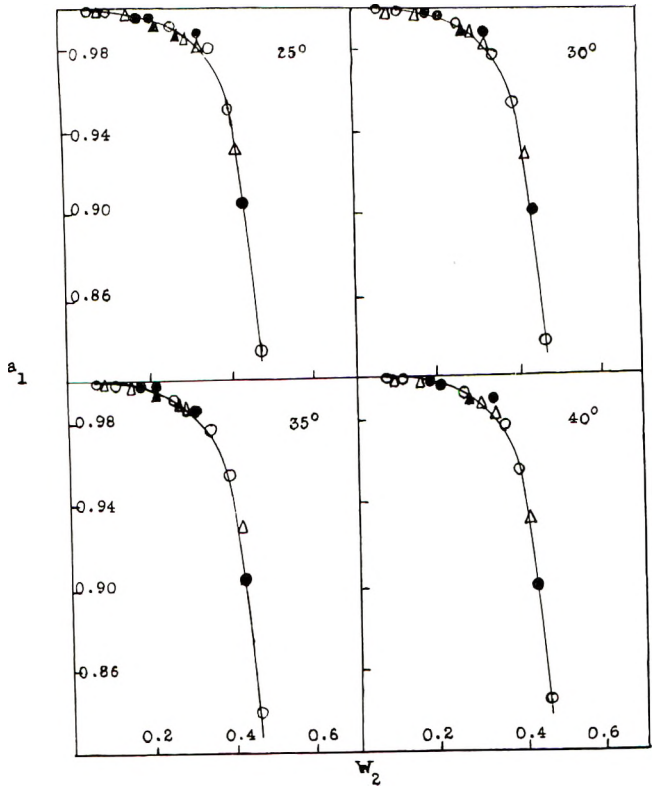

Fig. 6. a_1 as a function of polymer weight fraction for the cellulose nitrate–methyl acetate system. Points indicated as in Fig. 1.

concentrations. At higher concentrations, however, values of $T\Delta\bar{S}_1$ approach those predicted by lattice theories for comparable systems involving more flexible and less polar polymers. Where comparison is possible, values of $\Delta\bar{F}_1$ and $\Delta\bar{H}_1$ and $T\Delta\bar{S}_1$ for the cellulose nitrate–acetone system are in good agreement with those of Schulz.[1] In both the cellulose nitrate systems $-\Delta\bar{F}_1$ and $T\Delta\bar{S}_1$ tend to increase, and $\Delta\bar{H}_1$ tends to become less negative with increase of temperature.

Negative values of $\Delta\bar{H}_1$ and $\Delta\bar{S}_1$ imply strong polymer–solvent interaction and orientation of solvent. Cellulose derivatives are known to be solvated in solution.[22,23] In dilute solutions solvation should be complete or nearly so, and it has been suggested[6,7] that in such solutions solvated cellulose acetate may mix endothermally with solvents. At higher concentrations solvation may be incomplete, and dilution may result in further solvation and evolution of heat. The concentrations at which $\Delta\bar{H}_1$ changes sign might possibly be those at which solvation of the cellulose acetate is complete. They correspond, however, to more solvent molecules per glucose unit than is to be expected if only one solvent molecule were associated with each appropriate functional group in solvation. Numbers in excess of one per functional group have been suggested,[22] and it is possible

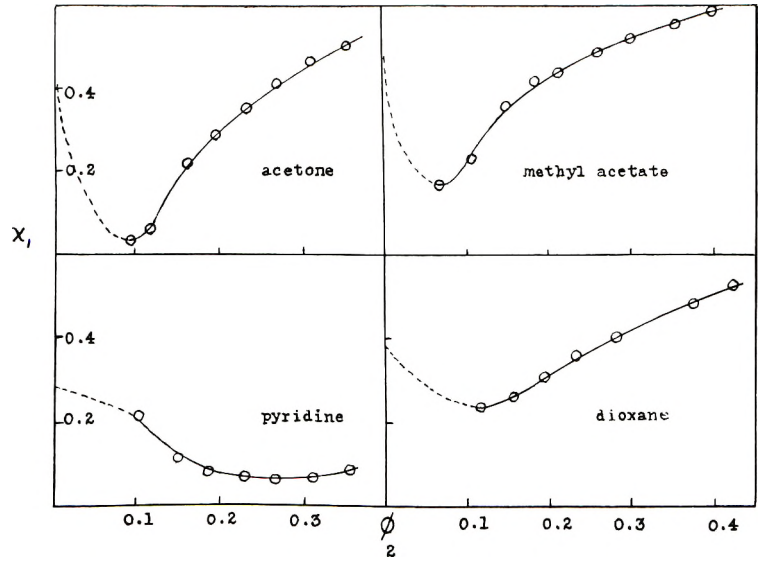

Fig. 7. χ_1 as a function of ϕ_2 for cellulose acetate–solvent systems.

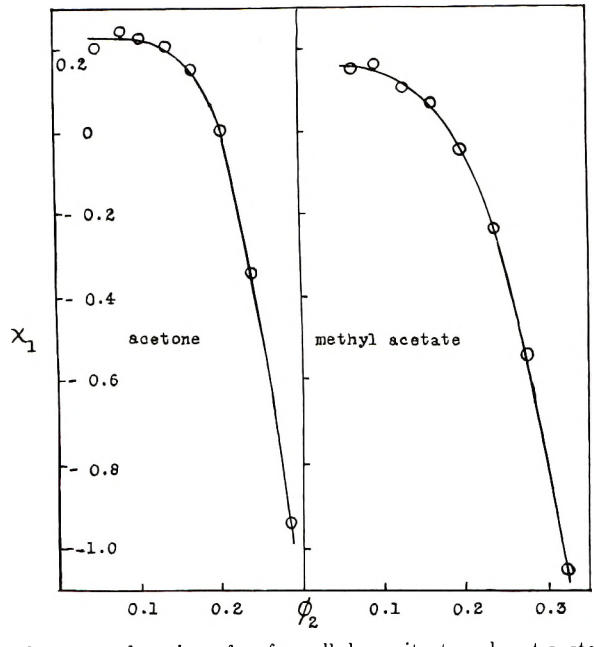

Fig. 8. χ_1 as a function of ϕ_2 for cellulose nitrate–solvent systems.

that solvation may involve some propagated attraction from a first firmly bound layer of solvent.[1] At any given concentration, not all the solvent molecules may take part in solvation. The exothermal nature of the cellulose acetate–dioxane system at all the concentrations studied is perhaps surprising. It has, however, been pointed out that, although dioxane

is nonpolar by internal compensation, the highly polar C=O groups are capable of considerable short-range interaction with polar groups of polymers.[24]

Except perhaps at the lowest concentrations, the variations of $T\Delta\bar{S}_1$ with concentration, with regard to both magnitude and sign, for the cellulose acetate systems involving acetone, methyl acetate, and dioxane are in general agreement with the concept of solvation. Values less than those for systems involving flexible, less polar polymers might be expected in view of solvation and chain stiffness. Values of $T\Delta\bar{S}_1$ for the pyridine system, however, are positive at all concentrations studied and large at the higher concentrations. Solvation effects may be less, and this is also suggested by the smaller negative values of $\Delta\bar{H}_1$. Viscosity–molecular weight relationships[10] and other considerations[25] suggest that chains of secondary cellulose acetate are less stiff in pyridine than in other solvents and may adopt more coiled forms.

The exothermal character of the cellulose nitrate systems at all concentrations studied suggests strong solvation and orientation effects. Munster[5] has suggested that dilution may free solvent clusters blocking nitrate groups, permitting further solvation and a reduction of $T\Delta\bar{S}_1$ to values not far from ideal. This might account for the values of $T\Delta\bar{S}_1$ at lower concentrations. Some flexibility of the chains of incompletely substituted nitrates[24] may account for larger values at higher concentrations. At concentrations of 1–45 wt.-% of polymer in the cellulose nitrate–acetone system Schulz[1] found that

$$\Delta\bar{H}_1 = kc^m \tag{9}$$

where c is the percentage polymer by weight and k and m are constants. A different relationship was found to hold for concentrations greater than 45%. The values of $\Delta\bar{H}_1$ in Table III lead to similar results. Schulz suggested that the two concentration ranges corresponded to different types of bonding between the polymer and solvent and that some propagated attraction from a first firmly bound solvent layer may occur at lower concentrations.

The variations of χ_1 with volume fraction of polymer for each of the cellulose acetate systems at 30°C. are shown in Figure 7. Values at the lowest concentrations are less than those obtained from osmotic studies of dilute solutions,[6] so that χ_1 should presumably increase as ϕ_2 is decreased below 0.1 in a manner perhaps similar to that indicated by the broken lines which intercept the ordinates at values obtained with dilute solutions. Errors in the values of χ_1 are likely to be greatest at the lowest concentrations, but somewhat similar behavior has been reported for the rubber–benzene system.[27] In the cellulose acetate–methyl acetate and cellulose acetate–dioxane systems χ_1 exceeds the critical value of approximately 0.5 at the highest concentrations, and this also appears possible in the cellulose acetate–acetone system if the polymer concentration is sufficiently increased. No evidence of phase separation, however, was observed in these cases.

TABLE IV
Values of χ_1, χ_h, and χ_s at 30°C.

System	ϕ_2	χ_1	χ_h	χ_s
Cellulose acetate–acetone	0.098	0.04	0.79	−0.75
	0.123	0.06	0.02	0.04
	0.158	0.22	−0.28	0.50
	0.194	0.29	−0.57	0.86
	0.232	0.35	−0.53	0.88
	0.315	0.46	−0.46	0.92
	0.360	0.49	−0.36	0.85
Cellulose acetate–methyl acetate	0.069	0.17	0.84	−0.67
	0.105	0.23	0.42	−0.19
	0.143	0.38	0.25	0.13
	0.182	0.42	0.12	0.30
	0.222	0.43	0.06	0.37
	0.264	0.49	0.02	0.47
	0.307	0.52	0.00	0.52
	0.353	0.56	−0.02	0.58
	0.400	0.59	−0.08	0.67
Cellulose acetate–pyridine	0.110	0.22	0.02	0.20
	0.149	0.11	−0.01	0.12
	0.189	0.07	−0.03	0.10
	0.231	0.06	−0.03	0.09
	0.274	0.05	−0.03	0.08
	0.318	0.06	−0.03	0.09
	0.364	0.07	−0.03	0.10
Cellulose acetate–dioxane	0.115	0.23	−0.01	0.24
	0.156	0.27	−0.15	0.42
	0.198	0.31	−0.21	0.52
	0.241	0.36	−0.25	0.61
	0.285	0.40	−0.24	0.64
	0.330	0.45	−0.24	0.69
	0.377	0.49	−0.23	0.72
	0.425	0.53	−0.23	0.76
Cellulose nitrate–acetone	0.051	0.20	−0.32	0.52
	0.079	0.24	−0.29	0.53
	0.108	0.23	−0.30	0.53
	0.139	0.21	−0.34	0.55
	0.172	0.16	−0.34	0.50
	0.206	0.02	−0.44	0.46
	0.244	−0.34	−0.70	0.36
	0.283	−0.93	−0.88	−0.05
Cellulose nitrate–methyl acetate	0.060	0.15	−0.31	0.46
	0.092	0.16	−0.33	0.49
	0.125	0.10	−0.34	0.44
	0.160	0.07	−0.35	0.42
	0.197	−0.04	−0.36	0.32
	0.235	−0.24	−0.38	0.14
	0.276	−0.54	−0.39	−0.15
	0.319	−1.06	−0.44	−0.62

The variation of χ_1 with ϕ_2 for the cellulose nitrate systems, shown in Figure 8, differs from those shown by the cellulose acetate systems. At the lowest concentrations χ_1 is positive, with values similar to those for dilute solutions,[6,7] but as ϕ_2 increases χ_1 falls rapidly to relatively large negative values. The variation of χ_1 with ϕ_2 in the cellulose nitrate–acetone system is similar to that obtained by Baughan et al.[9] but differs somewhat from that observed by Takenaka.[8]

According to simple lattice theories, χ_1 can be expressed as the sum of heat and entropy contributions, χ_h and χ_s:

$$\chi_1 = \chi_h + \chi_s \tag{10}$$

with $\chi_h = \Delta\bar{H}_1/RT\phi_2^2$. Values of χ_1, χ_h, and χ_s are given in Table IV. In the cellulose acetate systems, χ_h decreases from positive to negative values as ϕ_2 increases and becomes roughly constant at higher concentrations with pyridine and dioxane as solvents. χ_s tends to increase with concentration in the cellulose acetate–acetone, cellulose acetate–methyl acetate, and cellulose acetate–dioxane systems and to become roughly constant at higher concentrations in the first of these systems. The values of χ_s are larger than would be expected from simpler lattice theories. Values of χ_s are smaller in the cellulose acetate–pyridine system and are roughly constant at higher concentrations. In the cellulose nitrate systems, χ_h becomes increasingly negative as ϕ_2 increases and χ_s, although roughly constant at lower values, decreases and is negative at the highest values of ϕ_2.

The values of χ_s and their variations, and those of χ_1 and χ_h, with concentration, although not incompatible with the picture of solvation outlined above, show that simpler lattice theories are not applicable, without modification, to the polar systems studied. Both Tompa[28] and Munster[5,29] have suggested treatments for polar interacting systems. Tompa's treatment is not applicable to the present cases, since several empirical constants are involved in his expressions. More explicit expressions for $\Delta\bar{F}_1$, $\Delta\bar{H}_1$, and $\Delta\bar{S}_1$ are given by Munster, but these involve several parameters. Estimates can be made of some of these and the others can be obtained from values of $\Delta\bar{H}_1$ and $\Delta\bar{S}_1$ at a known concentration. The equations involved are, however, not easily solved by ordinary methods.

An alternative qualitative treatment may be possible. Values of ϕ_2 used in the calculation of χ_1 were calculated by assuming additivity of volumes and by using the density of the dry polymer. The assumption, although not strictly true, is unlikely to seriously affect values of ϕ_2. However, since at the concentrations used the polymers should be completely or partially solvated, the interaction occurring will be between solvated polymer and solvent, and ϕ_2 should more logically be expressed in terms of solvated polymer. For dilute solutions, in which solvation may be regarded as complete, it has been shown[7,30] that expression in such terms may lead to values of χ_1, χ_h, and χ_s in better agreement with the predictions of lattice theories. In the present cases, the degree of solvation is likely to

vary with concentration. In the absence of knowledge as to degree of solvation and its variation with concentration it is not possible to make estimates of ϕ_2 for the solvated polymers, but it is possible that expression in such terms would lead to values of x_1, x_u, and x_s more in keeping with those predicted by current polymer theory. Of the systems studied, the cellulose acetate–pyridine system, which seems likely to involve smaller degrees of solvation, is that more nearly resembling systems involving less polar and more flexible polymers in terms of lattice theories.

We are grateful for a Bradford City Research Scholarship held by one of us (R. S.).

References

1. Schulz, G. V., *Z. physik. Chem.*, **A184**, 1 (1939).
2. Boissonas, C. G., and K. H. Meyer, *Z. physik. Chem.*, **B40**, 118 (1938).
3. Hagger, C., and A. J. A. van der Wyck, *Helv. Chim. Acta*, **23**, 484 (1940).
4. Jeffries, R., *Trans. Faraday Soc.*, **53**, 1592 (1957).
5. Munster, A., *J. Polymer Sci.*, **8**, 633 (1952).
6. Moore, W. R., and B. M. Tidswell, *J. Polymer Sci.*, **29**, 37 (1958).
7. Moore, W. R., *Textile Research J.*, **30**, 965 (1960).
8. Takenaka, H., *J. Polymer Sci.*, **24**, 321 (1957).
9. Baughan, E. C., A. L. Jones, and K. Stewart, *Proc. Roy. Soc. (London)*, **A225**, 478 (1954).
10. Moore, W. R., and B. M. Tidswell, *J. Appl. Chem.*, **8**, 232 (1958).
11. Moore, W. R., and J. A. Epstein, *J. Appl. Chem.*, **6**, 168 (1956).
12. Felsing, W. A., and S. A. Durban, *J. Am. Chem. Soc.*, **48**, 2885 (1926).
13. Timmermans, J., *Physical Constants of Pure Organic Compounds*, Elsevier, Amsterdam, 1950.
14. Dippy, J. F. J., and S. R. C. Hughes, *J. Chem. Soc.*, **1954**, 953.
15. Dobry, A., and F. Boyer-Kawenski, *J. Polymer Sci.*, **2**, 90 (1947).
16. Højendahl, K., *Kgl. Danske Videnskab. Selskab, Mat. fys. Medd.*, **24**, 1 (1946).
17. Bawn, C. E. H., R. F. J. Freeman, and A. R. Kamillidin, *Trans. Faraday Soc.*, **46**, 862 (1950).
18. Bawn, C. E. H., and M. A. Wajid, *Trans. Faraday Soc.*, **52**, 1658 (1956).
19. Lambert, J. D., G. A. H. Roberts, J. S. Rowlinson, and V. J. Williamson, *Proc. Roy. Soc. (London)*, **A196**, 113 (1949).
20. Kunze, F., *Z. physik. Chem.*, **A188**, 90 (1941).
21. Flory, P. J., *Principles of Polymer Chemistry*, Cornell Univ. Press, Ithaca, N. Y., 1953, Chap. 12.
22. Moore, W. R., J. A. Epstein, A. M. Brown, and B. M. Tidwell, *J. Polymer Sci.*, **23**, 23 (1957).
23. Oh, E., H. M. Spurlin, and M. W. Grafflin, Eds., *Cellulose and Cellulose Derivatives*, 2nd Ed., Interscience, New York, 1955, p. 1094.
24. De Brouckere, L., and M. Mandel, in *Advances in Chemical Physics*, I. Prigogine, Ed., Vol. I. Interscience, New York, 1958, p. 99.
25. Moore, W. R., and J. Russell, *J. Colloid Sci.*, **9**, 338 (1954).
26. Moore, W. R., and G. P. Pearson, *Polymer*, **1**, 144 (1960).
27. Gee, G., and W. J. C. Orr, *Trans. Faraday Soc.*, **42**, 507 (1946).
28. Tompa, H., *J. Chem. Phys.*, **21**, 250 (1950).
29. Munster, A., *J. chim. phys.*, **49**, 128 (1952).
30. Moore, W. R., Communications International Symposium on Macromolecules, Weisbaden, 1959, II, B7.

Synopsis

Vapor pressure lowerings of solutions containing 10–50 wt.-% of a secondary cellulose acetate and of a cellulose nitrate of similar degree of substitution in representative solvents have been measured over a range of temperature. Solvent activities and free energies, heats and entropies of dilution are obtained. At low polymer concentrations the cellulose acetate systems are endothermal but become exothermal at higher concentrations. Entropies of dilution show a somewhat similar variation with concentration when acetone, methyl acetate, and dioxane are used as solvents for the cellulose acetate, but with pyridine as solvent entropies are positive and increase with increasing polymer concentration. The systems cellulose nitrate–acetone and cellulose nitrate–methyl acetate are exothermal at all concentrations, but entropies of dilution are positive and increase with concentration from values not far from ideal to relatively large ones. An attempt is made to interpret these results in terms of solvation and chain stiffness. Values of the polymer–solvent interaction parameter χ_1 are obtained by use of polymer volume fractions calculated from the densities of the dry polymers. As the volume fraction of polymer increases in the cellulose acetate systems, χ_1 would appear initially to fall from values characteristic of dilute solutions and then to increase. In the cellulose nitrate systems, χ_1 falls from small positive to relatively large negative values. Values of the heat χ_h and entropy χ_s contributions to χ_1 are also obtained. It is pointed out that it may be more logical to express polymer volume fraction in terms of solvated polymer and that this might lead to values of χ_1, χ_h, and χ_s more in keeping with theories of polymer–solvent interaction.

Résumé

On a mesuré à plusieurs températures les abaissements de tension de vapeur de solution contenant 10 à 50% en poids de diacétate de cellulose et de nitrate de cellulose de même dégré de substitution. On a déterminé les activités et énergies libres du solvant ainsi que les chaleurs et entropies de dilution. Pour des faibles concentrations en polymère, les systèmes contenant de l'acétate de cellulose sont endothermiques mais deviennent exothermes à des concentrations plus élevées. La variation des entropies de dilution en fonction de la concentration est à peu près du même type pour des solutions d'acétate de cellulose dans l'acétone, l'acétate de méthyle et le dioxanne, mais, lorsque le solvant et la pyridine, les entropies sont positives et augmentent avec la concentration en polymère. Les systèmes nitrate de cellulose–acétone et nitrate de cellulose–acétate de méthyle sont exothermiques à toutes les concentrations mais les entropies de dilution sont positives et augmentent avec la concentration depuis des valeurs presque idéales jusqu'à des valeurs relativement élevées. On a essayé d'interprèter ces résultats en termes de solvatation et de rigidité de chaîne. On a obtenu les valeurs du paramètre χ_1 d'interaction polymère–solvant en employant des fractions de volume de polymère calculées aux dépens des densités des polymères secs. Comme le fraction de volume du polymère augmente pour les systèmes à base d'acétate de cellulose, χ_1 diminuait au départ des valeurs caractéristiques des solutions diluées et ensuite augmentait. Dans les systèmes contenant du nitrate de cellulose, χ_1 tombe depuis les faibles valeurs positives jusqu'à des valeurs négatives relativement basses. Les valeurs des contributions enthalpiques χ_h et entropiques λ_s à χ_1 ont été également déterminées. On fait remarquer qu'il est peut-être plus logique l'exprimer les fractions de volume de polymère en termes de polymère solvaté; cela pourrait conduite à des valeurs de χ_1, χ_h et χ_s qui seraient plus en accord avec les théories de l'interaction polymère–solvant.

Zusammenfassung

Die Dampfdruckerniedrigung von Lösungen mit einem Gehalt von 10 bis 50 Gewichtsprozenten an sekundärem Celluloseacetat und an Cellulosenitat mit ähnlichem Substitutionsgrad wurde in ausgewählten Lösungsmitteln bei verschiedenen Temperaturen

gemessen. Die Aktivität des Lösungsmittels, sowie freie Verdünnungsenergien, Verdünnungswärmen und -entropien werden erhalten. Bei niedriger Polymerkonzentration sind die Celluloseacetatsysteme endotherm, werden jedoch bei höherer Konzentration exotherm. Die Verdünnungsentropie zeigt bei Verwendung von Aceton, Methylacetat und Dioxan als Lösungsmittel für das Celluloseacetat eine gewisse Ähnlichkeit der Konzentrationsabhängigkeit, bei Pyridin als Lösungsmittel ist jedoch die Entropie positiv und steigt mit zunehmender Polymerkonzentration an. Die Systeme Cellulosenitrat-Aceton und Cellulosenitrat-Methylacetat sind bei allen Konzentrationen exotherm, die Verdünnungsentropie ist aber positiv und steigt mit der Konzentration von einem annähernd idealen Wert zu relativ hohen Werten an. Es wurde versucht, diese Ergebnisse als Solvatisierungs- und Kettensteifigkeitseffekte zu deuten. Werte für den, Wechselwirkungsparameter χ_1 werden unter Verwendung aus der Dichte des trockenen Polymeren berechneten Volumbruchteils an Polymeren erhalten. Bei einem Ansteigen des Volumbruchteils des Polymeren in Celluloseacetatsystemen scheint χ_1 zuerst von den für verdünnte Lösungen charakteristischen Werten abzunehmen und dann anzusteigen. In Cellulosenitratsystemen fällt χ_1 von kleinen positiven zu relativ grossen negativen Werten ab. Weiters wurden Werte für die Wärme-χ_h und Entropiebeiträge χ_s zu χ_1 erhalten. Es wird betont, dass es richtiger sein mag, den Volumsbruchteil an Polymeren als solvatisiertes Polymeres in Rechnung zu stellen, und dass dies zu χ_1-, χ_h- und χ_s-Werten führen könnte, die mit den Theorien der Polymer-Lösungsmittel-Wechselwirkung besser übereinstimmen.

Received November 27, 1961

JOURNAL OF POLYMER SCIENCE: PART A VOL. 1, PP. 751–762 (1963)

Effect of Side-Chain Structure on Poly-α-Olefin Properties*

K. R. DUNHAM, J. VANDENBERGHE, J. W. H. FABER, and L. E. CONTOIS, *Research Laboratories, Eastman Kodak Company, Rochester, New York*

INTRODUCTION

The importance of catalyst[1,2] and solvent[3–5] in the propagation of growing stereoregular chains is well recognized. Monomer structure can also influence the stereoregularity of the polymers formed.[6,7] In order to explain further the effect of side-chain groups upon stereoregular polymerization and polymer properties, several series of α-olefins were polymerized.

The olefins studied were those having the structure:

$$[CH_2{=}CH]\text{—}(CH_2)_x\text{—}R$$

where X = 0–3, and R represents $—CH_3$, $—CH(CH_3)_2$, $—C(CH_3)_3$, $—C_6H_5$, and C_6H_{11}. A triethyl-aluminum–vanadium trichloride catalyst was used without solvent. Although the $Al(C_2H_4)_3$–VCl_3 system was less stereoregulating than other catalyst systems, such as AlR_3–$TiCl_4$, it had the advantage of high monomer conversion. The catalyst components did not react violently, and catalyst variations between experiments were minimized.

EXPERIMENTAL

A. Polymerization of α-Olefin Monomers

Monomers were distilled and dried over silica gel. A 135-ml. pressure bottle was flushed with dry nitrogen and charged with 0.27 mole of monomer and 0.01 mole of anhydrous VCl_3. The bottle was capped with a neoprene-lined self-sealing cap and 0.005 mole of $Al(C_2H_5)_3$ was injected by means of a hypodermic syringe. The bottle was placed inside a metal cage and tumbled for 16 hr. at 50°C. in a water bath.

B. Purification of Polymers

Generally, the catalyst was removed by placing the polymer in methanol containing hydrochloric acid, then extracting it with methanol in a Soxhlet

* Communication No. 2150 from the Kodak Research Laboratories.

extractor, and finally, extracting it with acetone in a Soxhlet extractor. The polymer was dried at 50°C. in a vacuum oven. Poly-α-olefins having low softening points were difficult to purify, and were washed with methanol and acetone in a Waring Blendor at solvent temperatures below the softening point of the polymers. In addition to removal of catalyst residues, the extraction treatment removed low molecular weight atactic material.

C. Crystallization of Polymers

Polymers were crystallized by heating in a hot Soxhlet extractor with boiling acetone for 48 hr. They were then filtered and dried for 24 hr. at 50°C. under vacuum.

D. Determination of Crystalline Melting Points

Melting points were determined by placing the sample in a standard metal melting-point block with a beam of light passing through the apparatus. After the light beam had passed through the sample, the intensity was measured by a light-intensity indicator. The block was heated at a standard rate of 1°C./min. As the sample melted, the disappearance of crystalline opacity was indicated by the increased light intensity at the meter. Melting points were reproducible and approximated those measured by differential thermal analysis or the polarized light-hot stage microscope combination.

E. Determination of Softening Points

Softening points were measured in the same apparatus as melting points. Samples were placed off-center between cover glasses so as to be out of the main light beam (Fig. 1). A metal cover with a small hole in the center was placed over the sample at an angle, thus blocking off part of the main light beam from the intensity recorder and placing the sample under load. At the softening point, plastic flow of the sample caused the cover to become more nearly horizontal, thus increasing the amount of light passing through the hole in the cover. The method was reproducible and sensitive to small changes in specimen softening. To determine softening points below room temperature, the apparatus was cooled with dry ice. A standard heating rate of 2°C./min. was employed. The data are in close agreement with glass transition temperatures determined by differential thermal analysis. Attempts were made to prevent crystallization of the sample in order to minimize secondary effects. In the molecular weight range studied, melt viscosity differences would be expected to influence the rate of change at the softening point. This influence was minimized by the low heating rate.

F. Measurement of Degree of Crystallinity

Approximately 0.5 mm. of polymer was placed in a Cu Kα x-ray beam and the diffraction pattern recorded on x-ray film. The sample-to-film distance was 4 cm., and the exposure time was 1 hr. The degree of crystallinity was estimated by visual observation of the photographs. Increased crystal-

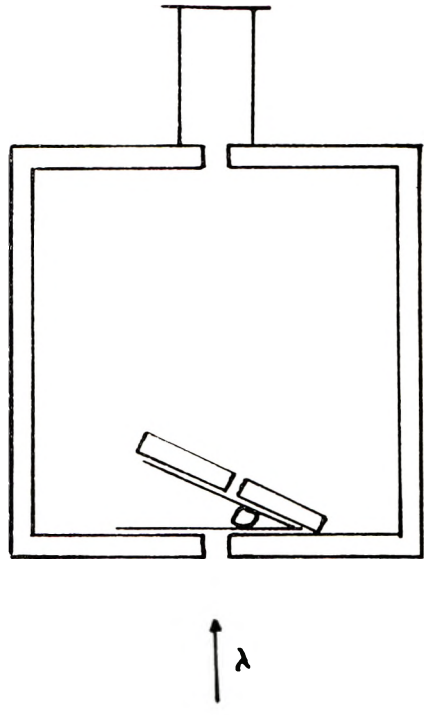

Fig. 1. Softening point apparatus.

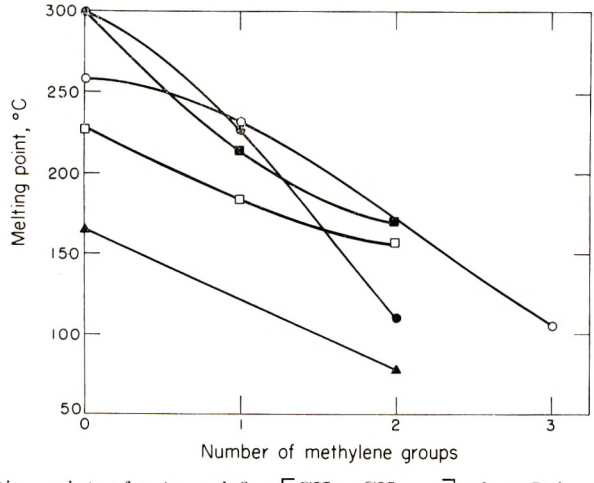

Fig. 2. Melting points of poly-α-olefins $\left[\begin{array}{l}CH_2—CH— \\ \quad\quad / \\ \quad (CH_2)_xR\end{array}\right]_n$ where R is: (▲) methyl, (●) isopropyl, (○) *tert*-butyl, (□) phenyl, or (■) cyclohexyl.

linity was seen in the photographs in terms of increased density of the sharp rings, characteristic of the crystalline phase, and decreased density of scattering in the region of the broad halos, characteristic of the amorphous phase.

DISCUSSION

Melting points, softening points, and degrees of crystallinity of the polymers are listed in Tables I–V. Melting points (Fig. 2) and softening points decreased with increasing side-chain length within each series.[8]

A plot of side-chain lengths against softening points gives the curves shown in Figure 3. In the phenyl, cyclohexyl, and isopropyl side-chain series, the softening point decreases gradually as side-chain length increases,

TABLE I
Physical Properties of Poly-α-Olefins

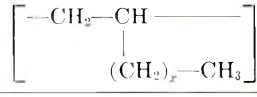

x	Name	Melting point, °C.	Softening point, °C.	Yield, %	Crystallinity
0	Polypropylene	165	−20	87	High
2	Poly-pentene-1	78	−29	77	Moderate
3	Poly-hexene-1	—	−36	95	None
5	Poly-octene-1	—	—	96	None

TABLE II
Physical Properties of Poly-α-Olefins

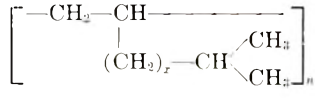

x	Name	Melting point, °C.	Softening point, °C.	Yield, %	Crystallinity
0	Poly-3-methyl-butene-1	300	53	90	Very high
1	Poly-4-methyl-pentene-1	228	36	93	High
2	Poly-5-methyl-hexene-1	110[a]	−14	87	None
3	Poly-6-methyl-heptene-1	—	−34	92	None

[a] Obtained from crystalline polymer prepared with $Al(C_2H_5)_3$–$TiCl_4$ catalyst.

TABLE III
Physical Properties of Poly-α-Olefins

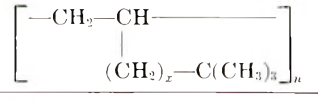

x	Melting point, °C.	$[\eta]$	Softening point, °C.	Yield, %	Crystallinity
0	260	—	64	0.2	High
1	231	—	59	0.4	Moderate
2	—	1.04	53	1.7	None
3	104	1.31	40	57.0	Moderate

TABLE IV
Physical Properties of Poly-α-Olefins

$$\left[\text{—CH}_2\text{—CH(—(CH}_2)_x\text{C}_6\text{H}_5\text{)—}\right]_n$$

x	Name	$[\eta]$	Melting point, °C.	Softening point, °C.	Yield, %	Crystallinity
0	Polystyrene	1.02	225	95	75	High
1	Poly-3-phenylpropene-1	0.86	185[a]	78	71	None
2	Poly-4-phenylbutene-1	1.19	159	40	91	Very low
3	Poly-5-phenylpentene-1	0.73	—	−28	82	None

[a] Obtained from crystalline polymer prepared with $Al(C_2H_5)_3$–$TiCl_4$ catalyst.

TABLE V
Physical Properties of Poly-α-Olefins

$$\left[\text{—CH}_2\text{—CH(—(CH}_2)_x\text{C}_6\text{H}_{11}\text{)—}\right]_n$$

x	Name	$[\eta]$	Melting point, °C.	Softening point, °C.	Yield, %	Crystallinity
0	Polyvinylcyclohexane	0.89	300	95	50	High
1	Polyallylcyclohexane	0.62	215[a]	75	30	None
2	Poly-4-cyclohexylbutene-1	0.61	170	40	31	Low
3	Poly-5-cyclohexylpentene-1	0.32	—	−25	90	None

[a] Obtained from polymer prepared with $Al(C_2H_5)_3$–$TiCl_4$ catalyst.

and then drops sharply. Loss of crystallinity occurs at this point. At longer side-chain lengths, the polymers are amorphous. The converse is not always true, however, although polymers having shorter side chains are generally crystalline. In the *tert*-butyl and *n*-alkyl side-chain series, the curves are nearly linear in the range under study. Since side-chain crystallization is known to occur with polyethylene having long branches and with polyalkyl acrylates and methacrylates with long linear side chains, the same phenomenon would probably be observed in the above series at long side-chain lengths. Within the range studied, however, the side chains were too short to influence either softening point or overall crystallinity through side-chain crystallization.

Within certain series (where R is *tert*-butyl, phenyl, and cyclohexyl, Table IV), crystallinity does not always decrease in a regular fashion with increasing side-chain length. The question has arisen whether amorphous polymers prepared with normally stereospecific catalysts are atactic or of

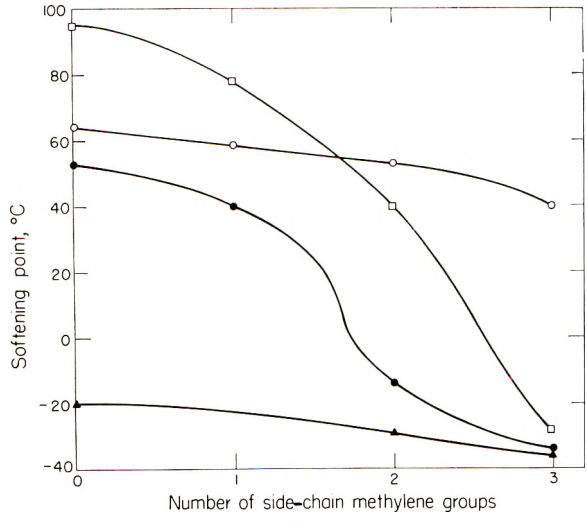

Fig. 3. Softening points of poly(α-olefin) $\left[\mathrm{CH_2{-}CH}\right]_n$ where R is: (▲) methyl, (●) isopropyl, (○) *tert*-butyl, (□) phenyl and cyclohexyl.

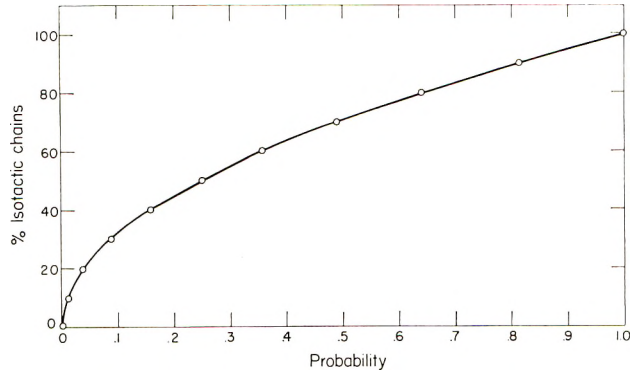

Fig. 4. Probability of adjacent isotactic chains in isotactic–atactic systems.

regular structure. Do side chains in the amorphous polymers reduce stereospecificity in initiation and propagation steps, causing random polymerization, or are regular chains formed, but prevented by the side chains from packing into crystallites?

Without a well-defined regular polymer which can be modified chemically, there is no direct quantitative evidence for the presence or absence of regular structure in a polymer which does not crystallize. Infrared, density, and solubility measurements made in these Laboratories tend to be inconclusive and define only qualitatively the presence or absence of regular structure. However, evidence has been presented to support the view that isotactic chains can exist in noncrystallizable systems.[9,10] On the basis of

these findings and those cited below, the systems under discussion are considered to be of regular structure whether or not they are crystallizable.

It has been demonstrated that the crystallinity of an isotactic polymer can be gradually reduced until it finally disappears as a result of chlorination.[11] In the present work, substitution of $-NO_2$ and $-SO_3H$ groups into the aromatic nucleus of isotactic polystyrene rendered the polymers noncrystallizable. Since it is difficult to envision the polymer backbone being altered in these reactions, it seems probable that isotactic structure can exist in noncrystallizable systems.

Statistical analysis of model isotactic–atactic systems, when used in conjunction with other data, can be useful in characterizing such systems. Several requirements must be met if crystallization is to occur.

(*1*) Two isotactic chains must be adjacent. Crystallization cannot occur if adjacent chains are both atactic or if one is isotactic and the other atactic. Both must be isotactic.

(*2*) The isotactic chains must be close to each other.

(*3*) Energy requirements must be favorable.[12]

(*4*) Impurities which influence crystallization must be absent. It is apparent that some impurities, such as solvent molecules or plasticizers, increase the rate of crystallization by decreasing the void between chains and increasing chain mobility. The discovery was made in these Laboratories that highly purified isotactic polystyrene having no measurable amount of catalyst residues crystallized more slowly than polystyrenes containing slight amounts of residue and were not as highly crystalline. [The catalyst in these experiments was $Al(C_2H_5)_3$–$TiCl_4$.] The significance of this finding is that impurities can affect not only rate of crystallization, as would be expected, but also the ultimate degree of crystallinity as seen by x-ray diffraction patterns. The presence or absence of impurities, then, is important in those systems wherein the tendency to crystallize is very slight.

The fact that two regular chains are adjacent does not necessarily mean that crystallization will occur. However, assuming ideal conditions, the assumption can be made that if two isotactic chains are adjacent to each other, crystallization will occur. If two atactic chains or an atactic and an isotactic chain are adjacent, crystallization cannot occur. The probability of two isotactic chains being adjacent will be zero in a completely atactic system, and unity in a completely isotactic system. The probability P for a system containing both atactic and isotactic chains can be determined by means of the formula,

$$P = \frac{[i!/2!(i-2)!]}{[n!/2!(n-2)!]}$$

where n is the total number of chains in the sampling (or universe) and i is the number of isotactic chains in the universe; $[i!/2!(i-2)!]$ is the total number of possible isotactic pairs, and $[n!/2!(n-2)!]$ is the total number of possible paired combinations.[13] This equation can be simplified to

$$P = [i(i-1)/n(n-1)]$$

In a system containing chains of approximately uniform length, 50% of which are isotactic and 50% atactic, with a sampling size of 100 chains,

$$P = 50(49)/100(99) = 0.25$$

Values of P for other atactic–isotactic systems are listed in Table VI. As the sampling size is increased, i approaches i-1 and n approaches n-1, and the value of P becomes more nearly $P = i^2/n^2 = (i/n)^2$ or the square of the per cent of isotacticity of the sample.

Systems having a low percentage of isotactic chains have extremely small probabilities of crystallizing. It is not until the percentage of isotactic chains is greater than 70% that conditions for crystallization become favorable (i.e., probability greater than 0.5). Under less than ideal conditions, spatial considerations may prevent crystallization along the entire length of even completely isotactic chains, and more than two adjacent chains can be required to produce a crystallite. Hence, the probability of crystallization occurring becomes less than in the ideal and $P < (i/n)^2$.

When allylbenzene was polymerized with $Al(C_2H_4)_3$–VCl_3 catalyst and the polymer subjected to crystallizing conditions, the x-ray diagram indicated the polymer was amorphous (Table IV). With $Al(C_2H_5)_3$–$TiCl_4$ catalyst under similar conditions, polyallylbenzene with a low degree of

TABLE VI
Probability of Adjacent Isotactic Chains in Isotactic–Atactic Systems

Isotactic chains, %	Probability
100	1.000
90	0.813
80	0.640
70	0.490
60	0.358
50	0.250
40	0.158
30	0.088
20	0.038
10	0.009
0	0.000

crystallinity was obtained. Previous work by the authors with several other α-olefins had demonstrated that more highly crystalline polymers could be prepared with the titanium catalyst than with the vanadium catalyst. The polymers prepared with the vanadium catalyst were crystalline, however. It is unlikely that the vanadium catalyst system would be nonstereospecific with allylbenzene and stereospecific for other monomers while the titanium catalyst system would be stereoregulating for allylbenzene as well as for the other monomers. Assuming both catalysts to be stereospecific, although to slightly different degrees, the results could be

explained by an inherent inability of polyallylbenzene chains to pack into crystal lattices, and by the fact that the titanium catalyst produces chains with a slightly higher degree of regularity or isotacticity. If the isotacticity with $Al(C_2H_5)_3$–$TiCl_4$ is of the order of 70% and with $Al(C_2H_5)_3$–VCl_3 somewhat lower, then conditions for crystallization would be favorable in the first case but not in the second.

Assuming the basic premise that vanadium-catalyzed polymers in this study are isotactic to a degree, it remains necessary to explain the sometimes erratic crystallinity results observed. In the isoalkene series, for example (Table II), poly-4-methyl-pentene-1 is highly crystalline but poly-5-methylhexene-1 is amorphous. In the polyphenylalkene series (Table IV), poly-4-phenylbutene-1 is crystalline, but poly-5-phenylpentene-1 is amorphous. In the polycyclohexylalkene series (Table V), a similar situation exists between poly-4-cyclohexylbutene-1, which is crystalline, and poly-5-cyclohexylpentene-1, which is amorphous. In the poly-*tert*-butylalkene series (Table III), poly-4,4-dimethylpentene-1 is crystalline, poly-5,5-dimethylhexene-1 is amorphous, and poly-6,6-dimethylheptene-1 is crystalline. Assuming isotactic conformation in each polymer, one may interpret these crystallinity results by considering side-chain length and side-chain lateral bulk.

A sudden large drop in softening point between two polymers of a given series is accompanied by loss of crystallinity. Since softening point is a measure of overall degrees of freedom within a polymer, a reduction in softening point would result from the removal of impediments to motion. Side chains can increase total polymer mobility as their length increases, or restrict movement when bulky side groups reinforce the backbone chain or each other.[14]

Natta[15] has deduced from x-ray diffraction evidence that formation of the ideal all-*trans* zigzag polymer chain is unlikely when the presence of substituent groups would lead to overcrowding. It has been shown that such polymers are more likely to exist in the *gauche* chain-bond conformation.[16] In this conformation, the side chains from adjacent isotactic helices will normally be aligned directly opposite one another in the crystalline state[17] (Fig. 5). The phenomenon of crystallization appears to involve the approach of two isotactic helices of opposite rotation, allowing the side chains to become locked in place by van der Waals attractive forces.

Where the side chain contains lateral bulk, polymers having relatively high softening points can crystallize because reduced side-chain mobility allows favorable positioning for van der Waals bonding. The abrupt drop in softening point and the concurrent loss of crystallinity observed with

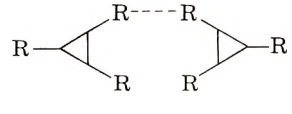

Fig. 5. Packing of adjacent isotactic helices (axis of chains normal to the plane of the paper).

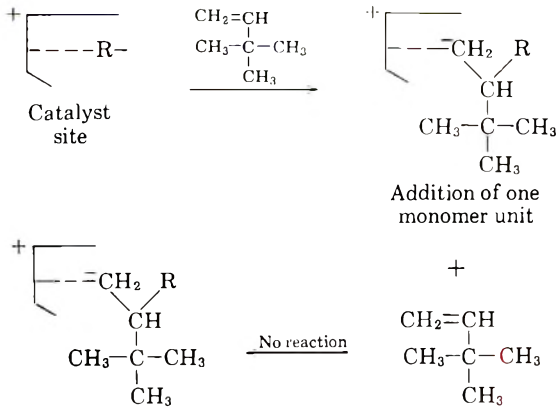

Fig. 6. Inhibiting effect of lateral bulk in side chains.

longer side chains is apparently due to removal of the bulky side-chain group from the vicinity of the backbone chain, introducing freedom of movement to the side chain.

It is surprising, however, that within a given series, the change in crystallinity with increasing side-chain length does not always progress smoothly. In the *tert*-butyl, phenyl, and cyclohexyl series, for example, loss of crystallinity occurs before any sudden drop in softening point takes place, that is, before side chains become highly mobile. It is known that the repeat distance along the chain axis varies with the length and nature of the side group, even within a given series. It is suggested that short blocks of atactic chains disrupt the regularity of the helix; this disruption, together with the alteration of repeat distances along portions of the chain, could interfere with crystallization. The influence of the atactic segments on crystallization may be more pronounced with helices of one pitch than with those of another. If this is the case, erratic crystallinity results observed in the *tert*-butyl, phenyl, and cyclohexyl series before any large drop in softening point has occurred, would seem reasonable.

Low conversions in the *tert*-butyl series (Table III) lead to speculation as to the polymerization mechanisms involved. In the first three members of the series, conversions were less than 2%; the conversion of 6,6-dimethylheptene-1 was 57.0%. The presence of lateral bulk in the side chain nearly, but not completely, prevented polymerization except when the *tert*-butyl group was removed from the immediate area of the vinyl group.

If the active catalyst center[18–20] is regarded simply as a restrictive site and no attempt is made to define its exact chemical or physical configuration, the effect of lateral bulk in the monomer can be understood. If a monomer containing a bulky side group adds to this catalyst site, the side group effectively blocks further monomer from entering (Fig. 6).

The effect may be compared to a key and a keyhole, where once the key becomes too large, it cannot fit the keyhole.

This blocking of the catalyst site by the bulky side chain of the first monomer unit explains the low conversions, but it is surprising that any

polymer is formed. The complete blocking of catalyst sites would lead to total deactivation of the catalyst, and no polymer should form under these conditions. The crystalline polymers of 3,3-dimethylbutene-1, 4,4-dimethylpentene-1, and 5,5-dimethylhexene-1 which were obtained in very low conversions may have been polymerized at sites other than the deactivated stereospecific sites. It is entirely possible that polymerization occurred by free-radical or ionic initiation or at edges or corners of the catalyst complex lattice. Since these catalyst sites are not normally stereoregulating, chain regularity is apparently determined by bulky side chains rather than by spatially restrictive catalyst sites. Fischer-Hirschfelder models of isotactic poly-α-olefin chains containing *tert*-butyl side chains show severe crowding even in the helical conformation, and the softening points are relatively high, indicating immobile molecules. The situation may be similar to polymerization of *tert*-butyl methacrylate or *tert*-butyl acrylate to crystalline polymers[21] where the catalysts employed do not impart stereoregularity to acrylates and methacrylates with smaller ester groups.

References

1. Natta, G. *Angew. Chem.*, **68**, 393 (1956).
2. Natta, G., *J. Polymer Sci.*, **34**, 531 (1959).
3. Williams, J. L. R., J. VanDenBerghe, K. R. Dunham, and W. J. Dulmage, *J. Am. Chem. Soc.*, **79**, 1716 (1957).
4. Korotkov, A. A., S. P. Mitsengendler, V. N. Krasulina, and L. A. Volkova, *Vysokomolekulyarnye Soedineniya*, **1**, 1319 (1960).
5. Ham, G. E., *J. Polymer Sci.*, **40**, 569 (1959).
6. Campbell, T. W., and A. C. Haven, Jr., *J. Appl. Polymer Sci.*, **1**, 73 (1959).
7. Natta, G., P. Corradini, and I. W. Bassi, *Gazz. chim. ital.*, **89**, 784 (1959).
8. Natta, G., *J. Am. Chem. Soc.*, **77**, 1708 (1955).
9. Dianesi, D., G. Natta, and F. Danusso, *Gazz. chim. ital.*, **89**, 775 (1959).
10. Braun, D., *J. Polymer Sci.*, **40**, 578 (1959).
11. Natta, G., P. Pino, and G. Mazzanti, *Chim. e ind. (Milan)*, **37**, 927 (1955).
12. Niegisch, W. D., *J. Polymer Sci.*, **40**, 263 (1959).
13. Uspensky, J. V., *Introduction to Mathematical Probability*, McGraw-Hill, New York 1937, Chapter I.
14. Simril, V. L., *J. Polymer Sci.*, **2**, 142 (1947).
15. Natta, G., *J. Polymer Sci.*, **16**, 143 (1955).
16. Bunn, C. W., and E. R. Howells, *J. Polymer Sci.*, **18**, 307 (1955).
17. Natta, G., *Makromol. Chem.*, **35**, 94 (1960).
18. Natta, G., P. Pino, G. Mazzanti, U. Giannini, E. Mantica, and M. Peraldo, *J. Polymer Sci.*, **26**, 120 (1957).
19. Corrick, W. L., *J. Am. Chem. Soc.*, **80**, 6455 (1958).
20. Patat, F., and H. Sinn, *Angew. Chem.*, **70**, 496 (1958).
21. Miller, M. L., M. C. Botty, and C. B. Rauhut, *J. Colloid Sci.*, **15**, 83 (1960).

Synopsis

Series of α-olefins were prepared and polymerized with $Al(C_2H_5)_3$–VCl_3 catalyst. Melting points, softening points, and degrees of crystallinity of the polymers were measured and the physical nature of the systems was discussed. Olefins studied were those having the general formula $CH_2{=}CH(CH_2)_xR$, where x = 0–3, and R is methyl, isopropyl, *tert*-butyl, phenyl, or cyclohexyl.

Résumé

Des séries d'α-oléfines ont été préparées et polymérisées par le catalyseur $Al(C_2H_5)_3$–VCl_3. On a mesuré les points de fusion, de ramollissement et le degré de cristallinité de ces polymères, et on a discuté la nature physique des systèmes. Les oléfines étudiées possèdaient la formule générale $CH_2{=}CH(CH_2)_xR$, où $x = 0$–3 et R est méthyle, isopropyle, *tert*-butyle, phényle, ou cyclohéxyle.

Zusammenfassung

Reihen von α-Olefinen wurden dargestellt und mit $Al(C_2H_5)_3$–VCl_3 als Katalysator polymerisiert. Die Schmelzpunkte, Erweichungspunkte und Kristallinitätsgrade der Polymeren wurden gemessen und die physikalische Natur der Systeme diskutiert. Die untersuchten Olefine besassen die allgemeine Formel $CH_2{=}CH{-}(CH_2)_x$-R, wobei $x = 0$ bis 3 und R = Methyl, Isopropyl, *tert*-Butyl, Phenyl, oder Cyclohexyl.

Received January 27, 1962
Revised December 13, 1961

JOURNAL OF POLYMER SCIENCE: PART A VOL. 1, PP. 763–788 (1963)

New Features in Polymer Crystal Growth from Concentrated Solutions

D. C. BASSETT, A. KELLER, and S. MITSUHASHI,* *H. H. Wills Physics Laboratory, University of Bristol, Bristol, England*

1. INTRODUCTION

Crystallization of polymers—polyethylene in particular—from dilute solution has been studied in some detail during the past few years. It has been established that it leads to tabular crystals consisting of layers of folded molecules.[1] The geometry of the simplest monolayer forms has been reasonably well explored,[2–5] in the course of which a particular type of pyramidal configuration has been deduced.[4,5] Much less is known, however, of crystals built of more than one layer. In a preliminary note it has been reported that multilayer polyethylene crystals are often found in a splayed configuration,[6] where consecutive chain folded layers are not in contact except in a small central region. Such crystals can be found even in the most dilute solutions where monolayers predominate. The splaying multilayer character of the crystals increases continuously with concentration up to about 0.3% and also beyond, for crystallization below about 75°C. in xylene, without showing any basic change otherwise. We shall refer to such crystals as simple multilayer crystals because of their readily recognizable relation to the familiar chain-folded lamellae. New observations on such crystals will be described in the first part of the paper.

At concentrations exceeding 0.3% for crystallization temperatures higher than 75°C., a new habit arises which by its much greater compactness is distinct from anything seen before. The description and discussion of these objects (to be termed "axialites") forms the second major part of the paper. In view of transition stages, this division of the subject matter cannot be made sharp, and occasional overlap of the presentation cannot readily be avoided.

2. OBSERVATIONAL TECHNIQUES

The starting point of this work was the realization that maximum information can only be obtained by examining the crystals while in the liquid.[6] Only in this way did even the simplest monolayer crystals reveal their true configuration.[5] In the case of multilayer crystals this method

* Present address: The Textile Research Institute of Japanese Government, 4, Sawatari, Kanagawa, Yokohama, Japan.

Fig. 1. A double pyramidal crystal viewed edge-on while floating in the liquid. Photomicrograph, 152×.

affords a means of seeing the same crystals in different projections without the distortions resulting from sedimentation and drying down. In addition, in the case of more complex objects the presence of a liquid medium also removes disturbing scattering effects, and clear features may arise in what can appear as a structureless opaque mass in the dried state. The details of the techniques have been described previously.[5,6] The dark-field technique was most suited for monolayer crystals, phase contrast microscopy for simple multilayer crystals, and conventional optical microscopy for axialites. In each case, however, the refractive index of the liquid had to be adjusted by the appropriate quantity of a suitable additive in order to obtain favorable viewing conditions.

3. SIMPLE MULTILAYER CRYSTALS: OBSERVATIONS AND COMMENTS

Previous observations[6] on splaying multilayer crystals have been extended. By continued observation of the crystals in the liquid it has been noticed that the simplest case of splaying is like the one shown in Figure 1. Here the crystal consists of two inverted pyramidal units connected at their apices. These units in Figure 1 are not themselves monolayers but packets of layers relatively close together. Figures 2 and 3 are transmission electron micrographs of such crystals, representing successive photographs of the same crystal. They show a crack and a fold along the lozenge short diagonal (the crack is visible better in Fig. 4). This is consistent with the double pyramidal configuration inferred from Figure 1, as pyramids flattening base and apex downwards are expected to crease and crack, respectively.[4,5] The replica in Figure 4 (of the detachment type[7]) reveals that the crack is on the top, while the crease is beneath in agreement with expectation. Spreading of the crease in Figures 2 and 3 indicates that collapse is still progressing during exposure to the electron beam. In special cases the contiguous screw terraces within the two pyramids can be rotated with respect to each other in a regular fashion. The curious twisted crystals in, for example, Figure 15 of an earlier report by Agar, Frank, and Keller[8] in fact now prove to be oppositely oriented, but otherwise compact, double pyramids, with often intermediate planar lamellae

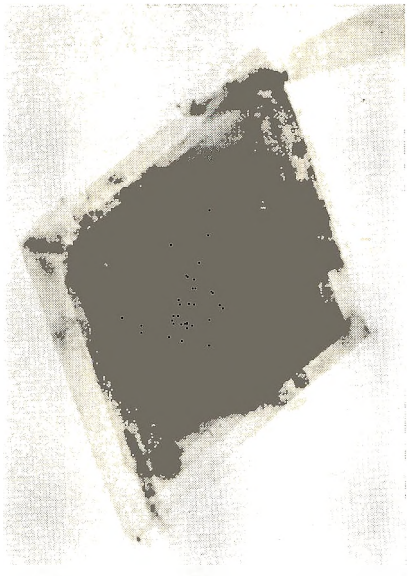

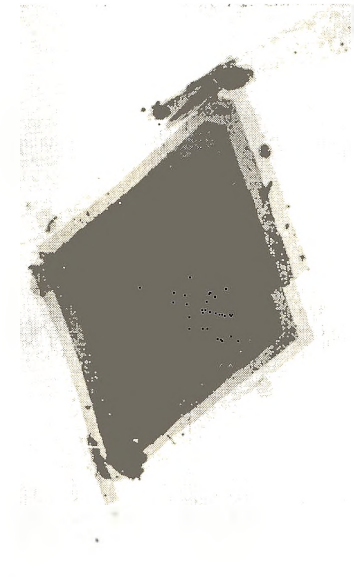

Fig. 2. (left) Electron micrograph of a crystal like that in Fig. 1. Unshadowed, 760×.
Fig. 3. (right) Electron micrograph of a crystal like that in Fig. 1; succeeding view of same crystal shown in Fig. 2. Unshadowed, 7600×.

Fig. 4. Electron micrograph of a shadowed detachment replica of a crystal like that in Fig. 1. 1075×.

Fig. 5. Layers folded over in a crystal like that in Fig. 1. Electron micrograph unshadowed, 1075×.

as well. This helps in explaining why sometimes only one half of a crystal is twisted while the other grows normally (further details to be published).

Electron micrographs also provide evidence for the splaying of layers. Figure 5 shows the common occurrence of layers which have folded back on themselves, presumably in the course of drying, which could arise if they were attached to each other near their centers only. Sometimes one finds crystals with two layers where both are closed polygons. Possibly these correspond to the simplest double pyramids. It is difficult to relate a double pyramid morphology to a screw dislocation geometry. It may be that one layer nucleated on the other in the early stages of growth, but alternatively the two might have formed from the same nucleus. According to the kinetic theories of chain-folded polymer crystal growth,[9–11] the crystal lamellae eventually grows with a thickness a little more than half the thickness of the primary nucleus, which should thus be left partially exposed as a tower in the crystal center. Such a tower may possibly nucleate a second layer in the way observed.

Less regularly splaying multilayer crystals can resemble the sheaving structure of spherulitic morphology,[1] if seen sideways. This has already been mentioned by Mitsuhashi and Keller.[6] Here we add photographs to illustrate two stages of the apparent sheaf formation (Figs. 6 and 7). These crystals also give spherulitelike birefringence effects in the polarizing microscope. The whole range of morphologies can be found by increasing the concentration of solutions crystallized at 76°C. from 0.01% to 0.5%. As

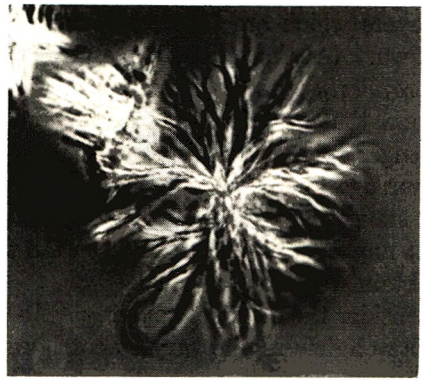

Fig. 6. Sheaving structures in multilayer crystal viewed edge-on in the liquid. Photomicrograph, 255×.

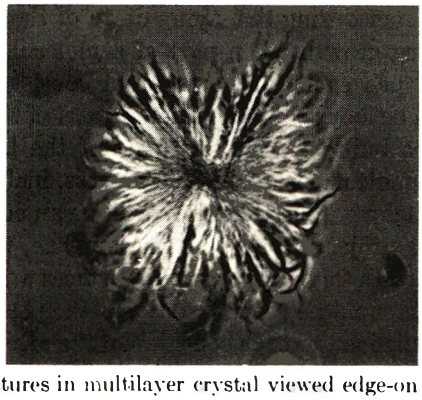

Fig. 7. Sheaving structures in multilayer crystal viewed edge-on in the liquid. Photomicrograph, 255×.

stated previously such structures would lead to "two-dimensional" spherulites, which, owing to the greater splaying of the long diagonals, would lead to *a* axis radial orientation. In melt-crystallized polyethylene spherulites,[12,13] the radial direction corresponds to the *b* axis; solution-crystallized ones have not been examined so far. Our arguments would imply the existence of two kinds of spherulites with either *a* or *b* radial, dependent on crystallization conditions, analogous to the known cases of polyamides.[12] Recent observations[14] also point in the same direction. Sheaving with maximum splay of the *b* crystal diagonals appears to occur in highly truncated lozenges (where *b* is the longest crystal direction). By the above analogy this could lead to *b* radial orientation in the spherulite. Speculative as this possibility may appear at present, it could provide a connection between spherulite type and crystal habit.

We may enquire about the structure underlying the progressively steeper pyramids forming the splaying crystals. If the pyramids are smooth they either contain structures of increasing obliquity (increasing fold staggering) or otherwise each crystal layer (defined as corresponding to a 360° lattice rotation in the helicoid) overlaps itself. The latter case could lead to rota-

tionally displaced layers which are frequently observed if crystals as in Figure 1 are dried down. (At the present stage we do not propose this as an explanation for the *regularly* twisted structures in Fig. 15 of reference 8.) Alternatively, we know that crystal layers can be corrugated, particularly in the large true lozenges and dendrites giving rise to crystals (as in Fig. 1 of reference 6), the corrugations corresponding to a periodic reversal in the direction of the fold staggering.[5] By varying the positions of reversal the lamellae could adopt any overall outline between the two extreme pyramidal configurations obtained without reversal.

This leads us to consider the origin of splaying. As the configuration of a single monolayer is well defined the varying configurations in the multilayer crystal are likely to be caused by constraints. It has been suggested to us by F. C. Frank that such a constraint could be provided by loose parts of chains projecting from the crystal surface. Such could originate as one molecule baulks another during the laying down of the segments along the crystal surface during growth when part of a molecule becomes excluded from the crystal. Such excluded parts could consist of end portions of chains, or they could be loops if another distant part of the excluded molecular portions becomes built into another part of the lamella. Moreover, the attachment of a molecule is a dynamic process, including finite rates of attachment and detachment, so that there will be an equilibrium length of unattached molecule projecting beyond the lamellae, this being longer at higher temperatures. In these ways, crystal surfaces would become "hairy" whereby the lamellae could be pushed apart, at the position of closest contact, and thus grow inclined to each other. On the other hand, "hairiness" could help in linking layers together by the "hairs" either becoming incorporated into consecutive lamellae or by their nucleating further layers.

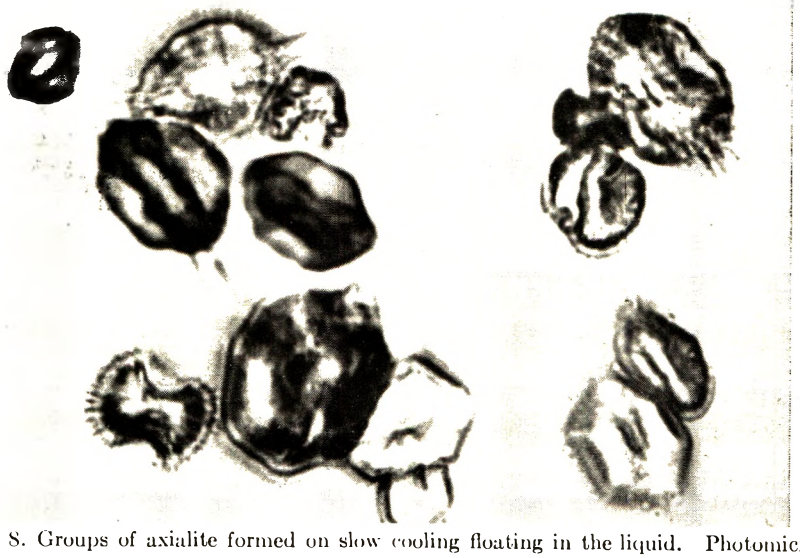

Fig. 8. Groups of axialite formed on slow cooling floating in the liquid. Photomicrograph, 750×.

In fact, the existence of lamellar linkages has been inferred from other results,[15] and nucleation of small islands on existing layers has been observed in studies of simple crystals.[16]

One may ask why some layers splay while others grow together. We are aware of having invoked the same cause (hairiness) to explain two opposed effects. We have no answer at this stage. It is worth noting, however, that lamellae which splay are usually found to be corrugated while in the liquid. On the other hand, those which form contiguous packets are smooth. Thus for geometric reasons alone, better or poorer fitting is expected, respectively.[17] Fitting geometry alone should not lead to splaying, though once layers are not in contact, they should splay more easily. A simple splaying of layers (as in Fig. 1 of reference 6) could be given by hair pressure in a small region near their joining. For a curving splaying, as in sheaving morphologies, however, hair pressure would be present from adjacent lamellae throughout the growth of a lamella. It is possible that this constraint could be eased by a systematic disposition of staggering reversals in a lamella which would then adopt an overall curved outline.

4. THE FORMATION AND APPEARANCE OF AXIALITES

As stated in the introduction, a novel, more compact type of crystallization product is observed from solutions more concentrated than ~0.3% when crystallized at temperatures exceeding about 75°C. This appears quite distinct from the usual multilayer crystals. Objects representing transition stages can also be observed, but these have not been explored systematically. In our standard experiments, Marlex 50 was crystallized from a 1% xylene solution. The resulting suspensions were examined optically in a cavity slide. The compact objects mentioned were seen best under ordinary illumination with the appropriate amount of acetone or ethanol added to the suspension. Figure 8 shows a few groups of objects seen under these conditions (taken from different photographs). The particular preparation was obtained by slow cooling of a 1% solution. From our experience, we know that crystallization must have occurred at 85–87°C. Of the different shapes visible, the simplest is an elongated hexagon reminiscent of single crystal outlines, but of much higher contrast. Other objects appear fibrous, e.g., sheaves often with curious twisted shapes, some of which have been illustrated before in accounts of the initial stages of spherulitic growth.[18] It was soon realized that the various shapes could appear from the same object when it was turning in the liquid, e.g., a hexagonal appearance could become sheaflike and vice versa; i.e., these objects have very different shapes when viewed from different directions.

This point was examined systematically by mounting a specimen on a universal stage. For this, the objects had to be in a medium rigid enough to prevent movement on tilting, and having a suitable refractive index, giving adequate contrast without excessive scatter. Drying down was thought to be best avoided as some changes were suspected to occur in the

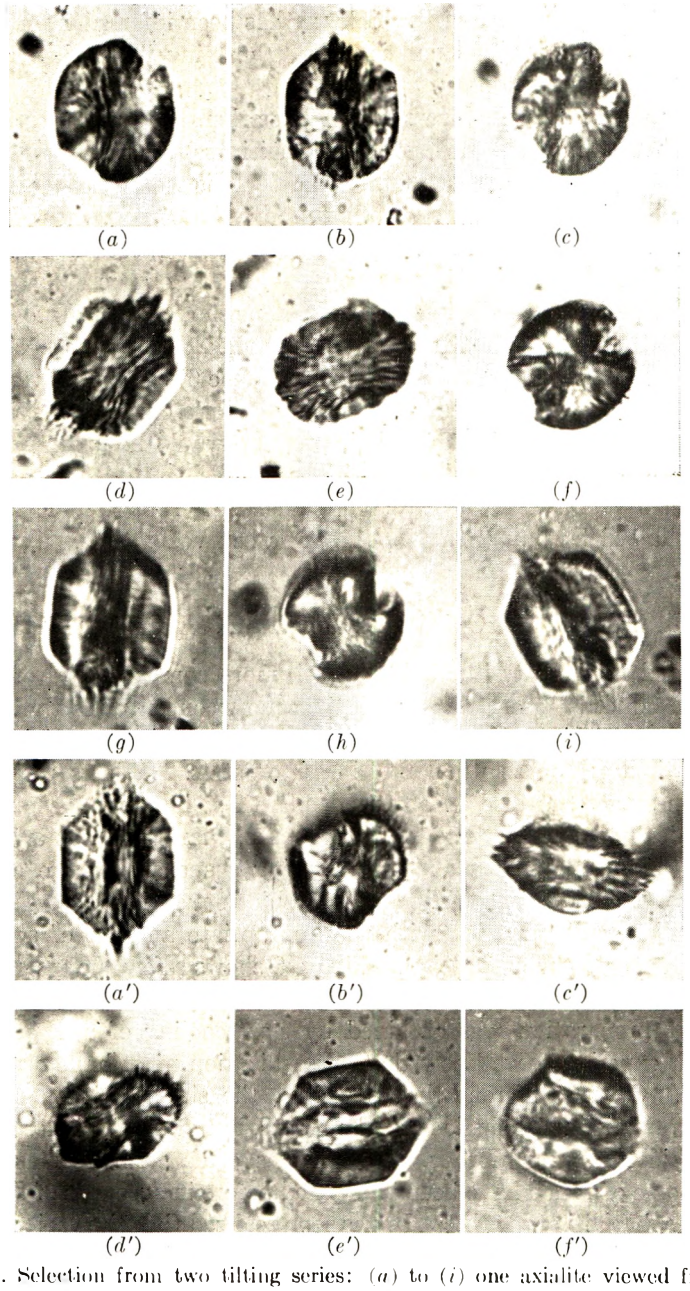

Fig. 9. Selection from two tilting series: (*a*) to (*i*) one axialite viewed from nine different directions; (*a′*) to (*f′*) another axialite viewed from six different directions. Photomicrographs, 750×.

course of it. These requirements were satisfied by mixing a drop of concentrated suspension in xylene with a large volume of ethanol and this mixture with a concentrated aqueous solution of polyvinyl alcohol to a syrupy consistency. Precipitation of the polyvinyl alcohol could be

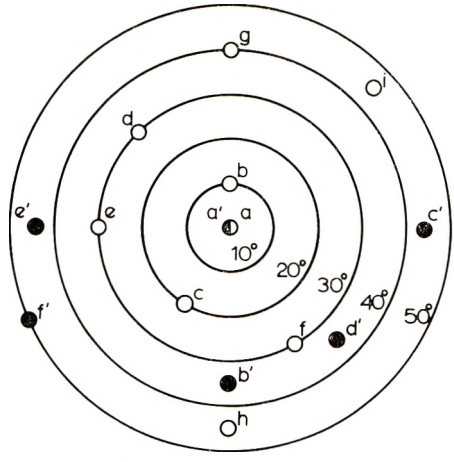

Fig. 10. Stereogram showing orientations (○) corresponding to (*a*) to (*i*) and (●) (*a'*) to (*f'*) of Fig. 9 (see note added in proof).

avoided by trial and error. The mixture was mounted between slide and coverglass, allowed to set sufficiently, and the coverglass was then sealed around. A Zeiss four-axial stage was used, permitting objectives up to 0.6 NA. Only a small selection of photographs (each set comprises ~60–70 photographs) can be shown here to illustrate some of the typical shapes (Fig. 9). Even these do not convey all the information even at a given setting of the stage, as photography through focus would be required for each. The tilt corresponding to each picture can be read off the accompanying stereogram (Fig. 10). The poles numbered correspond to the viewing directions with reference to that in the untilted state of the specimen i.e., (*a*, *a'*): center of stereogram. The convention adopted in mounting the photographs of Figure 9 is that each photograph when viewed up the page represents the view of the *same* object when observed inwards along the directions marked on the corresponding stereogram (Fig. 10) with the observed vertical and horizontal directions maintained so in the mounting. The circle corresponding to 50° tilt represents the observational limits of our stage. In view of this angular limitation, objects in different initial positions were required for a complete survey. The illustrations in Figure 9 are taken from two sets, referring to two objects with different initial positions, the corresponding poles being marked with open and full circles, respectively. It was most instructive to mount the photographs on the corresponding position of the stereogram; this cannot be illustrated, however, for reasons of size (see note added in proof).

The experiment confirms that the different shapes seen before arise from the same objects. It emerges from the full series that the objects resemble two partly opened books placed spine to spine, the pages having the shapes of half an elongated hexagon. The symmetrical sheaf appearance (Fig. 9*h*), arises from looking along the spine, the stretched hexagonal shape (Fig. 9 *g*,*i*) and the elongated fibrous appearance (Fig. 9*c'*) arise when

looking normal to the spine along the two mirror planes containing the spine. Figures 9*g*, 9*h*, and 9*c'*, 9*e'*, represent pairs of mutually (or nearly) perpendicular views. All other shapes correspond to intermediate viewing directions. The series show revealingly how inadequate a single microscopic image of three dimensional object can be. Some single crystals appear to show a pronounced twist (Figs. 9*a*, 9*f*, 9*d'*), which nevertheless turns out to be largely illusory, though in some cases a small twisting of the spine could not be ruled out completely. The same may be said of the apparent line of central thickening (Figs. 9*g*, 9*a'*). Most of these illusions are due to the limited focal depth of the objective plus the varying transmissivity in object details seen in different foreshortening. Objects of the above type will be termed axialites to denote the fact that they consist of assemblies of splaying crystal layers which appear to splay around a common axis (with some reservations to become apparent later).

By varying the temperature and concentration of crystallization, axialites of different shapes and compactness were obtained. The products were not always strictly identical under what was thought to be the same conditions; nevertheless, the general trend was observed that increase of either factor resulted in an increased relative elongation of the spine. In this way the shape of the axialites in their most regular view could range from that of a truncated lozenge, with small truncating faces, through a regular hexagon to hexagons highly elongated along the spine direction. This trend with increasing temperature is identical with that found in the simplest monolayer crystals in dilute solution.[16] It should follow from this resemblance that the spine corresponds to the *b* axis direction which has in fact been confirmed (see later).

Axialites with a nearly regular (though somewhat rounded) hexagonal outline were obtained from a 1% solution at 80°C. Figure 11 shows two of them in different positions. The double book appearance is again clear, the pages being quite distinct. Figure 12 shows a group of axialites grown at 85°C. These particular samples were dried down from the suspension, when as already said, the image becomes quite confused. If, however, they are vacuum-coated with carbon, visibility improves, and the

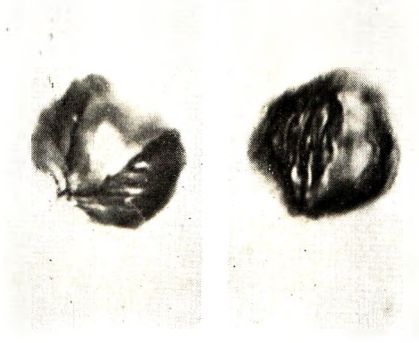

Fig. 11. Two axialites formed at 80°C. presenting different views. These were dried, carbon-coated, and covered with ethanol. Photomicrographs, 1000×.

Fig. 12. Group of axialites formed at 85°C. under conditions as in Fig. 11. Photomicrograph, 700×.

Fig. 13. Axialite with "wing" development in the liquid. Photomicrograph, 700×.

features as in Figures 11 and 12 emerge. The photographs were taken with these carbon-coated objects flooded with ethanol and covered afterwards, which reduced the rather excessive contrast. This is another illustration of the various means which can be used to achieve satisfactory viewing conditions, which is the underlying requirement for work on these objects.

Axialites reveal pronounced birefringence effects under the polarizing microscope. The effects are different for each orientation with respect to the microscope axis, and for each such orientation it is different for all positions with respect to the plane of polarization. Consequently, the number of illustrations even of the main effects would be prohibitive. Only two general features will be quoted. In the hexagonal view, most of the outer part of the objects appeared first-order grey or pale yellow, i.e., birefringence was low. This is consistent with the molecular orientation being about perpendicular to the layers. In the sheaf view, birefringence was strong and showed an extinction pattern which more or less resembled the Maltese cross characteristic of spherulites, depending on the sheaf development. Besides these typical axialites, related but more complicated objects can also appear. Thus one or several wings can grow out at an angle from the main body of the axialite. Again, suitable viewing conditions are required for interpreting the corresponding complex visual images. A simple example of wing formation is shown by Figure 13.

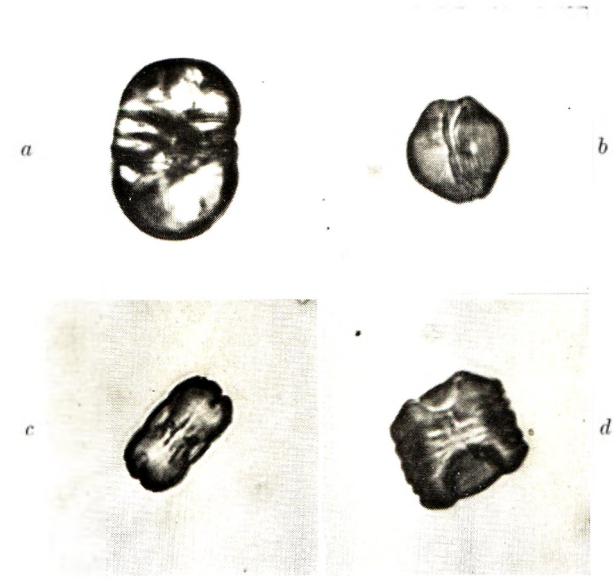

Fig. 14. Four types of a slightly different kind of axialite. Photomicrographs, 480×.

Another class of object is shown in Figure 14, which arose after a suspension was crystallized at 86.5°C. and held at that temperature for several days after crystallization. Here the objects are rounded and have smooth outlines. Most of them are oval (Fig. 14*a*), but others are somewhat rounded polygons (Fig. 14*b*). It was found that the two could represent different views of the same kind of object. An internal striation revealing a lamellar subdivision could often be seen also in the curious objects in Figures 14*c* and 14*d*. The refractive index being highest normal to this stratification, it follows that the lamination causing it probably corresponds to the usual crystal layer development. The appearance of these objects between crossed polars is particularly striking. In certain orientations, nearly complete extinction can be obtained, while other views show extinction brushes like those in biaxial interference figures or some elongated spherulites.

4.1. The Fine Structure of Axialites: Electron Microscopy

Axialites are not readily suited for fine structure studies with the electron microscope as they are opaque for work in transmission. In looser aggregates, some degree of transmission can be obtained, at the expense of some deformation, if the specimens are burned out by slow and gradual increase of the electron beam. Such micrographs are difficult to print and reproduce owing to their extreme contrast consistent with the double-book character of the objects. They do show, however, that the spines splay towards the edges, indicative of a pyramidal or conical habit with apices in contact. Accordingly, splaying would be rather about a central area than an axis as in the simpler multilayer crystals; however, splaying about an axis only is

Fig. 15. Shadowed transmission electron micrograph of an axialite formed at 85°C. Detachment replica, 3080×.

at least simulated when the objects become more compact, in which state they become totally unsuited for transmission electron microscopy. For the examination of finer structural elements replication was called for. In the several methods used carbon coating was applied first from several directions at large angles (60–80°) (in the latest experiments the specimen was continuously rotated during coating); then for rigidity, the carbon could be suitably backed. On sedimentation such an object usually lies on its flattest side, presenting a hexagonal outline. The pages at steeper angles could not be replicated without some deformation (because of their extreme reentrant angles and swelling during dissolution) and were often lost altogether. Dissolution of the polyethylene in hot xylene was carried out in a controlled manner so as to preserve a layer of polymer adhering to the carbon. This is the detachment replication technique developed by one of us earlier.[7] The most informative results were given by objects which consisted of relatively few pages only.

Figure 15 shows one example obtained. Most conspicuous is the page lying flat, giving a recognizable hexagonal outline. Other lacerated pages can be seen protruding outwards in a rather confused way. More of the latter feature is seen in the Figure 16 which agrees with photomicrographs like Figure 11. The replicas gave the diffraction pattern of polyethylene, confirming that a layer of the original crystalline polymer adhered to the carbon. The pages lying flat as in Figure 15 gave clear single crystal patterns with the b axis along the long diagonal of the hexagon. Thus the

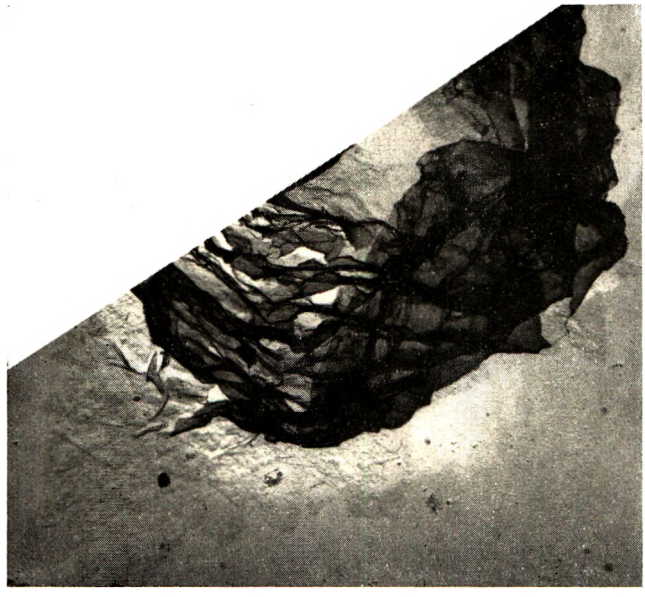

Fig. 16. Axialite formed at 80°C. Shadowed detachment replica, electron micrograph, 2385×.

spine of the book corresponds approximately to the *b* axis as already assumed. Single pages, as in Figure 15, are seen in much higher contrast than a normal 100 A. monolayer, and consequently must be much thicker. The flat page in Figure 15 would become nearly black if the substrate were brought out on printing. The thickness can be assessed roughly from unshadowed detachment replicas where standard multilayer crystals, obtained from dilute solution with 150 A. growth terraces, were sedimented on the grid after the replicas of the axialites were ready. The contrast in the axialite layer could be matched against that of the appropriate growth terrace in the single crystal. The flat pages in an object as in Figure 15 were found to have a layer thickness of ~1000 A. and those in one as in Figure 16 (but containing flatter pages) a layer thickness of ~600 A.

The thick layer in Figure 15 consists of a great number of the usual ~100 A. growth terraces (these may not be visible at the low magnification of Fig. 15; they should, however, be obvious from Figs. 17–19, which are from similar objects and to be discussed later). The contrast within the layer, however, is uniform. This means that the layer adhering to the carbon cannot contain the full growth pyramid, only a stratum of constant thickness, otherwise the thicker centres would appear darker, as they do in the standard transmission photographs of multilayer crystals. Neither can this stratum be the top surface only (as in the detachment replicas of single crystals[7]) because this would be too thin to give the contrast observed. Thus we must conclude that the carbon retains a thick (in case of Fig. 15), e.g., 1000 A. slice of ~100 A. layers, the thickness of which is uniform irrespective of the growth hills on them.

Low-angle x-ray photographs confirm that the axialites give reflections at ~130 A., the exact value depending on the temperature of crystallization as in the case of the standard single crystals. Thus they must consist of the usual chain folded lamellae found in single crystals which is also indicated by the growth terraces on them. We must conclude, therefore, that some coherence exists across a certain number of layers to produce the effect seen in Figure 15. The top layer bound to the carbon would accordingly keep a number of layers with it, while the rest dissolves. That dissolution conditions were adequate to remove the usual disconnected layers is evident from the fact that only the 100–150 A. top layer remains from the usual multilayer crystals lying on the same grids.

For greater ease of observation thick layer objects as simple as possible would be required. Figure 17 shows an example of more isolated thick layers obtained by ultrasonic fragmentation. The greater thickness, the growth terraces, and the uniformity of layers across the terraces are clearly discernible, but in addition some peeling effect is also seen. Ultrasonic disintegration has been applied also in connection with radiation studies.[15] It was stated there that cavitation produced by ultrasonics split the compact objects into fragments which, judging from their thickness, must still consist of a large number of layers. After detachment replication, however, the thick layers like those in Figure 17 became rare; mostly only standard ~100 A. layers adhere to the carbon. This would mean that the cohesion of layers in many still apparently multilayer fragments is reduced by the ultrasonic treatment, so that all but the layer in contact with the carbon can dissolve. However, in view of the occasional thick layers present, observation of the same fragment before and after dissolution would be needed in order to establish this effect rigorously.

Still simpler, thick-layer objects can be observed by interrupting crystallization in the early stages by removal of the crystallized solution (e.g. by

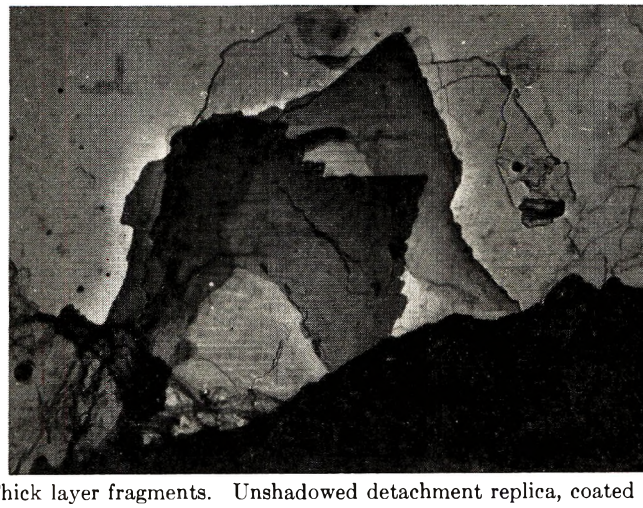

Fig. 17. Thick layer fragments. Unshadowed detachment replica, coated with carbon from different sides, with unequal intensity, electron micrograph, 8880×.

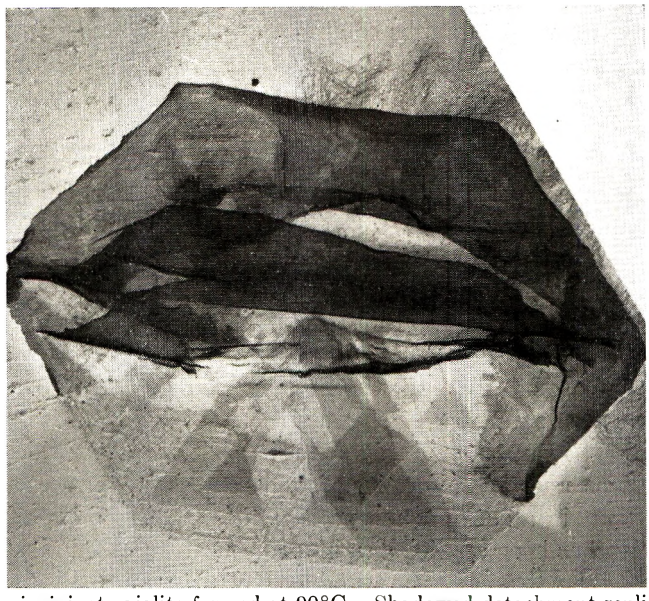

Fig. 18. An incipient axialite formed at 90°C. Shadowed detachment replica, electron micrograph, 4620×.

filtration). As both the thick-layer development and the habit of the layers are functions of concentration, such a preparation also ensures that the crystallization products are more uniform, and representative of the highest concentration range. Figure 18 shows one of the objects formed in this way. The optical microscope revealed that the books in this specimen consisted of only very few (2–5) pages. In Figure 18 the thick-layer development is absent on the lower side, which, except for thicker patches, is a detachment replica with the standard ~100 A. layers. The relation between the thick layers and the standard ~100 A. ones is by no means clear, but it is evident that in the axialite of Figure 18 some transition state must exist. Figure 19 shows the tip of an axialite in the same preparation representing an early development. The way thick layers join can be seen. Axialites representing still earlier stages of growth than those in Figures 18 and 19 show that this growth starts with the usual ~100 A. terraces as in simple crystals. From photographs like Figure 18, the thick parts appear to consist of layers folded back on themselves about the outer crystal edge. Peelings detaching themselves from the thick layers are often seen; this always starts in the interior, the peeling layers being hinged along the outer crystal edge.

The fact that the pages of the books are thicker than the standard crystal lamellae is also apparent from the optical micrographs of Figures 11 and 12; otherwise, the pages would not be seen so distinctly. This distinction is not so apparent when the axialites have not passed through a drying-down stage (Fig. 9). This might suggest that layers have stuck into packets in the course of drying. That drying does cause some disturbance can

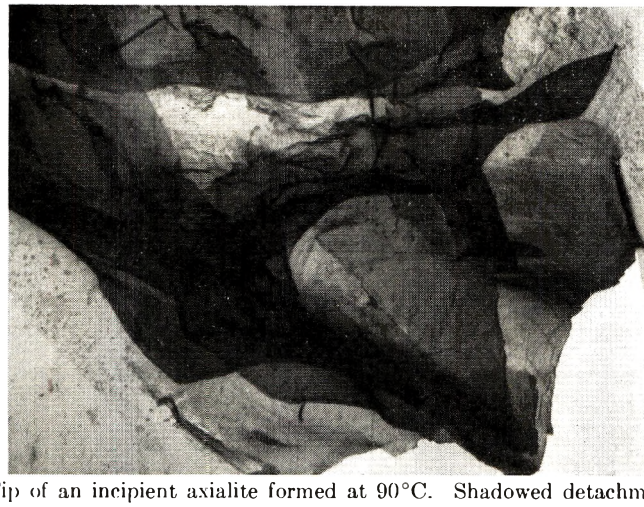

Fig. 19. Tip of an incipient axialite formed at 90°C. Shadowed detachment replica, electron micrograph, 5698.×

be judged from the threads pulled between pages (e.g., Fig. 22). These threads are not necessarily the result of the detachment replication, as they were also seen optically after drying and carbon coating, but before dissolution. Thus the pages could have all been connected while in the liquid, but on drying some pages would stick together and on pulling away from others produce threads. Even if folding back of layers on themselves or their sticking together were the sole origin of the thick-layer effect, these processes must be more than accidental, for otherwise those parts of layers not directly in contact with the carbon coating would dissolve in our treatment as do layers of simple crystals. For an explanation of the reduced solubility, cohesion greater than that produced by mere contact is required. It is possible that layers which are very steeply inclined to the substrate could become carbon coated from two sides during the process adopted, and thus be more protected from the solvent, but these are mostly torn up or lost during replication anyway, the most typical thick layer effects being seen on layers which lie flat, i.e., which can have coating on one side only. We must conclude, therefore, that these objects show ordering on a larger scale than their constituent chain-folded lamellae.

4.2. Some Properties of Axialites

It is found that the different kinds of axialites react differently on ultrasonically produced cavitation. The differences can be quite extreme. Thus axialites as in Figure 9 were not affected, except for some fringing on the surface, on treatment lasting more than ten times longer than that which broke up the axialites in Figure 11 completely into shreds and left little recognizable trace of the original objects. Thus the internal cohesion between components of the axialites formed under different conditions can be highly variable.

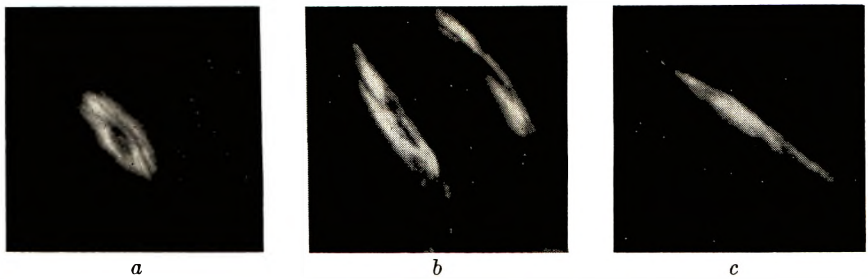

a *b* *c*

Fig. 20. Three axialites in stages of increasing elongation along their axial direction, photomicrographs, crossed polars: (*a*) 330×; (*b*) 220×; (*c*) 175×.

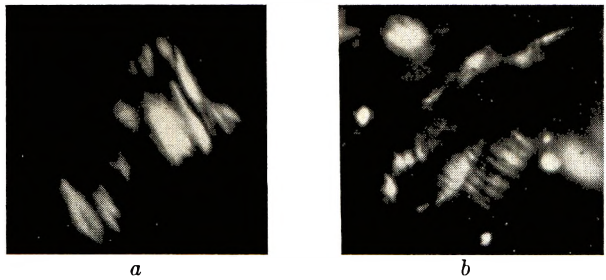

a *b*

Fig. 21. Axialites elongated normal to their axis, photomicrographs, crossed polars: (*a*) 600×, (*b*) 315×.

It has been possible to deform axialites by embedding and stretching in rubber. A suspension mixed with rubber solution and dried in to form a film was stretched with tweezers and examined after mounting in immersion oil or Canada balsam. Alternatively, the rubber was dissolved and washed away, leaving the axialites behind. In this rather crude process elongation could not be recorded quantitatively nor could examination be carried out during stretching or in the fully stretched state. Nevertheless, the effects observed are instructive. No effect has been observed for relatively small stretching of the rubber. It is thought that the axialites deform elastically and then recover as the stress is removed. With the highest elongation, deformation of the axialites is noted. The most frequent occurrences are those shown in Figure 20 (seen between crossed polars). They represent three stages of elongation in different objects. In Figure 20*a* the original splaying book structure is still recognizable, but in Figures 20*b* and 20*c* the resemblance is progressively lost. The remarkable fact is that the highest refractive index, i.e., the molecular direction, is normal to the elongation (negative birefringence) throughout this and other similar series. This suggests that the deformation consists of the pages sliding past each other like cards in a pack. Less frequently objects with a periodic banded structure have also been seen (Fig. 21), where the bright bands correspond to a higher concentration of matter. This can be interpreted as arising from stretching in a direction normal to the pages which would pull the pages or packets of them apart, the object elongating like

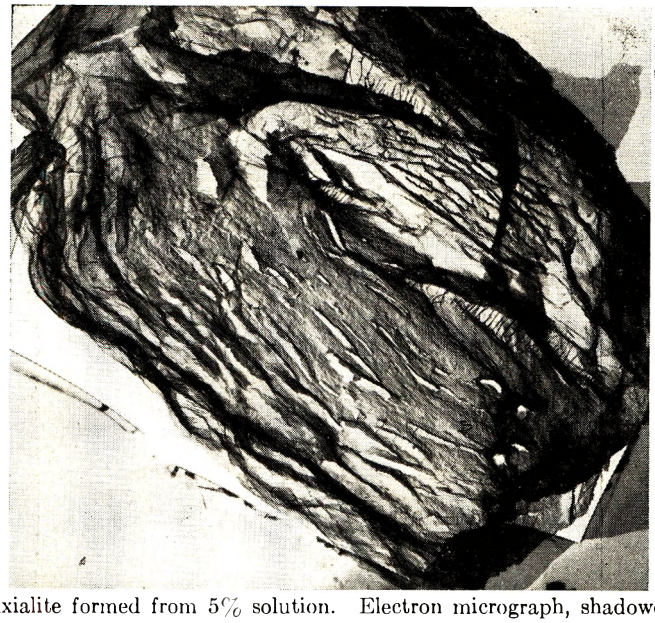

Fig. 22. Axialite formed from 5% solution. Electron micrograph, shadowed detachment replica, 4300×.

an accordion. In Figure 21 the highest refractive index is perpendicular to the stripes, again corresponding to the original molecular orientation in the lamellar packet in agreement with the previous interpretation. Thus in the first approximation elongation in either direction does not seem to disturb the lamellae, only their relative arrangements.

4.3. Crystallization from Very High Concentrations

The maximum concentration which can be achieved by simple dissolution of Marlex 50 in boiling xylene without unduly prolonged boiling is 1–2%. For higher concentrations, the polymer has been heated with the appropriate amount of solvent within a sealed tube to temperatures higher than the atmospheric boiling point. Stirring needed for achieving homogeneous mixing was done by sliding a metal rod sealed in the tube up and down, usually magnetically. In view of the danger of degradation the temperature was not raised above 200°C. In this way concentrations up to 20% have been achieved. Crystallization may then be conducted at chosen temperatures, which are necessarily above 80–85°C. owing to the rapid precipitation at such high concentrations. The products of crystallization are again of the axialite type in the whole concentration range. The objects are more compact and the outlines less regular than before. Figures 22 and 23 show detachment replicas of objects formed from 5% and 10% solutions, respectively. Single crystallike diffraction patterns can be obtained (with some arcing and spottiness), the b axis lying along the spine direction. A great number of pages are visible in the replicas, all consisting of thick layers. Enlarged details reveal ~100 A. growth

Fig. 23. Axialites formed from 10% solution. Shadowed detachment replica, election micrograph, 3950×.

terraces on them. The axial view between crossed polars is essentially fully spherulitic. Objects from higher concentration than in Figures 22 and 23 are essentially similar but more compact and with more pages and are consequently more difficult to replicate.

Concentrations higher than 20% have been achieved as follows. First a 20% polymer–xylene solution was prepared in one branch of a sealed, inverted U-tube in the above manner. Subsequently the other branch of the tube was cooled while the solution was kept at the dissolution temperature. Solvent distilled over into the cooler branch, so that the solution at the other end increased in concentration. The solution was stirred vigorously magnetically. After crystallization, the amount of liquid which had distilled over and hence the concentration at which crystallization occurred could be determined. It was found that with 30–33% concentration a gel formed which could largely be dispersed by adding more liquid to it and stirring. The dispersion consisted essentially of axialites as in Figures 22 and 23. At and beyond the ~40% concentration, the gel did not disperse any longer nor could the homogeneity of the solution be ensured. (The highest concentration, in our experiments, was a nominal 55% polymer.) The units building these gels still resemble the previous axialites with a lamellar morphology, but they are less regular and more tied together. For this reason, views from different sides of the same objects could not be observed. Between crossed polars the spherulitic appearance becomes more general, and also concentric extinction rings appear. Even so, as far as could be judged, these "spherulitic" effects still do not correspond to a truly three-dimensional morphology.

High pressure polyethylene has also been used in these studies. At low concentration, the crystals are less distinct and are smaller variants of axialites. At higher concentrations, however, they definitely start to resemble true spherulites. While the book character is still recognizable, sheaving becomes more three-dimensional, and the spherulitic extinction cross appears in a greater range of positions and more perfectly. The fine structure, however, is still lamellar, and even the ~100 A. spiral growth terraces are recognizable.[19]

5. SOME COMMENTS ON THE OBSERVATIONS ON AXIALITES

Most of the main conclusions should be self-evident from the description of the experiments. Here only three aspects will be commented on separately.

5.1. The Connectedness of Layers

The possibility of interlamellar ties has arisen firstly in connection with radiation studies,[15] where it emerges that the crosslinking effective in gel formation may take place between adjacent lamellae, and is more likely to occur, the more closely the lamellae are packed. While lamellar contact can be promoted by extraneous physical conditions, such as compacting the layers mechanically,[20] it would be ensured automatically by molecular ties running through several layers. As already mentioned in the first section, the tying of layers could be one of the consequences of the crystal surface being "hairy" on a molecular level. As stated there, these hairs should be longer at higher crystallization temperatures which, at least in principle, could lead to ties of longer range, in agreement with the stronger connectedness within crystals formed at higher temperatures. This has already been implied by the results of the radiation studies[15] and is further supported by the presently observed tendency towards the compact "axialite" formation with rising temperature. In the radiation work[15] it is reported that after ultrasonic disintegration samples would not gel for a particular radiation dose at which they had previously given more than 60% gel. Separation of layers, possibly associated with cutting of some of the tie molecules was suggested. Microscopic examination reveals that such ultrasonically treated samples still contain some multilayer fragments. In the course of the present detachment replication experiments, layer packets within such fragments seemed to be more readily soluble than those in the intact unit. This, pending further confirmation, would imply that the number of the tie molecules within the packets had become reduced.

The possibility of interlamellar tie molecules has arisen also in connection with standard multilayer crystals (Fig. 5 of reference 7). Here a layer formed at a higher temperature than the rest of the crystal was found to adhere to the detachment replica, in spite of its being buried deep in the crystal interior, and in spite of layers between it and the top layer attached to the carbon being dissolved away.

It would be desirable to find an independent physical measure of the connectedness of layers, but this is not readily available. The resistance to cavitation in the ultrasonic treatment is an indication of the degree of the connectedness in question. Similarly the deformation behavior is very illuminating. As deformation is seen to consist primarily of displacement of layers with respect to each other, the modulus (in the elastic range) and viscosity (in case of plastic flow) should be determined primarily by interlamellar links. This should also affect the relaxation times in time-dependent mechanical behavior. One would expect relaxation times associated with the motion of whole layers and layer packets, and those associated with displacements within a layer. Further, interlamellar linking should be decisive also for the ultimate strength of the sample. In principle, all this should be relevant to the mechanical behavior of polymers in general. However, it is difficult to make measurements on an individual axialite and place the present investigations on a quantitative basis.

The mode of development and detailed structure of the thick layers has eluded us so far. Despite some rather trivial possibilities (layers folding back on themselves or sticking together on drying), the experimental facts require a certain amount of molecular linkage between chain-folded ~100 A. layers which must have arisen in the course of growth, and must accordingly be fundamental.

5.2. Relation between Axialites and Spherulites

It is remarkable that one and the same entity when seen from different directions can simulate the appearance of single crystals on the one hand and that of objects characteristic of spherulitic morphology on the other. An example of this has already been encountered in connection with the simple multilayer crystals. With the more compact axialites, this dual resemblance is even more striking, as these can simulate nearly all stages in spherulitic development while still retaining the single-crystal appearance in the appropriate view. Thus, they may be intermediates between single crystals and spherulites.

Transitional objects between single crystals and spherulites have already been described in thin melt-crystallized films of polyoxymethylene and polyoxyethylene and were termed hedrites.[21,22] Such objects were seen also in poly-4-methylpentene-1,[23] in isotactic polystyrene,[24] and earlier in gutta-percha.[18] These hedrites are flat bodies; they can be polygonal, oval, or sheaflike, approximating two-dimensional spherulites. These different types of hedrites can now be correlated with different aspects of axialites. Thus hedrites might really correspond to such axialites, the development of which is restricted by the substrate. If hedrites grew with molecules normal to the substrate, polygonal forms would result as in simple crystals; if nucleation and growth is initiated by molecules lying along the substrate, the sheaf form would dominate. The axialites, as observed, could only account for pseudospherulites with axial symmetry.

Marlex axialites showed no obvious trend towards spherical symmetry, but those from the more branched high pressure polyethylene did. These were much smaller, and also structural features within them were on a smaller scale. It is possible that the trend towards spherical symmetry becomes manifest only over larger distances compared with the regularly developed axialite. The smaller size of the regular features in branched polyethylene is plausibly connected with the lowered regularity of the molecules of which they consist.

In view of the present observations it may be opportune to reconsider some of the earlier descriptions on initial spherulites. The twisted sheaf of gutta-percha (in Fig. 4 of reference 18) is likely to correspond to the appropriate view of an axialite-type object, particularly as such sheaves were obtained in melt-crystallized films which in the same specimen revealed the hedrites. Even the most typical fibrous sheaves as found in nylon 6,10 formed from suspension[18,25] may not be quite what they appear. Recent reexamination of these sheaves in the liquid revealed that in one preparation, at least, the loose fibers did not terminate in randomly situated fringes, but along the boundaries of an elongated polygon with straight sides. No material polygonal object was visible, yet the suggestion remains that such sheaves arose initially from a regular object of single-crystal type.

5.3. On the Relation between Crystallization from Solution and Melt

The pressurized-dissolution technique offers a means to approach the pure melt state from that of dilute solution continuously. The fact emerges that lamellar crystallization obtains up to concentrations where the amounts of polymer and solvent are comparable, i.e., in systems which correspond rather to the plasticized bulk than to solutions. Whenever diffraction studies have been made on detachment replicas of these objects, the lamellae have been found to be chain-folded. Images showing fine structural details become somewhat confused beyond 50% polymer; the final transition to the pure melt beyond this concentration needs more attention. Nevertheless, the experiments as they stand prove that lamellar crystallization representative of the whole specimen is not restricted to dilute solution where contact and interaction between different molecules is negligible.[10,26] Undoubtedly increasing molecular entanglement and defective crystalline structures are to be expected, but this should not obscure the basically chain-folded lamellar crystallization. What appears to happen is that with increasing concentration some connectedness develops progressively between the lamellae and in the later stages between the axialites or spherulites resulting therefrom. Accordingly, the development of molecular ties between otherwise chain-folded lamellae and the axialites or spherulites these give rise to would provide the transition between crystallization from dilute solutions and the bulk, also accounting for the increasing mechanical strength as the one-component system is approached.

Note added in proof: Since the paper was submitted the original stereograms with the photographs on them have been made more suitable for reproduction. They have been reproduced since in the review ref. 27 (added in the proof stage) where a full description of the mounting convention is also given.

We are indebted to Professor F. C. Frank, F.R.S. for much stimulating discussion. D. C. B. wishes also to acknowledge the award of a Postgraduate Scholarship by the Trustees of the Courtaulds Scientific and Educational Trust Fund, and S. M. a fellowship from the European Research Associates, Brussels.

References

1. Keller, A., *Makromol. Chem.*, **34**, 1 (1959).
2. Niegisch, W. D., and P. R. Swan, *J. Appl. Phys.*, **31**, 1906 (1960).
3. Reneker, D. H., and P. H. Geil, *J. Appl. Phys.*, **31**, 1916 (1960).
4. Bassett, D. C., and A. Keller, *Phil. Mag.*, **6**, 345 (1961).
5. Bassett, D. C., F. C. Frank, and A. Keller, to be published, see also ref. 27.
6. Mitsuhashi, S., and A. Keller, *Polymer*, **2**, 109 (1961).
7. Bassett, D. C., *Phil. Mag.*, **6**, 1053 (1961).
8. Agar, A. W., F. C. Frank, and A. Keller, *Phil. Mag.*, **4**, 32 (1959).
9. Price, F. P., *J. Polymer Sci.*, **42**, 49 (1960).
10. Lauritzen, J. I., and J. D. Hoffman, *J. Research Natl. Bur. Standards*, **64A**, 73 (1960).
11. Frank, F. C., and M. P. Tosi, *Proc. Roy. Soc. (London)*, **A263**, 323 (1961).
12. Keller, A., *J. Polymer Sci.*, **17**, 351 (1955).
13. Point, J. J., *Bull. Acad. roy. belg.*, **41**, 982 (1955).
14. Khoury, F., and F. J. Padden, *J. Polymer Sci.*, **47**, 455 (1960).
15. Salovey, R., and A. Keller, *Bell. Tech. J.*, **40**, 1397, 1409 (1961).
16. Bassett, D. C., and A. Keller, to be published.
17. Geil, P. H., and D. H. Reneker, *J. Polymer Sci.*, **51**, 569 (1961).
18. Keller, A., and J. R. S. Waring, *J. Polymer Sci.*, **17**, 447 (1955).
19. Geil, P. H., *J. Polymer Sci.*, **51**, S10 (1961).
20. Salovey, R., *J. Polymer Sci.*, **51**, S1 (1961).
21. Geil, P. H., in *Growth and Perfection of Crystals*, Wiley, New York, 1958, p. 579.
22. Geil, P. H., *J. Polymer Sci.*, **47**, 65 (1960).
23. Leugering, H. J., *Kolloid-Z.*, **172**, 184 (1960).
24. Danusso, F., and F. Sabioni, *Rend. ist. Lombardo Sci.*, **A92**, 435 (1958).
25. Keller, A., *J. Polymer Sci.*, **36**, 361 (1959).
26. Hoffman, J. D., and J. I. Lauritzen, *J. Research Natl. Bur. Standards*, **65A**, 297 (1961).
27. Keller, A., *Polymer*, **3**, 393 (1962).

Synopsis

The three-dimensional morphology of solution-crystallized low pressure polyethylene has been examined for concentrations to 50% in xylene. Lamellar crystallization is characteristic of the whole range, and whenever diffraction examination has been possible, the lamellae have been shown to contain chain-folded molecules. For crystallization from relatively dilute solutions (<0.3%) and below 75°C., earlier observations that the layers of multilayer crystals splay apart have been extended and the development of sheaving morphologies via the splaying of layers demonstrated. Sheaving has been interpreted as resulting from repulsion between portions of molecules excluded from the lamellar crystals. At higher concentrations and temperatures, molecules which crystallize through several lamellae become increasingly important. These are pro-

posed as an explanation for a new, more compact, type of object which appears under the above conditions. They are designated axialites, as they consist of layers or layer packets splaying about a common axis (b). Viewed along this axis they appear sheaving, but as hexagons or fibrous ovals perpendicular to the axis. They thus resemble single crystals in some projections and incipient spherulites in others. Electron-microscopic fine-structure examination has shown that physical cohesion exists between the 100 A. terraces forming a layer packet on a 1000 A. scale. This is attributed to the interlamellar ties referred to above. This tying together of otherwise chain-folded lamellae is considered as a plausible link between crystallization from dilute solution and from the melt. Disintegration and deformation of axialites has been studied in a preliminary way. Deformation has been found to consist of the relative displacement of otherwise intact layer packets. Some points concerning interlamellar connections and the possible relation between axialites and spherulites are also discussed.

Résumé

La morphologie tridimensionnelle du polyéthylène basse-pression cristallisé en solotion a été examinée pour des concentrations de 50% dans le xylène. La cristallisation lamellaire est la caractéristique de tous les domaines et lorsqu'il a été possible de faire un examen de diffraction, les lamelles contenaient des molécules en forme de chaîne-plissées. Pour la cristallisation de solutions relativement diluées ($<\sim 0.3\%$) et au-dessous de $\sim 75°C$ on a étendu les observations antérieures concluant que les couches (feuilles) des cristaux à plusieurs couches élargissent les unes sur les autres et on a démontré la formation d'une morphologie en faisceaux via le élargissement des couches. On a interprèté la formation des faisceaux comme résultant de la répulsion entre des portions de molécules exclues des cristaux lamellaires. A des températures et des concentrations croissantes, les molécules qui cristallisent au moyen de plusieurs lamelles deviennent de plus en plus nombreuses. On propose ceci comme explication de l'apparition dans les conditions décrites ci-dessus, d'espèces nouvelles et plus compacts. On les appelle "axialites" car elles sont constituées de couches ou paquets de couches réunis en faisceau autour d'un axe commun (b). Vus le long de cet axe, ils apparaissent en faisceau, mais perpendiculairement à cet axe, ils apparaissent commes des hexagones ou des ellipsoides fibreux. Dans une projection, ils ressemblent donc à de simples cristaux, dans l'autre, à des sphérulites débutants. L'examen de la structure fine au microscope électronique montre que la cohésion physique existe entre les couches successives de 100 Å formant un paquet de couches à une échelle de 1000 Å. Ceci est attribué aux assemblages interlamellaires vus plus haut. Cet assemblage de chaînes habituellement plissées est considéré comme le lieu plausible entre la cristallisation au départ de solution diluée et au départ d'une masse fondue. On a étudié préliminairement la désintégration et la déformation des "axialites." On a trouvé que la déformation consiste en un déplacement relatif de paquet de lamelles indépendantes les unes des autres. On discute également certains points concernant les connections interlamellaires et la relation possible entre axialites et sphérulites.

Zusammenfassung

Die dreidimensionale Morphologie von aus Lösung kristallisiertem Niederdruckpolyäthylen wurde bis zu einem Xylolgehalt von 50% untersucht. Eine lamellare Kristallisation ist für den gesamten Bereich charakteristisch und Beugungsuntersuchungen zeigten, dass die Lamellen Moleküle mit gefalteten Ketten enthalten. Für eine Kristallisation aus relativ verdünnter Lösung ($\sim 03.\%$) und unterhalb $\sim 75°C$. wurde die früher gemachte Beobachtung, dass die Schichten der Mehrschichtkristalle auseinanderstreben, erweitert und die Entwicklung von gebündelten Formen durch das Aufweiten der Schichten demonstriert. Die Bündelung wurde als Ergebnis einer Abstossung der aus den Kristallamellen ausgeschlossenen Molekülteile aufgefasst. Bei höherer Konzentration und Temperatur gewinnen die Moleküle an Bedeutung, die durch

mehrere Lamellen hindurch kristallisieren. Dies wird als Erklärung für einen neuem kompakteren Objekttyp angesehen, der unter diesen Bedingungen auftritt. Diese Typen werden als "Axialite" bezeichnet, da sie aus Schichten oder Schichtpaketen bestehen, die um eine gemeinsame Achse angeordnet sind (*b*). Entlang dieser Achse betrachtet erscheinen sie gebündelt, senkrecht zu ihr aber als Sechsecke oder faserige Ovale. Sie gleichen daher in einigen Projektionen Einkristallen und in anderen beginnenden Sphärolithen. Die elektronenmikroskopische Feinstrukturuntersuchung zeigte, dass eine physikalische Kohäsion zwischen den ein Schichtpaket bildenden $\sim$ 100 Å Terassen in einem Bereich von $\sim$1000 Å besteht. Dies wird den oben beschriebenen interlamellaren Verknüpfungen zugeschrieben. Dieses Zusammenknüpfen von Lamellen mit gefalteten Ketten wird als plausible Verbindung zwischen der Kristallisation aus verdünnter Lösung und aus der Schmelze betrachtet. Desintegration und Deformation von Axialiten wurde in Vorversuchen untersucht. Es wurde gefunden, dass die Deformation in einer relativen Verschiebung von sonst intakten Schichtpaketen besteht. Weiters wurden einige auf die interlamellare Verknüpfung und auf die mögliche Beziehung zwischen Axialiten und Sphärolithen bezügliche Punkte diskutiert.

Received December 20, 1961

JOURNAL OF POLYMER SCIENCE: PART A VOL. 1, PP. 789–798 (1963)

Fundamental Studies on Cationic Polymerization. III. Extension of Mechanism Studies to Homogenous Systems

I. KIRSHENBAUM, J. P. KENNEDY, and R. M. THOMAS,
Chemical Research Division, Esso Research & Engineering Company, Linden, New Jersey

INTRODUCTION

In the preceding paper,[1] we proposed a reaction mechanism to explain the behavior of the isobutene–$AlCl_3$ system at $-35°C.$ to $-78°C.$ in solvents with high dielectric constants. The proposed theory led to kinetic equations which explained quantitatively experimental results obtained in polar solvents (i.e., methyl chloride, ethyl chloride, and vinyl chloride). The theory predicted the dependence of degree of polymerization (DP) on temperature and the dependence of DP on monomer concentration: at low temperature, DP decreases with increasing monomer concentration, at high temperatures, DP increases with increasing monomer concentration, and at the inversion temperature DP is independent of monomer concentration, i.e., at the temperature at which the dependence of DP on monomer concentration changes sign.

The theory also explained the observed incorporation of C^{14} into polymer, when C^{14}-methyl chloride was used as solvent. Theoretical equations permitted the calculation of relative rate constants and activation energies.

In the presence of polar solvent, polymer precipitation occurs. Although our data indicated that the polymer molecule precipitates after it has stopped growing, i.e., after it has undergone a chain transfer or chain termination reaction, it was thought of interest to extend our work to homogeneous systems involving nonpolar solvents, specifically *n*-pentane and carbon disulfide. This has been done, and the experimental results have enabled us to broaden our theory to include factors considered unimportant in polar solvent systems.

EXPERIMENTAL

Equipment and Materials

The purification of isobutene, methyl chloride, and aluminum chloride,[2] together with general equipment used, has been described.[3] Gas chromatographic analysis of *n*-pentane has been disclosed.[4] Carbon disulfide (J. T.

Baker Chemical Company, Baker Analyzed Reagent grade) was dried and distilled over molecular sieves, cooled down to −78°C. and cold-filtered. Gas chromatographic analysis did not show the presence of any impurities.

Procedure

The general polymerization technique has been described previously.[4] The catalyst used was aluminum chloride dissolved in methyl chloride; its concentration, determined by titration, was 1.88×10^{-2} mole/l. Throughout these studies, the total volume of monomer and solvent was 25 ml. at −78°C. Since aluminum chloride is practically insoluble in either *n*-pentane or carbon disulfide, the catalyst had to be introduced in 0.5 ml. of methyl chloride. Preliminary experiments showed that conversions around 15% were obtained when about 0.5 ml. of the catalyst solution was introduced dropwise from a syringe into the flasks containing vigorously agitated 25 ml. of monomer mixtures. Polymerization ensued instantaneously. This could be seen from distinct Schlieren effects noticeable especially in flasks with higher monomer concentrations at lower temperatures. One minute after the last drop of catalyst was introduced, the reaction was quenched with cold methanol. Unreacted gases and solvents were evaporated on a steam bath and the product dried to constant weight in vacuo at 50°C. Unfractionated samples were subjected to molecular weight determination.[2]

RESULTS

Polymerization in *n*-Pentane

Previous studies showed that substantially homogeneous isobutene polymerizations can be achieved in *n*-pentane solvent.[4] Table I compiles results obtained in this solvent at various temperatures at different monomer concentrations.

TABLE I
DP's of Polyisobutenes Obtained in *n*-Pentane at Various Temperatures and at Various Monomer Concentrations

Mole fraction of isobutene[a]	DP			
	−35°C.	−55°C.	−78°C.	−100°C.
0.815 (9.76)	1,015	1,250	2,590	3,720
0.563 (6.32)	948	1,372	3,950	7,100
0.341 (3.64)	894	2,050	5,950	12,300
0.299 (3.16)	910	2,260	6,000	15,000
0.205 (2.12)	926	2,160	6,650	14,240
0.126 (1.28)	910	2,020	6,300	6,400(?)

[a] Figures in parentheses are corresponding values in mole/l. at −78°C.

Polymerization in Carbon Disulfide

Carbon disulfide is also an excellent medium for homogeneous polymerization of isobutene. Table II shows the results of isobutene polymerizations carried out in carbon disulfide diluent.

TABLE II
DP's of Polyisobutene Obtained in Carbon Disulfide at Various Temperatures and at Various Monomer Concentrations

Mole fraction of isobutene[a]	DP		
	−35°C.	−55°C.	−78°C.
0.643 (9.75)	625	1,100	3,450
0.412 (6.32)	440	1,210	5,940
0.219 (3.64)	375	1,810	11,500
0.188 (3.16)	500	3,180	12,950
0.123 (2.12)	456	5,340	16,000
0.073 (1.28)	910	6,000	20,000

[a] Figures in parentheses are corresponding values in mole/l. at −78°C.

DISCUSSION

A plot of log DP against $1/T$ for the *n*-pentane and carbon disulfide solvent systems does not give a clear-cut indication of an inversion temperature. This is in marked contrast to the results in polar solvents. It will be recalled that in polar solvents, the kinetic chain is determined by the relative rates of propagation and termination, but DP is determined by competing chain-breaking processes; namely, chain transfer to monomer and a reaction of the growing polymer chain with the solvent. The theoretical DP equation was found to be

$$\mathrm{DP} = k_1/[(k_3 - k_4)N_m C + k_4 C] \tag{1}$$

where N_m is the mole fraction of monomer and C is the number of moles (solvent + monomer) per liter. Thus, in polar solvents, the inversion temperature occurs when the rate constant for the chain breaking process involving the solvent (k_4) becomes equal to the rate constant for monomer transfer (k_3). However, this equation is not valid for the *n*-pentane and carbon disulfide systems, and, moreover, the rate constants for the two chain breaking processes do not become equal within the temperature range of interest. Accordingly, the same type of inversion phenomenon does not occur. This is developed in greater detail in the following discussion of mechanism.

A stepwise propagation is visualized:

$$\mathrm{R}_n{}^{\oplus}\mathrm{A}^{\ominus} \underset{k_{-1}}{\overset{k_1}{\rightleftharpoons}} \mathrm{R}_n{}^{\oplus} \ldots \mathrm{A}^{\ominus} \tag{2}$$

$$\mathrm{R}^{\oplus}{}_n \ldots \mathrm{A}^{\ominus} + \mathrm{M} \overset{k_2}{\rightarrow} \mathrm{R}^{\oplus}{}_{n+1}\mathrm{A}^{\ominus} \tag{3}$$

where $R^{\oplus}$ is the polymer cation, $A^{\ominus}$ is the gegenion, M represents the monomer, and the k's are the rate constants for the elemental steps. The growing polymer, especially in solvents of high dielectric constant, involves a highly solvated ion pair. The polymer ion pair has to be "activated" before the monomer can react with the growing carbonium ion. This "activation" is represented above by eq. 2. As pointed out previously,[1] this "activation" cannot require much energy but may, nevertheless, be the slow step in the propagation reaction, i.e., $k_1 < k_2$.[5]

The rate of propagation may be written as:

$$d[P]/dt = k_2[R_n^{\oplus} \ldots A^{\ominus}][M] \tag{4}$$

Since

$$[R_n^{\oplus} \ldots A^{\ominus}] = k_1[R^{\oplus}A^{\ominus}]/(k_{-1} + k_2[M]) \tag{5}$$

then

$$d[P]/dt = k_1k_2[R_n^{\oplus}A^{\ominus}][M]/(k_{-1} + k_2[M]) \tag{6}$$

This treatment is similar to that proposed by Mayo and Walling.[6]

The dielectric constant for polar solvents such as methyl chloride, ethyl chloride, and vinyl chloride at −35°C. to −78°C. is in the order of 13–17.[7,8] (Vinyl chloride has a dielectric constant of about 15 at −78°C.) Under these conditions, the activation reaction (k_1) as pictured in eq. 2, is much more important than the reverse reaction (k_{-1}). Accordingly, in polar solvents, $k_{-1} \ll k_2$,and eq. (6) simplifies to a monomer-independent expression. However, this approximation cannot be made for nonpolar solvents. The dielectric constants for *n*-pentane and carbon disulfide are about 2–3 in the temperature range of interest,[9,10] and k_{-1} must be considered important in the isobutene–$AlCl_3$–*n*-pentane system.

The average length of a polymer chain may be expressed as the ratio of the rate of chain propagation to the sum of the rates of all chain breaking and chain terminating processes. An important chain-breaking process is the monomer transfer reaction (i.e., proton transfer to the monomer).

$$R_n^{\oplus}A^{\ominus} + M \xrightarrow{k_3} R_n + M^{\oplus}A^{\ominus} \tag{7}$$

The rate of this reaction is

$$d[\text{Monomer transfer}]/dt = k_3[R_n^{\oplus}A^{\ominus}][M] \tag{8}$$

The rate of the chain breaking reaction involving the solvent is given by

$$d[\text{Solvent reaction}]/dt = k_4[R_n^{\oplus}A^{\ominus}][S]$$

where [S] is the concentration of solvent. Neglecting unimolecular chain termination and termination by poison as being small compared to monomer transfer or propagation yields

$$DP = \frac{k_1k_2[R_n^{\oplus}A^{\ominus}][M]}{(k_{-1} + k_2[M])(k_3[R_n^{\oplus}A^{\ominus}][M] + k_4[R_n^{\oplus}A^{\ominus}][S])} \tag{9}$$

Converting to mole fractions and simplifying yields

$$DP = \frac{N_m}{[(k_{-1}/k_2) + N_m C][(k_3 - k_4/k_1)N_m + (k_4/k_1)]} \quad (10)$$

where N_m is monomer mole fraction and C is the total number of moles of solvent plus monomer per liter.

Thus, for a solvent such as *n*-pentane, we no longer have a simple DP equation, and the monomer dependence is complex. The theoretical eq. (10) describes the DP data for the *n*-pentane system quite well over the investigated temperature range of −35 to −100°C. with a monomer mole fraction range of 0.12–0.81. A comparison of calculated and observed DP's for *n*-pentane is shown in Table III.

TABLE III
Comparison of Calculated and Observed DP's in *n*-Pentane Solvent

Mole fraction of monomer	DP at −100°C.		DP at −78°C.		DP at −55°C.		DP at −35°C.	
	Obs.	Calc.[a]	Obs.	Calc.[a]	Obs.	Calc.[a]	Obs.	Calc.[a]
0.126	—	—	6,300	6,600	2,020	2,300	910	800
0.205	14,240	15,000	6,650	6,300	2,160	2,300	926	970
0.299	15,000	11,000	6,000	5,550	2,260	2,200	910	1,050
0.341	12,300	9,700	5,950	5,200	2,050	2,100	894	1,070
0.563	7,100	6,000	3,950	3,900	1,372	1,650	948	1,040
0.815	3,720	3,800	2,590	2,800	1,250	1,260	1,015	910

[a] Calculated from eq. (10).

Values for relative rate constants are shown in Table IV. Internal consistency is shown by the Arrhenius plots in Figures 1 and 2. Activation energies calculated from these plots are shown in Table V.

TABLE IV
Relative Rate Constants in *n*-Pentane Solvent

Relative rate constants	−100°C.	−78°C.	−55°C.	−35°C.
k_3/k_1	2.5×10^{-5}	2.9×10^{-5}	6×10^{-5}	5.9×10^{-5}
k_4/k_1	$<0.1 \times 10^{-5}$	0.24×10^{-5}	0.6×10^{-5}	1.1×10^{-5}
k_{-1}/k_2	0.5	2	3	8

TABLE V
Activation Energies in *n*-Pentane Solvent

Activation energy, kcal./mole
$E_3 - E_1 \sim 1.2$
$E_4 - E_1 \sim 1.8$
$E_4 - E_3 \sim 0.6$
$E_{-1} - E_2 \sim 1.7$

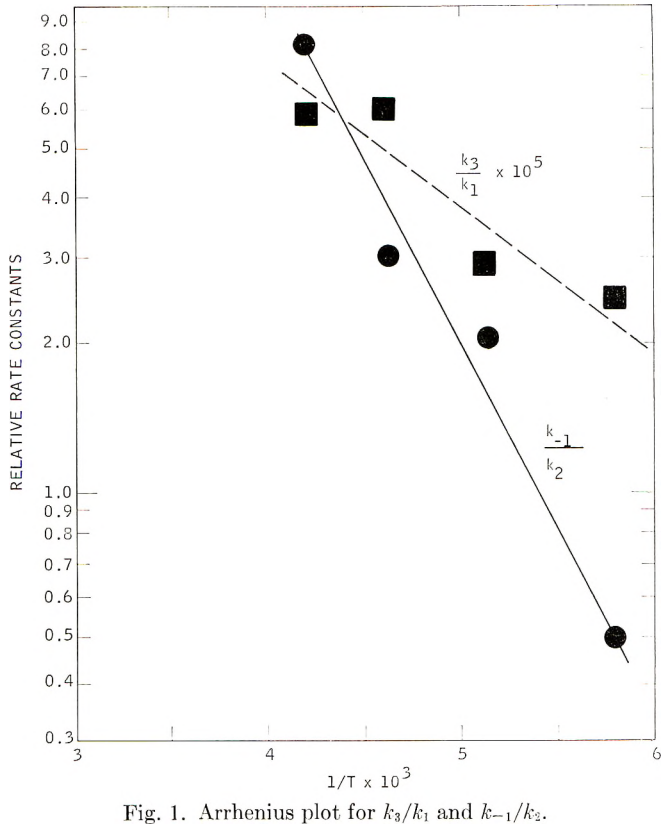

Fig. 1. Arrhenius plot for k_3/k_1 and k_{-1}/k_2.

As pointed out previously, the inversion temperature, observed in solvents with high dielectric constants, corresponds to the temperature at which k_3 becomes equal to k_4 in the theoretical DP eq. (1). In the *n*-pentane system, however, k_3 is significantly greater than k_4, even at -35°C., and, consequently,the same type of inversion temperature cannot be observed. As is evident from the data in Figure 3, there is some flattening of the DP versus N_mC curve at higher temperatures, primarily because of the high value for k_{-1}/k_2 (e.g., 8 at -35°C.).

Since carbon disulfide has a low dielectric constant, one might expect eq. (10) also to apply to the isobutene–$AlCl_3$–carbon disulfide system. Actually, however, the simple DP eq. (1) accounts for experimental data at -78°C. and 55°C. quite well, i.e. it seems as if "activation" of the polymer ion pair is rate-determining and $k_{-1} \ll k_2$ in carbon disulfide. A comparison of calculated and observed DP's for carbon disulfide is shown in Table VI. Values for the relative rate constants are listed in Table VII together with those for other solvent systems.

Unlike the behavior observed in polar solvent systems, solvent transfer in carbon disulfide does not become important as reaction temperature is raised. Temperature dependence of the relative rate constants is such that k_3/k_1 increases more rapidly with temperature than does k_4/k_1. The two do not become equal, and an inversion temperature is not observed.

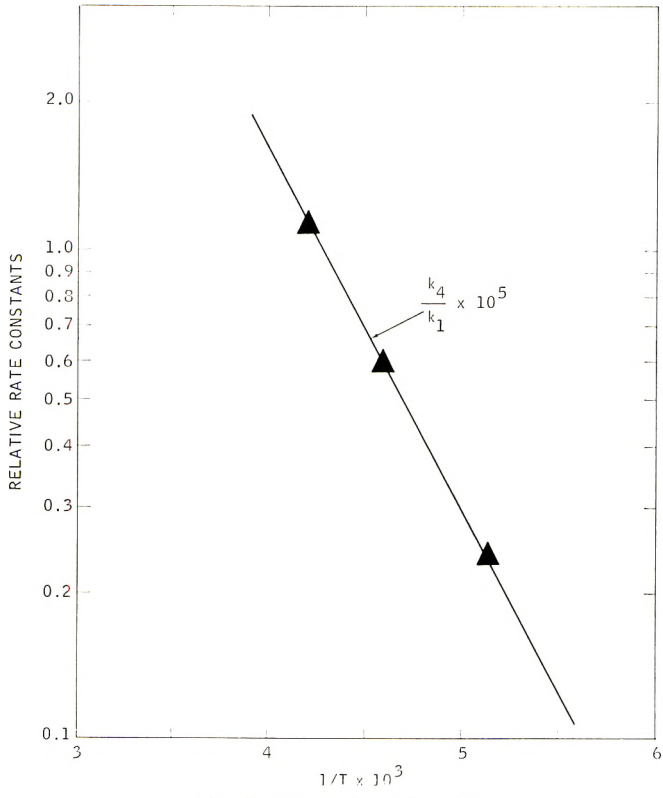

Fig. 2. Plot of k_4/k_1 vs. $1/T$.

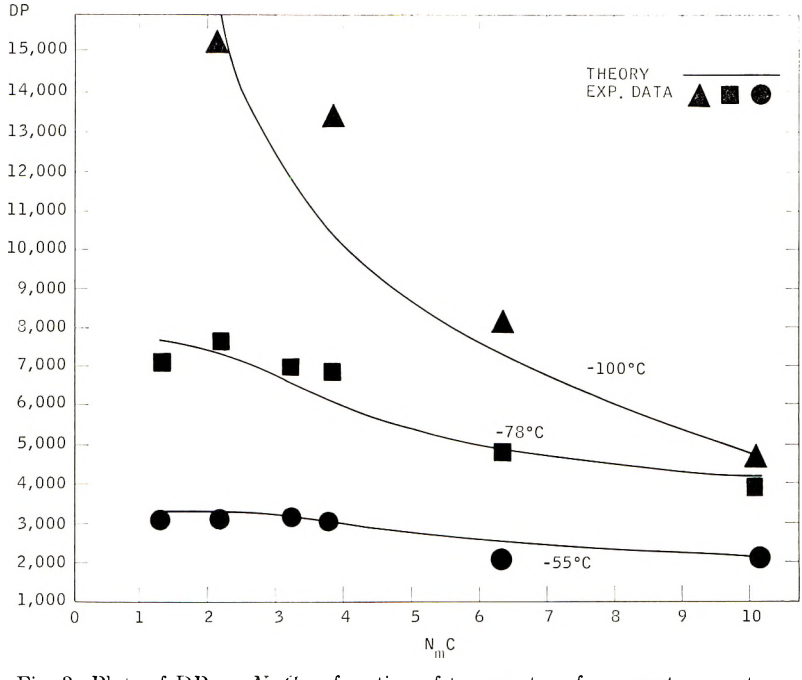

Fig. 3. Plots of DP vs. N_mC as function of temperature for n-pentane system.

Since −35°C. DP data for carbon disulfide scattered widely, it was not possible to use them to evaluate rate constants or activation energies.

In summary, the reaction mechanism proposed for the behavior of the isobutene–$AlCl_3$ system in polar solvents has been extended to the *n*-pentane and carbon disulfide systems. The kinetic equations for the *n*-pentane systems are more complex than those for the other systems because simplifying assumptions (which were possible for methyl chloride, vinyl chloride, etc.) do not appear valid in this case. However, in all systems studied, the molecular weight of the polymer is determined principally by two competing chain breaking processes; namely, chain transfer from polymer to monomer and chain transfer (or termination) involving the solvent. This reaction involving the solvent is important in polar solvents, especially at higher temperatures (e.g. −35°C.), but is much less important in either *n*-pentane or carbon disulfide systems.

TABLE VI
Comparison of Calculated and Observed DP's in CS_2 Solvent

Mole fraction of monomer	DP at −78°C.		DP at −55°C.	
	Obs.	Calc.[a]	Obs.	Calc.[a]
0.073	20,100	21,500	6,450	6,200
0.123	16,000	15,750	4,400	4,200
0.188	12,950	11,400	2,850	2,900
0.219	11,500	10,300	2,350	2,600
0.412	5,940	6,300	1,250	1,540
0.643	3,450	4,700	1,100	1,100

[a] Calculated from eq. (1).

TABLE VII
Comparison of Relative Rate Constants

Solvent	Relative rate constants × 10^5					
	−78°C.		−55°C.		−35°C.	
	k_3/k_1	k_4/k_1	k_3/k_1	k_4/k_1	k_3/k_1	k_4/k_1
Methyl chloride	2.3	0.09	3.6	1.2	—	—
Vinyl chloride	1.9	0.12	—	—	5.0	9.6
n-Pentane	2.9	0.24	6	0.6	5.9	1.1
Carbon disulfide	2.3	0.1	9.9	0.19	—	—

The reaction involving the solvent may be pictured as a chain transfer or a chain termination involving the diluent. The former concept can be pictured for a diluent such as methyl chloride, radioactive tracer experiments have shown C^{14} incorporation into the polymer when C^{14}-methyl chloride is used as solvent.[1] Chain transfer is, however, more difficult to

visualize for a material such as carbon disulfide. It may be that the small solvent effect (Table VII) noted in the various diluents is due to the small amount of methyl chloride introduced as catalyst carrier. On the other hand, the reaction with the solvent may in the various cases be merely a solvation associated with the kinetic or "spontaneous" termination reaction.

References

1. Kennedy, J. P., I. Kirshenbaum, R. M. Thomas, and D. C. Murray, *J. Polymer Sci.*, **A1**, 331 (1963).
2. Kennedy, J. P., and R. M. Thomas, *J. Polymer Sci.*, **46**, 481 (1960).
3. Kennedy, J. P., and R. M. Thomas, *Advances in Chem.*, in press.
4. Kennedy, J. P., and R. M. Thomas, *J. Polymer Sci.*, **46**, 233 (1960).
5. Kennedy, J. P., and R. M. Thomas, *J. Polymer Sci.*, **49**, 189 (1961).
6. Mayo, F. R., and C. Walling, *J. Am. Chem. Soc.*, **71**, 3845 (1949).
7. Landolt-Borstein, *Physicalisch Chemischen Tabellen*, 5th Ed., Vol. III, Springer-Verlag, Berlin, 1936, p. 1961.
8. Longworth, W. R., and P. H. Plesch, *J. Chem. Soc.*, **1959**, 1618.
9. Dornty, R. W., and C. P. Smyth, *J. Am. Chem. Soc.*, **52**, 3546 (1930).
10. *Table of Dielectric Constants of Pure Liquids*, B. S. Circular 514, August 10, 1961, p. 5.

Synopsis

Fundamental studies of the cationic polymerizations of isobutylene has been extended to the *n*-pentane and carbon disulfide systems. The kinetic equation for the *n*-pentane system is more complex than for other solvent systems because simplifying assumptions (which were possible for methyl chloride, ethyl chloride, and vinyl chloride) do not appear to be valid here. However, in all systems studied, the molecular weight of the polymer is determined principally by two competing chain breaking processes; namely, chain transfer from polymer to monomer and chain transfer or termination involving the solvent. The solvent reaction is important in polar solvents, especially at higher temperatures (e.g. −35°C.) but is much less important in either *n*-pentane or carbon disulfide systems.

Résumé

On a étendu les études fondamentales de la polymérisation cationique de l'isobutylène aux systèmes *n*-pentane et disulfure de carbone. Les équations cinétiques pour le système *n*-pentane sont plus complexes que pour les autres systèmes de solvants, car les simplifications (qui étaient possibles pour le chlorure de méthyle, d'éthyle et de vinyle) ne sont pas valides ici. Cependant, dans tous les systèmes étudiés, le poids moléculaire du polymère est essentiellement déterminé par deux processus de rupture de chaîne; à savoir, transfert de chaîne polymère/monomère et transfert de chaîne polymère/solvant. La réaction de transfert de chaîne sur solvant est importante dans les solvants polaires, spécialement à température élevée (p. ex. −35°C) mais est moins importante soit dans le système pentane, soit dans le système disulfure de carbone.

Zusammenfassung

Die grundlegende Untersuchung der kationischen Polymerisation von Isobutylen wurde auf das *n*-Pentan- und das Schwefelkohlenstoffsystem ausgedehnt. Die kinetischen Gleichungen sind für das *n*-Pentansystem komplexer als für andere Lösungsmittelsysteme, da vereinfachende Annahmen, wie sie für Methylchlorid, Äthylchlorid und Vinylchlorid möglich waren, hier nicht mehr gültig zu sein scheinen. In allen

untersuchten Systemen ist aber das Molekulargewicht des Polymeren hauptsächlich durch zwei kompetitive Kettenübertragungsprozesse bestimmt: nämlich Ketten übertragung zum Monomeren und Kettenübertragung zum Lösungsmittel. Die Lösungsmittelübertragungsreaktion gewinnt in polaren Lösungsmitteln, besonders bei höherer Temperatur (z.B. −35°C) Bedeutung, ist aber im *n*-Pentan- oder Schwefelkohlenstoffsystem viel weniger wichtig.

Received November 28, 1961
Revised December 28, 1961

JOURNAL OF POLYMER SCIENCE: PART A VOL. 1, PP. 799–815 (1963)

Kinetic Study of the Crosslinking of Gelatin by Formaldehyde and Glyoxal*

P. DAVIS and B. E. TABOR, *Research Laboratories, Kodak Ltd., Wealdstone, Harrow, Middlesex, England*

INTRODUCTION

The reaction of formaldehyde with proteins[1–4] normally involves formation of crosslinks between molecules to give an increase in molecular weight and finally an insoluble product.

There is considerable doubt as to the position of the crosslinks on the protein molecule: crosslinks either between two amino groups or between an amino group and some other group have been postulated. For collagen (or gelatin) molecules, guanidine, hydroxyl, amide and peptide amino groups have been suggested as second sites.[4a] Most of the reported work is on the stoichiometry of the reaction and on attempts to isolate products both for protein[5] and for model systems.[2]

The dialdehyde, glyoxal, is another recognized crosslinking agent for gelatin and collagen.[6]

A study of the crosslinking of gelatin by the simplest monofunctional and difunctional aldehydes, formaldehyde and glyoxal, is reported in this paper, a kinetic method being used to follow the reaction.

The kinetics of the crosslinking reaction, for proteins, has received no detailed study. For a kinetic study of the crosslinking of gelatin a method of measuring the rate of formation of crosslinks is required. Crosslinking results in an increase in molecular weight. The viscosity of a gelatin solution is a function of molecular weight, and therefore the rate of change of viscosity with time was used as the measure of the rate of the crosslinking reaction. In some cases the results from this method are not strictly comparable. Reasons for this are advanced in the text.

From this study of the dependence of rate of viscosity increase on reactant concentrations, a kinetic relationship is derived. While it is not possible, from a kinetic study alone, to determine a unique reaction mechanism, those which are kinetically in agreement with the results of this study have been assessed. In addition to the kinetic evidence, results obtained with different types of gelatin and modified gelatins have been used to decide the most probable mechanisms to reaction.

* Communication No. 2209H from the Kodak Research Laboratories.

EXPERIMENTAL

Gelatins

For most of the work with formaldehyde, an acid-processed pigskin gelatin (high viscosity) and three deionized[7] alkali-processed gelatins (high, medium, and low viscosities) were used. For the work with glyoxal, the high and low viscosity alkali- processed gelatins were used. For part of the work, a wider range of both acid- and alkali-processed gelatins and three calfskin gelatins of low arginine and high ornithine content[8] were used. Various modified gelatins prepared from alkali-processed gelatins have also been studied. The modifications were methylation (methanol–hydrochloric acid[9]) of the carboxy groups and deamination (nitrous acid[9]); guanidination (O-methylisourea[10]), and acetylation (sodium acetate; acetic anhydride[11]) of amino groups.

Allowance was made for the moisture content of all gelatins used.

Reagents

The formaldehyde solutions were prepared by dilution of AnalaR 36% (w/v) formaldehyde. The glyoxal solutions were prepared from a B.D.H. sample of glyoxal monohydrate. All other reagents were of AnalaR quality.

Experimental Method

The gelatin was soaked overnight at 5°C., then dispersed at 50°C. in the presence of phosphate buffer. The solution was cooled to 40°C., and the final pH adjustment was made. A buffered solution of the crosslinking agent, at 40°C., was then added, with thorough mixing. Samples were then transferred to viscometers of either the normal or miniature U-tube types (described in Brit. Standard 188-1957) in a thermostat at 40°C. Viscosity measurements were made at suitable time intervals from the addition of the crosslinking agent, until the viscosities of the solutions had approximately doubled their initial value. Plots of viscosity, on both log and linear scales, were drawn against time of reaction. Allowance was made, where necessary, for the change of viscosity during the viscosity measurement (Appendix I).

The variables (concentration of crosslinking agent, pH, gelatin concentration) were studied over as wide a range as practicable, one factor being varied while the others were kept constant. The gelatin concentration was only varied over the range 7–14%. Higher concentrations were difficult to handle. At low concentrations, below 2%, in the presence of formaldehyde the viscosity either remained constant or fell with time, owing to the preponderance of intramolecular bonding. This has previously been demonstrated for chrome alum hardening.[12] For the present work it seemed unwise to approach this concentration region, so 7% was taken as the lower limit.

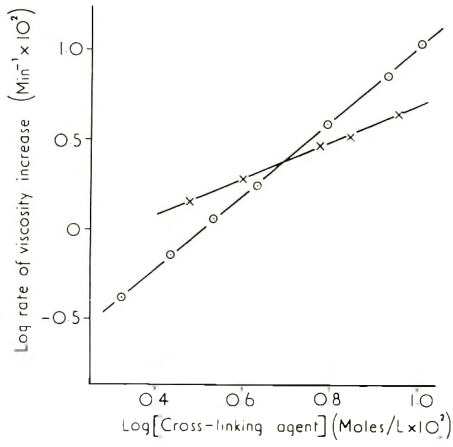

Fig. 1. Dependence of rate of viscosity increase on crosslinking-agent concentration for alkali-processed gelatins, 10%, pH 6.5, temperature 40°C.: (⊙) formaldehyde; (×) glyoxal.

Determination of the Rate of Viscosity Increase

The plots of log viscosity against time differed for formaldehyde and glyoxal. With formaldehyde, it was convenient to take the rate of viscosity increase as the reciprocal of the time (in minutes) required to give a doubling of the initial viscosity. With glyoxal, the shape of the curves indicated a significant degree of reactions which did not produce an increase in viscosity (e.g., intramolecular linkages). To minimize the effect of these, the initial slope of the plot of viscosity against time was taken as the measure of the rate of viscosity increase.

Kinetics calculated for formaldehyde on the basis of the initial slope criterion gave the same results as those based on the doubling of the viscosity. Where it can be applied, measurement of the time to double the viscosity is more convenient and precise than measurement of the initial slope of a viscosity/time curve.

RESULTS

The dependencies of rate of viscosity increase on the concentrations of crosslinking agent, hydrogen ion, and gelatin have been studied. Plots of log rate of viscosity increase against log concentration were drawn (Fig. 1) and the slopes of these plots used to determine the exponent x in the general relationship:

$$(\text{Rate of viscosity increase}) \propto (\text{Concentration})^x$$

Provided that the viscosity increase criteria chosen correspond to the same amount of crosslinking reaction in each case, the experimentally determined exponent x will be the same as the "true" kinetic exponent for the rate of the crosslinking reaction.

A. Crosslinking Agent Concentration: Rate $\propto$ [crosslinking Agent]^n

The slopes n of the plots of log rate against log [crosslinking agent] are shown in Table I. For formaldehyde, these are dependent on the range of formaldehyde concentration used. Provided that the concentration is below 0.1M, good straight lines (Fig. 1) with a slope $n = 2$ were obtained in all cases. At higher formaldehyde concentrations, the slope decreases, giving values of n below 2.0. The value of n at these high formaldehyde concentrations is independent of gelatin type, but depends on pH, as shown in Table II. The results at high formaldehyde concentration and higher pH's refer to experiments in which the time required to produce a gel at 40°C. was used as the criterion of hardening. Under these conditions rates of viscosity increase were too rapid for measurement to be practicable by the viscometric method.

TABLE I. Dependence of Rate of Viscosity Increase on Crosslinking Agent Concentration (Values of n)
(Gelatin, 10%; Temp., 40°C.; Concn. of Crosslinking Agent 0.01–0.10M)

Crosslinking agent	pH	n for alkali-processed gelatins			n for acid-processed pigskin gel
		Low viscosity	Medium viscosity	High viscosity	
Formaldehyde	5.5		1.95	2.0	2.0
Formaldehyde	6.5	1.95	2.0	2.0	2.05
Glyoxal	6.5	1.04		1.09	

TABLE II. Dependence of Rate of Viscosity Increase on Formaldehyde Concentration at High Concentration (Average Values of n for Stated Concentration Range)
(Formaldehyde, 0.02–3.0M; Gelatin, 10%; Temperature, 40°C.)

		n for various formaldehyde concn. ranges[a]			
	pH	0.02–0.1M	0.1–0.3M	0.3–1.0M	1.0–3.0M
Alkali-processed gelatin	6–7	2.0	1.65	1.2	(0.8)
	3–4		1.9	1.65	1.35
Acid-processed gelatin	6–7	2.0	1.6	1.2	(0.7)
	3–4		1.9	1.6	1.3

[a] Figures in parentheses refer to rate of setting experiments. Other figures refer to "viscosity rise" experiments.

The rate exponent n was independent of the glyoxal concentration over the range investigated (Table I).

B. Hydrogen-Ion Concentration: Rate $\propto 1/[H^+]^p$

The slopes p of the plots of log rate against pH are shown in Table III. For formaldehyde, the study was extended to include nine alkali-processed and nine acid-processed gelatins. The glyoxal results refer to alkali-processed gelatins only.

With glyoxal, it was decided to extend the investigation of the pH dependency to cover as high a range as possible (Table IV). This was done by choosing a suitable glyoxal concentration which would give a tractable experiment at the pH required. These experiments were then related to a standard hardener concentration by use of the previously determined glyoxal rate dependency.

TABLE III
Dependence of Rate of Viscosity Increase in pH (Values of p)
(Gelatin, 10%; Temperature, 40°C.; Crosslinking agent concentration, 0.025–0.07M; pH 5.5–7.5)

Crosslinking agent	Values of p	
	Alkali-processed gelatins	Acid-processed gelatins
Formaldehyde[a]	1.09 (±0.015)	0.91 (±0.015)
Glyoxal	0.97	

[a] Mean value of p for nine gelatins.

TABLE IV
Dependence of Rate of Viscosity Increase on pH for Glyoxal (Extended Range)

	Alkali-processed gelatins	
	Low viscosity	High viscosity
pH range	7.5–9.4	6.4–7.9
p	1.28	1.07

C. Gelatin Concentration: Rate $\propto$ [Gelatin]^m

The results for formaldehyde and glyoxal are given in Table V.

TABLE V
Dependence of Rate of Viscosity Increase on Gelatin Concentration (Values of m)
(Temperature, 40°C.)

Cross-linking agent	Reaction conditions			Values of m			
				Alkali-processed gelatin			Acid-processed gelatin (high viscosity)
	pH	Concn. cross-linking agent, M	Gelatin concn. range, %	Low viscosity	Medium viscosity	High viscosity	
Formaldehyde	6.5	0.02	7–14		2.4	2.6	2.6
		0.05		2.3	2.5		
	4.0	0.5	7–14		2.4	2.6	2.7
Glyoxal	6.5	0.07					
		0.025	8–12	2.6		2.5	

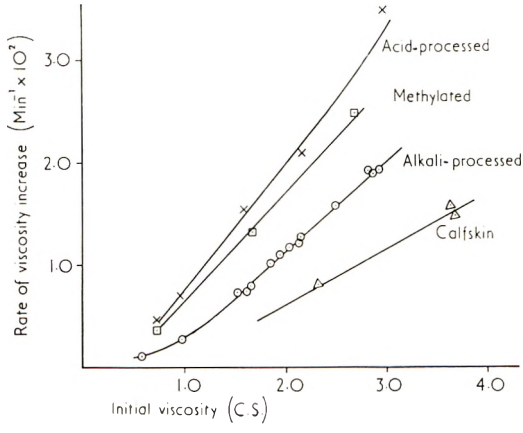

Fig. 2. Effect of initial viscosity and gelatin type on rate of viscosity increase.

D. Effect of Gelatin Type and Viscosity

A good correlation was found between rate of viscosity increase (reciprocal of time to double initial viscosity) and initial viscosity, provided the gelatins were divided into three classes (Fig. 2). For the same initial viscosity, acid-processed gelatins give greater rates of viscosity increase and calfskin gelatins give lower rates of viscosity increase than do normal alkali-processed gelatins.

E. Modified Gelatins

1. Methylated Alkali-Processed Gelatins. These behave more like acid-processed gelatins in that, for the same initial viscosity, they show greater rates of viscosity increase than do alkali-processed gelatins (Fig. 2).

2. Amino-Modified Gelatins. Complete removal (deamination) or complete blockage (guanidination and acetylation) of the amino groups gives a product which is not crosslinked by formaldehyde (Table VI). Similarly, blockage by guanidination prevents crosslinking by glyoxal (Table VI).

With formaldehyde, partial removal of blockage of amino groups gives a decrease in the rate of viscosity increase. For acetylated gelatins, the rate of viscosity increase is proportional to the amino-group content. Deaminated and guanidinated gelatins show a different effect in that, at low extents of modification, the rate of viscosity increase is higher than would be expected from the amino-group content. Thus, a guanidinated gelatin in which 37% of the amino groups had been blocked showed only a 10% reduction in rate of viscosity increase. This gelatin had the same 10% viscosity as the original gelatin.

Mixtures of alkali-processed gelatins with completely deaminated or guanidinated derivatives having the same 10% viscosity have also been

TABLE VI
Rates of Viscosity Increase for Amino-Modified Gelatins
(Gelatin, 10%, pH 6.5; Temperature, 40°C.)

Crosslinking agent	Gelatin	Amino content, mmole/g. gel	10% viscosity, cstokes	Rate of viscosity increase, min.$^{-1}$ × 10^2
Formaldehyde (0.025*M*)	Parent gelatin	0.40	29	1.9
	Deaminated	0.03	25	0.02[a]
	Guanidinated	0.05	20	0.04[a]
	Acetylated	0.04	24	0.04[a]
Glyoxal (0.035*M*)	Parent gelatin	0.40	30	1.38
	Guanidinated	0.03	26	0.06[a]

[a] These values refer to small initial rise in viscosity; the viscosity never reached twice its initial value.

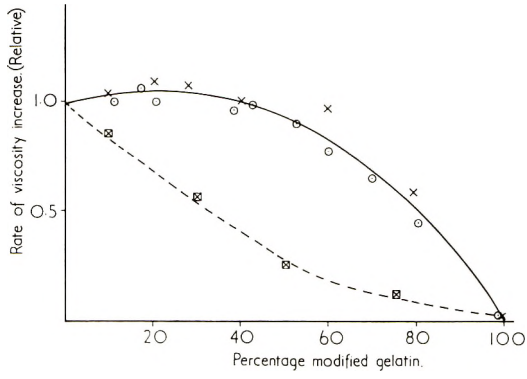

Fig. 3. Rates of viscosity increase for mixtures of modified and normal gelatins, 10% gelatin, pH 6.5, temperature 40°C.: (×) deaminated gelatin, formaldehyde 0.025*M*; (⊙) guanidinated gelatin, formaldehyde 0.025*M*; (⊠) guanidinated gelatin, glyoxal 0.035*M*.

examined. These modified gelatins are not crosslinked by formaldehyde or glyoxal (Table IV), and a reduction in rate of viscosity increase with increase in proportion of modified gelatin might be expected. This occurred with glyoxal but only with formaldehyde when the modified gelatin was present as over 40% of the mixture (Fig. 3).

DISCUSSION

1. General

The method of following the rates of crosslinking made use of the change in viscosity with time of a relatively concentrated solution. Dilute solution viscosity would have been more directly related to molecular weight. However, attempts to use a dilution technique on samples taken from the reacting mixture gave very irreproducible results. This is probably due to the effect of dilution on the reaction equilibria involved.

With the concentrated solutions, provided that the criteria chosen correspond to the same degree of reaction in each case and that the ratio of intramolecular to intermolecular bonds is constant, the experimentally determined exponents for the dependence of the rate of viscosity increase on concentration of the reactions can be taken as the kinetic exponents for the crosslinking reaction.

Concentration of Crosslinking Agent. These basic assumptions are reasonable when the crosslinking agent concentration is varied. The results for concentrations of both crosslinking agents up to 0.1*M* are, within the limits of experimental error, integral values which can be considered in terms of simple kinetics (2 and 1 for formaldehyde and glyoxal, respectively). With formaldehyde at higher concentrations, the value fell below 2.0 with increase in concentration, the values being independent of gelatin type but dependent on pH. The value of 2.0 for the rate exponent, determined over the lower formaldehyde range, is taken as applying to the kinetics of the actual crosslinking reaction. The significance of the fall, with increasing formaldehyde concentration, is discussed later in connection with the mechanism of the crosslinking reaction.

Hydrogen-Ion Concentration. With variation of pH, the idea that a given proportional increase in viscosity represents the same degree of reaction is still quite reasonable, particularly at the gelatin concentrations used. For both formaldehyde and glyoxal over the pH range of 5.5–7.5, a rate inversely proportional to the hydrogen-ion concentration is taken as the kinetic exponent.

With formaldehyde, acid-processed gelatins show a lower pH-dependence than alkali-processed gelatins. This difference, although small, was substantiated by experiments with nine gelatins of each type. The effect of charge on the variation of viscosity with pH is a possible explanation.

Gelatin Concentration. For the formation of a simple crosslink between two molecules, a kinetic exponent of 2.0 would be expected. Experimental values between 2.3 and 2.7 were, however, obtained. The experimental values do not represent true kinetic exponents as the criteria chosen for judging a given degree of reaction are not valid in this case. The reasons for this are as follows:

(*1*) For a given number of crosslinks per molecule, the number of crosslinks required will be proportional to the amount of gelatin present. From this it may be argued that the expected experimental dependency should be unity.

(*2*) The viscosity of a gelatin is not simply proportional to its concentration; thus, a given proportional increase in viscosity does not indicate the same number of crosslinks per molecule at different concentrations.

(*3*) Increase in viscosity only indicates intermolecular bond formation. A true reaction rate will also include that of intramolecular bond formation. The data of Pouradier and Chateau[12] show this factor to be very important, and to be dependent on gelatin concentrations.

This study is based on the assumption that a crosslink is formed between

two gelatin molecules and a bimolecular reaction is implicit. The experimental values obtained result from a combination of the effects mentioned. They are, however, not incompatible with a true bimolecular reaction and a value of 2 has been taken as the kinetic exponent.

The Kinetic Relationship. The kinetic dependence of rate of crosslinking on the reactant concentrations is therefore:

$$\text{Rate of crosslinking} \propto \frac{[\text{Gelatin}]^2\ [\text{Crosslinking agent}]^n}{[\text{H}^+]}$$

where $n = 2$ for formaldehyde and 1 for glyoxal. This applies over normal concentration ranges but not to the results with formaldehyde at high concentration or to the results with glyoxal at high pH.

2. Mechanism of the Formaldehyde–Gelatin Reaction

The importance of the side-chain amino groups on gelatin, in aldehyde crosslinking, is generally accepted.[4] Their removal by nitrous acid or blockage by guanidination and acetylation gave products which are not crosslinked by formaldehyde (Table VI). Charged amino groups on gelatin react with aldehydes to give methylol compounds, a hydrogen ion being liberated in the reaction (Appendix II).

Stage 1. It is assumed that the crosslinking reaction involves an initial equilibrium formation of a methylol derivative of the side-chain amino groups.

$$\text{Gel NH}_3^+ + \text{CH}_2\text{O} \overset{(K_1K_2)}{\rightleftharpoons} \text{Gel—NH—CH}_2\text{OH} + \text{H}^+$$

This reaction has been studied, and values of K_1 and K_2 have been determined (Appendix II).

The crosslinking reaction will then be:

$$\text{Gel—NH—CH}_2\text{OH} + \text{Unknown} \rightarrow \text{Crosslinked product.}$$

Comparison with the kinetics shows that the crosslinking reaction involves a second molecule of both gelatin and formaldehyde (i.e., unknown = gelatin + CH_2O) and this suggests a further stage.

Stage 2. The second molecule cannot react through an uncharged amino group without involving a further hydrogen-ion dependence. It is, however, probable that the second stage involves the formation of another methylol compound; the aldehyde reacting with an active hydrogen atom (Gel—H). No assumption is at present made as to the nature of this methylol compound.

$$\text{Gel—H} + \text{CH}_2\text{O} \overset{K_3}{\rightleftharpoons} \text{Gel—CH}_2\text{OH}$$

The existence of a second methylol stage in the reaction is supported by the results obtained at high formaldehyde concentration, where the exponent falls below 2.0 with increase in concentration.

If the initial concentrations of gelatin and formaldehyde are G and F, respectively, and x is the methylol concentration at equilibrium then,

$$(G - x)(F - x) = K_3x. \tag{1}$$

Taking logarithms and differentiating with respect to x, we then have

$$dF/dx = (GF - x^2)/[x(G - x)] \tag{2}$$

and thus

$$d \log x/d \log F = Fdx/xdF = (G - x)/[G - (x^2/F)] \tag{3}$$

If we consider a single methylol stage, the rate exponent n^* is the slope of the plot of log rate of reaction against log F, i.e.,

$$n^* = d \log \text{Rate}/d \log F.$$

If the rate of reaction is assumed to be proportional to the methylol concentration, then from eq. (3), we obtain

$$n^* = d \log x/d \log F = (G - x)/[G - (x^2/F)]$$

At low formaldehyde concentrations, x will be very small compared with G and $n^* \simeq 1.0$. At high formaldehyde concentrations when conversion to the methylol compound is nearly complete, $x \rightarrow G$ and $n^* \rightarrow 0$. Thus, n^* would be expected to vary from 1.0 at low formaldehyde concentrations to 0 at very high formaldehyde concentrations.

This effect will be shown by any methylol equilibrium including the proposed first stage (amino-methylol). If this were the only equilibrium (i.e., no second-stage equilibrium), then n should decrease from 2.0 to 1.0 with increase in formaldehyde concentration, always providing that the second stage does not have an overall controlling effect on the rate-dependency. If, however, a second-stage methylol equilibrium is also present, n should decrease from 2.0 to 0 with increase in formaldehyde concentration.

The experimental values of n (Table II) vary between 2.0 and 0.7, indicating the presence of two equilibria.

The experimental values of n are the sum of values for these two equilibria ($n = n_1 + n_2$). These values can be corrected for formation of the amino-methylol compound (n_1) with values of the equilibrium constants (K_1, K_2) derived from the results quoted in Appendix II. By this method values of n_2 have been calculated. The results are shown in Figure 4, where values of n_2 are plotted against formaldehyde concentration (on a log scale). These values of n_2 refer to the second-stage equilibrium only. The theoretical curve corresponding to $K_3 = 1.0$, also shown, agrees well with the experimental points. Experimental values ($n_1 + n_2$) showed a dependence on pH (Table II), due to variation of n_1 with pH; the calculated

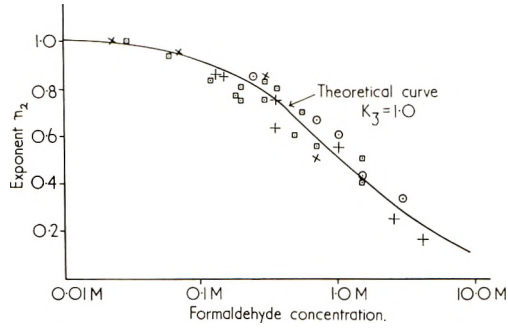

Fig. 4. Values of the exponent n_2 at various formaldehyde concentrations, where rate of crosslinking $\propto$ [Gel—NHCH$_2$OH][Gel][CH$_2$O]^{n_2}: (⊡) alkali-processed gelatin, pH 6-7; (⊙) alkali-processed gelatin, pH 3–4; (×) acid-processed gelatin, pH 6–7; (+) acid-processed gelatin, pH 3–4.

values of n_2 are independent of pH and the gelatin used.

The gelatins used differ in amide content. The acid-processed gelatin has an amide content of 0.415 mmoles/g. gelatin, while that of the alkali-processed gelatin is very low. These gelatins showed no difference in results, which indicates that the amide groups are not involved in the crosslinking. The independence of n_2 of pH is further evidence that the second stage does not involve the release of a hydrogen ion.

There is evidence that the second stage does not involve amino groups. If only amino groups were involved in crosslinking, the addition of completely deaminated or guanidinated gelatins to normal gelatins would be expected to produce a large reduction in rate of viscosity increase. This is not supported by the experiments where such mixtures had to contain over 40% amino-modified gelatin before a reduction was observed (Fig. 3).

Proposed Mechanisms for the Crosslinking Reaction. The kinetics of the cross-linking reaction are satisfied by a mechanism involving: (*1*) formation of two gelatin methylol compounds which then react to give a crosslink:

$$\text{Gel—NH—CH}_2\text{OH} + \text{Gel—CH}_2\text{OH} \rightarrow \text{Crosslinked product}$$

(*2*) formation of a dimethylol amino compound which then reacts with a gelatin molecule:

$$\text{Gel—N}\begin{matrix}\diagup\ \text{CH}_2\text{OH} \\ \diagdown\ \text{CH}_2\text{OH}\end{matrix} + \text{Gel—H} \rightarrow \text{Crosslinked product}$$

The exact nature of the second site of the crosslink (Gel—H) in mechanisms (*1*) and (*2*) is not known. Uncharged amino groups and amide groups have been excluded and the imino groups of the peptide backbone is unlikely from calculations of bond-bridging distances.[13] The hydroxyl groups are a possible site and are known to form methylol compounds with formalde-

hyde. A third possible mechanism would be (*3*) reaction of an amino-methylol group with a charged amino-methylol group:

$$\text{Gel—NH—CH}_2\text{OH} + \text{Gel—NH}_2^+\text{—CH}_2\text{OH} \rightarrow \text{Crosslinked product.}$$

This would agree with the kinetics if either the reaction was irreversible (i.e., the system was not in equilibrium), or the charge was retained by the crosslinkage. This reaction, involving two amino groups, is not supported by the evidence from mixtures of amino-modified and normal gelatins.

Nature of the Crosslink. Methylene bridges ($—CH_2—$) are usually proposed for the crosslinking of proteins by formaldehyde. It has been pointed out[13] that this may be sterically difficult with such a short crosslink (2.4–2.5 A.). Methylene ether crosslinks ($—CH_2—O—CH_2—$) have also been proposed[14] and are about twice the length of the methylene link. The kinetics of the reaction support the initial formation of a methylene-ether type of crosslink. It is possible that these linkages could later reorganize (e.g., in a dried gelatin layer) to form more stable methylene crosslinks.

3. Effect of Gelatin Type and Viscosity

The higher the initial viscosity of a gelatin, the larger will be the molecular weight and the lower the number of crosslinks/g. gelatin required to give a doubling of viscosity. The observed dependence of the rate of viscosity increase on initial viscosity, was, therefore, to be expected.

The difference between acid- and alkali-processed gelatins may be explained by a difference in either the viscosity–molecular weight relationship or the pK of amino groups. Any difference in the gelatin, particularly one involving a variation of charged groups, is likely to change both these parameters. Methylation is an example of such a change, and has been found to give an increase in rate of viscosity increase (Fig. 2). It is difficult, however, to see how these effects can explain the following observations: (*a*) calfskin gelatins with high amino-group contents (0.63 mmole/g. gelatin) gave lower rates of viscosity increase than gelatins with normal amino-group content (0.39 mmole/g. gelatin); (*b*) partially deaminated and guanidinated gelatins gave rates of viscosity increase higher than expected from amino-group content; (*c*) mixtures of completely deaminated or guanidinated gelatins with normal gelatins showed no reduction in rate of viscosity increase until the modified gelatin was present as over 40% of the mixture.

For these effects it is suggested that the efficiency of crosslinking (ratio of intermolecular to intramolecular crosslinks) is the determining factor. Intramolecular crosslinks should be favored by a large number of amino groups as reaction sites (calfskin gelatin), and intermolecular crosslinks by a small number (partially deaminated or guanidinated gelatins). Completely deaminated or guanidinated gelatins cannot form intramolecular crosslinks, as they only contain one of the two types of reaction sites neces-

sary. Intermolecular links should therefore be favored in reactions involving mixtures of these gelatins with normal gelatins.

All these experiments support the hypothesis that the crosslink is between an amino group and some other group. Experiments with hydroxyl-modified gelatins would have been of interest, but difficulties in obtaining an undegraded hydroxyl-modified gelatin have prevented this.

4. Mechanism of the Glyoxal Gelatin Reaction

As with formaldehyde, the most probable first reaction is to give a methylol derivative, thus

$$\text{Gel—NH}_3^+ + \text{OHC—CHO} \rightarrow \text{Gel—NHCH(OH)CHO} + \text{H}^+$$

On the assumption that this takes part in the crosslinking reaction, comparison with the experimental kinetics shows that a second gelatin molecule is involved in the formation of the linkage. The hydrogen-ion dependency excludes the obvious course, the reaction of the second aldehyde group with another amino group to form a second methylol derivative in the same way as the first.

This leaves a number of alternative sites for reaction. The gelatins used were alkali-processed, of low amide content. Hence, as with formaldehyde, it is unlikely that this is the second reacting site. The amino groups of the peptide backbone may be excluded by evidence for the inability of simple substances containing this group to react with the aldehyde group. Other possibilities are the hydroxyl group or reaction with charged amino groups giving rise to charged crosslinks:

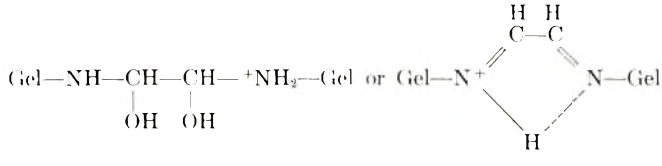

The symmetry of this latter possibility might help to stabilize such a linkage. The charge is, however, less likely to persist at higher pH values and this should lead to a higher order of hydrogen-ion dependence. There is some evidence indicating that this occurs (Table III).

The idea of a linkage between a charged and an uncharged amino group is also supported by the experiments with mixtures of a completely guanidinated gelatin and a normal gelatin (Fig. 3). With glyoxal, in contradistinction to formaldehyde, the addition of the amino-modified gelatin produces a large reduction in rate of viscosity increase in a manner which would be expected for the addition of an inert diluent.

5. Application of Results to Dried Layers

This kinetic study and discussion refer only to the rate of the crosslinking reaction in solution. It seems probable that the same mechanisms will apply to dried gelatin layers although the relative importance of

factors, such as efficiency of crosslinking, may differ. All the results refer to rates of cross-linking and not to the final degree of crosslinking (e.g., melting point of an aged dried layer). Factors having a large effect on rate (e.g., pH) may have little effect on this final degree of crosslinking.

APPENDIX I

The Measurement of a Rapidly Changing Viscosity

When the flow time of the reacting mixture is short, or when relatively little reaction and viscosity change occurs during this period, the viscosity measured can be taken to represent the degree of reaction at the beginning of the measurement. However, if the flow times are long or the reaction is rapid, this is no longer true. Allowance must be made for the change in viscosity during measurement to avoid a spurious effect on the viscosity/reaction-time plots.

Experimentally the plots of log viscosity against reaction time were either straight lines or gently curved. Even these latter were practically straight over the longest flow times. Thus, the viscosity at a given time t during the measurement may be expressed as

$$\eta_t = \eta_0 e^{\alpha t} \tag{1}$$

where η_0 is the viscosity at the beginning of the determination, and α is the slope of the plot of log viscosity versus reaction time over the time interval of the measurement.

From Poiseuille's law, the volume flowing through the viscometer,

$$V = P\pi a^4/8\eta_t l \text{ cc./sec.},$$

where a is the radius, l is the length of the capillary, and P is the mean pressure head of the liquid.

For the Ostwald-type viscometer, a constant volume, Q (the viscometer volume), will pass through in the flow time t'. Thus

$$Q = (P\pi a^4/8l) \int_0^{t'} dt/\eta_t \tag{2}$$

When eqs. (1) and (2) are combined, integrated, and rearranged, we obtain

$$\eta_0 = (P\pi a^4/8lQ)t'[(1 - e^{-\alpha t'})/\alpha t']$$

Thus η_0, the viscosity at the beginning of the measurement, is given by the expression

(Viscometer constant) $\times$ (Flow time) $\times$ (Correction factor)

The correction factor, in the form, $(1 - e^{-\Delta})/\Delta$, where $\Delta = \alpha t'$, is readily calculable.

APPENDIX II

Equilibrium Constants for the Formation of Formaldehyde–Gelatin Amino–Methylol Compounds

Under the conditions normally used (pH < 8) where the gelatin amino groups are predominantly in the $—NH_3^+$ form, the concentration of formaldehyde-methylol compound is determined by the following equilibria:

$$\text{Gel}—NH_3^+ \overset{K_1}{\rightleftharpoons} \text{Gel}—NH_2 + H^+$$

$$\text{Gel}—NH_2 + CH_2O \overset{K_2}{\rightleftharpoons} \text{Gel}—NH—CH_2OH$$

This methylol formation has been followed by measurement of the hydrogen ion liberated on addition of a formaldehyde solution at a given pH to a gelatin solution at the same pH. Experiments were made on a series of formaldehyde concentrations at pH values between 6 and 11.

Determination of K_1. The total content of charged amino groups at each pH value was determined by extrapolation of a plot of hydrogen ion liberated ($[x]$) against $[x]$/[Formaldehyde] to $[x]$/[Formaldehyde] = 0. The values obtained are in excellent agreement with titration-curve values.

Experimental values of pK_1 were calculated from these data (Table VII). As gelatin contains amino groups having different pK values, a variation of pK_1 with pH was expected. Theoretical values for pK_1 (Table VII) were calculated on the assumption that the following amino-group contents and pK values hold: α-amino, 0.016 mmole/g., pK 7.0: ϵ-hydroxylysine, 0.064 mmole/g., pK 9.5; ϵ-lysine, 0.320 mmole/g., pK 10.3.

Determination of K_2. Values of K_2 have been calculated for each pH value on the basis of data on the amount of hydrogen ion liberated at different formaldehyde additions, together with values of K_1 determined

TABLE VII
Values of pK_1 and K_2
(Temperature, 40°C.; Gelatin Concentration, 2%)
Average Values for Alkali- and Acid-Processed Gelatins

pH	$[NH_3^+]$, mmoles/g. dry gelatin	pK_1		K_2
		Experimental	Theoretical	
6.0	0.39	—	—	160
7.0	0.385	8.8	8.8	110
7.5	0.38	9.1	9.1	130
8.0	0.37	9.3	9.3	160
8.5	0.36	9.5	9.6	210
9.0	0.34	9.8	9.8	230
9.5	0.30	10.0	10.0	250
10.0	0.22	10.1	10.1	—
10.5	0.12	10.2	10.2	—
11.0	0.05	10.2	10.2	—

above. Results for low extents of reaction only were used to minimize errors from an expected variation of K_1 with amount of reaction and from dimethylol formation. The value of K_2 at higher pH's agrees with the literature value[15] for lysine as an amino acid (K_2 = 240). Results are set out in Table VII.

References

1. French, D., and J. T. Edsall, *Advances in Protein Chem.*, **2**, 277 (1945).
2. Fraenkel-Conrat, H., and H. S. Olcott, *J. Am. Chem. Soc.*, **67**, 950 (1945).
3. Gustavson, K. H., *Advances in Protein Chem.*, **5**, 353 (1949).
4. Gustavson, K. H., *The Chemistry of Tanning Processes*, Academic Press, New York, 1956, (a) p. 253, (b) p. 246.
5. Howarth, R. D., R. MacGillivary, and D. H. Peacock, *J. Chem. Soc.*, **1952**, 298.
6. Mees, C. E. K., *The Theory of the Photographic Process*, Macmillan, New York, 1954, Chap. 3, p. 82.
7. Janus, J. W., A. W. Kenchington, and A. G. Ward, *Research*, **4**, 247 (1951).
8. Hamilton, P. B., and R. A. Anderson, *J. Biol. Chem.*, **211**, 95 (1954).
9. Davis, P., in *Recent Advances in Gelatin and Glue Research*, Pergamon Press, London, 1958, p. 225.
10. Janus, J. W., in *Recent Advances in Gelatin and Glue Research*, Pergamon Press, London, 1958, p. 214.
11. Green, R. W., K. P. Ang, and L. C. Lam, *Biochem. J.*, **54**, 818 (1953).
12. Pouradier, J., and H. Chateau, *J. chim. phys.*, **53**, 726 (1956); J. Pouradier, *Discussions Faraday Soc.*, **16**, 180 (1954).
13. Carpenter, D. C., *Arch. Biochem.*, **9**, 159 (1946).
14. Wormell, R. L., *New Fibres from Proteins*, Butterworths, London, 1954, p. 93.
15. Levy, M., and D. E. Silberman, *J. Biol. Chem.*, **188**, 723 (1937).

Synopsis

A study has been made of the effect of concentration of the crosslinking agent, gelatin concentration, and pH on the rate of increase of viscosity with time, for gelatin solutions containing either formaldehyde or glyoxal. The results are consistent with the kinetic relationship:

$$\text{Rate of crosslinking} \propto [\text{Gelatin}]^2[\text{Crosslinking agent}]^n/[H^+]$$

For formaldehyde, n is 2. For glyoxal, n is 1, as was expected for this bifunctional hardener. Initial formation of gelatin–methylol compounds is proposed in both cases. With formaldehyde, it is suggested that this leads to a methylene-ether crosslink between a gelatin amino-methylol compound and an unspecified gelatin–methylol compound, while in the case of glyoxal, there is evidence to suggest that the crosslinkage involves two side-chain amino groups and results in a charged crosslink.

Résumé

On a effectué l'étude de l'effet de la concentration de l'agent de pontage, de la concentration en gélatine et du pH sur la vitesse d'augmentation de viscosité en fonction du temps, de solutions de gélatines contenant soit du formaldéhyde soit du glyoxal. Les résultats sont accord avec la formule:

$$\text{Vitesse de pontage} = \text{fonction}\ \frac{[\text{Gélatine}]^2[\text{agent de pontage}]^n}{[H^+]}$$

Pour le formaldéhyde, n est égal à 2. Pour le glyoxal n est égal à 1, comme prévu pour cet agent bifonctionnel. On propose dans les deux cas la formation initiale de composés

de méthylol–gélatine. Avec le formaldéhyde on suggère que cela conduit à la formation d'un pont méthylène-éther entre un composé d'amino-méthylol-gélatine et un composé non-spécifié de méthylol–gélatine, tandis que dans le cas du glyoxal, il va de soi que le pontage fait intervenir deux groupements amines latéraux et il en résulte un pont intermoléculaire, porteur de charges.

Zusammenfassung

Eine Untersuchung des Einflusses der Vernetzerkonzentration, der Gelatinekonzentration und des pH auf die Geschwindigkeit der Viskositätszunahme in Gelatinelösungen, die entweder Formaldehyd oder Glyoxal enthielten, wurde durchgeführt. Die Ergebnisse entsprechen der kinetischen Beziehung:

$$\text{Vernetzungsgeschwindigkeit} \propto \frac{[\text{Gelatine}]^2[\text{Vernetzer}]^n}{[H^+]}$$

Für Formaldehyd beträgt n zwei; für Glyoxal ist n, wie für dieses bifunktionelle Härtungsmittel zu erwarten, gleich eins. In beiden Fällen wird eine anfängliche Bildung von Gelatine-Methylolverbindungen angenommen. Bei Formaldehyd soll diese zu einer Methylen-Äthervernetzung zwischen einer Gelatine-Aminomethylolverbindung und einer nicht spezifizierten Gelatine-Methylolverbindung führen, während in Falle des Glyoxals Hinweise für den Aufbau der Vernetzung aus zwei Seitenkettenaminogruppen bestehen, was zu Vernetzungsstellen mit Ladungen führt.

Received September 15, 1961
Revised December 22, 1961

JOURNAL OF POLYMER SCIENCE: PART A VOL. 1, PP. 817–821 (1963)

Diffusion Constants of a Maltosaccharide Series*

M. C. BOURNE, C. O. CHICHESTER, and C. STERLING, *Department of Food Science and Technology, University of California, Davis, California*

Previous studies of sugar diffusion have been concerned principally with mono- and disaccharides.[1–6] These have been investigated in dilute, as well as concentrated, solutions, and coefficients for both integral and self diffusion have been obtained. However, the relationship of molecular size to the diffusion constants of oligosaccharides has been ascertained only in a limited way. The present investigation considers diffusion coefficients of a maltosaccharide series, ranging from glucose to maltohexaose.

Experimental

^{14}C-labeled starch was prepared from tobacco leaves[7] and diluted with inactive tobacco starch as carrier. The starch was put into solution and hydrolyzed with 0.1*N* H_2SO_4. After neutralization with $Ba(OH)_2$ the mixture was centrifuged, and the supernatant was allowed to stand over a mixture of ion exchange resins (Amberlite IR 120 and Duolite A4) and then decanted and dried.

The maltosaccharides were separated, by the paper chromatographic method of Jeans et al.[8] as modified by Hughes et al.,[9] with a mixture of isoamyl alcohol, pyridine, and water (1:1:1). Eight 18-hr. developments were given. Radioautographs were made, the bands of radioactive sugars were carefully excised, and the sugars were eluted from each band. After drying, the individual oligosaccharides were further purified by paper chromatography of each sugar. Maltosaccharides with a degree of polymerization (DP) of 1–6 (glucose through maltohexaose) were thus separated and dried.

The diffusion cell, which was developed for this study, will be described fully elsewhere.[10] Briefly, the cell is of the diaphragm type, with solutions separated by a fritted-glass disk, whose outer surfaces are continually swept by a magnetic stirrer. The cell constant was determined with 0.04*M* KCl.[11,12] The temperature was held at 25 ± 0.02°C., and each solution had 10 ppm $HgCl_2$ for prevention against microbial activity. Solutes were used at tracer levels (usually at levels below 1 ppm). Initial sampling was performed after the establishment of a uniform diffusion gradient, and the second sampling was made about 98 hr. afterwards.

* This work was supported by a grant-in-aid from the American Maize-Products Co.

Because of the presumptive adsorption of the oligosaccharides on the frit surface, experiments were carried out in solvents which would saturate the active adsorbing sites and show the effect of solvent concentration as well. The solvents were 0.05 and 0.25*M* glucose, 20% sucrose (ca. 0.585*M*), and 20% corn syrup solids. The approximate oligosaccharide distribution in the corn syrup solids was as follows:[13]

Oligosaccharide DP	Per Cent
1	30.0
2	17.9
3	13.2
4	9.6
5	7.3
6	5.3
7	4.3
>7	12.1

If it be assumed that the oligosaccharides of higher DP than 7 have a mean number-average molecular weight corresponding to DP 9, the corn syrup solution has a molarity of 0.569.

Except for the self-diffusion coefficient of glucose in 0.05*M* glucose, all diffusion coefficients determined here are integral coefficients. (In two additional experiments, the pores of the disk were filled with 0.05*M* inactive glucose, and labeled glucose in 0.05*M* inactive glucose was allowed to diffuse into water.)

After being withdrawn, each sample was weighed and then dried in a counting vial. Phosphor solution (0.6 gm. 2,5-diphenyloxazole, 0.05 gm. 1,4-bis-2(5-phenyloxazolyl)benzene, 67 ml. toluene, 33 ml. ethanol) was added to dissolve the sugars, and radioactivity was determined in an automatic Tri-carb liquid scintillation spectrometer (Packard Instrument Co. Model 314X). Because radioactivity was the sole measure of concentration, materials balances were made for total radioactivity in each experiment. When these were not accurate to within 1.0%, the results were discarded. The same phosphor solution was used in all samples, and each sample set was measured at the same time. Hence, the counting efficiency was constant for all samples. Because of the long life of ^{14}C no correction was made for radioisotope decay, and it was assumed that the ^{14}C-containing molecules diffuse at the same rate as molecules with ^{12}C. All experiments were made in duplicate.

Results

Table I presents the diffusion coefficients for the maltosaccharide series. The mean value of the diffusion coefficient of glucose into water at 25°C., 6.70×10^{-6} cm.^{2} sec.$^{-1}$, is to be compared with Longsworth's[6] value of 6.728×10^{-6} cm.^{2} sec.$^{-1}$. Note that the integral diffusion coefficients decrease with increasing degree of polymerization.

TABLE I
Diffusion Coefficients of Maltosaccharides at 25°C.

DP of Saccharide	Solvent[a]	Diffus. coeff., cm.^{2} sec.$^{-1}$ × 10^6
1	0.05*M* glucose → water	6.70
1	0.05*M* glucose	6.28
2	0.05*M* "	4.94
3	0.05*M* "	4.00
4	0.05*M* "	3.63
5	0.05*M* "	3.22
6	0.05*M* "	3.04
5	0.25*M* "	2.92
2	20% sucrose	2.57
4	20% "	1.87
6	20% "	1.50
2	20% corn syrup solids	3.96
4	20% "	2.46
6	20% "	1.52

[a] All solvents with added 10 ppm $HgCl_2$.

In more concentrated systems, the diffusion constant is considerably diminished. Except for maltosaccharides of DP 6, there is a greater decrease in 20% sucrose solution than in 20% corn syrup solution. The physical properties of the solvent systems are given in Table II.

TABLE II
Physical Properties of Solvent Systems

Solvent	Molarity	Sp. gr. at 25°C.	Viscosity at 25°C., cpoise
0.05*M* glucose	0.05	0.9996	0.899
20% sucrose	0.585	1.0720	1.474
20% corn syrup solids	0.569	1.0744	1.759

In all cases, it is possible to construct a more or less rectilinear plot of diffusion coefficient versus the logarithm of the degree of polymerization. This relationship is as follows:

Solvent	Relationship
0.05*M* glucose	$D = 6.28–4.37 \log DP$
20% sucrose	$D = 3.25–2.2 \log DP$
20% corn syrup solids	$D = 5.47–5.0 \log DP$

Discussion

A rectilinear relationship of diffusion coefficient/log (DP) may also be found in a paraffin hydrocarbon series of Douglass and McCall[14] but not in a similar series of aliphatic alcohols.[15] On theoretical grounds, such a rela-

tionship does not seem to be particularly meaningful. However, it does call attention to a departure from the curvilinear relationship which is to be expected when diffusion coefficients of spherical molecules are calculated on the basis of the Einstein[16] equation: $D = RT \cdot 1/N6\pi\eta r$. Thus, if the molecular volume of maltohexaose were considered to be 5.3 times the molecular volume of glucose, spheres of the former would have a diffusion coefficient approximately 0.57 of that of the latter. In reality, the relationship is about 0.49. The most probable explanation is that the molecule is asymmetric. From the equation of Herzog et al.[17] it is possible to determine an axial ratio of 3:1 for maltohexaose, considered as a prolate ellipsoid, and smaller ratios for the lower polymers. Obviously, the average configuration of these molecules must be that of a partial coil.

According to the Einstein equation, the general diminution of the diffusion coefficients in concentrated sugar solutions may be related to the greater viscosity of those solutions. However, the decrease in absolute value of the coefficient (in the case of maltose and maltotetraose) is greater in sucrose solution than in corn syrup solution—despite the fact that the latter solvent is considerably more viscous. In measuring diffusion coefficients of glucose and sucrose solutions, Gladden and Dole[3] failed to find a close relationship between diffusion coefficient and viscosity as a function of concentration. Probably, as a result of molecular association, the Einstein equation cannot be expected to be valid for concentrated solutions.

According to Eyring,[18] an increase in molarity of solute or of solvent will be related with a decreased diffusion coefficient. Thus, like the Einstein equation, this relationship could account for the smaller values of the coefficient in the more concentrated solvents. However, because of the very slight differences in molarity between the sucrose and corn syrup solutions, Eyring's[18] equation similarly cannot explain the marked differences between the diffusion coefficients in these solutions.

Perhaps it may be assumed that effective association between the smaller maltosaccharides and the sucrose molecules is greater than that among the smaller maltosaccharides. With larger maltosaccharide molecules, the affinity between the like molecules presumably is greater, as is the case in starch.

References

1. Clark, D. M., and M. Dole, *J. Am. Chem. Soc.*, **76,** 3745 (1954).
2. English, A. C., and M. Dole, *J. Am. Chem. Soc.*, **72,** 3261 (1950).
3. Gladden, J. E., and M. Dole, *J. Am. Chem. Soc.*, **75,** 3900 (1953).
4. Gosting, L. J., and M. S. Morris, *J. Am. Chem. Soc.*, **71,** 1998 (1949).
5. Longsworth, L. G., *J. Am. Chem. Soc.*, **74,** 4155 (1952).
6. Longsworth, L. G., *J. Am. Chem. Soc.*, **75,** 5705 (1953).
7. Calvin, M., C. Heidelberger, J. C. Reid, B. M. Tolbert, and P. F. Yankwith, *Isotopic Carbon*, Wiley, New York (1949).
8. Jeans, A., C. G. Wise, and R. J. Dimler, *Anal. Chem.*, **23,** 415 (1951).
9. Hughes, R. E., C. O. Chichester, and C. Sterling, *Food Technol.*, **12,** 111 (1958).
10. Bourne, M. C., C. O. Chichester, and C. Sterling, in press.
11. Harned, H. S., and R. L. Nuttall, *J. Am. Chem. Soc.*, **71,** 1460 (1949).

12. Gosting, L. J., *J. Am. Chem. Soc.*, **72**, 4421 (1950).
13. Lewis, F. A., *Western Canner and Packer*, **48** (10), 26 (1956).
14. Douglass, D. C., and D. W. McCall, *J. Phys. Chem.*, **62**, 1102 (1958).
15. McCall, D. W., D. C. Douglass, and E. W. Anderson, *J. Chem. Phys.*, **31**, 1555 (1959).
16. Einstein, A., *Ann. Physik.*, [4] **17**, 549 (1905).
17. Herzog, R. O., R. Illig, and H. Kudar, *Z. physik. Chem. Leipzig*, **A167**, 329 (1934).
18. Eyring, H. J., *J. Chem. Phys.*, **4**, 283 (1936).

Synopsis

A series of maltosaccharides, from glucose through maltohexaose, was prepared from starch labeled with ^{14}C. Self and integral diffusion coefficients were measured in dilute and in concentrated solvents. The coefficients were related more or less rectilinearly with the logarithm of degree of polymerization, presumably because of molecule asymmetry. A greater diminution in the coefficient occurred in 20% sucrose than in 20% corn syrup of approximately equal molarity but considerably greater viscosity.

Résumé

On a préparé une série de maltosaccharides, du glucose au maltohexaose, à partir d'amidon marqué au ^{14}C. On a mesuré les coefficients d'autodiffusion et de diffusion intégrale dans des solutions diluées et concentrées. Les coefficients varient plus ou moins linéairement avec le logarithme du degré de polymérisation, ce qui est probablement dû à l'asymétrie de la molécule. Le coefficient diminue plus fort dans une solution à 20% de sucrose que dans 20% de sirop de grain de molarité environ égale mais d'une viscosité considérablement plus élevée.

Zusammenfassung

Eine Reihe von Maltosesacchariden, von Glucose bis Maltohexaose, wurde aus ^{14}C-markierter Stärke hergestellt. Selbstdiffusionskoeffizienten und integrale Diffusionskoeffizienten wurden in verdünnter und konzentrierter Lösung gemessen. Die Koeffizienten standen in mehr oder weniger linearer Beziehung zum Logarithmus des Polymerisationsgrades, offenbar wegen der Molekülasymmetrie. Bei einer 20%igen Rohrzuckerlösung trat eine grössere Abnahme der Koeffizienten auf als bei einem 20% igen Mais-Sirup mit ungefähr gleicher Molarität, aber bedeutend grösserer Viskosität.

Received January 25, 1962

JOURNAL OF POLYMER SCIENCE: PART A VOL. 1, PP. 823–830 (1963)

Polymerization of Phosphonitrilic Chloride Trimer at High Pressures and Temperatures

J. R. SOULEN and M. S. SILVERMAN, *Research and Development Department, Pennsalt Chemicals Corporation, Wyndmoor, Pennsylvania*

Introduction

It has been known for a long time that the lower members of the homologous phosphonitrilic chloride series, $(PNCl_2)_n$, $n = 3, 4, \ldots$, undergo thermal polymerization at 250–350°C. to a high polymer with rubberlike properties.[1] Depolymerization requires temperatures above 350°C.,[1] although recent work[2] indicates it may take place slowly at somewhat lower temperatures. Nevertheless, the —P—N— backbone structure in the high polymer has considerable thermal stability. Thus the phosphonitrilic chlorides and their derivatives, such as $(PNF_2)_n$ and $(PNPh_2)_n$, have received attention as potential high temperature inorganic or semiorganic elastomers, although there has been no useful product of this type reported to date. The rubbery polymers thus far obtained are unsuitable for practical applications due to their ease of hydrolysis. Recently there have been several studies[3,4] of catalyzed polymerizations of $(PNCl_2)_3$, including some cases in which nearly complete polymerization to the elastomer has been obtained at 210°C. The data were consistent with a rate law first-order in the trimer, and a number of substances including ethers, ketones, alcohols, and organic acids accelerated the rate greatly over that of purified trimer with no deliberately added catalyst.

The purpose of the work reported here was to polymerize $(PNCl_2)_3$ at very high pressures and to use this variable to obtain information on the polymerization equilibrium and rate, as well as properties of the elastomer obtained. There was a possibility that if this substance could be formed under conditions radically different from those usually employed, a product with more desirable properties would result.

Experimental

Phosphonitrilic chloride trimer obtained from Hooker Chemical Corp. was used without further purification (Found: N, 12.08; Cl, 61.81; calc.: N, 12.08; Cl, 61.19). Infrared and x-ray diffraction analyses showed $(PNCl_2)_3$ only.

The density of phosphonitrilic chloride rubber was obtained from weights in air and in acetone of a sample of this material obtained by polymerization of the trimer at 300° and one atmosphere.

A tetrahedral anvil high pressure apparatus of the type developed at the National Bureau of Standards[5] was used. The only differences from the description cited was that $^5/_8$-in. rather than $^9/_{16}$-in. tetrahedral sample holders were used in the present work, and a sheet of 5-mil Mylar was used between the anvil assemblies and the Teflon sheet. Force was applied to the tetrahedral anvil system by a Watson-Stillman 100-ton hydraulic laboratory press. Pressure calibration was done by measuring the electrical resistance change of bismuth as a function of ram force, and the three discontinuities were considered to occur at 25.4, 27.0, and 88 kbars. In all experiments a thin sleeve of spectroscopic-grade graphite was used as the heating element around the sample, and end-plugs of the same material isolated the sample from the platinum or silver tabs that carried the current from the anvils to the heating sleeve. Temperature calibrations were done by measurement of the electrical power input required to obtain temperatures indicated by a chromel–alumel thermocouple, the tip of which was in good contact with the center of this sleeve. The temperatures reported here are thus the highest to which any part of the sample is subjected, and it must be recognized that the ends of the sample are in each case somewhat cooler. Further, from experience in repeated calibrations, it is apparent that temperature values are uncertain by ± 50°C., but the differences between temperature levels of the experiments should be quite reliable.

In each run the sample (25–75 mg.) was first compressed in the high pressure apparatus, then heated, and held at the desired conditions for a measured period of time. The high pressure was maintained until the power was turned off and the sample had cooled to near ambient temperature. From measurements during temperature calibration, it was determined that the cooling rate was very rapid.

The amount of polymerization to the relatively nonvolatile high polymer was determined by weighing the reaction products, heating them in an oven under house vacuum (170–260 mm. Hg) at 180–190°C. for 1 hr. and then reweighing them. In separate experiments with mixtures of trimer and rubber prepared in the same way as that used for the density determination, the error of this method was shown to be less than 2%. It was apparent by microscopic examination of the products that in some cases graphite contaminant remained occluded even after careful attempts to separate it completely. In a number of runs the amount of carbon in the vacuum oven residue was determined and this correction, which was in almost all cases small, was subtracted from the total residue weight to obtain the weight of the high polymer.

Hydrolytic stabilities were determined by weighing samples of the product before and after exposure to atmospheric moisture for periods of the order of a week.

Thermal stability comparisons were made on a Chevenard thermobalance (obtained from Cooke, Troughton, and Simms, Inc., Malden, Mass.) with the use of a dry, high-purity nitrogen atmosphere (flow rate

over the sample about 400 ml./min.) and a nominal heating rate of 5°C./min. Because of the small weights of the high pressure products (about 10% of the sample weight generally used on this thermobalance), the precision of the thermogravimetric curves is considerably less than usual. Their general appearance, however, is undoubtedly reliable.

Discussion

Conclusions about the equilibrium between phosphonitrilic chloride trimer and rubber from this high pressure study are complicated to some extent by the temperature gradient in the sample, the possibilities of a number of intermediate degrees of polymerization, and the question of whether equilibrium has been obtained. Visual observations of the products indicate, however, that certain of the runs do yield valid equilibrium information. In each series of runs carried out at a single pressure level, at the lowest temperature the product was unchanged, white, crystalline solid. At higher temperatures, the center part of the sample contained increasing amounts of darker elastomer until a pellet of spongy rubber filled the entire sample cavity. At higher temperatures still, the middle section of the sample began to contain a tan to grey fluffy powder which increased in amount with temperature, and the remaining elastomeric part of the product was much less coherent. In a run at 65 kbars and 1600°C., the grey powder was isolated, and $(PNCl_2)_3$ was shown to be its major constituent by infrared analysis.

Figure 1 summarizes the high pressure, high temperature equilibrium findings. Time for each run was 5 min. At 70 kbars and temperatures of

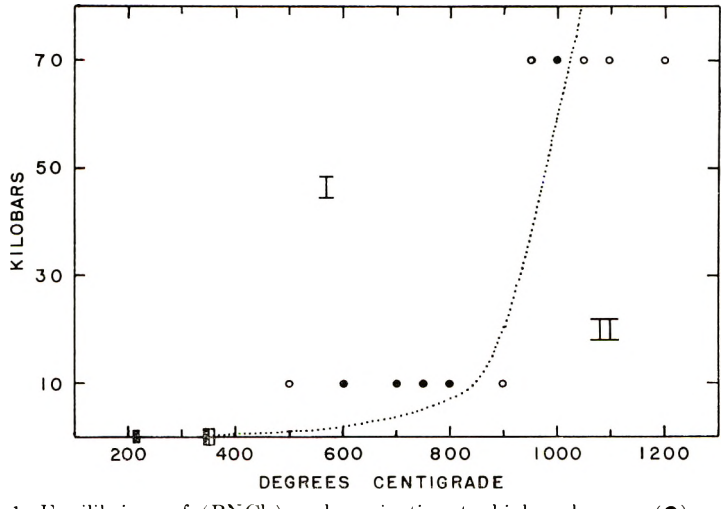

Fig. 1. Equilibrium of $(PNCl_2)_3$ polymerization to high polymer: (●) over 90% conversion to high polymer; (○) depolymerization in Region II, incomplete polymerization (due to slow rate) in Region I (1-atm. results indicated on abscissa); (■) over 90% conversion to high polymer, data of Stokes[1] and Konecny et al.;[3] (□) depolymerization, data of Stokes.[1] Region I: high polymer favored, region II: depolymerization occurs.

1050°C. and above, depolymerization of the high polymer was observed. At 1000°C., no depolymerization was noted, and over 90% conversion to the high polymer was obtained. In a run at 950°C., starting material was present and only 67% high polymer was found. This is no doubt due to limitation of the rate by the temperature of the coolest part of the sample. At 10 kbars, visual decomposition of the high polymer was observed at 900°C., and it was not possible to analyze complete samples from runs above this temperature because they blew out of the apparatus. At 600–850°C., over 90% conversion to high polymer was obtained with no evidence of its depolymerization. A 500°C. run in which only 53% conversion to high polymer was obtained in 5 min. indicates the rate limitation at the 10-kbar level.

To determine how rapidly the final state is achieved under partial conversion conditions, runs of 1 and 25 min. durations were also made at 70 kbars, 900°C. and at 10 kbars, 500°C. As shown in Figure 2, the per cent polymerized in 1 min. is in the same range as that obtained in 5 min., but at 25 min. a significant further amount of polymerization has occurred. If the entire sample were at the temperature of the hottest middle section, complete polymerization would no doubt have been observed under these temperature and pressure conditions.

Figure 1 indicates that the equilibrium is shifted toward the high polymer by increasing pressure and decreasing temperature. The pressure dependence is consistent with theory, in that our measured density of the rubbery high polymer is 2.343 g./cc at 25°C., whereas the density of the trimer has been found previously[6] to be 1.99 g./cc. Thus $(PNCl_2)_3$ has a volume of 58.2 cc./mole of $PNCl_2$ and $(PNCl_2)_x$ rubber has a volume of only 49.5 cc./mole of $PNCl_2$. For the reaction,

$$^1/_3\,(PNCl_2)_3 \rightarrow 1/x(PNCl_2)_x \text{ rubber}$$

$\Delta V = -8.7$ cc. Because $(d\Delta F/dP)_T = \Delta V$, the free energy change becomes more negative, and the reaction, as written, becomes more favorable as pressure is increased. The temperature dependence of these high pressure studies is in agreement with previous findings on the gas-phase equilibrium which showed the polymerization to be exothermic.[7]

In addition to information from this high pressure study, several rectangles which summarize the equilibrium at one atmosphere are indicated on the abscissa of Figure 1. As stated earlier, polymerization has been carried out up to 350°C., but depolymerization is said to begin above this temperature.[1] Recent catalyzed polymerizations have been essentially complete at 210°C.[3] Based on these and the high pressure points, Figure 1 has been divided into Region I, in which polymerization has been found to be favored thermodynamically, and region II, in which depolymerization has been found to occur. The dividing line is only approximate.

Although increasing pressure has a favorable influence on the polymerization equilibrium, it is seen in Figure 3 that it slows significantly the rate of polymerization. All runs in this figure are 5 min. in duration, and

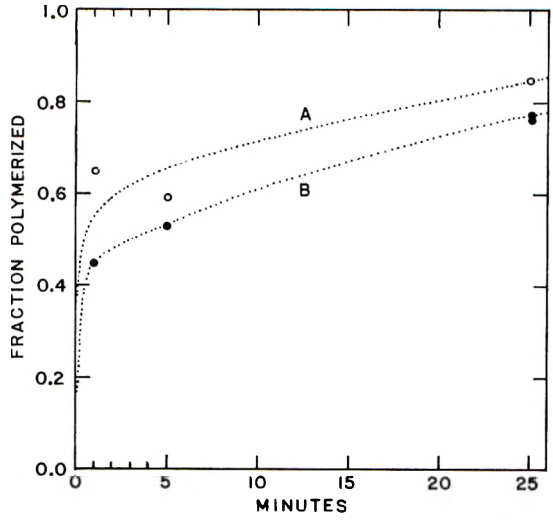

Fig. 2. Rate of polymerization of $(PNCl_2)_3$ to high polymer in high pressure apparatus: (*A*) 70 kbars, 900°C.; (*B*) 10 kbars, 500°C.

it can be seen that at 700°C. the reaction at 10 kbars is over 90% complete, while at 70 kbars it is less than 10% complete in this time. Too much reliability cannot be placed on the values of any one point because of the temperature uncertainties mentioned in the experimental section and the small error in the vacuum oven separation determination of the high polymer. In addition, carbon analyses, which resulted in small corrections, were not performed on all the vacuum oven residues. Nevertheless, the curves in Figure 3 are certainly correct enough to demonstrate the pressure inhibition of the reaction rate.

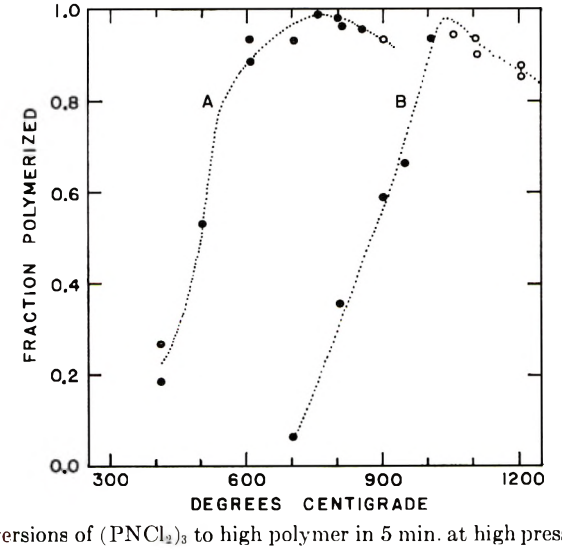

Fig. 3. Conversions of $(PNCl_2)_3$ to high polymer in 5 min. at high pressure: (*A*) at 10 kbars; (*B*) at 70 kbars; (●) incomplete or nearly complete polymerization; (O) depolymerization of high polymer noted.

This indicates that the transition state in the rate determining step of the polymerization must have a larger volume than the reactants in that step. In general, for a reaction A + B → $AB^{\ddagger}$ → Products, $AB^{\ddagger}$ being the intermediate configuration of highest energy, the pressure dependence of the rate is given by $[(d \ln k)/dP]_T = \Delta V^{\ddagger}/RT$, where ΔV is the change in volume for the reaction A + B → $AB.^{\ddagger}$ Since increasing pressure slows the polymerization, $\Delta V^{\ddagger}$ must be positive. Konecny et al. have proposed[4] an ionic mechanism whose initiation step apparently involves the loss of a chloride ion from $(PNCl_2)_3$, with formation of $P_3N_3Cl_5^+$. The latter, it is suggested, is responsible for propagation of the polymerization:

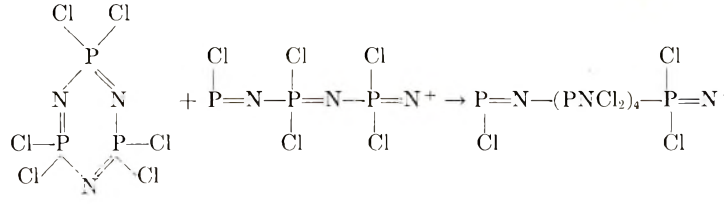

In both the loss of Cl^- by the trimer and the transfer of Cl during propagation, it is reasonable to expect that the transition state would have a larger molar volume than the reactants, and both these steps would therefore be slower at higher pressure. Assuming a first-order rate law, from the data of the runs at 700°C. at 10 and 70 kbars, it is calculated that $\Delta V^{\ddagger}$ is +5.1 cc. This is about 9% of the molar volume of the trimer.

Elastomeric products from a number of high pressure runs, along with the high polymer made at one atmosphere, were exposed to atmospheric moisture for a number of days. Under these conditions, the high polymer loses HCl by hydrolysis, forming a hard, solid residue which is most likely a polymer of $PN(OH)_2$. There was no significant difference between the per cent weight losses of the high pressure and one atmosphere elastomers which underwent this hydrolysis, and the product obtained at high-pressure thus appears to have no greater hydrolytic stability.

As an indication of the relative thermal stabilities, samples of the rubbers made at 1 atm. and the high pressure product were heated in an inert atmosphere in a thermobalance. In addition, a high pressure rubber which had been exposed for a much greater time to the atmosphere was also run. In Figure 4 it is seen that the rubber obtained at 1 atm. undergoes a relatively smooth, continuous loss in weight which is complete at 550°C. under the condition of the thermobalance run. The h gh pressure product shows considerable loss below 200°C., indicating its content of the volatile lower polymers, and then undergoes its major weight loss in approximately the same temperature region as the rubber obtained at 1 atm. Thus the thermal stability of the high polymer is not enhanced by making it under high pressure conditions. About $^1/_6$ of the original weight remains after heating to 700°C. Analysis of this is complicated by the small residue

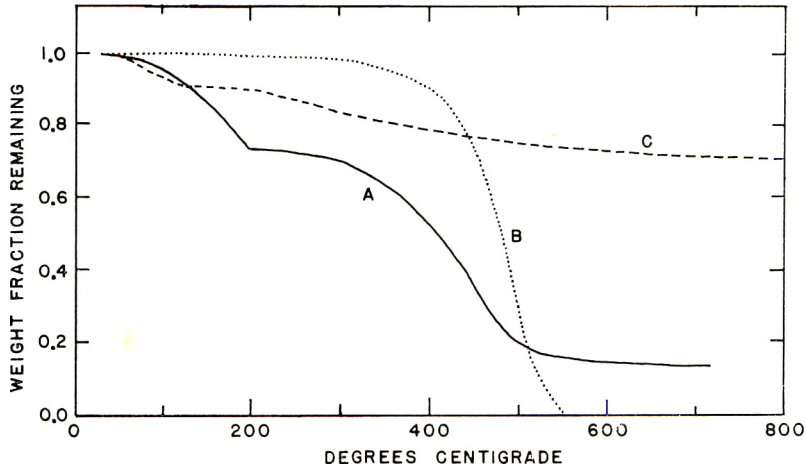

Fig. 4. Thermogravimetric curves of phosphonitrilic polymers: (*A*) partially polymerized high pressure product; (*B*) rubbery high polymer made at 1 atm.; (*C*) partially polymerized high pressure product exposed to atmospheric moisture before thermogravimetric analysis.

weights, only a few milligrams. However, from chemical and infrared analyses, it appears to be a mixture of graphite from the heating sleeve and the hydrolysis product of a fraction of the high polymer which reacted with atmospheric moisture during handling. The third curve in Figure 4 shows the considerable thermal stability of a high pressure rubber which has undergone considerable hydrolysis with accompanying loss of its elastomeric properties.

In further study of the high pressure formation of phosphonitrilic chloride rubber, it would be advantageous to use larger sample container and apparatus without a corresponding increase in sample size, in order to obtain a more nearly uniform temperature throughout the sample. This might also be accomplished by suitable contouring of the heating sleeve. Use of the tetramer $(PNCl_2)_4$, as the starting material would be of interest. Recent measurements of the heats of formation of the trimer and the tetramer[8] show identical values per mole of $PNCl_2$, and thus their heats of polymerization would be the same. On the other hand, the reported density of the tetramer[6] is about halfway between that of the trimer and the high polymer. One would therefore expect to find the equilibrium of the tetramer polymerization less pressure-dependent than that of the trimer, whereas the temperature dependence should be the same.

The authors are indebted to W. H. Chappell, Jr., who performed a considerable part of the experimental work, the analytical and shop groups of our Research and Development Department for their help, and U. O. Hutton of the National Bureau of Standards for a number of suggestions with regard to the high pressure apparatus. This work was supported in part by the Office of the Naval Research.

References

1. Stokes, H. N., *Am. Chem. J.*, **19**, 782 (1897).
2. Patat, F., and P. Derst, *Angew. Chem.*, **71**, 105 (1959).
3. Konecny, J. O., and C. M. Douglas, *J. Polymer Sci.*, **36**, 195 (1959).
4. Konecny, J. O., C. M. Douglas, and M. Y. Gray, *J. Polymer Sci.*, **42**, 383 (1960).
5. Lloyd, E. C., U. O. Hutton, and D. P. Johnson, *J. Research Natl. Bur. Standards*, **63C**, 59 (1959).
6. Paddock, N. L., and H. T. Searle, in *Advances in Inorg. Chem. and Radiochem.*, Vol. 1, Academie Press, Inc., New York, 1959, p. 354.
7. Schmitz-Dumont, O., *Z. Elektrochem.*, **45**, 651 (1939).
8. Hartley, S. B., N. L. Paddock, and H. T. Searle, *J. Chem. Soc.*, **1961**, 430.

Synopsis

Polymerization of phosphonitrilie chloride trimer at pressures of 10 kbars and above has shown that increasing pressure favors the formation of the rubbery high polymer thermodynamically, but slows its rate of formation. There appears to be no difference in hydrolytic or thermal stability between elastomer formed under high pressure conditions and that obtained by the more usual polymerization at 1 atm.

Résumé

La polymérisation du trimère du chlorure phosphonitrilique à des pressions de 10 kilobare et plus, à montré que l'augmentation de pression favorise thermodynamiquement la formation d'un haut polymère caoutchouteux, mais diminue sa vitesse de formation. Il apparait qu'il n'y a pas de différence de stabilité hydrolytique ou thermique entre l'élastomère formé sous des conditions de haute pression et celui obtenu par la polymérisation plus usuelle, à la pression d'une atmosphère.

Zusammenfassung

Die Polymerisation von Phosphornitrilchlorid bei Drucken von 10 Kilobar und mehr hat gezeigt, dass Druckzunahme die Bildung des kautschukartigen Hochpolymeren zwar thermodynamisch begünstigt, seine Bildungsgeschwindigkeit aber herabsetzt. Zwischen den bei hohem Druck gebildeten Elastomeren und den durch Polymerisation bei einer Atmosphäre erhaltenen scheint kein Unterschied in der hydrolytischen und thermischen Stabilität zu bestehen.

Received September 8, 1961
Revised October 20, 1961

BOOK REVIEWS

N. G. GAYLORD, Editor

Polyamino Acids, Polypeptides and Proteins. MARK A. STRAHMANN, Ed. The University of Wisconsin Press, Madison, 1962. 394 pp. $8.00.

In the last fifteen years methods were discovered by which synthetic high molecular weight polypeptides can be obtained. These substances may be considered models of proteins occurring in living organisms although they lack, of course, the unique sequence of the amino acid residues and the intricate precisely defined folding to which protein molecules owe their functional specificity. In spite of—or possibly because of—this simplification in the structure of the model, the study of synthetic polypeptides has led to a variety of developments which have advanced very significantly the understanding of proteins. The time is certainly ripe for a summary of these developments. We are indebted to the organizers of an international symposium, which was held at the University of Wisconsin in 1961, for having assembled the leading scientists working in this field and to Prof. Stahmann for having edited papers presented at the symposium and discussion remarks following these presentations.

The 36 papers contained in this volume are subdivided into five sections entitled I. Synthesis and Chemical Properties of Poly-α-Amino Acids and Polypeptides, II. Kinetics and Mechanism of Polymerization Reaction, III. Properties of Polyamino Acids in Solution, IV. Protein and Polypeptide Structure and V. Biological Properties of Poly-α-Amino Acids.

The papers are generally of the highest quality and they summarize work carried out in a most active area of polymer research. While they are of most immediate value to specialists in the field of protein and polypeptide structure, it is to be hoped that polymer chemists concentrating on other areas will also pay due attention to these developments. The discovery of the existence of helical conformations of synthetic chain molecules in solution—first discovered for the synthetic polypeptides—may well have its analogs for a much broader class of polymers than is suspected at the present time. In any case, the phenomenon is of such fundamental interest that every polymer chemist should aim at an understanding of it.

H. Morawetz

Polytechnic Institute of Brooklyn
Brooklyn, New York

Direct Analysis of Diffraction by Matter. R. HOSEMANN and A. N. BAGCHI. North-Holland Publishing Co., Amsterdam, 1962. xxi + 734 pp.

In reviewing this book for the *Journal of Polymer Science* it is necessary to point out that the book was not written for polymer chemists. This is essentially a treatise for the serious crystal structure physicist. The highly mathematical presentation with its complicated nomenclature and symbols, which help to make the book an outstanding contribution to the structure worker, provide an "iron curtain" for most polymer chemists.

This book is important for the field of polymers because it provides techniques and mathematical treatments of diffraction phenomena which are applicable to high polymer structures. Optical diffraction is emphasized as a means of simplifying tedious mathematical calculations. This approach presents the possibility of checking models of structures in a single step; from the model of the system to the diffraction pattern. The authors have also included a very complete and elegant analysis of small angle scattering.

The book is extremely valuable too because it presents a detailed discussion of paracrystallinity and its associated diffraction effects.

The paracrystalline state (which may be defined qualitatively as a partially disordered crystalline state or a partially ordered amorphous state) has been the subject of considerable interest to polymer structure workers. This has come about due to realization that this concept may be very useful in understanding and explaining polymer structure-property relationships. It provides an alternate approach to polymer structure which traditionally has been considered in terms of mixed amorphous and crystalline volume elements in a type of "salt and pepper" mixture.

It may be hoped that the availability of this book will provide a basis for the application of the techniques to appropriate high polymer systems and that practical results will develop. It is in fact unfortunate that the authors did not include more practical applications, for this would have stimulated use of the ideas.

H. S. Kaufman

Allied Chemical Corporation
New York, New York

ERRATUM

Infrared Study of the Reaction of Polyisoprene and Polybutadiene With Sulfur by Use of Deuterated Polymers

(*J. Polymer Sci.*, **58**, 1063–1082, 1962)

By J. J. Shipman and M. A. Golub

Stanford Research Institute, Menlo Park, California

On page 1079 the formula IV should be